Lancaster Environment Centre, Lancaster University

Modelling the Fate and Bioaccumulation Potential of Organic Chemicals in China

Shizhen Zhao

Submitted for the degree of Doctor of Philosophy

January 2016

Abstract

An extensive array of chemicals are used in industry and commerce, many produced in large volumes, but their fate in the environment and corresponding exposure to organisms (including humans) has only been measured for a limited number of substances. Modelling tools have been demonstrated to be an economical alternative to measurement data for the assessment of chemical fate and exposure. Therefore, many fate and bioaccumulation models have been developed in Western countries while progress on the development of tools and legislation are relatively far behind in China. In this thesis, the application of modelling tools in environmental fate and exposure assessment of organic pollutants has been explored in China. The first aspect of this research was the adaptability of Western dietary exposure models to the Chinese population. In **Paper I**, three established Western-based exposure models were used for China using specific Chinese dietary scenarios and modified human characteristics to explore their potential adaptability to be used for the Chinese population. The second aspect was to explore the possibility of extending existing bioaccumulation models to a wider range of organic pollutants by incorporation of newly developed poly-parameter linear free energy relationships (pp-LFERs) for individual biological phases in **Paper II**. Compared to traditional single-parameter (sp) K_{OW}-based (sp-LFERs) methods, the pp-LFERs only indicated limited advantages when evaluated with measurements, implying that the choice of approach should be based on other factors beyond methodology of calculating partitioning coefficients (e.g., accuracy of input data and uncertainty from biotransformation). The studies described in **Paper III** and **Paper IV** took polychlorinated biphenyls (PCBs) as a case study, to comprehensively evaluate and demonstrate the ability of a global dynamic fate model （BETR-Global） linked to a bioaccumulation model (ACC-HUMAN) in the reconstruction of historical trends and predicting future of emission trends and exposure profiles for the Chinese population. Meanwhile, controlling sources of intentional and unintentional emissions were thoroughly explored within China in **Paper III**. **Paper IV** more focused on human exposure under the combined effect of emission trends and dietary transition for the Chinese population. The delayed peak time of the human body burden of PCBs has mainly been caused by rapid dietary shifts and on-going emissions from sources, such as imported e-waste in China. The Large uncertainty in the prediction of human body burdens suggests that the choice of model system could be relevant for exposure assessment and that the model should be tailored to the system of interest. Finally, preliminary suggestions to conduct effective controlling measures were also made for the policy makers.

Acknowledgments

I would like to give many thanks to my supervisors Dr. Andy Sweetman and Professor Kevin Jones, for offering me this fantastic opportunity to study for a Ph.D. at Lancaster University. Without your faith in my ability, I would have never considered the further postgraduate study. This unforgettable four-year period has been the most precious experience in my life. It is my great honour to be a member of this excellent research group at Lancaster Environment Centre.

Many thanks to Dr. Andy Sweetman for the daily support from the first day I arrived in Lancaster. I cannot finish my Ph.D. without your continuous support and encouragement, particularly for all the quick chats and invaluable discussions. Thank you so much!

I would like to express my sincere gratitude to Prof. Kevin Jones for providing me this fantastic chance to join in the research group and taking me on board towards the amazing world of scientific research. You are always supportive when I need suggestions and helps.

Thank you to Dr. Oliver Price for providing a new perspective from the industry society, all continuous inputs, valuable suggestions and taking the time to visit us from your busy schedule. Your frequent communications over the years have been tremendously helpful and always encouraging.

I gratefully acknowledge Dr. Knut Breivik for kindly offering insightful comments on my manuscripts, providing discussions and suggestions on my research work.

Dr. Hong Li, many thanks for guiding me when I just arrived the UK and help me to go through all the complicated formalities. You are so kind to assist me in getting used to life abroad.

Thanks to Unilever and Chinese Scholarship Council (CSC) for funding my research work and living at Lancaster University.

Many thanks to all of my fellow mates for the exciting discussions and all the fun we had in the last four years. Special thanks to my landlord, Claudia, you are the best housemate I have ever met. Thanks for sharing your house and all the valuable research and life experiences with me.

I would like to thank my family: my parents and my brother for supporting me spiritually throughout working on this project and my general life. You are my greatest motivation to move forward. 爸爸妈妈，我爱你们！

Last but not least, thank you to Jinjin Wang. You are the best lover, companion and friend that I could have ever asked for. Thanks for your patience on my moody days. You are always supporting me and my dreams, and never trying to hold me back from what I want in my life. I am so lucky to have your love and support to keep me going.

Contents

Abbreviations

BAF	Bioaccumulation Factor
BCF	Bioconcentration Factor
BMF	Biomagnification Factor
BSAF	Biota-sediment Accumulation Factor
BTF	Biotransfer Factor
bw	Body Weight
C	Concentration
CAS	Chemical Abstracts Service
cVMS	Cyclic Volatile Methyl Siloxanes
DSD	Dangerous Substances Directive
dw	Dry Weight
EAF	Electric Arc Furnaces
EC	European Commission
EINECS	European Inventory of Existing Commercial Chemical Substances
EU	European Union
f	Fugacity, Pa
FAO	Food and Agriculture Organization of the United Nations
IECSC	Inventory of Existing Chemical Substances Produced or Imported in China
IP-PCBs	Intentionally Produced Polychlorinated Biphenyls
IVIVE	In Vitro-In Vivo Extrapolation
K_{AW}	Air-Water Partition Coefficient
K_{OA}	Octanol-Air Partitioning Coefficient
K_{OW}	Octanol-Water Partition Coefficient
LRAT	Long-range Atmospheric Transport
NOLM	Non-lipid Organic Matter
OC	Organic Carbon
PBL	Planetary Boundary Layer
PBTK	Physiologically based Toxicokinetic Model
PCBs	Polychlorinated Biphenyls
PEC	Predicted Environmental Concentration
PFOA	Perfluorooctanoic Acid
PNEC	Predicted No Effect Concentration

POC	Particle Organic Carbon
POPs	Persistent Organic Pollutants
PPCP	Pharmaceutical and Personal Care Products
QSAR	Quantitative Structure-Active Relationship
RAIDAR	Risk Assessment, IDentification, And Ranking Model
RCR	Risk Character Ratio
REACH	Registration, Evaluation, Authorization and Restriction of Chemicals
RQ	Risk Quotient
SE	Standard Deviation
TDS	Total Diet Survey
TGD	Technical Guidance Document on Risk Assessment
TOC	Total Organic Carbon
TSCA	Toxic Substances Control Act
UP-PCBs	Unintentionally Produced Polychlorinated Biphenyls
USEPA	Environmental Protection Agency, USA
WHO	World Health Organization
ww	Wet Weight
Z	Fugacity Capacity, mol m^{-3} Pa^{-1}

List of Papers

I Shizhen Zhao, Oliver Price, Kevin C. Jones, Andy J. Sweetman. 2015. Applicability of western chemical dietary exposure models to the Chinese population. Environ Res. 140:165-176; 2015

I was responsible for designing the study, collection of the data for model parameterization, deriving model inputs and scenarios, analysing model outputs and took the lead role in writing the manuscript for publication. Dr. Andy Sweetman, Prof. Kevin Jones and Dr. Oliver Price provided supervision, manuscript editing and general advice.

II Shizhen Zhao, Oliver Price, Kevin C. Jones, Andy J. Sweetman. 2015. Modelling bioaccumulation in fish by poly-parameter linear-free energy relationships (PP-LFERs). (Unpublished manuscript)

I was responsible for designing the study, writing the model equations, collection of the data for model parameterization, deriving model inputs and scenarios, analysing model outputs and took the lead role in writing the manuscript for publication. Dr. Andy Sweetman, Prof. Kevin Jones and Dr. Oliver Price provided supervision, manuscript editing and general advice.

III Shizhen Zhao, Oliver Price, Guorui Liu, Minghui Zheng, Kevin C. Jones, Andy J. Sweetman. 2015. Long-term temporal trends of PCBs and their controlling sources in China. (Unpublished manuscript)

I was responsible for designing the study, writing the model equations, collection of the data for model parameterization, deriving model inputs and scenarios, analysing model outputs and took the lead role in writing the manuscript for publication. Dr. Andy Sweetman, Prof. Kevin Jones and Dr. Oliver Price provided supervision, manuscript editing and general advice. Prof Guorui Liu and Prof Minghui Zheng offered the measured emission factors of UP-PCBs and offered general suggestions on modelling outputs.

IV Shizhen Zhao, Oliver Price, Kevin C. Jones, Andy J. Sweetman. 2015. Time-variant dietary exposure of POPs in China –a PCB case study. (Unpublished manuscript)

I was responsible for designing the study, writing the model equations, collection of the data for model parameterization, deriving model inputs and scenarios, analysing model outputs and took the leading role in writing the manuscript for publication. Dr. Andy

Sweetman, Prof. Kevin Jones and Dr. Oliver Price provided supervision, manuscript editing and general advices.

List of Figures and Tables

1 Background

1.1 Chemicals in the environment

There are more than 100 million unique chemical substances registered in the CAS database until November 2015 (http://www.cas.org/). A new chemical substance is being added to a large amount of already registered chemicals every second (Hendriks, 2013). In Europe, more than 100,000 chemicals are on the market and compiled in the European Inventory of Existing Commercial Chemical Substances (EINECS) during 1970-1982 and are awaiting assessment. The vast majority of the 30,000 substances in wide commercial use (>1 t y^{-1}) are not measured in the environment. Their emission, fate and exposure to biota are still unknown (Muir and Howard, 2006). The situation is similar in China with more than 45,000 chemicals registered under the Inventory of Existing Chemical Substances Produced or Imported in China updated in 2013 (IECSC). This inventory only covers the chemicals produced or imported during 1992-2003 within mainland China, which does not account for substances manufactured out of this period.

Chemical substances can be emitted into the physical environment through a wide range of pathways during each stage of their life cycle, e.g., the production or transportation of goods. Later on, they could harm human health via multiple exposure pathways (e.g., dietary intake, inhalation and dermal contact), possibly causing disorders, cancers and reproductive issues (Grandjean and Landrigan, 2006; Janjua et al., 2007; Jobling et al., 1995). Most of these chemicals have not been measured and evaluated in the environment, and limited information is known about their emission, environmental fate and exposure. Therefore, human exposure to numerous potential hazardous chemicals is unknown. Considering the huge number of commercially used chemicals and the high cost of environmental monitoring, modelling tools are becoming important approaches used in chemical risk assessment as well as screening and identifying emerging new contaminants. Also, models are particularly useful to integrate current knowledge and identify the corresponding gaps on the transfer of chemicals from different sources, through the environment and food web to the organisms (e.g. the source-receptor relationship).

1.2 Regulatory progress

The need to establish legally binding frameworks for the control of chemicals was recognized and started in the 1960's in Europe and the US, evolving from hazard identification to safety risk assessment (Christensen et al., 2011; van Leeuwen and Vermeire, 2007). The legislation addressing industrial chemicals in Europe began with the Dangerous Substances Directive 67/548/EEC (DSD) in 1967, which specified the management requirements for the

classification, packing and identification of hazardous chemicals (Commission of the European Communities, 1967). Subsequently, in order to further improve risk assessment of industrial chemicals produced in or imported into Europe, the chemical legislation of REACH (Registration, Evaluation and Authorisation of Chemicals (EC) No 1907/2006) was adopted in December 2006 and came into force on 1 June 2007 (Parliament and Union, 2006). Under EU REACH, chemical substances and mixtures produced or imported in more than one tonne per year are required to undergo a registration process. In the United States, the "Toxic Substances Control Act" (TSCA) was issued in 1976 (Congress US, 1976), which specified a systematic review process for the evaluation of new chemicals before they enter the market as well as an array of tools for estimating potential risk from existing chemicals.

In China, chemical-related legislation was not initiated until 1994 (Wang et al., 2012). The "Measures on Environmental Managements of New Chemical Substances" was issued by State Environmental Protection Administration (SEPA) in 2003 and revised in 2010 (MEP China, 2010), which is known as China REACH due to its similarity to EU REACH. Different from EU REACH, it is only applicable to new chemicals. Meanwhile, the "Guidelines for the Hazard Evaluation of New chemical substances" (HJ/T154/2004), "Guidelines for the Testing of Chemicals" (HJ/T153-2004), and "Guidelines for Chemical Testing Good Laboratory Practices" (HJ/T155-2004) were also successively issued by SEPA to promote the application of hazard assessments, related test methods and laboratory management. Despite the regulatory progress made in China, its technical development is behind methodologies in developed countries (Wang et al., 2012). For example, the technical guidance for chemical assessment is still lacking so far, and no specified modelling tools to conduct hazard and exposure assessment are available. Although the well-developed assessment frameworks, modelling approaches and exposure scenarios by developed countries could offer insightful references for Chinese cases, the application and adaption of the methodologies would vary case by case in China and should be used with caution. This is a result of China being such a large country with multiple environmental conditions, chemical industry processes, the design and operation of sewage treatment plants and many other essential influential factors (Wang et al., 2012).

1.3 Exposure assessment

Driven by the increasing pollution issues and rapid legislation processes, chemical risk assessment plays a crucial part in various directives and regulations. For example, it is mandatory for the notification of new chemicals under EU REACH regulations (TGD EU, 2003). Chemicals risk assessment means determining and quantifying any risk stemming from exposure to a certain substance, including identifying a relationship between a dose and its effect as well as target populations. As one of the core steps in the risk assessment of chemicals, exposure assessment (illustrated in

Figure 1) is defined as the "determination of the emissions, pathways, and rates of movements of a substance and its transformation or degradation, in order to estimate the concentrations/dose to which human population or environmental compartments are exposed" (van Leeuwen and Vermeire, 2007). The endpoint in the exposure assessment could have different departure points. The exposure to humans could be calculated from measured concentration in indirect exposure vectors (e.g., food items and air), or from the predicting concentrations in environmental media and then modelling their transfer to biotic media.

The fate models are often combined with human exposure models to predict the chemical concentrations in the environment and hence the human body. The exposure considered in this work is environmental exposure, excluding the exposure under special scenarios (e.g., occupational exposure). Figure 1 provides a general conceptual overview for the indirect far-field chemical exposure to humans. Firstly, chemicals are emitted to the physical environment (e.g., air, water, soil and sediment). Then, these chemicals are subject to environmental fate and transport processes (e.g., intermedia transport and distribution). Subsequently, these chemicals could accumulate in aquatic and terrestrial food chains, reaching various human food sources (e.g., vegetation and cow). Eventually, humans are exposed to chemicals via different contact routes (e.g., ingestion and inhalation) from multiple environmental media (e.g., air, water, meat and vegetables).

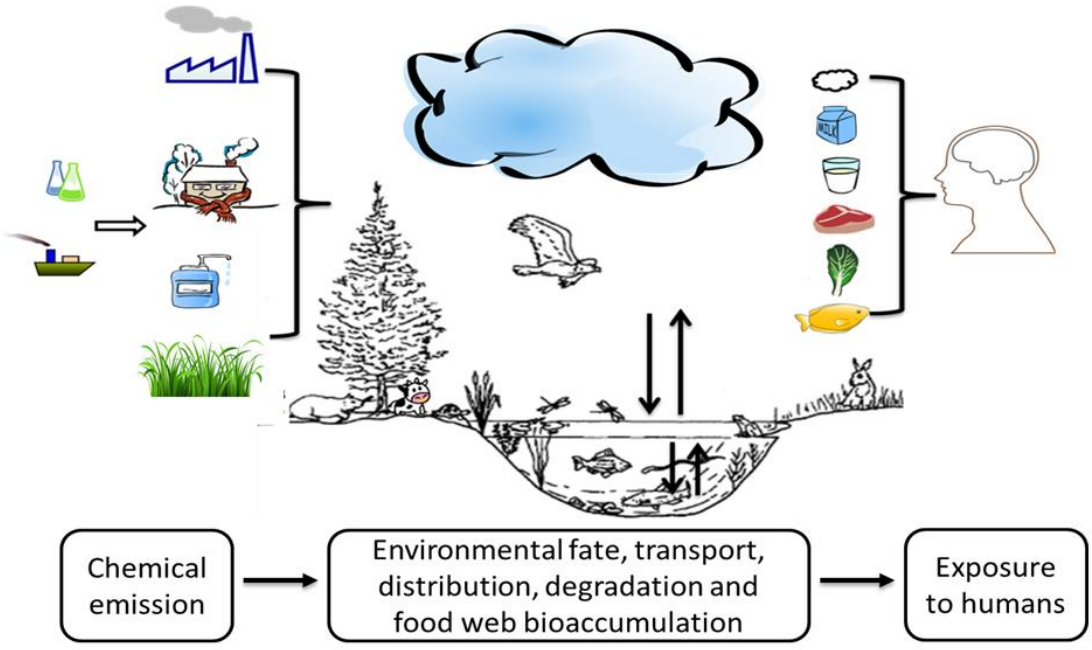

Figure 1. A conceptual model of indirect far-field human exposures to chemicals released to the environment (from source to receptor).

1.4 Aim and outline of this thesis

The top-level objective of this research is to provide a general overview of the potential adaption of Western-based fate and bioaccumulation models to predict human exposure in China. The main exposure pathway focussed on the dietary intake pathway (including inhalation). Therefore, the aims of this thesis were to:

1) Systematically review the applicability of established Western-based multimedia fate and bioaccumulation models for the Chinese population and define any research gaps for model adaption (**Paper I**);
2) Based on the identified research gaps in existing bioaccumulation models, develop traditional octanol-water partition coefficient (K_{OW})-driven bioaccumulation models to extend their applicability domain to more polar and complex chemicals by incorporating newly developed poly-parameter free energy relationships (pp-LFER), using the fish model as a starting point (**Paper II**);
3) Demonstrate that multimedia fate models coupled with bioaccumulation food web models are helpful tools for understanding the source-receptor relationship and offer guidance on setting effective control measures in China (**Paper III** and **IV**);
4) Investigate the impact of different emission sources on a chemical's fate in the physical environment and its bioaccumulation potential along the food chain, with humans as the end receptor (**Paper III** and **IV**);
5) Examine the impact of dietary pattern and change in dietary composition and habits on the human exposure for Chinese population (**Paper I** and **IV**).

A tiered approach was used to achieve the above aims. Firstly, **Paper I** selected three well-established multimedia fate and bioaccumulation models developed by Western countries, to systematically explore the applicability of these models in China. This included identification of predominant exposure pathways and making suggestions to improve their performance in China. In addition, research gaps were identified for traditional K_{OW} -driven bioaccumulation models, including their limited applicability domain caused by directly treating lipid solubility as equal to octanol solubility. Consequently, **Paper II** describes a novel approach to the incorporation of poly-parameter relationships to address the limited applicability domain of existing empirical equations used in traditional K_{OW}-driven bioaccumulation models. It is also an attempt to understand how these newly developed approaches could offer insights on partitioning between biota and the physical environment as well as the interpretation of biomonitoring results. Finally, **Papers III** and **IV** utilize an advanced unsteady-state fate model linked to a bioaccumulation food chain model, in order to thoroughly investigate chemical source-receptor relationships and to aid the development

of successful control measures. PCBs were selected as a case study due to their well-studied profile of chemical properties, emission trends and available measured data. Finally, preliminary suggestions on how to conduct effective controlling measures are made for consideration by policy makers.

2 Introduction to Modelling Tools

The ultimate goals of environmental modelling are to understand the relevant processes and to make predictions regarding the impact of human activities on the environment (Schwarzenbach et al., 2005). In addition, in order to understand the environmental fate and transport, bioaccumulation and exposure of chemicals to biota, the lack of monitoring data for most chemicals of commerce also necessitates the use of modelling tools (Arnot et al., 2006). As a result, numerous mathematical models have been developed from simple box models (Brandes et al., 1996) to complex spatially-resolved models combined with geographic information systems (MacLeod et al., 2011). In this thesis, coupled multimedia fate models and bioaccumulation models used to estimate human exposure are described in the following sections. Several models have been developed for the prediction of environmental fate and bioaccumulation along the food web based on different temporal and spatial solutions, e.g., the regional scale steady-state models SimpleBox (Brandes et al., 1996; Van de Meent, 1993), the dynamic CozMoPOP (Wania et al., 2006) and the dynamic model Globo-POP (Wania and Mackay, 1995).

2.1 Multimedia fate model

Chemical fate models are an essential tool for risk management and chemical regulation. In addition, accurate quantification of a chemical's fate in environmental compartments is the premise for understanding their exposure to biota. Typically, the environment is divided into bulk compartments representative of the atmosphere, water, sediment and soil. Other compartments like vegetation can be added when necessary.

2.1.1 Fugacity concept

The fugacity concept was firstly introduced as a criterion of equilibrium by Gilbert N. Lewis in 1901 (Lewis, 1901) and introduced to environmental modelling by Don Mackay in 1979 (Mackay, 1979). Fugacity is often described as the "escaping" tendency of a chemical in a given phase whereas the fugacity capacity presents the partitioning capacity of the phases. It is based on the understanding that chemical present in a system with different phases (e.g. water, air, and soil) will tend to be distributed at equilibrium, and thus the chemical potential is equal in all phases. Whereas chemical potential is logarithmically related to concentration, fugacity is logarithmically related to chemical potential and thus linearly (or near linearly) related to the concentration at low concentration. Consequently, fugacity is a more practical parameter to model contaminant behaviour in the environment. In addition, it can also indicate the equilibrium status of a system (when fugacities are equal), which cannot be achieved by concentration alone. The fugacity is estimated as:

$f_i = C_i/Z_i$

where f is the fugacity (Pa) of a chemical in phase i, C_i is the concentration (mol m^{-3}) of a chemical in phase i and Z_i is the fugacity capacity (mol m^{-3} Pa^{-1}). The net diffusive flux between phases will always be from phases with higher fugacity to phases with lower fugacity. A phase with higher fugacity capacity will also reach a higher concentration than a phase with low fugacity capacity under the same fugacity ($C=Z\times f$). This equation does not necessarily imply that concentration and fugacity are always linearly related. As a rule of thumb, the linearity assumption may be considered valid for concentrations less than 10% of saturation. Nonlinearity at higher concentrations can be accommodated by allowing Z to vary as a function of concentration and fugacity.

Multimedia environmental models based on the fugacity approach have been developed by Professor Donald Mackay since 1979 at the University of Toronto and Trent University, Canada. In multimedia fate models, the total environment is represented by a set of spatially homogeneous boxes. Fugacity box models typically divide the environmental medium as bulk compartments of air, water, soil and sediment. Chemicals are assumed evenly distributed in each box. More compartments could be added when it is necessary, e.g., vegetation and biota. At equilibrium, fugacities are equal when a system achieves the minimal Gibbs free energy. As a result, two individual compartments (e.g., water, air and soil) will have the same fugacity when reaching equilibrium, though they may have different concentrations.

The complexity of the model depends on the application, geographical size, target chemicals, the number of phases and connectivity, the number of subdivisions included in each phase and spatial resolution. Mackay divided multimedia fate models into four levels based on different complexity (Mackay, 2001) as detailed in Table 1, each with different assumptions of thermodynamic equilibrium, steady/unsteady state and intermedia mass transfer. Mass transfer is modelled by advective transport, such as deposition. These multimedia models could offer insights into the dynamics of environmental transport and transformation of organic substances. Therefore, they are an essential part of the risk assessment of new and existing chemicals. Level I model calculates equilibrium partitioning of a given mass of chemical in a closed system without degradation or advection processes. In a Level II model, the system is open and in thermodynamic equilibrium, considering inflows and outflows of chemicals and processes of advection and degradation. At Level III, the system is open and not in thermodynamic equilibrium, depending on the rate of transport and transformation. Under such conditions, the mode of emission (e.g. to water, air or soil) will have an impact on the predicted results. The model with the highest complexity is a Level IV model, which is an unsteady-state (dynamic)

model, allowing a given mass of a chemical in a compartment to change over time. Therefore, the output is expressed as a function of time.

Table 1. Levels of multimedia fate models with corresponding required information and model outputs (Mackay et al., 1996; van Leeuwen and Vermeire, 2007).

Model level	Conditions	Required inputs	Outputs
Level I	Equilibrium partitioning under steady state	Physiochemical properties; environmental parameters; amount of chemical	Chemical distribution between the compartments
Level II	Level I plus transport and degradation	Level I plus overall emission; advection and transformation rates	Chemical distribution; residence time; dominant loss mechanisms
Level III	Steady-state and nonequilibrium	Level II plus emission to each compartment; intermedia transfer rates	Level II plus dominant transport process
Level IV	Unsteady-state and nonequilibrium	As Level III	Level III plus time-course concentration; time to reach steady-state; recovery time

2.1.2 Steady-state model

Under the condition of steady-state emission and assuming all properties are independent of time, a given mass of a chemical would partition between various phases considered within the model. Its relatively simplified structure and low data requirements, make it easy to apply. However, such models have several limitations. Firstly, they are difficult to validate, since the assumption of steady state is not always true in the real environment. They may introduce errors when complex dynamic processes significantly affect the chemical transport, accumulation and elimination processes. Furthermore, they are not able to provide the required time to achieve steady state, nor do they describe the time course of recovery after emission reduction or cessation (Sweetman et al., 2002). Therefore, steady-state models may not be suitable for compartments that are slow to respond, e.g., concentrations in sediments located in remote environments would be overestimated by steady-state models. **Paper I** presents examples of three Level III multimedia models, using the steady-state assumption.

2.1.3 Dynamic model

The dynamic (unsteady-state model) can be used to predict chemical concentrations changing over time, which is more realistic, compared to steady-state models. However, it requires more

detailed information on parameterisation and input data, leading to relatively longer simulation times than steady-state models. The mass of a chemical released into the environments could be varied with time, so such models are able to predict the past and future trends when the emission inventory is available. In addition, they could evaluate the effectiveness of banning a chemical from use and offer guidance for policy maker on setting controlling strategies. **Paper III** used a dynamic Level IV model (BETR-Global) to predict the chemical fate and identify control sources in China, with PCBs as a case study.

Unsteady-state models would be most useful when the rate of chemical input does not equal the output rate, which can be shown as (Mackay, 2001):

d (chemical mass)/dt = total input rate-total output rate

where the input rate means the chemical entering into the model system and the output rate refers to chemical loss through a range of pathways, e.g., advection, degradation and reaction.

2.2 Food chain bioaccumulation model

2.2.1 Why model bioaccumulation?

After xenobiotics are released into the environment, aquatic and terrestrial organisms can be exposed to these chemicals. Chemicals may accumulate in organisms through multiple mechanisms (e.g., from air, water and soil). Bioaccumulation describes processes by which chemicals are taken up and retained by the organism from their environment and/or diet (Mackay and Fraser, 2000). It causes an increased chemical concentration in an organism compared to that in its ambient environment through all exposure routes. The bioaccumulative potential of a chemical depends on several factors, including physicochemical properties, (e.g., hydrophobicity (Kelly et al., 2008) and volatility (Kömp and McLachlan, 1997)), the tendency of a chemical to become associated with tissue components (Li et al., 2003), and the degradability by various metabolic pathways (Klecka et al., 2000). Most persistent organic pollutants generally pose very high bioaccumulation potential. e.g., PCBs and PBDEs (Kelly et al., 2007).

The bioaccumulative potential of an organic chemical in an organism of interest is normally measured by a range of empirical bioaccumulation matrices. They are mainly expressed by the concentration ratio of a chemical in a target organism relative to the chemical concentration in a given environmental media or foodstuff. Widely used metrics include the bioconcentration factor (BCF: $C_{water}/C_{organisms}$ measured in the laboratory), the bioaccumulation factor (BAF: $C_{water}/C_{organism}$ measured in field including dietary intake), biota/sediment accumulating factor (BASF, $C_{organism}/C_{sediment}$) and biomagnification factor (BMF, $C_{organism}/C_{intake\ food}$). The expression of the test chemical concentration units would greatly affect the way of interpretation relative

bioaccumulation metric. For instance, using wet weight or dry weight would result in difficult bioaccumulative level (Burkhard et al., 2012). These values could be obtained by measuring or modelling. Due to growing public concern over the ethical considerations of animal testing, cost of testing (both financial and time) and legislation requirements, modelling can provide a valuable approach for the prediction of bioaccumulation (Cronin, 2004; Guillen et al., 2012). Bioaccumulation food chain models involve a range of necessary simplifications to understand the complex processes that result in chemical exposure. The key differences of exposure models include how they are parameterized (e.g. human dietary intake rates) and the treatment of food web bioaccumulation. There are two general approaches to quantifying bioaccumulation, which are empirical and mechanistic models both for aquatic and terrestrial food chains. The empirical approach involved the calculation of BCFs or BAFs by deduction from concentration in the organisms of interest (e.g., fish) and concentration in their prey and an environmental compartment (e.g. water and/or sediment). These values are necessarily subject to errors, in the case of field samples and biological variabilities. In order to better characterize underlying processes, mechanistic bioaccumulation models treat chemical distribution as a function of trophic level in the ecosystem, which could help to interpret bioaccumulation related to contaminant dynamics with possible changes in the environment (e.g., temperature, trophic conditions and prey contamination levels). For instance, the sensitivity or uncertainty could be tested on environmental input parameters.

2.2.2 Aquatic food chain model

Due to direct emission and transport processes of a chemical, the aquatic environment is often the final sink of many organic pollutants. Building the relationship between concentrations in the aquatic environment and organisms of interest could help to interpret chemical and biological effects in biota. A number of useful aquatic bioaccumulation models (empirical and mechanistic) have been proposed and we briefly introduced below.

2.2.2.1 Empirical aquatic model

Much effort has been made to predict bioconcentration in aquatic organisms using molecular structure or measured properties since the 1970s. The most commonly used approach is to establish an empirical relationship with K_{OW}. Neely et al. (1974) reported the first linear relationship between K_{OW} and BCFs for fish (Neely et al., 1974). This approach was then extended to more chemicals by Veith. Several non-linear K_{OW}-BCF relationships have also been suggested, e.g., bilinear (Bintein et al., 1993) and polynomial (Connell and Hawker, 1988). These equations should be used with caution when applying to compounds out of the domain of the training dataset. Since bioconcentration reflects the net flux of lipid-water partition and other biological processes, such Kow-based models may not work well for chemicals subject to

specific interaction processes (Hermens et al., 2013). Empirical models are normally preferred for initial screening, since they often only require simple physicochemical properties as inputs.

2.2.2.2 Mechanistic aquatic models

Mechanistic food chain models can treat chemicals with the potential for increasing in concentration along trophic levels. Concentrations in organisms are calculated sequentially up the food web, e.g., those calculated for benthos are used as food for fish. Therefore, they are able to treat a large number of organisms and developed a comprehensive method for assessing contaminant migration into and within a complex ecosystem (Mackay and Fraser, 2000). A number of mass balance mechanistic models have been developed and applied to quantify chemical flux in (by dietary intake and gill uptake) and out (by gill elimination, growth dilution, biotransformation and faecal egestion) of fish as illustrated in Figure 2 (Arnot and Gobas, 2004; Barber et al., 1991; Erickson and Mckim, 1990; Gobas, 1993; Gobas et al., 1988; Kelly et al., 2004; Nichols et al., 1990). It is preferable to simple regression-based bioconcentration or biotransfer parameterization of bioaccumulation, especially for very hydrophobic chemicals (Arnot et al., 2010; Birak et al., 2001). There are one-compartment and multi-compartment fish models. One-compartment models assume a chemical is homogeneous within the whole fish body, while multi-compartment models treat the target organism as a set of connected organs or tissue groups and chemicals are transferred by blood. **Paper II** used a one-compartment fish model and a multi-compartment fish model to explore whether the newly developed poly-parameter relationships (pp-LFERs) for partition coefficients of biological phases could improve predictions of BCFs.

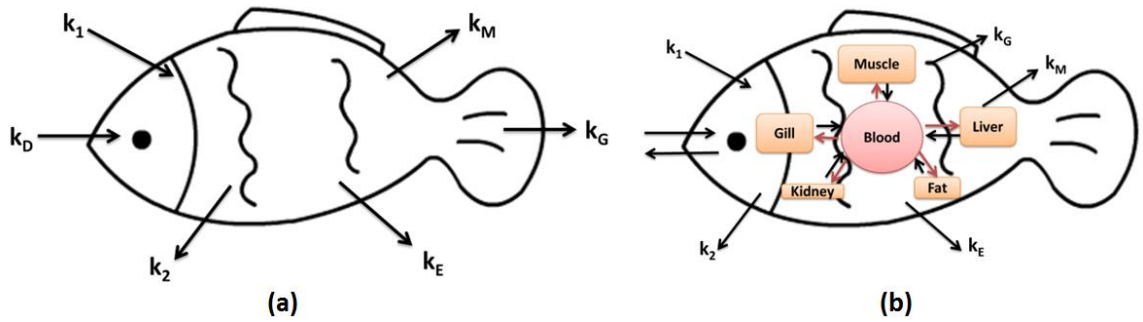

Figure 2. The conceptual diagrams of the one-compartment fish model (adapted from (Arnot and Gobas, 2004)) and multi-compartment PBTK fish model. The arrows represent the major routes of uptake, elimination and transport processes in a fish. k_1 means gill uptake rate constant; k_2 means gill elimination rate constant; k_D means the dietary uptake rate constant; k_M means metabolic transformation rate constant; k_E means the fecal egestion rate constant; k_G means the growth dilution rate constant.

Physiologically-based one-compartment models quantify chemical-specific differences in absorption, biomagnification, biotransformation (metabolism) and elimination processes leading to more refined chemical-specific estimates of exposure and internal concentrations in target receptors (e.g., fish and shrimp) as illustrated in Figure 2-(a). A widely used mechanistic steady-state fish model was developed by Gobas on 1993 (Gobas, 1993) and further improved by Arnot and Gobas on 2004 (Arnot and Gobas, 2004). Using chemical concentrations in water and sediment, the trophic transfer of hydrophobic organic chemicals to organisms (e.g., fish and benthos) was examined. This relatively simple approach has the advantage of enabling feeding interactions to be accounted for in the bioaccumulation process.

When the elimination rates differ in two or more stages or the organ-specific concentration is needed, a one-compartment model is not sufficient to describe the bioaccumulative behaviour. The simplest form of a multi-compartment model is a two-compartment model. Its rationale is that one compartment undergoes fast release of xenobiotics while the second compartment only slowly releases the chemical to the first compartment (van Leeuwen and Vermeire, 2007). A more complicated example of modelling tool is the multi-compartment physiologically based pharmacokinetic (PBPK) models as illustrated in Figure 2- (b), particularly well-suited to calculate tissue doses of chemicals and their metabolites over a wide range of exposure conditions in different species (Leung, 1991; Nichols et al., 1990). It is based on three groups of parameters: physiological information (e.g., blood flow), partition coefficients and metabolism. Each considered compartment corresponds to discrete tissues or organs with appropriate parameterized volume, blood flow rates and pathways of metabolism to the target chemicals. A mass-balance differential equation is used to describe each compartment and equations are solved by numerical integration to predict time-course concentration (Andersen, 2003).

2.2.3 Terrestrial food chain model

The bioaccumulation of chemicals in terrestrial food chains is a process in which pollutants are transferred from contaminated sources (e.g., ambient air and soil to agricultural systems - including crops and dairy products) then to humans as the endpoint. Modelling and simulation techniques for bioaccumulation and biotransformation processes have been developed for both general and specific vegetables with large consumption volumes (e.g., apples, potatoes and lettuce) (Juraske et al., 2011; Trapp, 2007; Trapp, 2015). These submodels have also been incorporated into regulatory exposure assessment tool in Europe and North America, e.g. EUSES (European Commision, 2004) and RAIDAR (Arnot et al., 2006). These two models were used as references for model adaptations to China in **Paper I**.

The terrestrial food web can be divided into agricultural and wildlife food webs. The agricultural food web includes chemical transfer from air and soil to plants, from plants to

herbivores (e.g., cow and livestock), from cow to milk and beef, then taken up by humans (McLachlan, 1996). The wildlife food web examines the chemical bioaccumulation in wildlife species (e.g., deer and shrew) (Armitage and Gobas, 2007), with less relevance to general human exposure. Therefore, only agricultural food webs were further explored in this thesis.

2.2.3.1 Plant model

Fruit and vegetables constitute a considerable fraction of the Chinese diet. Organic chemicals are taken up by plants from both air and soil (Collins et al., 2005). Vegetation is then consumed by herbivores, resulting in the transfer of contaminants along the terrestrial food chain and eventually reaching humans (McLachlan, 1994). Therefore, uptake into edible plants is an important process for assessing the exposure of humans to toxic organic chemicals. This indirect exposure makes vegetation the important source of human exposure to some organic pollutants, such as pesticides (McLachlan, 1996).

During the last few decades, a range of plant uptake models has been constructed and used in a wide range of applications (e.g., chemical safety assessment laid down in Technical Guidance Documents (TGD EU, 2003)). The uptake of organic chemicals by plants occurs via several pathways as illustrated in Figure 3. Organic chemicals can directly become in contact with plant tissues (e.g., leaf) through vapour and particle deposition or via below ground tissues (e.g., roots) uptake (Collins et al., 2011). Most plant models assess uptake from the air (McLachlan, 2010) or soil (Travis and Arms, 1988) while several models have been developed for both pathways (Collins and Finnegan, 2010; Trapp, 2015; Trapp and Legind, 2011). Recently, models were also developed to estimate specifically the foliar uptake and translocation of chemicals intentionally applied to crops (e.g., pesticides and herbicides) (Fantke et al., 2011; Fantke et al., 2012). However, models with specific direct chemical usage patterns are out of the scope of this thesis. Both empirical and mechanistic models have been developed to treat chemical bioaccumulation in plants.

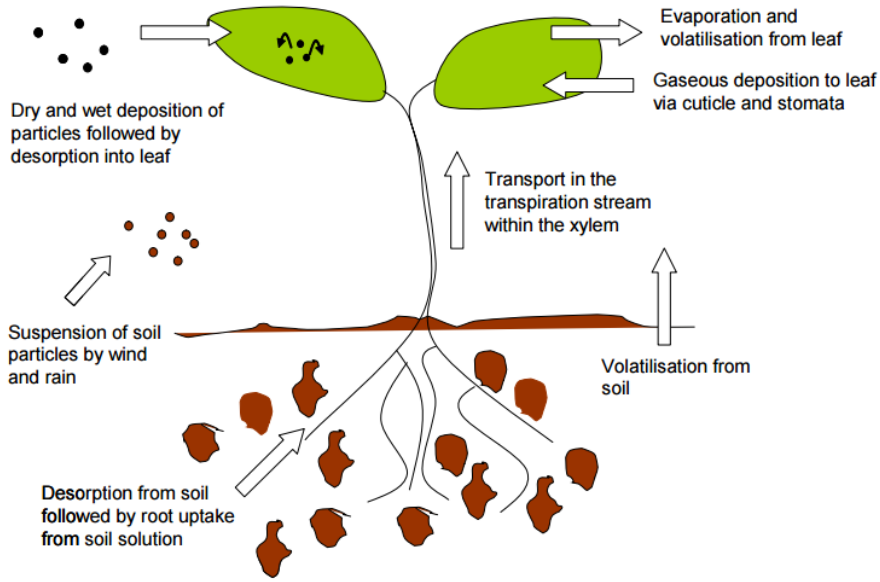

Figure 3. Main pathways for plant uptake of organic chemicals (Collins et al., 2006).

2.2.3.1.1 Empirical plant model

Empirical models describe chemical uptake by plant roots expressed as the ratio of chemical concentration in plant compartments (e.g., leafs and roots) to that in corresponding measured exposure media (e.g., soil and air) when samples are collected (Collins et al., 2011). These ratios are generally referred to as bioconcentration ratios, but they cannot reflect steady-state or equilibrium status. Travis and Arms (1988) developed one of the earliest and most widely used empirical plant models using the relationship between BCF and chemical properties derived as (Travis and Arms, 1988):

$$log\ BCF = 1.588 - 0.578\ log\ K_{OW}$$

where *BCF* is the ratio of chemical concentration in aboveground plant parts (mg kg^{-1} dry plant) to the concentration in the soil (mg kg^{-1} dry soil). This type of plant model is easy to use with very simple inputs needed (only K_{OW} needed in this case). However, empirical relationships strongly depend on a limited number of data points and do not say much about the uptake mechanisms. As a result, special caution should be taken when applying the empirical model to the chemical out of the applicable property domain.

2.2.3.1.2 Mechanistic plant model

Mechanistic mass balance plant models normally include one or more compartments with rates of input, output, and accumulation describing partitioning, degradation, flow or diffusion rates to estimate plant tissue concentrations from chemical exposure (Paterson et al., 1991; Paterson

et al., 1994; Paterson et al., 1990; Rein et al., 2011; Ryan et al., 1988; Topp et al., 1986; Trapp, 2000; Trapp, 2002; Trapp, 2004; Trapp, 2007; Trapp and Matthies, 1995). The main processes involved include: diffusion and bulk flow of chemicals between soil and root; transport within the plant in the phloem; transpiration streams between root, stem and foliage; exchange between air-soil and leaf-air; metabolism and growth. Mechanistic models need more parameters than empirical models, which include the physicochemical properties of a target chemical (e.g. K_{OW}, K_{AW} and K_{OC}), plant properties (e.g., masses and volumes of considered compartments, growth and transpiration rates) and environmental properties (e.g., temperature, organic carbon content and air composition). These three types of inputs contribute variability to plant uptake modelling (Trapp, 2015). However, the model performance was not positively related to the model complexity. The lack of experimental plant uptake data greatly limits model development and evaluation (Mckone and Maddalena, 2007).

2.2.3.2 Mammalian model

Higher trophic organisms such as mammals tend to be subject to adverse effects caused by increasingly accumulated chemical concentrations. Humans are at the top of the food web and can be particularly sensitive to exposure. Animal-origin foodstuffs account for the majority dietary exposure to a wide range of persistent organic chemicals in humans, e.g., PCBs (Wang et al., 2010). Therefore, bioaccumulation in mammalian models is essential to understand the biotransfer of chemicals through food webs to humans, as the endpoint.

2.2.3.2.1 Empirical mammalian model

Several K_{OW}-based empirical relationships have been developed based on empirical data from animal feeding studies (Garten and Trabalka, 1983; Kenaga, 1980; Mclachlan et al., 1990; Stephens et al., 1995; van Asselt et al., 2013). Many factors will influence these relationships, e.g., different biotransformation abilities (Ronis and Walker, 1985; Wallace, 1989). A good example is that Travis and Arms (1988) proposed simple regressions between K_{OW} and biotransfer factor (BTF) for milk and beef from experimental data (Travis and Arms, 1988). This model has been extensively used and has been incorporated by international regulatory authorities into chemical exposure assessment tools to protect human health (Takaki et al., 2015). However, it has been criticized, due to the limited range of investigated chemicals, most of which are persistent within a narrow K_{OW} range ($3<\log K_{OW}<7$). Subsequently, new K_{OW}–based empirical models using more experimental data have been proposed (MacLachlan and Bhula, 2008). However, the metabolism of a chemical was demonstrated to have more significant impact on BTFs than the chemical hydrophobicity (Hendriks et al., 2007). So the K_{OW}-based model may be limited by lacking a solid theoretical basis.

2.2.3.2.2 Mechanistic mammalian model

Mechanistic mammalian models are based on a mass balance of chemicals between inputs (e.g., ingestion and inhalation) and outputs (e.g., excretion with milk, faeces/urine and metabolism), which could provide a quantitative description of the absorption, distribution, metabolism and excretion process of chemicals in biotas. They have been developed for several species, such as cows (Rosenbaum et al., 2009) and humans (Czub and McLachlan, 2004; Mackay and Fraser, 2000; McLachlan, 1996). Much effort has been devoted to the development of physiological parameters (e.g., cardiac output, blood flows, ventilation rates, organ volumes and composition of tissues/organ) (Krishnan and Peyret, 2009). In addition, partitioning coefficients to organs/tissues, absorption rates and biotransformation rates are also required. The model reliability strongly depends on the accuracy of physiological parameters, partitioning coefficients and biotransformation rates. Experimental data and Quantitative structure–activity relationship (QSAR) submodels for estimating the dietary assimilation efficacy in mammals are limited (Gobas et al., 2015). So far, terrestrial bioaccumulation models use relationships with octanol (Kelly et al., 2004) or assume a constant value (e.g., 90%) for bioavailability (Gobas et al., 2003).

The largest uncertainties originate from the biotransformation rates due to extremely limited measurements and estimation approaches, particularly for mammalian species. Due to the data gaps, screening-level bioaccumulation and exposure assessments often assume that biotransformation rate can be neglected as the worst-case assumption. This would result in overestimation of bioaccumulation and exposure for chemicals subject to biotransformation (Arnot et al., 2010). Also, when examining human bioaccumulation and exposure from a multimedia perspective, the biotransformation indicated greater importance than a chemical's partitioning properties (McLachlan et al., 2011). Arnot et al. (2014) developed a screening-level QSAR model to estimate biotransformation half-lives in mammals (Arnot et al., 2014). In addition, in vitro-in vivo extrapolation (IVIVE) methods are used to estimate biotransformation half-lives for high throughput exposure and risk assessment (Nichols et al., 2007; Nichols et al., 2006; Rotroff et al., 2010), which was used in **Paper II**.

3 Used Models

In this thesis, both steady state models and dynamic models were used to achieve different aims in each chapter/paper. Most model approaches were the combination of fate models and bioaccumulation food chain models, except for the BETR-Global model. This model only considers the vegetation and does not cover the bioaccumulation food chain. These models were selected mainly due to their widespread and established use in chemical regulation. EUSES, RAIDAR and ACC-HUMANsteady models are widely used in Europe and North America and thus they were chosen in **Paper I** to study the impact of different dietary pathways on chemical exposure. The fish submodel extracted from RAIDAR was used as a reference for a one-compartment fish model in **Paper II**, since it is one of the most widely used fish models in risk assessment. BETR-Global model was selected for use in **Paper III** and **IV**, since it can provide a long-term time-course prediction of concentrations in environmental compartments under dynamic (Level IV) calculations. All models used are introduced below.

3.1 EUSES

Since the early 1980s, the EU initiated projects to develop a systematic approach towards the hazard and risk assessment of substances, along with the enforcement of European legislation for new chemicals. Therefore, USES 1.0, an integrated risk assessment tools for new and existing substances was developed (Jager, 1995; Jager et al., 1994a; Jager et al., 1994b; Linders and Luttik, 1995; Van der Poel, 1994; Vermeire et al., 1997; Vermeire et al., 2005; Vermeire et al., 1994). Subsequently, it was updated to evolve into the European Union System for the Evaluation of Substance (EUSES), which implements the methods described in the Technical Guidance Document (TGD) (TGD EU, 2003). Therefore, EUSES is selected as a typical regulatory-based risk assessment tool developed by Europe in **Paper I**.

EUSES offers three model spatial scales, which are local, regional and global. Its structure and main considered processes of chemical distribution and transport are presented in Figure 4. It consists of several models with a great number of elements, including SimpleBox and SimpleTreat. SimpleBox is a core part of the model, which predicts chemical fate in compartmental environments (Brandes et al., 1996; Van de Meent, 1993). SimpleTreat is a sub-model used to predict the distribution and elimination of chemicals through sewage treatment plants (Franco et al., 2013; Struijs, 1996). The EUSES model divides the environment into air, soil (natural/agricultural/industrial soil), water (freshwater and seawater and sediment (freshwater/seawater sediment). It uses empirical equations to simply predict chemical concentrations in biota relevant to human diet (e.g., meat, fish and vegetables). The main outputs of EUSES are local and regional risk characterisation ratios (RCR) in considered environmental compartments. The required inputs mainly include physicochemical properties,

emission rate and use pattern. The RCR is the ratio of the predicted environmental concentration (PEC) and the predicted no-effect concentration (PNEC, defined as the environmental concentration of a chemical below which there is no predicted effect). A chemical would be flagged as a concern if its RCR calculated greater than 1.

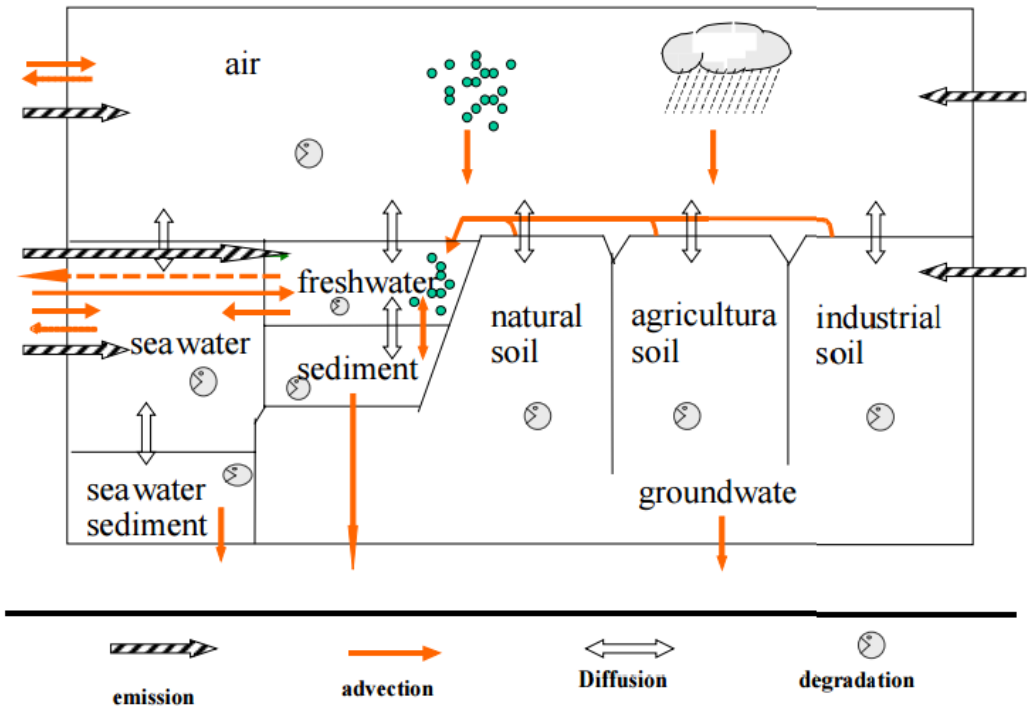

Figure 4. The principal processes of chemical distribution, transportation and degradation in the EUSES model (European Commision, 2004).

3.2 RAIDAR

Paper I selected another established screening level multimedia model, the Risk Assessment, IDentification, And Ranking (RAIDAR) model (Arnot et al., 2006). This model is designed to assess and prioritize chemicals by estimating environmental fate, transport, bioaccumulation and exposure to humans and wildlife for a unit emission rate. The RAIDAR model uses a 'back-tracking' or reverses modelling approach to avoid highly uncertain emission rate data as model input, in contrast to traditional risk assessment models like EUSES which use the risk quotient (RQ, ratio of estimated and measured concentration) as an endpoint. The model can be especially useful when actual emission rates are difficult to obtain for a particular region. It provides fate calculations of simple Level II and more complex Level III. It also defines an

evaluative region in which all chemicals can be assessed without the use of real regional descriptions.

In order to quantitatively evaluate human exposure to chemical substances through multimedia exposure pathways, the RAIDAR model also incorporates a bioaccumulation food chain model linked to the fate model (Arnot et al., 2006). Its treatment of key processes in bioaccumulation is different from the EUSES model (Arnot et al., 2010). EUSES uses empirical equations to identify bioaccumulation in food chains while RAIDAR includes mechanistic mass balance models to address the organism bioaccumulation process. For instance, the BCF in EUSES is derived from regressions with K_{OW} whilst the one-compartment fish in RAIDAR provides insights into the multiple exposure pathways of chemical uptake and elimination in an aquatic organism (Arnot and Gobas, 2004).

3.3 ACC-HUMAN & ACC-HUMANsteady

ACC-HUMAN is a fugacity-based, non-steady state mechanistic model. It is designed to describe the bioaccumulation of lipophilic organic pollutants from air, water, soil to humans (Czub and McLachlan, 2004). The physical environment is linked through a marine and agricultural bioaccumulation food chain to humans as the end receptor. The default model is parametrized for southern Sweden. The uptake pathways of contaminants considered were mainly from the dietary intake of animal-origin food, namely fish and dairy products. Also, uptake by inhalation and water consumption were also considered to include partitioning for less hydrophobic chemical substances. More recently, an unsteady-state model of bioaccumulation in plants was incorporated including uptake and elimination processes and time to reach steady-state (Undeman et al., 2009). ACC-HUMAN was used in **Paper IV** to predict the long-term time trends for contaminant bioaccumulation in human body burdens for the Chinese population.

ACC-HUMANsteady is a steady-state version of ACC-HUMAN. It is a nested Level I fate model (steady-state, equilibrium, no in- or out-flows or degradation reactions) linked to a steady-state bioaccumulation model, which calculates equilibrium concentrations. This model was selected in **Paper I** as a standard model used in European-based exposure models.

3.4 BETR-Global

The BETR-Global multimedia contaminant fate model was introduced in 2005, as a global-scale mass-balance model (Macleod et al., 2005). This model was used to predict the fate and exposure of PCBs in **Paper III** and **IV** under dynamic Level IV conditions. The BETR-Global model describes the global environment with a spatial resolution of 15 °latitude ×15 °longitude and 288 multimedia regions linked by flows of air and water illustrated in Figure 5 (Macleod et al., 2005; MacLeod et al., 2001). It has been evaluated and applied successfully for a range of

organic contaminants and can provide fate simulations both for Level III and Level IV (Armitage et al., 2009; Macleod et al., 2005; MacLeod et al., 2011). Within each multimedia region, the model calculates the distribution of chemicals, the exchange between seven bulk environmental compartments, which include sea water, fresh water, planetary boundary layer (PBL), free atmosphere, soil, freshwater sediments and vegetation (MacLeod et al., 2001). The model accounts for advective transport between regions by air/water and inter-compartmental transport processes, such as dry and wet deposition and reversible partitioning.

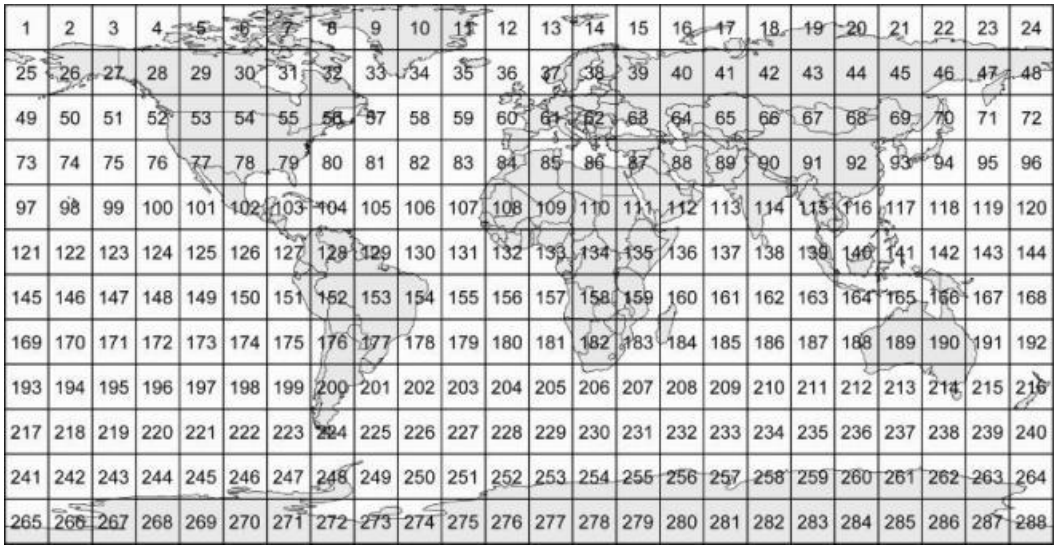

Figure 5. The regional segmentation of the BETR-Global model showing numbers used to identify different regions/cells (Macleod et al., 2005).

4 Studied Chemicals

A wide range of chemical substances was selected to test the model approaches or used as a case study in this thesis, including real chemicals and hypothetical chemicals. These chemicals were selected due to their potential exposure hazard for humans, their potential ability to reach in remote regions (e.g., Arctic), wide usage/large production volumes, well-documented emission estimations and extensive data sets for model evaluation. Meanwhile, the hypothetical chemicals were defined to thoroughly understand the behaviours of a whole range of environment-related chemicals with possible combination of properties.

4.1 Hypothetical chemicals

In order to comprehensively investigate the sensitivity and uncertainty of model outputs, hypothetical chemicals were defined with a wide range of combined partitioning properties (K_{OA}, K_{AW} and K_{OW}) covering those of environmentally relevant chemicals. All the hypothetical chemicals are presented in a partitioning map (Meyer et al., 2005). Its advantage is allowing comprehensive investigation of model sensitivity and uncertainty for all defined hypothetical chemicals at the same time. This approach has been demonstrated to be useful when a large set of diverse chemicals are modelled with a fixed environmental scenario offering insights for real chemicals with unknown properties (Undeman and McLachlan, 2011). In addition, it could help to mechanistically understand a model's behaviour, with regard to how model outputs change with different partitioning properties. This approach was employed in **Paper I** to visualize the uncertainty and sensitivity of dietary pattern on the different dominant exposure pathways for three selected multimedia models.

4.2 Emerging contaminants

Recently, pharmaceuticals and personal care product ingredients (PPCPs) have received increasing attention from the scientific, regulatory and business communities, as emerging contaminants with possible threats to the aquatic environment and human health (Boxall et al., 2012; Daughton and Ternes, 1999; Liu and Wong, 2013). They are widely used in high quantities throughout the world and have been frequently detected in range different environments (Carballa et al., 2004; Kasprzyk-Hordern et al., 2009; Lishman et al., 2006).

In **Paper I**, several typical PPCPs were selected to study their dietary exposure to the Chinese population. One important category is the cyclic volatile methyl siloxanes (cVMS), such as octamethylcyclotetrasiloxane (D4), decamethylcyclopentasiloxane (D5), and dodecamethylcyclohexasiloxane (D6), which are hydrophobic silicone fluids. They are used either as precursors in the synthesis of high-molecular-weight silicone polymers, or as ingredients in the formulation of personal care products (Alleni et al., 1997). They have unique

partitioning properties with high K_{AW} and low K_{OA} Consequently, much concern has been raised about their potential for environmental persistence and bioaccumulation (Whelan and Breivik, 2013).

Parabens are a class of preservatives widely used in cosmetics and food products and selected in **Paper I** for evaluation (Rastogi et al., 1995; Zhang et al., 2005). Another selected chemical is triclosan, which is an antimicrobial compound widely used in household and personal health care products (Rodricks et al., 2010). They enter the natural environment through effluent discharges and bio-solids produced by municipal and industrial wastewater treatment plants. Although a high proportion of these chemicals are biodegraded during wastewater treatment, the remainder can be adsorbed to sludge, which may ultimately be applied to land as biosolids and cause adverse effects on ecological receptors (Fuchsman et al., 2010).

The perfluoroalkyl acids (PFAA) and their salts are chemicals with extensive consumer and industrial applications, including protective coatings for fabrics and carpets, paper coatings, insecticides, paints, cosmetics, and fire-fighting foams. In recent years, a number of studies have reported the ubiquitous distribution of perfluorinated compounds (PFCs) in humans and wildlife (Calafat et al., 2006; Wang et al., 2013; Wu et al., 2012b). In addition, they are extremely persistent, bioaccumulative and of toxicological concern (Fuentes et al., 2007; Shin et al., 2014). Perfluorooctanoate (PFOA) was selected as one of the most extensively studied chemicals in **Paper I**.

4.3 PCBs

Polychlorinated biphenyls (PCBs) are a class of chemicals consisting of 209 congeners containing a varying number of chlorine atoms substituted onto a biphenyl molecule (see Figure 6). About 130 PCB congeners have been observed in commercial mixtures and released into the environment. They were produced commercially in 1929 for the first time and identified as one of twelve original persistent organic pollutants (POPs) under Stockholm Convention (UNEP, 2001). Although their production ceased in the 1970s globally, they are still widely being detected in the environment and biota (Bjerregaard et al., 2013; Diefenbacher et al., 2015; Jaward et al., 2005; Schuster et al., 2010; Tato et al., 2011). The manufacturing history of PCBs is relatively short in China (1965-1974), compared to other developed countries. During this period, approximately 10,000 tonnes of PCBs were produced, including 9000 tonnes of tri-CBs and 1000 tonnes of penta-CBs, accounting for less than 1% among the global production. Nevertheless, PCBs are also frequently detected in the environment and organisms in China (Wang et al., 2010; Wu et al., 2012a; Zhang et al., 2013a; Zhang et al., 2013b; Zheng et al., 2014). Once they are released into the environment, they are very slow to degrade and can undergo long-range transport among various environmental compartments. Due to their high

lipid solubility, PCBs readily bind to the lipid in fat tissue and accumulate in biota along food chains. Consequently, the ingestion of contaminated foods represents the most important exposure pathway for most POPs including PCBs.

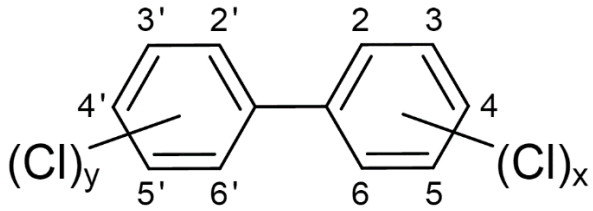

Figure 6. The general structure of PCBs.

In China, two kinds of commercial PCBs (#1 PCB and #2 PCB) were produced and which were mainly used in transformers and other electrical products. #1 PCB contained 42% chlorine, which was similar to Aroclor 1242, and #2 PCB contained 53% chlorine, similar to Aroclor 1254 (Jiang et al., 1997). Around 90% of accumulative tonnage was utilized in the electrical supply and distribution industry (e.g. as dielectric fluid in capacitors and transformers) and mostly made up of tri-PCBs. The remainder was used as additives for paint with penta-CBs being the dominant homologue. Assuming that these two technical mixtures (#1 PCB and #2 PCB) were produced in the ratio of 9:1, congener production in China was estimated using congeners composition of Aroclor 1242 for #1 PCB and Aroclor 1254 for #2 PCB (Ren et al., 2007). As a result, the major congeners produced and used in China were tri-CBs, followed by tetra-PCBs. Although the major congener profile for global PCBs production was also tri-CBs followed by tetra-CBs (Breivik et al., 2002), the compositions of these two congeners are higher in Chinese products than in global products (40.4–25.2% for tri-PCB, and 31.1–24.7% for tetra-PCB) (Ren et al., 2007).

PCBs were used in **Paper III** and **Paper IV** as substances for a case study. Since they are classical legacy POPs with very well-studied emission profiles and rich data availability, they could facilitate model evaluation and aid in one identification of potential model improvements. In addition, they could offer a good reference for other similar types of chemicals for the identification of effective regulatory control measures. As a result, these two studies modelled the temporal trends of PCB concentrations in the physical environment (**Paper III**) and the human body (**Paper IV**). Seven indicator PCB congeners spanning a wide range of physical-chemical properties were used. This study successfully demonstrated that a dynamic fate model

coupled with a bioaccumulation food chain model could help to reconstruct the chemical historical profile of emission and compartment trends along with human exposure.

5 General Discussion

5.1 Impact of diet pattern on human exposure

The typical dietary pattern of the Chinese population is significantly different to that for most Western populations, with a much higher consumption rate of vegetables and cereals and much less animal-origin food products. Consequently, **Paper I** examined the impact of dietary pattern on determining the predominant dietary exposure pathways using three established multimedia fate and bioaccumulation models for the Chinese population, which are EUSES, RAIDAR and ACC-HUMANsteady. The predicted dietary exposure pathways were compared using scenarios with a range of hypothetical and current emerging contaminants. Model predictions indicated that dietary preference could have a significant impact on human exposure, with the relatively high consumption of vegetables and cereals, resulting in higher exposure via plants-based foodstuffs under Chinese consumption patterns compared to Western diets, although the differences across inherent model structures were greater than those between dietary scenarios.

Paper IV also investigated regional dietary exposure using a reference year 2002, which assumed that people only eat locally produced food in defined regions. However, the difference was relatively small among different regions in China, with a factor of three between the highest and lowest values of human body burden. The highest body burden was observed for populations living in a contaminated region, which had a high preference for consumption of animal-origin food, especially fish. In reality, there is a high uncertainty in quantifying the dietary pattern for a population of interest, particularly for China having such a large population with varying dietary habits. Although the Total Diet Study offered a good database to support the examination of biomonitoring studies, participants may tend to underreport their dietary intake (Livingstone et al., 1990), which could potentially cause the underestimation of human dietary exposure.

5.2 Applicability of Western exposure models to the Chinese population

Paper I systematically demonstrated that the selected models had a good ability to identify key dietary exposure pathways, which can be used for screening purposes and evaluative risk assessment. However, more assessment of the performance of exposure models with several potential adaptations is required before they can be applied to China with confidence. Since China has a very large population with varying regional dietary habits, the comprehensive evaluation of sensitivity and uncertainty of dietary preference is required for the future study. The fish model, which has been developed so far based on wild seafood products, needs to be expanded to consider different bioaccumulation models for the freshwater food chain covering farmed fish, which could be significantly more contaminated by some chemicals such as PCBs

(Carlson and Hites, 2005; Hites et al., 2004). Furthermore, despite the importance of consumption of vegetables, especially cereals in China, there is currently no specific model for organic chemical uptake into cereals that we are aware of (Legind and Trapp, 2009). Therefore, the development of a more specialized crop model (like wheat and grains) should be explored. In summary, some model adaptations will be required to cover a number of important Chinese exposure pathways, e.g., freshwater farmed fish, grains and pork.

5.3 pp-LFERs vs. pp-LFERs

In an attempt to examine the possibility of the extended application of bioaccumulation models, **Paper II** evaluated the influence of implementing newly developed pp-LFERs approaches into a one-compartment fish model and a multi-compartment physiologically-based toxicokinetic (PBTK) model. The BCFs of fish were used as the evaluation metric to compare the predictions with compiled measurements. Overall, preliminary results indicated that pp-LFERs incorporated models (R^2=0.75) slightly outperformed those using the sp-LFERs in a one-compartmental fish model (R^2=0.72). In addition, pronounced enhancement was achieved for compounds with log K_{OW} between 4 and 5 with R^2 increasing from 0.52 to 0.71. Furthermore, the greatest improvement was observed using a multi-compartment PBTK models with consideration of metabolism. Using the pp-LFERs, all predictions fell within a factor of 10 of the measured BCFs.

In theory, the pp-LFERs should have a better ability to predict bioconcentration with less deviation from the measurements, since they describe the partitioning behaviour according to the individual sorptive capacity of each involved biological phase (e.g., neutral lipid, phospholipid, protein and water). The traditional K_{OW}-driven bioaccumulation model using sp-LFERs approach simplifies the sorptive phases (e.g. lipid and non-lipid organic matter) using empirical equations with log K_{OW}. The underlying explanation for the limited improvement of the one-compartment model could be that the sp-LFERs tend to underestimate partitioning to protein and overestimate that to lipid. As a result, the underestimation and overestimation could cancel out resulting in no pronounced improvement in terms of the predicted BCFs values. For screening purposes, the K_{OW}-based (sp-LFERs) approach should be sufficient to quantify the main partitioning characteristics. On the other hand, the case for using pp-LFERs is more positive for multi-compartment PBTK models, with obvious improvement across the whole set of evaluated chemicals. This could be attributed to the fact that more pp-LFERs for different biological phases were incorporated in the multi-compartment PBTK models than in the one-compartment models. Improved quantification of each considered tissues/organ would cumulatively result in better prediction of the total body concentration of fish.

However, though the limited improvement was identified for this replacement, it still could provide new perspectives on understanding and interpretation of biomonitoring studies. The PBTK model is designed to predict the site-specific burden in fish or other target organisms. Better prediction of contaminant concentrations in specific organs could facilitate a more detailed toxicity assessment. For example, the concentration specifically in the phospholipid (main composition for membrane) would help to understand membrane toxicity (Endo et al., 2013). In addition, for some chemicals such as bisphenol A, which are prone to binding with phospholipid instead of neutral lipid (fat lipid), which would result in large discrepancies.

The quantification of biotransformation rates in biota is the most difficult aspect of predicting the bioaccumulation of chemicals susceptible to degradation. The extrapolation of biotransformation rates from the total degradation rates could potentially result in large errors. In vitro-in vivo extrapolation is a common way of using the hepatic metabolism to calculate the whole body biotransformation rate. Since directly measured metabolism rates are too limited to conduct the systematic evaluation, **Paper II** used measured/predicted biotransformation rates of the whole fish body to back-calculate hepatic metabolism rates. This is just a first approximation to consistently compare the influence of biotransformation on BCFs and large errors could potentially be incurred. In addition, it is important that ionization of chemicals should be included, since the partitioning properties of ionic species would be considerably different from neutral species. Further developments are required for the consideration of ionization and more accurate quantification of biotransformation in biota.

5.4 PCB case study in China

Paper III and **Paper IV** investigated and demonstrated the benefits gained from combined use of multimedia fate and bioaccumulation models to understanding source-receptor relationships. PCBs were used to conduct this case study, due to their well-studied profile. Similar studies could be transferred to other chemicals when necessary data become available.

5.4.1 Primary emission vs. secondary emission

PCBs can be emitted from both primary and secondary sources. Primary sources are predicted to account for the main direct release of PCBs to the environment from their major use categories, while secondary sources represent re-emission from environmental reservoirs (e.g., soils and vegetation). Several studies suggest that the main contribution to PCB emission will move from primary to secondary sources as production and use of PCBs declines (Cousins et al., 1999; Harner et al., 1995). In order to study the current role of primary and secondary emission in China, **Paper III** studied the contribution of these sources by applying multiple emission scenarios. When China started to produce PCBs in 1964, primary sources became increasingly important and provided a constant contribution of approximately 70% until 2030. After 2030,

PCB-28 and PCB-153 were predicted to have different behaviours with PCB-28 being mainly dominated by regional primary emission and PCB-153 being mostly controlled by secondary sources. This could be because PCB-28 was mainly supplied by ongoing and increasingly important unintentionally produced sources. Whilst the primary sources for PCB-153 will gradually cease within China, it is likely that secondary emission will gradually replace the role of primary emission. This type of result is difficult to confirm with observations. However, several pilot studies could indirectly support this. For instance, Li et al. (2010) investigated the soil-air equilibrium status using fugacity ratios and suggested that the soils may be secondary sources to the very volatile PCBs and likely continue to be sinks for heavier PCBs.

Understanding the existing role and future trend of primary and secondary emissions of PCBs, would provide insights for policy makers on making effective controlling measures. An overestimate of the relative importance of primary emission could lead to costly and unnecessary measures to reduce future environmental exposure, whereas an underestimation of the importance of secondary emissions could lead to an over-optimistic assessment of reducing environmental and human exposure to PCBs (Breivik et al., 2004). For instance, **Paper III** observed PCB-28 and PCB-153 would have congener-specific rates for transfer from controlling by primary emission to secondary emission. As a result, the corresponding regulatory measures should also be substance-specific.

5.4.2 Role of UP-PCBs

There are two types of primary PCB emissions into the atmosphere, intentionally produced (IP-PCB) and unintentionally produced PCBs (UP-PCBs) (Cui et al., 2015; Cui et al., 2013). The relative importance of these two types of emissions on a chemical's fate in the environment and its bioaccumulative potential in the human body for the Chinese population was investigated in **Paper III** and **IV**. **Paper III** focuses on the reconstruction and prediction of the long-term emission trend of intentionally produced seven indicator PCBs with additional consideration of the unintentional emissions (from the manufacture of steel, cement and sinter iron) during 1930-2100. In general, the total concentration of seven indicator PCBs was mainly controlled by intentionally produced PCBs during 1930-2040. After 2040, UP-PCBs were predicted to be the dominant contributor to the total concentration of seven indicator PCBs. Due to the different congener profiles in UP-PCBs, the unintentional emission has a congener-specific impact on its environmental fate. PCB-28 is the predominant congener in the unintentional sources and thus a good indicator to stand for the environmental behaviour of seven indicator PCBs from UP sources.

Paper IV also examined the contribution of UP-PCBs on the human body burden of PCBs for the Chinese population. The results suggested that the UP-PCBs did not dominate (<5%) the total human body burden for seven indicator congeners. The underlying explanation could be

that the dominant congener PCB-28 in UP-PCBs has a relative low bioaccumulation potential compared to other heavier PCBs (e.g., PCB138/153). However, the calculation of the future significance of the sources of UP-PCBs involves large uncertainties, and could be improved significantly with further domestic measurements of emission factors for a wider range of emission sources, which would enable better determination of emission trends.

In addition, **Paper III** also pointed out the difficulty in making a clear distinction between UP-PCBs and IP-PCBs in reality. During these considered thermal processes, particularly for the cement manufacturer, which is often utilized to deal with hazardous waste, PCBs could also be present in the raw material. If this applies, the measured so-called UP-PCBs from the waste stream could also contain the IP-PCBs. Although several preliminary calculations of the mass balance indicated that the PCBs in the waste stream should be mainly formed during the incineration process (Liu et al., 2015a), the precise quantification is very challenging.

5.4.3 Role of imported e-waste

The transport of e-waste from developed countries to developing regions and the primitive recycling or disposal of e-waste in these regions have received increased attention (Breivik et al., 2014). As one of the world's largest importers of e-waste and manufacturer of electrical and electronic equipment, China plays a key role in the production and recycling of e-waste worldwide. **Paper III** used an emission inventory to consider the worldwide transport of e-waste transport (Breivik et al., 2015), to quantify the contribution of imported e-waste on chemical concentrations in China. Subsequently, **Paper IV** further examined its impact on human body burden for humans living in regions near e-waste cycling sites (polluted regions) and far away from that (background regions).

The accumulative emissions from imported e-waste contributed 30% to the total emissions for seven indicator congeners during 1930-2100 while PCB-180 received the highest percentage (45%) from imported e-waste. The influence of e-waste on air concentrations could be potentially be shifted from a regional scale to a national level in the future. In terms of the cumulative atmospheric concentrations in different study regions, the contribution from imported e-waste was largest for the heavily polluted e-waste regions, accounting for more than 30% of all congeners. During 1930-1990, the contribution from imported-e-waste on human body burdens was negligible. This was because China did not start to import e-waste until 1980. Since 2000, imported e-waste started to increase its contribution (46%) to the total human body burden (ng g^{-1} lipid) in e-waste heavily polluted region, and was predicted to peak at 2040, responsible for more than 90% of seven indicator PCBs. On the contrary, remote regions far away from recycling sites of e-waste received a negligible contribution to environmental concentration and human body burden from imported e-waste.

If the exposure from imported e-waste was excluded, the peak of human body burden in the polluted region would occur in the year 2000, but it was predicted to occur in 2020 with inclusion of imported e-waste. Consequently, the on-going import of e-waste may also cause the time lag of peak burden occurred in human body up to 20 years.

5.4.4 Is China a sink or source?

In order to understand the role that China plays in terms of sink or source, **Paper III** divided the emission sources from the domestic region (China) or the extra-region (rest of the world excluding China) for two reference years (1980 and 2050). It appears that China could possibly move from a net sink with a net input of 800 kg $year^{-1}$ during 1980 to a potential source to neighbouring regions with a net output of 444 kg $year^{-1}$ by 2050. This result is particularly challenging to confirm with observations.

5.4.5 Impact of diet transition on human body burden

The Chinese population has been through rapid dietary transitions with increased daily consumption of animal-origin food products during the last decades, e.g., dairy product, meat and fish. **Paper IV** investigated the impact of this dietary transition combined changing emission trends on human body burdens in China. Under the combined effect of changing emission and cohort dietary transition, the body burden of a 30-year-old female cohort increased 75 times over the last 70 years (1940-2010), despite a 4-fold reduction in Chinese environmental concentration driven by declining emission. As a result, the dietary transition could possibly result in an additional increase in human body burdens of over two orders of magnitude. Also, the peak time of human body burden occurred in 2010 for a 30-year-old female cohort of Chinese population while this occurred in 1980 for Western females. The combined effect of emission trends and dietary transition resulted in an approximate 30 years' delay of peak human body burden between the Chinese and Europeans.

This time lag could be attributed to two main reasons. One is the relatively fast diet transition from 1959-2100 with rapidly increased consumption of animal-origin food (milk, meat and fish) in China. For example, the contrast trend was observed for Arctic population by replacing locally traditional food (with high accumulative concentration of PCBs) with imported food, where Quinn et al. (2012) reported that the rapid diet transition could cause up to a 50-fold reduction over a 40 year period (Quinn et al., 2012). Another reason could be more intensive on-going emission sources compared to Western countries, though the manufacture of PCBs has been ceased around the world. For instance, China received more than 70% of the e-waste waste stream from the rest of the world. In addition, China is the largest industrial country in the world, with unintentionally emitted PCBs from various industrial thermal processes (e.g., production of

steel and cement) which may also provide an on-going contribution to human body burdens (Liu et al., 2015b).

5.4.6 Comparison with measurements

Comparing model predictions and experimental measurements is a direct way to understand the ability of modelling tools to predict a chemical's fate behaviour and bioaccumulation potential applied to real scenarios. In addition, such comparison could help build confidence on model performance and identify further improvements. Therefore, **Paper III** and **Paper IV** provided a preliminary comparison of the modelled environmental concentrations and human body burdens with measured values in the literature. As the combination of BETR-Global model and ACC-HUMAN model could not provide information on urban-rural gradients, model predictions were compared against observed general background concentrations in **Paper III** and **Paper IV**. The peak concentration is difficult to confirm with measurements, which happened around 1970 as predicted by modelling. However, several preliminary findings from dated sediment cores could potentially support the model estimation. The historical trend was shown to increase until the mid-1970s in a dated sediment core from Yangtze River Estuary adjacent to the East Sea region and Pearl River Delta (Mai et al., 2005; Yang et al., 2012).

Atmospheric PCBs concentrations have been measured in China by several researchers over the last decade (Jaward et al., 2005; Xing et al., 2005). According to the comparison with observations over the period 2001 to 2008, the model generally captures the main trends during this period in the atmosphere. Most modelled concentrations are within a factor of three, compared to the limited observations in background air. Surveys providing PCB concentration data for background soils have been conducted in 2005 and 2013 (Ren et al., 2007; Zheng et al., 2014). Measured surface soil concentrations from 2005 (Ren et al., 2007) and 2013 for forest soil (Zheng et al., 2014) were compared with model predictions and agreed well, within a factor of four except for tri-PCB, although the measured concentrations varied over a wide range.

The task to evaluate the predictions on human body burden with biomonitoring studies is more challenging. Since most studies aimed at populations living in or near the heavily polluted regions, e.g., e-waste recycling sites (Song and Li, 2014; Wu et al., 2008; Zhao et al., 2009), which are unlikely to represent human body burdens of the general population. In addition, national biomonitoring studies were not initiated until the late 1980s, so the temporal trend before cessation cannot be confirmed by observations. Although there are many assumptions and uncertainties (e.g. the dietary consumption pattern, food origins, lipid content in food) in this modelling exercise, the modelled human body burden broadly corresponds to the varied biomonitoring data within a factor of two.

Developed countries, like Norway, observed substantially decreasing trends of POP serum concentrations in humans sampled between 1979 and 2007 (Nost et al., 2013). Relevant longitudinal biomonitoring studies on a single population are very limited in China. Sun et al. (2011) reported that the dioxin like-PCB concentrations increased from 2002 to 2007 in human milk in northern China with a positive correlation with age (Sun et al., 2011), which is consistent with the trend of human body burden predicted in this study.

6 Conclusions

The papers presented in this thesis and the research undertaken have demonstrated the useful application of a series of modelling tools to assist in the understanding and evaluation of a chemical's fate in the physical environment and bioaccumulative behaviours along food chains. In a broader context, this thesis has provided insights into how to appropriately apply models and how to handle model complexity in exposure assessment. Selection of system parameters (e.g. environmental and diet characteristics), emission estimation (e.g., UP-PCBs vs. IP-PCBs), approaches to predicting physical-chemical properties (e.g., partition coefficients), may be guided by the methodologies evaluated in **Papers I-IV**. The main conclusions drawn are highlighted as below:

1) Dietary patterns greatly affect the human exposure, although the significance is less than uncertainties in model inherent structure and inputs.

2) The established human dietary exposure models developed by Western countries are promising to adapt for the Chinese population. The main identified improvements include the further specialization of crop models and a farmed-fish model.

3) The traditional K_{OW}-driven one-compartmental bioaccumulation model is sufficient to be used for screening purposes and first-tier chemical risk assessment. Multi-compartmental PBTK fish model can benefit from the incorporation of pp-LFERs due to a better quantification of the site-specific toxicity.

4) The case study of PCBs successfully demonstrated the combined application of multimedia fate and bioaccumulation models for the reconstruction and prediction of a chemical's fate in the physical environment and its bioaccumulative potential along food chains. This exercise also further demonstrated that Western-based bioaccumulation models could be adapted for Chinese populations and could be a valuable starting point for further model development in China.

5) Various influential factors for predicting environmental concentration and human body burden were examined to thoroughly understand the source-receptor relationship for PCBs in China, including dietary transition and multiple emission sources. The rapid change in dietary patterns and imported e-waste were the main drivers for the delayed peak time of human body burdens for the Chinese population.

6) Preliminary suggestions for the policy makers could include: developing substance-specific (lighter PCBs vs heavier PCBs) and site-specific (e.g., background site vs e-waste heavily polluted site) control measures instead of imposing a single solution;

building a biobank to facilitate human biomonitoring and constructing a comprehensive tracking system to record geographical information of food origins.

7 Recommendations and Future Work

Currently, there are several bottlenecks in chemical exposure assessment in China, including difficulty with food categorisation, access to food origin information, and limited data on chemical concentrations in the environment and biota. Although a significant number of studies have been conducted in China, substantial data gaps still exist. Long-term monitoring studies are urgently needed to comprehensively confirm the output of this thesis and to assess the effectiveness of international programmes on cessation of POPs production (e.g., PCBs), such as the Stockholm Convention. National-scale monitoring campaigns should be initiated with a greater focus on background sites, where most people live instead of the heavily polluted sites, which are more relevant to the general chemical exposure in humans. In addition, developing the design of biomonitoring campaigns, particularly the study of a single population, instead of randomly selecting target populations over different time points, would be helpful. A biobank network would greatly facilitate data collection by storing the frozen biosamples of target populations. This is would be particularly useful to track back historical exposure and understand exposure mechanisms, if new pollutants were discovered in future.

In addition, fate models with spatial resolution (such as BETR-Global) and nonspatial models (like RAIDAR) were used for multiple purposes in this thesis. A generic non-spatial fate model is essential for screening chemicals with simple input requirements. However, such models do not provide insights into the likely variations. Since human intake is closely associated with emission locations, particularly for chemicals that are not subject to significant dispersive transport at a regional scale, spatial models could provide more detailed information on human exposure with specific regional emission information. However, existing models are not good at capturing gradients between urban and rural areas and recognizing potential ‘hot spots’. Therefore, models are also needed to estimate the intake at a population level for emissions at specific locations, e.g., the residents living near an e-waste recycling sites.

Furthermore, different exposure scenarios covering the wide variability found in China need to be developed and incorporated into current exposure models, with additional consideration of the variation in the Chinese diet. e.g., more specialized crop models and farmed-fish models due to their significance in the daily food consumption patterns for the Chinese population. Further assessment of the performance of exposure models with several potential adaptations is required before they can be applied to China with confidence. Since China has a very large population with varying regional dietary habits, the comprehensive evaluation of sensitivity and uncertainty of dietary preference is required for future studies. To expand the current work to other chemicals, high-quality emission profiles are required as the starting point of a systematic life

cycle analysis of a chemical. Large uncertainties exist in the current emission inventories, for example, the illicit trade of e-waste is difficult to track in the case of PCBs.

In a broader context, not only for the Chinese population, some suggestions were made for the potential development of bioaccumulation food chain models. Firstly, more and more chemical used in industry and commerce are ionic in nature, but their environmental partitioning behaviour is still unclear. Most available models for risk assessment do not consider ionic chemicals in their applicability domain. Consequently, model algorithms are required to assess the risks from ionic organic chemicals. For instance, how will they contribute to the environmental distribution? Can they be biodegraded? Which molecular descriptors are able to predict their biological effects? Another issue is the uncertainty from the biotransformation. It has been demonstrated that hydrophobic chemicals are particularly sensitive to biotransformation. Better quantifying biotransformation rates and dietary assimilation efficiency is important to improve the performance of bioaccumulation food chain model.

At present, various sources of information are used for chemical assessment in multiple media represented using different units, e.g., in vitro, in vivo or in situ. Converting data to consistent units of chemical activity or fugacity would facilitate the interpretation and application of information for hazard and risk assessment (Arnot et al., 2015; Mackay et al., 2011). It allows data for different species and food webs to be intergraded into the same evaluation for comparison purposes. For instance, the chemical concentration in an organism or a tissue/organ is often normalized to lipid content. **Paper II** demonstrated this is not appropriate in some cases and different biological phases would have different partition properties; lipid-normalized concentrations should be replaced with activities or fugacities with additional consideration of sorptive capacities of individual sub-compartments (e.g. neutral lipid, phospholipid and protein). Direct measurements of fugacities by passive sampling methods would be useful to avoid normalization issues when calculating fugacities (Jahnke et al., 2011).

8 References

Alleni R, Kochs P, Chandra G. Industrial organosilicon materials, their environmental entry and predicted fate. Organosilicon Materials. Springer, 1997, pp. 1-25.

Andersen ME. Toxicokinetic modeling and its applications in chemical risk assessment. Toxicology Letters 2003; 138: 9-27.

Armitage JM, Gobas FA. A terrestrial food-chain bioaccumulation model for POPs. Environ Sci Technol 2007; 41: 4019-25.

Armitage JM, MacLeod M, Cousins IT. Modeling the global fate and transport of perfluorooctanoic acid (PFOA) and perfluorooctanoate (PFO) emitted from direct sources using a multispecies mass balance model. Environmental Science & Technology 2009; 43: 1134-1140.

Arnot J, Armitage J, Brown T, Escher B, Scholz S, Jahnke A, et al. Expanding the applicability domain of the chemical activity approach for hazard and risk assessment. 2015.

Arnot JA, Brown TN, Wania F. Estimating screening-level organic chemical half-lives in humans. Environ Sci Technol 2014; 48: 723-30.

Arnot JA, Gobas F. A food web bioaccumulation model for organic chemicals in aquatic ecosystems. Environmental Toxicology and Chemistry 2004; 23: 2343-2355.

Arnot JA, Mackay D, Parkerton TF, Zaleski RT, Warren CS. Multimedia modeling of human exposure to chemical substances: The roles of food web biomagnification and biotransformation. Environmental Toxicology and Chemistry 2010; 29: 45-55.

Arnot JA, Mackay D, Webster E, Southwood JM. Screening level risk assessment model for chemical fate and effects in the environment. Environmental Science & Technology 2006; 40: 2316-2323.

Barber MC, Suárez LA, Lassiter RR. Modelling bioaccumulation of organic pollutants in fish with an application to PCBs in Lake Ontario salmonids. Canadian Journal of Fisheries and Aquatic Sciences 1991; 48: 318-337.

Bintein S, Devillers J, Karcher W. Nonlinear dependence of fish bioconcentration on n-octanol/water partition coefficient. SAR and QSAR in Environmental Research 1993; 1: 29-39.

Birak P, Yurk J, Adeshina F, Lorber M, Pollard K, Choudhury H, et al. Travis and Arms revisited: a second look at a widely used bioconcentration algorithm. Toxicology and Industrial Health 2001; 17: 163-175.

Bjerregaard P, Pedersen HS, Nielsen NO, Dewailly E. Population surveys in Greenland 1993-2009: Temporal trend of PCBs and pesticides in the general Inuit population by age and urbanisation. Science of the Total Environment 2013; 454: 283-288.

Boxall A, Rudd MA, Brooks BW, Caldwell DJ, Choi K, Hickmann S, et al. Pharmaceuticals and personal care products in the environment: what are the big questions? Environmental Health Perspectives 2012; 120: 1221-1229.

Brandes L, Den Hollander H, Van de Meent D. SimpleBox 2.0: a nested multimedia fate model for evaluating the environmental fate of chemicals. RIVM Rapport 719101029 1996.

Breivik K, Alcock R, Li YF, Bailey RE, Fiedler H, Pacyna JM. Primary sources of selected POPs: regional and global scale emission inventories. Environmental Pollution 2004; 128: 3-16.

Breivik K, Armitage JM, Wania F, Jones KC. Tracking the global generation and exports of e-waste. Do existing estimates add up? Environ Sci Technol 2014; 48: 8735-43.

Breivik K, Armitage JM, Wania F, Sweetman AJ, Jones KC. Tracking the global distribution of persistent organic pollutants accounting for e-waste exports to developing regions. Environ Sci Technol 2015.

Burkhard LP, Arnot JA, Embry MR, Farley KJ, Hoke RA, Kitano M, et al. Comparing laboratory and field measured bioaccumulation endpoints. Integrated Environmental Assessment and Management 2012; 8: 17-31.

Calafat AM, Kuklenyik Z, Caudill SP, Reidy JA, Needham LL. Perfluorochemicals in pooled serum samples from United States residents in 2001 and 2002. Environmental science & technology 2006; 40: 2128-2134.
Carballa M, Omil F, Lema JM, Llompart M, Garcia-Jares C, Rodriguez I, et al. Behavior of pharmaceuticals, cosmetics and hormones in a sewage treatment plant. Water Res 2004; 38: 2918-26.
Carlson DL, Hites RA. Polychlorinated biphenyls in salmon and salmon feed: global differences and bioaccumulation. Environ Sci Technol 2005; 39: 7389-95.
Christensen FM, Eisenreich SJ, Rasmussen K, Sintes JR, Sokull-Kluettgen B, Van de Plassche EJ. European experience in chemicals management: integrating science into policy. Environ Sci Technol 2011; 45: 80-9.
Collins C, Fryer M, Grosso A. Plant uptake of non-ionic organic chemicals. Environmental Science & Technology 2005; 40: 45-52.
Collins C, Martin I, Fryer M. Evaluation of models for predicting plant uptake of chemicals from soil: Environment Agency, 2006.
Collins CD, Finnegan E. Modeling the plant uptake of organic chemicals, including the soil−air−plant pathway. Environmental Science & Technology 2010; 44: 998-1003.
Collins CD, Martin I, Doucette W. Plant uptake of xenobiotics. Organic Xenobiotics and Plants. Springer, 2011, pp. 3-16.
Commission of the European Communities. Council Directive 67/548/EEC of 27 June 1967 on the approximation of laws, regulations and administrative provisions relating to the classification, packaging and labelling of dangerous substances. OJ L196, 1967.
Congress US. Toxic Substances Control Act. Public Law 1976; 99: 469.
Connell DW, Hawker DW. Use of polynomial expressions to describe the bioconcentration of hydrophobic chemicals by fish. Ecotoxicology and Environmental Safety 1988; 16: 242-257.
Cousins IT, Beck AJ, Jones KC. A review of the processes involved in the exchange of semi-volatile organic compounds (SVOC) across the air-soil interface. Science of the Total Environment 1999; 228: 5-24.
Cronin MT. Predicting chemical toxicity and fate: CRC press, 2004.
Cui S, Fu Q, Ma W-L, Song W-W, Liu L-Y, Li Y-F. A preliminary compilation and evaluation of a comprehensive emission inventory for polychlorinated biphenyls in China. Science of The Total Environment 2015; 533: 247-255.
Cui S, Qi H, Liu LY, Song WW, Ma WL, Jia HL, et al. Emission of unintentionally produced polychlorinated biphenyls (UP-PCBs) in China: Has this become the major source of PCBs in Chinese air? Atmospheric Environment 2013; 67: 73-79.
Czub G, McLachlan MS. A food chain model to predict the levels of lipophilic organic contaminants in humans. Environmental Toxicology and Chemistry 2004; 23: 2356-2366.
Daughton CG, Ternes TA. Pharmaceuticals and personal care products in the environment: Agents of subtle change? Environmental Health Perspectives 1999; 107: 907-938.
Diefenbacher PS, Bogdal C, Gerecke AC, Gluge J, Schmid P, Scheringer M, et al. Emissions of polychlorinated biphenyls in Switzerland: a combination of long-term measurements and modeling. Environ Sci Technol 2015; 49: 2199-206.
Endo S, Brown TN, Goss KU. General model for estimating partition coefficients to organisms and their tissues using the biological compositions and polyparameter linear free energy relationships. Environ Sci Technol 2013; 47: 6630-9.
Erickson RJ, Mckim JM. A simple fow-limited model for exchange of organic-chemicals at fish gills. Environmental Toxicology and Chemistry 1990; 9: 159-165.
European Commision. European Union System for the Evaluation of Substances Version 2.0 (EUSES 2.0). Prepared for the European Chemical Bureau By the National Institute of Public Health and the Environment (RIVM), Bilthoven, The Netherlands (RIVM, Report no. 601900005). 2004.

Fantke P, Charles R, de Alencastro LF, Friedrich R, Jolliet O. Plant uptake of pesticides and human health: Dynamic modeling of residues in wheat and ingestion intake. Chemosphere 2011; 85: 1639-1647.
Fantke P, Wieland P, Juraske R, Shaddick G, Itoiz ES, Friedrich R, et al. Parameterization models for pesticide exposure via crop consumption. Environ Sci Technol 2012; 46: 12864-72.
Franco A, Struijs J, Gouin T, Price OR. Evolution of the sewage treatment plant model SimpleTreat: Applicability domain and data requirements. Integrated environmental assessment and management 2013; 9: 560-568.
Fuchsman P, Lyndall J, Bock M, Lauren D, Barber T, Leigh K, et al. Terrestrial ecological risk evaluation for triclosan in land - applied biosolids. Integrated environmental assessment and management 2010; 6: 405-418.
Fuentes S, Colomina MT, Vicens P, Franco-Pons N, Domingo JL. Concurrent exposure to perfluorooctane sulfonate and restraint stress during pregnancy in mice: effects on postnatal development and behavior of the offspring. Toxicological sciences 2007; 98: 589-598.
Garten CT, Trabalka JR. Evaluation of models for predicting terrestrial food chain behavior of xenobiotics. Environmental Science & Technology 1983; 17: 590-595.
Gobas FA, Burkhard LP, Doucette WJ, Sappington KG, Verbruggen EM, Hope BK, et al. Review of existing terrestrial bioaccumulation models and terrestrial bioaccumulation modeling needs for organic chemicals. Integr Environ Assess Manag 2015: n/a-n/a.
Gobas FAPC. A model for predicting the bioaccumulation of hydrophobic organic chemicals in aquatic food-webs: application to Lake Ontario. Ecological Modelling 1993; 69: 1-17.
Gobas FAPC, Kelly BC, Arnot JA. Quantitative structure activity relationships for predicting the bioaccumulation of POPs in terrestrial food-webs. Qsar & Combinatorial Science 2003; 22: 329-336.
Gobas FAPC, Muir DCG, Mackay D. Dynamics of dietary bioaccumulation and faecal elimination of hydrophobic organic chemicals in fish. Chemosphere 1988; 17: 943-962.
Grandjean P, Landrigan PJ. Developmental neurotoxicity of industrial chemicals. The Lancet 2006; 368: 2167-2178.
Guillen D, Ginebreda A, Farre M, Darbra RM, Petrovic M, Gros M, et al. Prioritization of chemicals in the aquatic environment based on risk assessment: Analytical, modeling and regulatory perspective. Science of the Total Environment 2012; 440: 236-252.
Harner T, Mackay D, Jones KC. Model of the long-term Exchange of PCBs between soil and the atmosphere in the southern U.K. Environ Sci Technol 1995; 29: 1200-9.
Hendriks AJ. How to deal with 100,000+ substances, sites, and species: overarching principles in environmental risk assessment. Environ Sci Technol 2013; 47: 3546-7.
Hendriks AJ, Sm íkov á H, Huijbregts MA. A new twist on an old regression: Transfer of chemicals to beef and milk in human and ecological risk assessment. Chemosphere 2007; 70: 46-56.
Hermens JLM, de Bruijn JHM, Brooke DN. The octanol-water partition coefficient: Strengths and limitations. Environmental Toxicology and Chemistry 2013; 32: 732-733.
Hites RA, Foran JA, Carpenter DO, Hamilton MC, Knuth BA, Schwager SJ. Global assessment of organic contaminants in farmed salmon. Science 2004; 303: 226-9.
Jager D. Feasibility of validating the Uniform System for the Evaluation of Substances (USES). RIVM Rapport 679102026 1995.
Jager D, Vermeire Tt, Slooff W, Roelfzema H. Uniform system for the evaluation of substances II effects assessment. Chemosphere 1994a; 29: 319-335.
Jager D, Visser C, Van de Meent D. Uniform system for the evaluation of substances IV distribution and intake. Chemosphere 1994b; 29: 353-369.
Jahnke A, Mayer P, Adolfsson - Erici M, McLachlan MS. Equilibrium sampling of environmental pollutants in fish: Comparison with lipid - normalized concentrations and homogenization effects on chemical activity. Environmental Toxicology and Chemistry 2011; 30: 1515-1521.

Janjua NR, Mortensen GK, Andersson A-M, Kongshoj B, Skakkebæk NE, Wulf HC. Systemic uptake of diethyl phthalate, dibutyl phthalate, and butyl paraben following whole-body topical application and reproductive and thyroid hormone levels in humans. Environmental science & technology 2007; 41: 5564-5570.
Jaward TM, Zhang G, Nam JJ, Sweetman AJ, Obbard JP, Kobara Y, et al. Passive air sampling of polychlorinated biphenyls, organochlorine compounds, and polybrominated diphenyl ethers across Asia. Environmental Science & Technology 2005; 39: 8638-8645.
Jiang K, Li L, Chen Y, Jin J. Determination of PCDD/Fs and dioxin-like PCBs in Chinese commercial PCBs and emissions from a testing PCB incinerator. Chemosphere 1997; 34: 941-950.
Jobling S, Reynolds T, White R, Parker MG, Sumpter JP. A variety of environmentally persistent chemicals, including some phthalate plasticizers, are weakly estrogenic. Environmental health perspectives 1995; 103: 582.
Juraske R, Vivas CS, Velasquez AE, Santos GG, Moreno MB, Gomez JD, et al. Pesticide uptake in potatoes: model and field experiments. Environ Sci Technol 2011; 45: 651-7.
Kasprzyk-Hordern B, Dinsdale RM, Guwy AJ. The removal of pharmaceuticals, personal care products, endocrine disruptors and illicit drugs during wastewater treatment and its impact on the quality of receiving waters. Water Res 2009; 43: 363-80.
Kelly BC, Gobas F, McLachlan MS. Intestinal absorption and biomagnification of organic contaminants in fish, wildlife, and humans. Environmental Toxicology and Chemistry 2004; 23: 2324-2336.
Kelly BC, Ikonomou MG, Blair JD, Gobas FA. Bioaccumulation behaviour of polybrominated diphenyl ethers (PBDEs) in a Canadian Arctic marine food web. Science of the Total Environment 2008; 401: 60-72.
Kelly BC, Ikonomou MG, Blair JD, Morin AE, Gobas FA. Food web–specific biomagnification of persistent organic pollutants. Science 2007; 317: 236-239.
Kenaga EE. Correlation of bioconcentration factors of chemicals in aquatic and terrestrial organisms with their physical and chemical properties. Environmental Science & Technology 1980; 14: 553-556.
Klecka G, Boethling R, Franklin J, Grady L, Graham D, Howard PH, et al. Evaluation of persistence and long-range transport of organic chemicals in the environment: SETAC, 2000.
Kömp P, McLachlan MS. Interspecies variability of the plant/air partitioning of polychlorinated biphenyls. Environmental science & technology 1997; 31: 2944-2948.
Krishnan K, Peyret T. Physiologically based toxicokinetic (PBTK) modeling in ecotoxicology. Ecotoxicology modeling. Springer, 2009, pp. 145-175.
Legind CN, Trapp S. Modeling the exposure of children and adults via diet to chemicals in the environment with crop-specific models. Environmental Pollution 2009; 157: 778-785.
Leung HW. Development and utilization of physiologically based pharmacokinetic models for toxicological applications. Journal of Toxicology and Environmental Health, Part A Current Issues 1991; 32: 247-267.
Lewis GN. The law of physico-chemical change. Proceedings of the American Academy of Arts and Sciences. JSTOR, 1901, pp. 49-69.
Li H, Drouillard KG, Bennett E, Haffner GD, Letcher RJ. Plasma-associated halogenated phenolic contaminants in benthic and pelagic fish species from the Detroit River. Environmental science & technology 2003; 37: 832-839.
Linders JB, Luttik R. Uniform System for the Evaluation of Substances. V. ESPE, risk assessment for pesticides. Chemosphere 1995; 31: 3237-48.
Lishman L, Smyth SA, Sarafin K, Kleywegt S, Toito J, Peart T, et al. Occurrence and reductions of pharmaceuticals and personal care products and estrogens by municipal wastewater treatment plants in Ontario, Canada. Science of the Total Environment 2006; 367: 544-558.
Liu G, Zhan J, Zheng M, Li L, Li C, Jiang X, et al. Field pilot study on emissions, formations and distributions of PCDD/Fs from cement kiln co-processing fly ash from municipal solid waste incinerations. Journal of Hazardous Materials 2015a; 299: 471-478.

Liu G, Zheng M, Jiang X, Jin R, Zhao Y, Zhan J. Insights into the emission reductions of multiple unintentional persistent organic pollutants from industrial activities. Chemosphere 2015b; 144: 420-424.
Liu JL, Wong MH. Pharmaceuticals and personal care products (PPCPs): A review on environmental contamination in China. Environment International 2013; 59: 208-224.
Livingstone M, Prentice A, Strain J, Coward W, Black A, Barker M, et al. Accuracy of weighed dietary records in studies of diet and health. BMJ: British Medical Journal 1990; 300: 708.
Mackay D. Finding fugacity feasible. Environmental Science & Technology 1979; 13: 1218-1223.
Mackay D. Multimedia environmental models: the fugacity approach: CRC press, 2001.
Mackay D, Arnot JA, Wania F, Bailey RE. Chemical activity as an integrating concept in environmental assessment and management of contaminants. Integrated Environmental Assessment and Management 2011; 7: 248-255.
Mackay D, Di Guardo A, Paterson S, Kicsi G, Cowan CE. Assessing the fate of new and existing chemicals: A five-stage process. Environmental Toxicology and Chemistry 1996; 15: 1618-1626.
Mackay D, Fraser A. Bioaccumulation of persistent organic chemicals: mechanisms and models. Environmental Pollution 2000; 110: 375-391.
MacLachlan D, Bhula R. Estimating the residue transfer of pesticides in animal feedstuffs to livestock tissues, milk and eggs: a review. Animal Production Science 2008; 48: 589-598.
Macleod M, Riley WJ, Mckone TE. Assessing the influence of climate variability on atmospheric concentrations of polychlorinated biphenyls using a global-scale mass balance model (BETR-global). Environmental Science & Technology 2005; 39: 6749-6756.
MacLeod M, von Waldow H, Tay P, Armitage JM, Wöhrnschimmel H, Riley WJ, et al. BETR Global–A geographically-explicit global-scale multimedia contaminant fate model. Environmental Pollution 2011; 159: 1442-1445.
MacLeod M, Woodfine DG, Mackay D, McKone T, Bennett D, Maddalena R. BETR North America: a regionally segmented multimedia contaminant fate model for North America. Environmental Science and Pollution Research 2001; 8: 156-163.
Mai BX, Zeng EY, Luo XJ, Yang QS, Zhang G, Li XD, et al. Abundances, depositional fluxes, and homologue patterns of polychlorinated biphenyls in dated sediment cores from the Pearl River Delta, China. Environmental Science & Technology 2005; 39: 49-56.
Mckone TE, Maddalena RL. Plant uptake of organic pollutants from soil: Bioconcentration estimates based on models and experiments. Environmental Toxicology and Chemistry 2007; 26: 2494-2504.
McLachlan MS. Model of the Fate of Hydrophobic Contaminants in Cows. Environmental Science & Technology 1994; 28: 2407-2414.
McLachlan MS. Bioaccumulation of hydrophobic chemicals in agricultural feed chains. Environmental Science & Technology 1996; 30: 252-259.
McLachlan MS. Mass Transfer between the Atmosphere and Plant Canopy Systems. Handbook of Chemical Mass Transport in the Environment, 2010, pp. 137.
McLachlan MS, Czub G, MacLeod M, Arnot JA. Bioaccumulation of organic contaminants in humans: a multimedia perspective and the importance of biotransformation. Environ Sci Technol 2011; 45: 197-202.
Mclachlan MS, Thoma H, Reissinger M, Hutzinger O. PCDD/F in an Agricultural Food-Chain .1. PCDD/F Mass Balance of a Lactating Cow. Chemosphere 1990; 20: 1013-1020.
MEP China. Decree No. 7 of the Ministry of Environmental Protection of the People's Republic of China, Measures of Environmental Administration of New Chemical Substances, 2010.

Meyer T, Wania F, Breivik K. Illustrating sensitivity and uncertainty in environmental fate models using partitioning maps. Environmental Science & Technology 2005; 39: 3186-3196.
Muir DC, Howard PH. Are there other persistent organic pollutants? A challenge for environmental chemists. Environmental science & technology 2006; 40: 7157-7166.
Neely WB, Branson DR, Blau GE. Partition coefficient to measure bioconcentration potential of organic chemicals in fish. Environmental Science & Technology 1974; 8: 1113-1115.
Nichols JW, Fitzsimmons PN, Burkhard LP. In vitro-in vivo extrapolation of quantitative hepatic biotransformation data for fish. II. Modeled effects on chemical bioaccumulation. Environmental Toxicology and Chemistry 2007; 26: 1304-1319.
Nichols JW, McKim JM, Andersen ME, Gargas ML, Clewell HJ, 3rd, Erickson RJ. A physiologically based toxicokinetic model for the uptake and disposition of waterborne organic chemicals in fish. Toxicol Appl Pharmacol 1990; 106: 433-47.
Nichols JW, Schultz IR, Fitzsimmons PN. In vitro–in vivo extrapolation of quantitative hepatic biotransformation data for fish: I. A review of methods, and strategies for incorporating intrinsic clearance estimates into chemical kinetic models. Aquatic Toxicology 2006; 78: 74-90.
Nost TH, Breivik K, Fuskevag OM, Nieboer E, Odland JO, Sandanger TM. Persistent organic pollutants in Norwegian men from 1979 to 2007: intraindividual changes, age-period-cohort effects, and model predictions. Environmental Health Perspectives 2013; 121: 1292-1298.
Parliament E, Union tCotE. Regulation (EC) no. 1907/2006 of the European Parliament and of the Council of 18 December 2006 concerning the registration, evaluation, authorization and restriction of chemicals (REACH), establishing a European Chemicals Agency, amending Directive 1999/45/EC and repealing Council Regulation (EEC) no. 793/93 and Commission Regulation (EC) no. 1488/94, as well as Council Directive 76/769/EEC and commission Directives 91/155/EEC, 93/67/EEC, 93/105/CE and 2000/21/EC. Official Journal of the European Union 2006; 396.
Paterson S, Mackay D, Bacci E, Calamari D. Correlation of the equilibrium and kinetics of leaf-air exchange of hydrophobic organic chemicals. Environmental Science & Technology 1991; 25: 866-871.
Paterson S, Mackay D, McFarlane C. A model of organic chemical uptake by plants from soil and the atmosphere. Environmental Science & Technology 1994; 28: 2259-2266.
Paterson S, Mackay D, Tam D, Shiu WY. Uptake of organic chemicals by plants: A review of processes, correlations and models. Chemosphere 1990; 21: 297-331.
Quinn CL, Armitage JM, Breivik K, Wania F. A methodology for evaluating the influence of diets and intergenerational dietary transitions on historic and future human exposure to persistent organic pollutants in the Arctic. Environment International 2012; 49: 83-91.
Rastogi S, Schouten A, Kruijf Nd, Weijland J. Contents of methyl‐, ethyl‐, propyl‐, butyl‐ and benzylparaben in cosmetic products. Contact Dermatitis 1995; 32: 28-30.
Rein A, Legind CN, Trapp S. New concepts for dynamic plant uptake models. Sar and Qsar in Environmental Research 2011; 22: 191-215.
Ren N, Que M, Li YF, Liu Y, Wan X, Xu D, et al. Polychlorinated biphenyls in Chinese surface soils. Environ Sci Technol 2007; 41: 3871-6.
Rodricks JV, Swenberg JA, Borzelleca JF, Maronpot RR, Shipp AM. Triclosan: a critical review of the experimental data and development of margins of safety for consumer products. Critical reviews in toxicology 2010; 40: 422-484.
Ronis M, Walker C. Species variations in the metabolism of liposoluble organochlorine compounds by hepatic microsomal monooxygenase: comparative kinetics in four vertebrate species. Comparative Biochemistry and Physiology Part C: Comparative Pharmacology 1985; 82: 445-449.
Rosenbaum RK, McKone TE, Jolliet O. CKow: a dynamic model for chemical transfer to meat and milk. Environ Sci Technol 2009; 43: 8191-8.

Rotroff DM, Wetmore BA, Dix DJ, Ferguson SS, Clewell HJ, Houck KA, et al. Incorporating human dosimetry and exposure into high-throughput in vitro toxicity screening. Toxicological Sciences 2010: kfq220.
Ryan J, Bell R, Davidson J, O'connor G. Plant uptake of non-ionic organic chemicals from soils. Chemosphere 1988; 17: 2299-2323.
Schuster JK, Gioia R, Breivik K, Steinnes E, Scheringer M, Jones KC. Trends in European background air reflect reductions in primary emissions of PCBs and PBDEs. Environ Sci Technol 2010; 44: 6760-6.
Schwarzenbach RP, Gschwend PM, Imboden DM. Environmental organic chemistry: John Wiley & Sons, 2005.
Shin HM, Steenland K, Ryan PB, Vieira VM, Bartell SM. Biomarker-based calibration of retrospective exposure predictions of perfluorooctanoic acid. Environ Sci Technol 2014; 48: 5636-42.
Song Q, Li J. A systematic review of the human body burden of e-waste exposure in China. Environment International 2014; 68: 82-93.
Stephens RD, Petreas MX, Hayward DG. Biotransfer and bioaccumulation of dioxins and furans from soil: Chickens as a model for foraging animals. Science of the Total Environment 1995; 175: 253-273.
Struijs J. SimpleTreat 3.0: a model to predict the distribution and elimination of chemicals by sewage treatment plants. 1996.
Sun S-J, Kayama F, Zhao J-H, Ge J, Yang Y-X, Fukatsu H, et al. Longitudinal increases in PCDD/F and dl-PCB concentrations in human milk in northern China. Chemosphere 2011; 85: 448-453.
Sweetman AJ, Cousins IT, Seth R, Jones KC, Mackay D. A dynamic level IV multimedia environmental model: Application to the fate of polychlorinated biphenyls in the United Kingdom over a 60-year period. Environmental Toxicology and Chemistry 2002; 21: 930-940.
Takaki K, Wade AJ, Collins CD. Assessment and improvement of biotransfer models to cow's milk and beef used in exposure assessment tools for organic pollutants. Chemosphere 2015; 138: 390-397.
Tato L, Tremolada P, Ballabio C, Guazzoni N, Parolini M, Caccianiga M, et al. Seasonal and spatial variability of polychlorinated biphenyls (PCBs) in vegetation and cow milk from a high altitude pasture in the Italian Alps. Environmental Pollution 2011; 159: 2656-2664.
TGD EU. Technical guidance document on risk assessment in support of commission directive 93/67/EEC on risk assessment for new notified substances, Commission Regulation (EC) No 1488/94 on Risk Assessment for existing substances, and Directive 98/8/EC of the European Parliament and of the Council concerning the placing of biocidal products on the market. Part I–IV, European Chemicals Bureau (ECB), JRC-Ispra (VA), Italy, April 2003. Part II. European Commission Joint Research Centre. EUR 2003; 20418.
Topp E, Scheunert I, Attar A, Korte F. Factors affecting the uptake of 14 C-labeled organic chemicals by plants from soil. Ecotoxicology and Environmental Safety 1986; 11: 219-228.
Trapp S. Modelling uptake into roots and subsequent translocation of neutral and ionisable organic compounds. Pest Management Science 2000; 56: 767-778.
Trapp S. Dynamic root uptake model for neutral lipophilic organics. Environmental Toxicology and Chemistry 2002; 21: 203-206.
Trapp S. Plant uptake and transport models for neutral and ionic chemicals. Environmental Science and Pollution Research 2004; 11: 33-39.
Trapp S. Fruit tree model for uptake of organic compounds from soil and air. SAR & QSAR in Environmental Research 2007; 18: 367-387.
Trapp S. Calibration of a plant uptake model with plant- and site-specific data for uptake of chlorinated organic compounds into radish. Environ Sci Technol 2015; 49: 395-402.
Trapp S, Legind CN. Uptake of organic contaminants from soil into vegetables and fruits. Dealing with Contaminated Sites. Springer, 2011, pp. 369-408.

Trapp S, Matthies M. Generic one-compartment model for uptake of organic chemicals by foliar vegetation. Environmental science & technology 1995; 29: 2333-2338.
Travis CC, Arms AD. Bioconcentration of organics in beef, milk, and vegetation. Environmental Science & Technology 1988; 22: 271-274.
Undeman E, Czub G, McLachlan MS. Addressing temporal variability when modeling bioaccumulation in plants. Environmental Science & Technology 2009; 43: 3751-3756.
Undeman E, McLachlan MS. Assessing model uncertainty of bioaccumulation models by combining chemical space visualization with a process-based diagnostic approach. Environmental Science & Technology 2011; 45: 8429-8436.
UNEP. The Stockholm Convention on Persistent Organic Pollutants. United Nations Environmental Programme, 2001.
van Asselt ED, Kowalczyk J, van Eijkeren JCH, Zeilmaker MJ, Ehlers S, Fuerst P, et al. Transfer of perfluorooctane sulfonic acid (PFOS) from contaminated feed to dairy milk. Food Chemistry 2013; 141: 1489-1495.
Van de Meent D. SIMPLEBOX: a generic multimedia fate evaluation model. RIVM Bilthoven,, The Netherlands, 1993.
Van der Poel P. Uniform system for the evaluation of substances III. Emission estimation. Chemosphere 1994; 29: 337-352.
van Leeuwen CJ, Vermeire TG. Risk assessment of chemicals: an introduction: Springer Science & Business Media, 2007.
Veith GD, Defoe DL, Bergstedt BV. Measuring and estimating the bioconcentration Factor of chemicals in fish. Journal of the Fisheries Research Board of Canada 1979; 36: 1040-1048.
Vermeire T, Jager D, Bussian B, Devillers J, Den Haan K, Hansen B, et al. European union system for the evaluation of substances (EUSES). Principles and structure. Chemosphere 1997; 34: 1823-1836.
Vermeire T, Rikken M, Attias L, Boccardi P, Boeije G, Brooke D, et al. European union system for the evaluation of substances: the second version. Chemosphere 2005; 59: 473-485.
Vermeire T, Van der Zandt P, Roelfzema H, Van Leeuwen C. Uniform system for the evaluation of substances I principles and structure. Chemosphere 1994; 29: 23-38.
Wallace KB. Glutathione‐dependent metabolism in fish and rodents. Environmental Toxicology and Chemistry 1989; 8: 1049-1055.
Wang H, Yan ZG, Li H, Yang NY, Leung KMY, Wang YZ, et al. Progress of environmental management and risk assessment of industrial chemicals in China. Environmental Pollution 2012; 165: 174-181.
Wang N, Kong D, Cai D, Shi L, Cao Y, Pang G, et al. Levels of polychlorinated biphenyls in human adipose tissue samples from southeast China. Environ Sci Technol 2010; 44: 4334-40.
Wang S, Huang J, Yang Y, Hui Y, Ge Y, Larssen T, et al. First report of a Chinese PFOS alternative overlooked for 30 years: its toxicity, persistence, and presence in the environment. Environ Sci Technol 2013; 47: 10163-70.
Wania F, Breivik K, Persson NJ, McLachlan MS. CoZMo-POP 2–A fugacity-based dynamic multi-compartmental mass balance model of the fate of persistent organic pollutants. Environmental Modelling & Software 2006; 21: 868-884.
Wania F, Mackay D. A global distribution model for persistent organic chemicals. Science of the Total Environment 1995; 160: 211-232.
Whelan MJ, Breivik K. Dynamic modelling of aquatic exposure and pelagic food chain transfer of cyclic volatile methyl siloxanes in the Inner Oslofjord. Chemosphere 2013; 93: 794-804.
Wu J-P, Luo X-J, Zhang Y, Luo Y, Chen S-J, Mai B-X, et al. Bioaccumulation of polybrominated diphenyl ethers (PBDEs) and polychlorinated biphenyls (PCBs) in wild aquatic species from an electronic waste (e-waste) recycling site in South China. Environment International 2008; 34: 1109-1113.

Wu S, Xia XH, Zhang SW, Liu Q, Xu L. Distribution of Polychlorinated Biphenyls (PCBs) and toxic equivalency of dioxin-like PCB congeners in rural soils of Beijing, China. Journal of Environmental Informatics 2012a; 20: 12-19.
Wu YN, Wang YX, Li JG, Zhao YF, Guo FF, Liu JY, et al. Perfluorinated compounds in seafood from coastal areas in China. Environment International 2012b; 42: 67-71.
Xing X, Lu YL, Dawson RW, Shi YJ, Zhang H, Wang TY, et al. A spatial temporal assessment of pollution from PCBs in China. Chemosphere 2005; 60: 731-739.
Yang H, Zhuo S, Xue B, Zhang C, Liu W. Distribution, historical trends and inventories of polychlorinated biphenyls in sediments from Yangtze River Estuary and adjacent East China Sea. Environmental Pollution 2012; 169: 20-26.
Zhang H, Luo Y, Teng Y, Wan H. PCB contamination in soils of the Pearl River Delta, South China: levels, sources, and potential risks. Environmental Science and Pollution Research 2013a; 20: 5150-5159.
Zhang L, Li J, Liu X, Zhao Y, Li X, Wen S, et al. Dietary intake of PCDD/Fs and dioxin-like PCBs from the Chinese total diet study in 2007. Chemosphere 2013b; 90: 1625-1630.
Zhang Q, Lian M, Liu L, Cui H. High-performance liquid chromatographic assay of parabens in wash-off cosmetic products and foods using chemiluminescence detection. Analytica Chimica Acta 2005; 537: 31-39.
Zhao GF, Wang ZJ, Zhou HD, Zhao Q. Burdens of PBBs, PBDEs, and PCBs in tissues of the cancer patients in the e-waste disassembly sites in Zhejiang, China. Science of the Total Environment 2009; 407: 4831-4837.
Zheng Q, Nizzetto L, Mulder MD, Sanka O, Lammel G, Li J, et al. Does an analysis of polychlorinated biphenyl (PCB) distribution in mountain soils across China reveal a latitudinal fractionation paradox? Environmental Pollution 2014; 195: 115-122.

PAPER I

Environmental Research 140 (2015) 165–176

Contents lists available at ScienceDirect

Environmental Research

journal homepage: www.elsevier.com/locate/envres

Applicability of western chemical dietary exposure models to the Chinese population

Shizhen Zhao [a], Oliver Price [b], Zhengtao Liu [c], Kevin C. Jones [a], Andrew J. Sweetman [a,*]

[a] Lancaster Environment Centre, Lancaster University, Lancaster LA14YQ, UK
[b] Safety and Environmental Assurance Centre, Unilever, Sharnbrook MK44 1LQ, UK
[c] State Key Laboratory of Environmental Criteria and Risk Assessment, State Environmental Protection Key Laboratory of Ecological Effect and Risk Assessment of Chemicals, Chinese Research Academy of Environmental Science, Beijing 100012, PR China

ARTICLE INFO

Article history:
Received 10 December 2014
Received in revised form
25 March 2015
Accepted 26 March 2015

Keywords:
Dietary exposure
Risk assessment
Exposure models
Chinese population

ABSTRACT

A range of exposure models, which have been developed in Europe and North America, are playing an increasingly important role in priority setting and the risk assessment of chemicals. However, the applicability of these tools, which are based on Western dietary exposure pathways, to estimate chemical exposure to the Chinese population to support the development of a risk-based environment and exposure assessment, is unclear. Three frequently used modelling tools, EUSES, RAIDAR and ACC-HUMANsteady, have been evaluated in terms of human dietary exposure estimation by application to a range of chemicals with different physicochemical properties under both model default and Chinese dietary scenarios. Hence, the modelling approaches were assessed by considering dietary pattern differences only. The predicted dietary exposure pathways were compared under both scenarios using a range of hypothetical and current emerging contaminants. Although the differences across models are greater than those between dietary scenarios, model predictions indicated that dietary preference can have a significant impact on human exposure, with the relatively high consumption of vegetables and cereals resulting in higher exposure via plants-based foodstuffs under Chinese consumption patterns compared to Western diets. The selected models demonstrated a good ability to identify key dietary exposure pathways which can be used for screening purposes and an evaluative risk assessment. However, some model adaptations will be required to cover a number of important Chinese exposure pathways, such as freshwater farmed-fish, grains and pork.

1. Introduction

Many chemicals are released into the environment which have the potential to be taken up into organisms, where they may be transferred through food chains and potentially threaten human health. Human exposure to chemicals can occur via direct and indirect exposure. Indirect human exposure via the environment comprises intake through inhalation, drinking water and diet. The evaluation and quantification of human exposure to chemicals through multimedia exposure pathways is required for both priority setting and risk assessment, and is becoming increasingly important in the global assessment of chemicals (Undeman and McLachlan, 2011). In many previous studies, diet has been highlighted as an important human exposure pathway for a wide range of organic chemicals, such as polychlorinated dibenzo-p-dioxins, polychlorinated dibenzo-furans (PCDD/F, dioxins) and polychlorinated biphenyls (PCBs). For some chemicals, dietary exposure has been demonstrated to account for more than 90% of total human exposure (Domingo et al., 2012; Harrad et al., 2004; Herzke et al., 2013; Kiviranta et al., 2004; Vestergren et al., 2012; Xia et al., 2010; Zhou et al., 2012). However, owing to limited time and resource, many existing chemicals still lack detailed information on human exposure via the consumption of food, which makes risk assessment both difficult and incomplete. Therefore, multimedia fate modelling approaches have been demonstrated to be helpful to screen and prioritize chemical compounds of concern for the environment and human health (Rodan et al., 1999).

A number of different models are currently used in Europe and North America to assess human dietary exposure and risk. For example, the European Union System for the Evaluation of Substances (EUSES), USEtox, CALTOX, ACC-HUMAN and the Risk Assessment Identification And Ranking (RAIDAR) models have been used to estimate human exposure to chemicals via the environment (Arnot and Mackay, 2008; Czub and McLachlan, 2004; McKone et al., 2007; Rosenbaum et al., 2008; Vermeire et al., 2005). All these models represent the current state of science and

* Corresponding author.
E-mail address: a.sweetman@lancaster.ac.uk (A.J. Sweetman).

http://dx.doi.org/10.1016/j.envres.2015.03.025
0013-9351/

have been developed to meet the needs of chemical risk assessment for government regulators, industry and academia in developed countries (Fryer et al., 2006). The key differences between the models are their parameterization of geographic and environmental conditions, human receptor characteristics, and treatment of the food web (Arnot et al., 2010).

As a developing country China has become one of the most important chemical manufacturing nations in the world, and there are thousands of chemicals used in commerce daily. Under rapid industrialization there are potential health risks associated with chemical residues in food resources which may be significant in China (L. Zhang et al., 2013). Unfortunately, prioritization schemes and risk assessment procedures for these chemicals in China are currently underdeveloped and national technical guidance for risk assessment has not yet been established, nor have the modelling tools required (Wang et al., 2012). As a result, there is an urgent need for China to develop suitable approaches and modelling tools.

The models and approaches currently being used in developed countries could significantly help for both priority setting and risk assessment for chemical management in China, and much effort has been made to adapt Western-developed models to estimate emission and fate of persistent organic chemicals (POPs) in China, mainly by the revision of environmental parameters and emission scenarios (Xu et al., 2013; Q.Q. Zhang et al., 2013; Zhang et al., 2014). However, human exposure to organic pollutants has also been shown to be highly variable in different regions of the world (Undeman et al., 2010). Recent measurement campaigns have found large variations of daily intake in the relative contributions from different food groups among regions in China for a number of POPs, which are different from Western countries (Shi et al., 2013; Yu et al., 2013; L. Zhang et al., 2013). However, the uncertainty from dietary patterns and its potential impact on human exposure have not been explored for Chinese population. Therefore, this study was designed to assess whether Western-based dietary modelling tools could be directly applied to China or how they could be reconfigured to investigate Chinese exposure scenarios to support environmental and human risk-based assessments.

In order to model human dietary exposure to chemicals in China, it is important to understand which models are potentially suitable and how they can be adapted to the Chinese population, or indeed need to be modified. Therefore, the aims of this study are: (1) to compare three commonly used modelling approaches and evaluate their performance in Europe and Canada to assess dietary exposure routes; (2) to identify dominant dietary exposure pathways both under Western and Chinese scenarios and explore the impact of dietary preferences for a wide range of hypothetical chemicals; (3) to explore the potential application of these models to China. To pursue these objectives, firstly, the dominant dietary exposure pathway was identified for a wide range of hypothetical chemicals covering chemical partitioning space defined by their octanol–water (K_{OW}) and octanal–air (K_{OA}) partition coefficients for each of the three models. Secondly, the three models were evaluated by applying them to a range of legacy and emerging contaminants with different properties under both Western and Chinese scenarios. Finally, this analysis was used to identify potential adaptions to facilitate better risk assessment in China.

2. Methods

2.1. Model overview

RAIDAR 2.0, EUSES (spreadsheet version 1.24) and ACC-HUMANsteady (a steady-state version of ACC-HUMAN) were selected to be assessed in this study. Each model was accessed from their respective websites; namely the Canadian Centre for Environment Modelling and Chemistry (http://www.trentu.ca/academic/aminss/envmodel/models/RAIDAR100.html), Netherlands Centre for Environmental Modelling (http://cem-nl.eu/eutgd.html) and Department of Applied Environment Science, Stockholm University (http://www.itm.su.se/page.php?pid=117). These models are described in detail elsewhere (Arnot et al., 2006; Czub and McLachlan, 2004; Vermeire et al., 1997).

In general, the three models are conceptually similar as they are all based on the Mackay-type steady-state fugacity-based box models as summarized in Table 1 (Mackay et al., 2009). EUSES is a harmonized quantitative risk assessment tool, which is designed to support decisions for regulators and industry to undertake chemical risk assessments (Vermeire et al., 2005, 1997). Details are given in the EU Technical Guidance Document (TGD) (European Commision, 2003). Default values for food consumption rates are representative of the highest country-average levels among the EU member states. RAIDAR and ACC-HUMANsteady are research models based on more recent research in exposure assessment (Arnot et al., 2010; Czub and McLachlan, 2004; Undeman and McLachlan, 2011). These models were chosen as they are widely used in Europe, Canada and U.S. for screening purposes using assumed 'generic' environment.

However, one significant difference among the three models is the treatment of food web bioaccumulation and transfer and thus their predictions for substances in various food groups vary (Arnot et al., 2010). EUSES employs simple empirical regression models to estimate concentrations in organisms from concentrations in environmental media, whilst RAIDAR and ACC-HUMANsteady use mechanistic models to address the bioaccumulation processes. Mechanistic bioaccumulation models incorporate chemical specific biomagnification and biotransformation processes, resulting in more refined exposure estimation, provided additional input requirements are available (Arnot et al., 2010). Different food groups are considered according to locally applicable food chains. Additionally, EUSES includes a spatial assessment of

Table 1
Comparison of three selected models.

Model	EUSES	RAIDAR	ACC-HUMANsteady
Sponsor	RIVM European Commission	Environment Canada, Health Canada, Industry	Baltic Sea Research Institute, Stockholm University
Source distance	Near field and far field	Far field	Far field
Human exposure pathways	Inhalation, water, fish, meat, dairy and vegetables (root, leaf)	Inhalation, water, fish, meat (poultry, beef and pork), vegetables (root, leaf)	Inhalation, water, beef, dairy, fish, vegetables (root, leaf, fruit and grain)
Exposure algorithm	Empirical regression models to estimate concentrations in organisms in equilibrium with environmental media	Combined fate and food web mass balance models for estimating exposure and ranking	Steady-state, mechanistic-based fugacity approach
Data input	Physical–chemical data and chemical emission information for initial screening assessment	Physical–chemical data and degradation half-life parameters from databases or QSARs	Physical–chemical data and environmental concentration

Table 2
Defaults of media area volume in regional EUSES, RAIDAR and ACC-HUMANsteady.

Media volume	Air, m^3	Water, m^3	Soil, m^3	Sediment, m^3
Regional scale in EUSES	4.03×10^{13}	Freshwater: 3.59×10^9 Seawater: 3.99×10^9 Sum: 7.58×10^9	Agricultural soil: 4.79×10^9 Natural soil: 5.39×10^8 Industrial soil: 2×10^8 Sum: 5.53×10^9	4.79×10^7
RAIDAR	1×10^{14}	2×10^{11}	1.8×10^{10}	5×10^8
ACC-HUMANsteady	4.03×10^{13}	7.64×10^9	5.43×10^9	5×10^7

environmental distribution covering global, regional and local scales whilst RAIDAR and ACC-HUMANsteady only consider regional scales.

2.2. Parameterization of selected models

2.2.1. Environmental properties

ACC-HUMANsteady is a unit world model (steady state, equilibrium, no in- or out-flows or degradation reactions) linked to a bioaccumulation model which calculates the equilibrium concentrations in air (gaseous and aerosol bound), water (dissolved) and soil (bulk soil and pore water). In RAIDAR and EUSES, the model simulations are level III (steady state, non-equilibrium, in- and out-flows and degradation reactions included) and require information on chemical mode of entry to the environment, which are considered to be equal for emissions to air, water and soil in this study. An arbitrary unit chemical emission rate E_U of 1 kg h^{-1} was used for the simulations in three models (Arnot et al., 2010).

The default regional compartment volumes of air, water, soil and sediment for the three models are given in Table 2. ACC-HUMANsteady and EUSES have similar default dimensions of their physical environments, whilst the regional scale of EUSES is about 40% of the RAIDAR evaluative environment. EUSES contains soil sub-categorise (agricultural, natural and industrial soil type) and water sub-categories (surface water and seawater), whereas RAIDAR and ACC-HUMANsteady do not sub-divide bulk soil and water compartments. Therefore, chemical emissions to soil and water were assumed to enter the agricultural soil and freshwater compartments in EUSES. When calculating mass distribution in EUSES, the total amount of chemical in sub-categories of water and soil are taken into account.

The differences of default parameterization of the physical environments and fate prediction in three models will lead to a divergence of the predictions of human dietary exposure. Therefore, the mass distributions (m_i, kg kg^{-1}) in each compartment were calculated as

$$m_i = M_i/M_T \quad (1)$$

where M_i is the mass in an environmental medium i (kg), M_T is the chemical mass in the total system (kg). Thus the maximum percentage of mass distributed in the considered compartments can be plotted on partitioning space diagrams, i.e. two-dimensional chemical space as a function of log K_{OW} (x-axis) and log K_{OA} (y-axis). Where, each point in this space corresponds to a hypothetical chemical with specific combination values of log K_{OW} and log K_{OA} (Meyer et al., 2005).

2.2.2. Dietary intake

Default daily food intake rates for the three models were assumed to be typical dietary patterns for the corresponding regions as shown in Table 3. Since EUSES considers a hypothetical worst scenario by taking the maximum consumption for each food item across EU countries, its total food intake rate is 2.5 fold higher than ACC-HUMANsteady. These provide a reference for comparison with Chinese dietary patterns to explore the impact of dietary preference. Drinking water and inhalation were regarded as dietary intake in this study. RAIDAR and ACC-HUMANsteady directly use the predicted concentrations in water and air to calculate exposure via drinking water without any treatment, while EUSES employed two different surface water purification systems for calculations (Rikken and Lijzen, 2004). Each of the three models uses different food groups and parameters for the calculation of intake. For example, ACC-HUMANsteady uses fruit (apple), leafy vegetables (lettuce), grains, tubers (potato), and root vegetables (carrot) to estimate exposure from plants, whilst EUSES and RAIDAR simply classify a distinction between root (underground) and leaf (above ground) vegetables. For meat, RAIDAR divides intake via poultry, pork and beef in a separate calculation, whilst EUSES only considers a general meat group and ACC-HUMANsteady only considers intake via consumption of beef. Dairy intake in EUSES assumes the consumption of milk only, whereas RAIDAR and ACC-HUMANsteady includes bulk dairy, which is a weighted average of dairy products, with a further separate consideration of milk. In order to facilitate the comparison between models, the predicted concentrations in poultry, pork and beef calculated in RAIDAR were combined into one meat category. In ACC-HUMANsteady, fruit, lettuce and grain were classified into the category of leaf vegetables, and potato and carrot are included in the calculation of root vegetable. In ACC-HUMANsteady, ingestions rates, body mass and lipid content are considered as a function of age and a 30 years old woman is used as the model default. However, in EUSES and RAIDAR, an average human individual is assumed to have a body weight of 70 kg (Undeman and McLachlan, 2011).

In order to adapt the three models to a Chinese population scenario, parameters for human characteristics and daily dietary intake rates were modified based on the measured survey data from China. China has conducted four Chinese Nutrition and Health Surveys, since 1959 organized by Chinese Centre for Disease Control and Prevention, namely in the years 1959, 1982, 1992 and 2002, covering 31 provinces within the mainland. The information of Chinese dietary pattern was extracted from the most recent National Nutrition Survey in 2002 (Jin, 2008), however, as

Table 3
Daily intake rates in model defaults and Chinese diet pattern.

Food group	Units	EUSES	RAIDAR	ACC-HUMANsteady	Chinese diet[a]
Drinking water	L d^{-1}	2	2	0.6	2.7[a]
Inhalation	m^3 d^{-1}	20	20	15	19[a]
Fish	g_{WW} d^{-1}	115	96	29	30
Leaf crops[b]	g_{WW} d^{-1}	1200	1077	319	676
Root crops[b]	g_{WW} d^{-1}	380	360	132	106
Meat[c]	g_{WW} d^{-1}	300	360	75	79
Dairy products	g_{WW} d^{-1}	560	455	351	27
Eggs	g_{WW} d^{-1}	N/A	48	N/A	24
Total intake	g_{WW} d^{-1}	2555	2396	904	941
Bodyweight	kg	70	70	63	61

[a] Statistics related to diet pattern in China are extracted from Chinese Nutrition and Health Survey (Jin, 2008). Drinking water and inhalation rate are from other literatures (Xiaoli et al., 2010; Zongshuang et al., 2009).

[b] For ACC-HUMANsteady, intake rates of lettuce 37 g_{WW} d^{-1}, fruit 190 g_{WW} d^{-1} and grain 92 g_{WW} d^{-1} were classified into general categorization of leaf crops; intake rates of carrot 21 g_{WW} d^{-1} and potato 111 g_{WW} d^{-1} were regarded as root crops.

[c] RAIDAR separated meat group into poultry, pork and beef with 120 g_{WW} d^{-1}, whilst ACC-HUMANsteady only considered beef.

there was no individual classification data for leaf and root vegetables, it was assumed that 20% of total vegetable consumption comes from root vegetables (Song et al., 2009). The selected food consumption rates for the Chinese population are listed in Table 3.

The three models considered in the study all calculate total daily dietary intake rate from environmental contamination of foodstuffs. Thus daily intake rates were used as a metric to estimate human exposure. The calculation of chemical daily intake rate R_i (ng kg^{-1} d^{-1}) on a bodyweight basis from exposure to multimedia sources was carried out using

$$R_i = G_i \times C_i/\text{Bodyweight} \quad (2)$$

where the C_i values relate to concentration in the corresponding media with units of (ng g^{-1}) for food items, G_i represents the ingestion rates (g_{WW} day^{-1}) or air inhalation rates (m^3 day^{-1}) of exposure media. The total daily chemical intake via diet or inhalation (R) (ng kg^{-1} d^{-}) is therefore a sum of exposure from each media (i), which is calculated on an individual body weight basis.

$$R = \sum R_i \quad (3)$$

The fractional contribution P_i of the dominant exposure pathway to total intake (P_i) was calculated by Eq. (4) and plotted as an evaluated endpoint in Fig. 2.

$$P_i = \max(i)[R_i/R] \quad (4)$$

2.3. Hypothetical chemical test

2.3.1. Partitioning space map

To investigate the sensitivity of each model to chemicals with a wide range of properties and to explore how this might affect their ability to predict dietary exposure, a chemical partition space was defined as a function of equilibrium partition coefficients between air, water and octanol (Meyer et al., 2005). Each model was used to predict both mass distribution and dietary exposure for a range of combinations of log K_{OW} and log K_{OA}. Each point within these space plots corresponds to a hypothetical chemical with a specific combination of partitioning properties. For the purposes of these calculations, log K_{OW} was assumed to equal log K_{OA}+log K_{AW}. The boundaries of the investigated space are defined by log K_{OA} from 4 to 12 and log K_{OW} from −2 to 12 in steps of 0.5 log units, such that most known chemicals fall within this range. It is important to note that both RAIDAR and ACC-HUMANsteady were originally designed for hydrophobic chemicals and the domain of applicability common to all regression equations in EUSES is only from log K_{OW} 3–4.7 (Legind and Trapp, 2009). Caution should be taken when applying these regressions to substances outside of these ranges.

2.3.2. Physicochemical properties

Another assumption was that all hypothetical chemicals were perfectly persistent in all compartments. This assumption provides a conservative assessment for these hypothetical chemicals. Thus for EUSES, “not biodegradable” was chosen for the biodegradability test results. For the calculation of organic carbon–water partitioning in EUSES, the “predominantly hydrophobic” option was selected for chemicals with log $K_{OW} \geq 2$, and “non-hydrophobic” for chemicals with log $K_{OW} < 2$. Half-life values of 1×10^{11} h in all environmental media were assumed in RAIDAR, which could be interpreted as having negligible reaction rates (Mackay et al., 1996). The values of other parameters, like molecular weight, heat transfer coefficients were assigned as shown in Table 4 and used elsewhere (Undeman and McLachlan, 2011).

2.4. Selection of real chemical properties

The three models were also assessed for their ability to predict the dietary exposure for a suite of emerging pollutants and chemicals in current production. The physicochemical property data required for each of the three models included molecular weight, K_{OW}, Henry's Law constant, water solubility, vapor pressure, and estimated biodegradation half-lives in water, soil, sediment and in biota. Biodegradation half-life data were collected and processed using the regression equations derived from outputs of the Biowin model (a submodel in EPISuite) (Arnot et al., 2010). Metabolism within organisms was not considered in the calculations as the metabolism rates for many chemicals are not available and thus their inclusion would increase the uncertainty of output. This conservative assumption is often considered acceptable practice for chemical assessment and screening (Meyer et al., 2005; Undeman and McLachlan, 2011).

All temperature-dependent parameters were adjusted to a temperature of 25 °C. The publicly accessible free tool EPISuite™ Version 4.11 (US EPA, 2012), which includes both QSA(P)R tools and experimental databases was employed to provide property estimates where measured data were unavailable. Table 5 contains the physicochemical property data of fifteen selected organic chemicals covering a wide range of property combinations. Triclosan, nonylphenol, pentachlorophenol are also ionizable, however, the correction for ionization is not included in three models. Data from pharmaceutical studies suggests that ionized species are absorbed by humans with 3–10% of the efficiency of the neutral species, thus the effect of ionization was assumed to be minimal compared to the neutral species and ignored in this study (Abraham et al., 2002; Arnot and Mackay, 2007).

3. Results and discussion

3.1. Mass distribution linked to exposure

To explore the impact of the environmental distribution calculated within the models, individual chemical burdens in different environmental compartments were estimated using the default scenarios. The maximum mass distributions in the physical compartments of three selected models were contoured onto the partitioning space maps as shown in Fig. 1, using two-dimensional chemical space as a function of log K_{OW} (x-axis) and log K_{OA} (y-axis). Each point in this space corresponds to a hypothetical chemical with specific combination values of log K_{OW} and log K_{OA} (Meyer et al., 2005). The solid lines in plots depict the border between two compartments where the burden is equally shared. Four representative hypothetical chemicals H1–H4 are also included in Figs. 1 and 2 to provide reference points. They have been chosen to represent persistent superhydrophobic (H1), hydrophobic (H2), volatile (H3) and soluble chemicals (H4).

The maximum mass distributions predicted by the three models are similar for water and soil, where water is the predominant storage media for chemicals with log $K_{OW} \leq 2$ for ACC-HUMANsteady and log $K_{OW} \leq 3.5$ for RAIDAR, soil being more important for chemicals with log $K_{OW} > 2$. For highly hydrophobic chemicals (log $K_{OW} > 4$ and 8 for RAIDAR and EUSES, respectively) and the more volatile chemicals (log $K_{OA} < 6$ and 5 for RAIDAR and EUSES, respectively), they were predicted to be found predominantly in sediment in RAIDAR and EUSES compared with air in ACC-HUMANsteady. This disparity is mainly due to differences in model structure. RAIDAR and EUSES are level III fate models whilst ACC-HUMANsteady uses a simplified level I model, which does not account for advective and intermedia exchange processes (such as volatilization, deposition, precipitation and

Table 4
Assigned values of properties for the hypothetical chemicals in three selected models.

Parameters	Unit	Values
Molecular weight	g mol^{-1}	300
ΔU_{AW}	kJ mol^{-1}	60[a]
ΔU_{OW}	kJ mol^{-1}	−20[a]
ΔU_{OA}	kJ mol^{-1}	80[a]
Henry's law constant	Pa m^3 mol^{-1}	$K_{aw} \times R \times T$[b]

[a] The heat of phase transfer was chosen based on the study of Undeman and McLachlan (2011).
[b] R is the universal gas constant and T is the environmental temperature of 288 K.

sedimentation). Additionally, different environmental properties shown in Table 2 and/or the environmental scenarios, also lead to the distinct mass distributions in three models, including the estimations of partition coefficients, area fractions of individual compartments, fraction of organic carbon, mass transfer coefficients and so on (Meyer et al., 2005).

3.2. Multiple exposure pathways of hypothetical chemical

To investigate the most important pathways of human exposure as a function of a chemical's partitioning profile, the maximum dietary exposure pathway contribution has been plotted in Fig. 2. This represents the largest percentage contribution to total exposure among all considered food groups. For example, a chemical with a log K_{OW}=7 and log K_{OA}=8, such as H2, would appear in the upper-right red domain using outputs of ACC-HUMANsteady and RAIDAR (Fig. 2(a) and (c), respectively), and identify fish as the primary source of total daily intake (>90%). Overall, differences across models are greater than differences in diet patterns, and both are discussed in this study. In this study, relative mass ratios were compared, and so the significance of individual exposure routes was proportional to overall exposure. Some exposure routes, however, may also present appreciable risk to humans under high emission scenarios.

EUSES predicted that root crop consumption could be an important exposure pathway for a wide range of chemical partition space, particularly in the domain with log K_{OW} ranging from 4 to 12. RAIDAR and ACC-HUMANsteady, however, suggested that the contribution from root vegetable consumption was minimal. The consumption of leaf vegetables, however, was suggested to be important using RAIDAR and ACC-HUMANsteady within a similar domain for both high and low K_{OW} values. EUSES indicated leaf vegetable consumption was important only for chemicals with low K_{OW} values. For instance, hypothetical chemical H1 represents a superhydrophobic chemical with a log K_{OW} of 11 and a log K_{OA} of 10. EUSES predicted for H1 that root vegetable consumption was likely to be the main exposure pathway (Fig. 1e), whilst both RAIDAR and ACC-HUMANsteady indicated leafy vegetable consumption would be dominant. When linked to predictions of environmental distribution, as shown in Fig. 1, the three models consistently suggested that bulk soil as the dominant sink for H1. There are important differences between EUSES and RAIDAR model predictions in terms of the uptake via leaf and root vegetable consumption for chemicals with low volatility and high hydrophobicity (Mitchell et al., 2013). This may be due to the assumption that root crops are in equilibrium with the surrounding soil in EUSES which leads to a potential overestimation (Undeman and McLachlan, 2011). The uptake of chemicals into roots occurs mainly via the transpiration stream from soil pore water to xylem, a process which is retarded for hydrophobic chemicals that are strongly adsorbed to organic matter in soil. So, there may be insufficient time to reach equilibrium between root and soil, which was assumed in RAIDAR and ACC-HUMANsteady (Arnot and Mackay, 2007; Undeman and McLachlan, 2011).

An important difference among RAIDAR, ACC-HUMANsteady and EUSES is the calculation of the bioaccumulation in cattle and fish. EUSES uses an empirical regression equation relating log K_{OW} and BAF/BCF to calculate chemical concentration in milk, meat and fish with little mechanistic basis. In contrast, both RAIDAR and ACC-HUMANsteady use mechanistically based mass balance models of bioaccumulation (Arnot and Mackay, 2007; Undeman and McLachlan, 2011). The empirical model structure in EUSES has the advantage of requiring limited input data. However, such models have limitations and often include limited or no mechanistic description of processes. They also contain a number of empirical relationships with limited functionality. For example, BAFs calculated within the model are derived using an empirical relationship with a limited log K_{OW} range of between 1.5 and 6.5. As a result, calculated BAFs for compounds with log K_{OW} values outside of this range must therefore be used with caution (Rikken and Lijzen, 2004). More complex mechanistic models provide a more realistic assessment of chemical fate and behavior, especially for food chain accumulation. However, they often require significantly more chemical and biological input data. If measurements of uptake and loss processes are available as model input, a validated mechanistic model will provide valuable insights into food chain accumulation and hence provide more realistic

Table 5
Physicochemical properties of studied chemicals.

CAS	Compound	Abbreviation	Molar mass, g mol^{-1}	log K_{OW}	log K_{OA}	Vapor pressure, Pa	Watersolubility, mg L^{-1}
95-50-1	1,2-Dichlorobenzene	1,2-D	147.00	3.38	4.54	196	155.8
1163-19-5	Decabromodiphenyl ether	DecaBDE	959.17	9.45	15.76	4.63×10^{-6}	1×10^{-4}
335-67-1	Perfluorooctanoic acid	PFOA	414.07	N/A[a]	6.8	4.2	1.42×10^{4}
3380-34-5	Triclosan	TCS	289.55	4.80	11.54	6.93×10^{-4}	0.012
84-66-2	Diethyl phthalate	DEP	222.24	2.24	7.02	0.22	988
87-68-3	Hexachlorobutadiene	HCBD	260.76	4.90	5.16	20	3.2
81-15-2	Musk xylene	MX	297.27	4.90	11.82	3×10^{-5}	0.15
115-96-8	Tris (2-chloroethyl) phosphate	TCEP	285.49	1.44	5.31	1.14×10^{-3}	7.82×10^{3}
25154-52-3	Nonylphenol	NP	220.36	4.48	8.62	0.3	6
87-86-5	Pentachlorophenol	PCP	266.34	3.69	11.12	9.8×10^{-3}	14
25637-99-4	Hexabromocyclododecane	HBCD	641.70	5.63	11.89	6.27×10^{-5}	2.09×10^{-5}
99-76-3	Methylparaben	MeP	152.15	1.96	8.79	0.114	2.50×10^{3}
556-67-2	Octamethylcyclotetrasiloxane	D4	296.62	6.98	6.06	132	0.056
541-02-6	Decamethylcyclopentasiloxane	D5D5	370.78	8.07	6.93	33.2	0.017
540-97-6	Dodecamethylcyclohexasiloxane	D6	444.93	9.06	8.43	4.6	5.3×10^{-3}

[a] For perfluorooctanoic acid (PFOA), K_{OW} is not regarded as useful indicator of environmental partitioning, K_{OC} value is used to describe the sediment–water and soil–water partitioning, so the value of 3.53 for log K_{OC} and −2.4 for log K_{AW} were selected (Armitage et al., 2009).

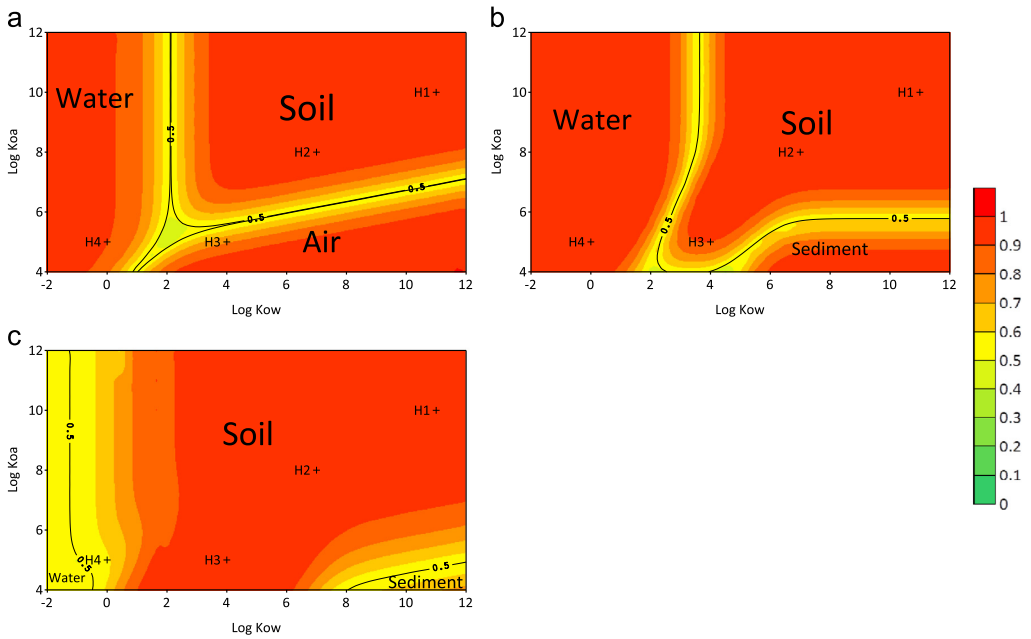

Fig. 1. Maximum mass distribution (kg kg^{-1}) in water, air, soil and sediment compartment of (a) ACC-HUMANsteady, (b) RAIDAR and (c) EUSES.

predictions. However, it is often the case that large uncertainties exist for input data for biological processes and these data are unavailable for many chemicals. In this study, although metabolism is ignored, the assumption of perfect persistency makes it less significant. These models also consider dairy and beef cattle separately to predict milk and meat concentrations.

Amongst all of the considered products of animal-origin, fish consumption is predicted to be one of the most important dietary exposure pathways, since there is a high potential for bioaccumulation of hydrophobic chemicals. As seen from Fig. 2, fish consumption is predicted to be the major exposure pathway for chemicals in the range of log K_{OW}=5–8 for EUSES, 3.5–10 for RAIDAR and 4–12 for ACC-HUMANsteady. For EUSES, the domain for high exposure from consumption of fish is much smaller than those domains predicted by RAIDAR and ACC-HUMANsteady. Take hypothetical chemical H2 for example, which represents a hydrophobic chemical. EUSES predicts the majority of exposure occurs via consumption of root vegetables whilst RAIDAR and ACC-HUMANsteady suggest that consumption of fish is more important. When considering the predicted environmental distribution shown in Fig. 1, the majority of H2 is predicted to be found in soil by three models. There are several possible explanations for this. One is that the mass distribution in water predicted by EUSES is lower than that for other two models, which is demonstrated in Fig. 1. Another explanation is that EUSES uses an empirical K_{OW}-based regression for the calculation of bioconcentration factors, which assumes fish reaches equilibrium with water and adopts multiple treatments for different ranges of K_{OW}, that is a simple linear model for chemicals with a log K_{OW} range of 1–6 and a parabolic equation applied for chemical with a log K_{OW} range 6–10 (Connell and Hawker, 1988; Veith et al., 1979).

The ratios of chemical concentrations of fish and total water were calculated and plotted in Fig. 3, which means BAFs in ACC-HUMANsteady and RAIDAR and BCFs in EUSES. The BCF predicted from EUSES is less than RAIDAR and ACC-HUMANsteady for a wide range of chemicals (log K_{OW} < 10). It also neglects dietary uptake and growth dilution, which can be important for substances with log K_{OW} > 5 (Undeman and McLachlan, 2011). So, as with many studies discussed previously, EUSES often underestimates fish concentrations (Rikken and Lijzen, 2004). Further, the overestimation of chemical concentration in roots, leads the exposure via fish to be proportionally less dominant in EUSES. As a result, this type of risk assessment as suggested by EUSES may not be suitable for use in 'non-standard' populations. Besides, when log K_{OW} > 10, BAFs predicted by ACC-HUMANsteady decrease gradually whilst those from RAIDAR drops rapidly, which results in the fish domain extending to a wider range of log K_{OW} in the partitioning space of ACC-HUMANsteady. This is because RAIDAR quantifies bioavailability and assumes only freely dissolved chemical is available to pass through fish gills (Arnot and Gobas, 2004). For the extremely hydrophobic compounds with high affinity to organic matter, the fraction of freely dissolved chemical concentration calculated by RAIDAR is low. However, the fish model in RAIDAR is applicable for organic chemicals with log K_{OW} values from 1 to 9, thus anything beyond this should be treated with caution (Arnot and Gobas, 2004).

Exposure via the consumption of meat and dairy products was indicated to be less significant than exposure via the consumption of vegetables and fish by all three models, as shown in Fig. 2. RAIDAR and ACC-HUMANsteady, however, did suggest that the intake of meat and dairy products as the dominant exposure routes for chemicals with K_{OW} values 2–4, although EUSES suggested that neither represented an important exposure pathway. For example, hypothetical chemical H3 represents a volatile and moderately hydrophobic chemical, for which ACC-HUMANsteady suggests human exposure occurs mainly via inhalation; whilst RAIDAR suggests that exposure via the consumption of fish and meat has a similar significance. EUSES predicted that exposure via root vegetable consumption was likely to be dominant. These predicted trends were unaltered under the Chinese dietary scenario. When linked to the predicted environmental distribution, as shown in Fig. 1, ACC-HUMANsteady predicted the maximum mass distribution would occur in air, whilst RAIDAR and EUSES predicted soil would be dominant. As a result, the high mass

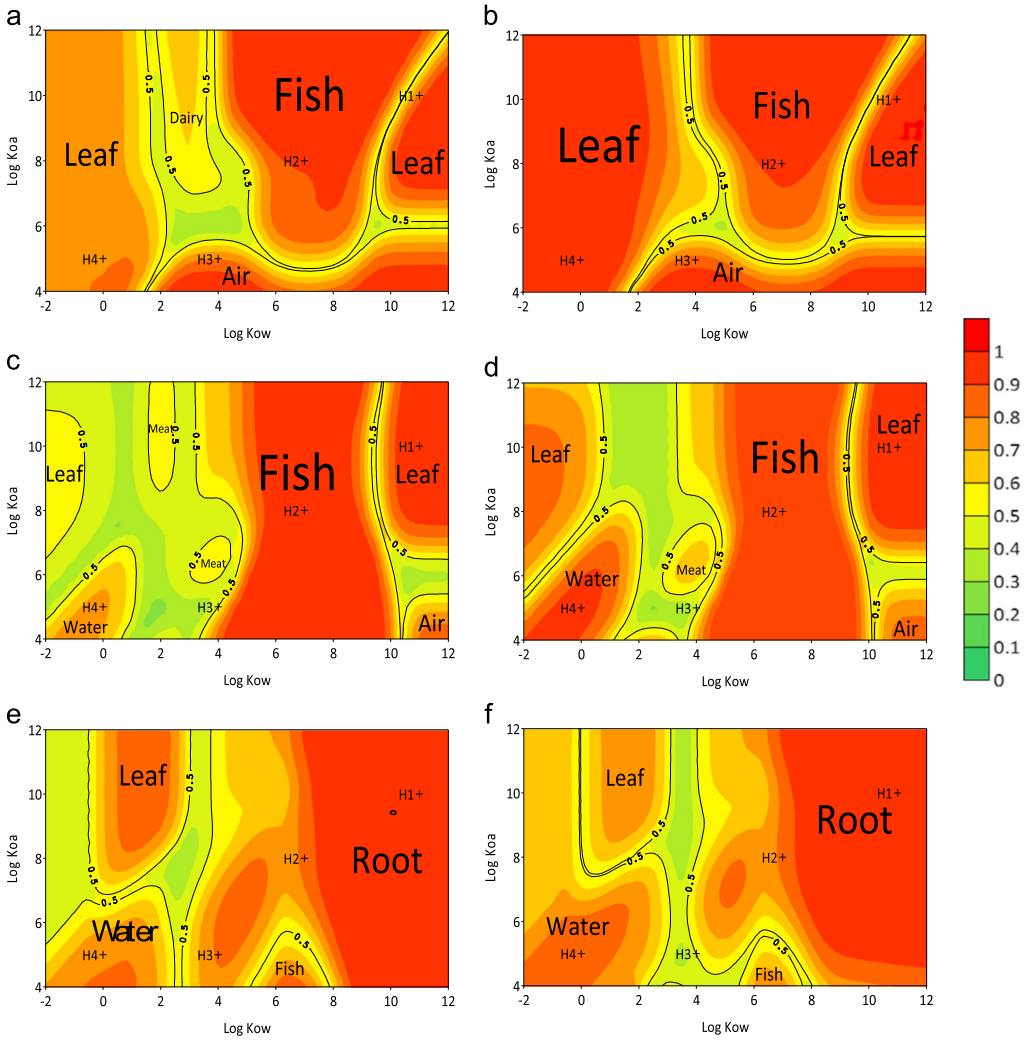

Fig. 2. Maximum exposure contribution (ng kg^{-1} d^{-1}/ng kg^{-1} d^{-1}) to total dietary intake using default model settings and Chinese dietary scenarios for ACC-HUMAN-steady, RAIDAR and EUSES. The solid lines indicate borders where one exposure pathway contributes to 50% of the total dietary intake (including inhalation and drinking water). Four representative hypothetical chemicals H1–H4 are also included.

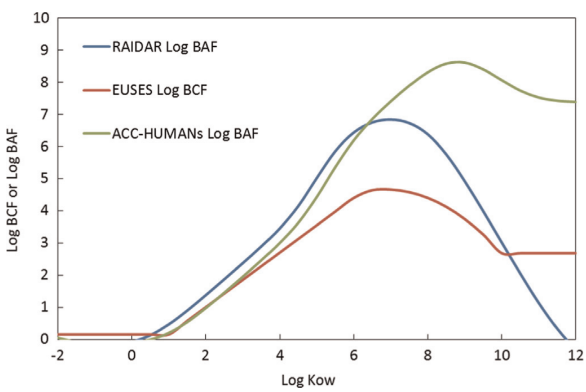

Fig. 3. The comparison of the logarithmic bioconcentration/bioaccmulation factor used by RAIDAR, EUSES and ACC-HUMANsteady for the calculation of chemical concentration in fish.

distribution in air results in high inhalation exposure using ACC-HUMANsteady. Furthermore, RAIDAR additionally includes poultry, pig and beef as dietary pathways in the agricultural food chain, thus the predicted proportion of exposure occurring via meat consumption in RAIDAR was higher than ACC-HUMANsteady and EUSES.

For chemicals with $\log K_{OW} < 2$, EUSES and RAIDAR consistently predicted that the consumption of both drinking water and leafy vegetables are important contributors to total exposure, while ACC-HUMANsteady suggests consumption of leafy vegetables as the most import contaminant exposure pathway. For example, for the hypothetical chemical H4, the predictions from both RAIDAR and EUSES suggested that the consumption of drinking water was the predominant exposure pathway, whilst ACC-HUMANsteady suggested that the consumption of leafy vegetables was the most important. When combined with the mass distribution information in Fig. 1, ACC-HUMANsteady and RAIDAR indicate water as the dominant compartment. However, EUSES predicted that soil contained a greater mass burden than water.

The three models employ multiple assumptions to predict chemical uptake in leafy vegetables. EUSES utilizes a K_{OW}-driven regression equation to calculate a transpiration stream concentration factor (TSCF), whilst RAIDAR assumes that chemical uptake into leaf occurs mainly from atmospheric deposition. K_{OA} is used to characterize the partitioning between the plant and gas phase of air (Arnot and Mackay, 2007). However, ACC-HUMANsteady assumes translocation from soil pore water to leaves via the transpiration stream is the main uptake process for hydrophilic chemicals, and the transpiration stream is in equilibrium with the soil pore water. Therefore, higher uptake is predicted for hydrophilic chemicals ($\log K_{OW} < 2$) by ACC-HUAMNsteady than either RAIDAR or EUSES.

The EUSES model combined with the Chinese dietary scenario suggests the importance of exposure via the consumption of drinking water is increased as a result of the relatively higher consumption of water in the Chinese scenario (Table 3). However, the importance of exposure via root vegetable consumption was reduced due to lower consumption rates in China compared to the default settings in EUSES. For ACC-HUMANsteady, the most significant change resulting from the Chinese dietary scenario is that the consumption of dairy as the important contributor to overall exposure under the default scenario was replaced by the consumption of leafy vegetables. This is due to increased vegetable consumption and decreased dairy product consumption as shown in Table 3. Similar trends were observed using RAIDAR. As a result, the increased consumption of leafy vegetables in Chinese diet suggests that this exposure pathway requires further investigation. A representative crop-specific plant model in China, such as for Chinese leaf instead of lettuce as used in Europe would also need to be considered (Legind and Trapp, 2009).

3.3. Predicted exposure pathways for real chemicals

To illustrate the output from the models for the study chemicals using both Western and Chinese scenarios, the predicted predominant exposure pathways from each model using default values (for Western countries) and modified Chinese consumption patterns are shown in Figs. 4–6. EUSES predicted that exposure via consumption of root vegetables is the most important exposure pathway for 10 of the 15 chemicals considered. This is also the case for EUSES when changing the dietary input to the Chinese scenario. RAIDAR predictions suggest that fish consumption was the most important exposure pathway for 10 out of 15 chemicals. However, these predictions changed for 1,2-dichlorobenzene, tris (2-chloroethyl) phosphate (TCEP) and methylparaben (MeP) under the Chinese dietary scenario using RAIDAR, as a result of the increased inhalation rate and water consumption relative to total consumption in the Chinese scenario compared to RAIDAR defaults (Table 3). In addition, predicted main exposure pathways for PCP, MeP and PFOA changed from dairy to leafy vegetable consumption using ACC-HUMANsteady under the Chinese dietary scenario, as dairy product consumption in China is much lower than that for Western diets. For remaining chemicals, ACC-HUMANsteady predicted similar primary exposure pathways for both Western and Chinese dietary scenarios.

TCEP, diethyl phthalate (DEP) and MEP have relatively low K_{OW} values and high water solubilities. As a result, they are expected to be mostly present in surface waters and show lower bioaccumulation potential. Interestingly, however, there are no consistent predictions from three models for these chemicals. For DEP, as an example, RAIDAR and ACC-HUMANsteady suggested that the consumption of leafy vegetables would be a dominant exposure pathway, whilst EUSES estimated that consumption of drinking water would be the predominant exposure route with consumption of leafy vegetables ranking as the second most important exposure pathway. Under the Chinese dietary scenario, the three models predicted consistent dominant exposure pathways for DEP. According to the UK Total Diet Study, the consumption of fish provided the greatest contribution to human exposure for DEP, although, drinking water was not considered in this study (Bradley et al., 2013). A survey carried out in China suggested that the consumption of beverages and cereals are the main exposure route for DEP (Guo et al., 2012), which is consistent with the prediction from EUSES. Another recent study carried out in New York State indicated the highest mean concentration of DEP was present in grain products (Schecter et al., 2013), which agrees with the predictions from the RAIDAR and ACC-HUMANsteady models. It

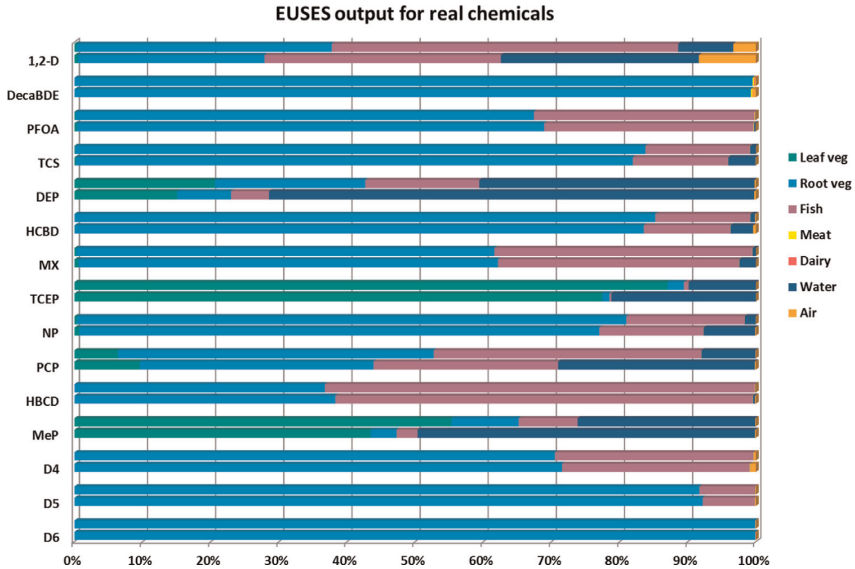

Fig. 4. The relative contribution of multiple food sources predicted by EUSES for real chemicals (ng kg^{-1} d^{-1}/ng kg^{-1} d^{-1}). The upper bars indicated the output with defaults diet pattern and lower bars showed the output with Chinese diet pattern.

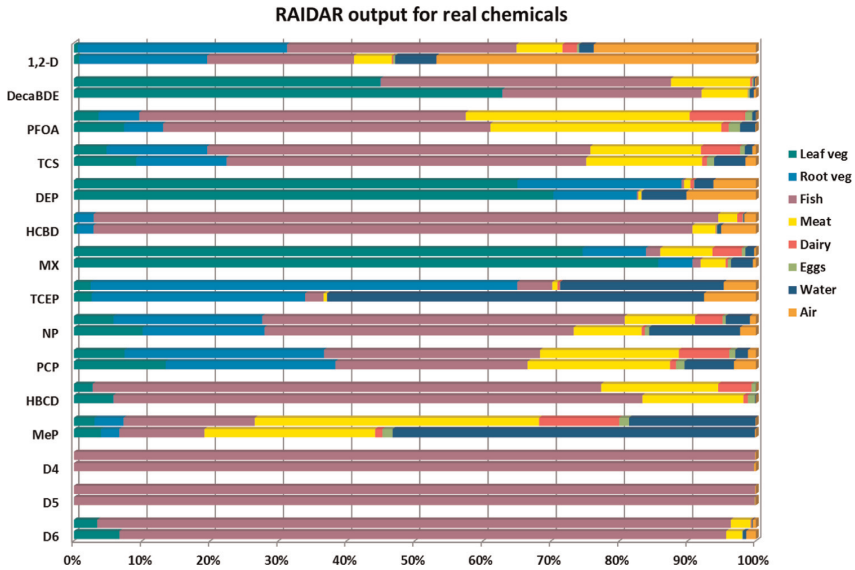

Fig. 5. The relative contribution of multiple food sources predicted by RAIDAR for real chemicals (ng kg^{-1} d^{-1}/ng kg^{-1} d^{-1}). The upper bars indicated the output with defaults and lower bars showed the output with Chinese diet pattern.

appears, therefore, that EUSES may underestimate the level of relative importance of plant uptake for hydrophilic chemicals using default settings.

For chemicals with moderate K_{OW} values and water solubilities, such as PFOA, PCP and NP, RAIDAR predicts consumption of fish as the major exposure pathway whilst EUSES estimates consumption of root vegetables as the most important route. In contrast, ACC-HUMANsteady suggested that consumption of dairy products may be the most important exposure route for PFOA and PCP whilst the fish consumption is the most important exposure route for NP. Under the Chinese dietary scenario, ACC-HUMANsteady predicted that the key exposure route for PFOA and PCP would be leafy vegetables rather than dairy. This may be due to the decreased dairy consumption and increased leafy vegetable intake in the Chinese diet as shown in Table 3. A modelling study showed that PCP mainly partitions into soil, thus vegetable consumption accounts for 99.9% of human exposure in U.S. and root uptake is the major source for vegetation contamination (Hattemerfrey and Travis, 1989), which is consistent with predictions from EUSES.

Hydrophobic chemicals with low volatilities and water solubilities, like hexabromocyclododecane (HBCD) and musk xylene (MX), generally have a high potential to bioaccumulate in fish. Predictions from the three models suggested that consumption of fish would be the major exposure pathway for HBCD. The predicted main exposure pathway remained the same for each model using the Chinese dietary scenarios. The concentration of HBCD in food samples has been measured in both Europe and China. According to data from the UK Total Diet Study, the consumption of

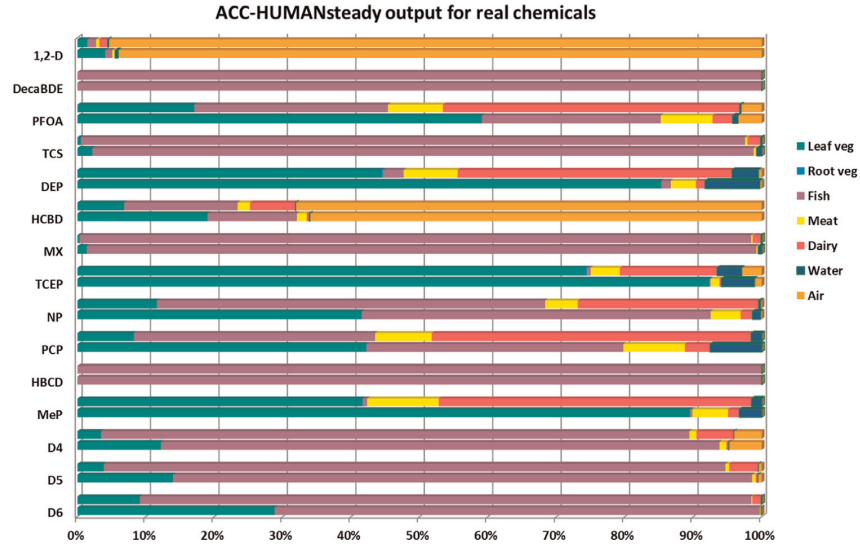

Fig. 6. The relative contribution of multiple food sources predicted by ACC-HUMANsteady for real chemicals (ng kg^{-} d^{-1}/ng kg^{-1} d^{-1}). The upper bars indicated the output with defaults and lower bars showed the output with Chinese diet pattern.

green vegetables and foods from animal origins were found to be the major source of dietary HBCD intake (Driffield et al., 2008). A study performed on Swedish food samples suggested that fish was a major source of dietary HBCD intake due to the high proportion of fish in the Swedish diet and the relatively high HBCD levels in fish (Remberger et al., 2004). In contrast, in China, meat and meat products accounted for up to 52% of estimated total dietary intake, with aquatic food groups accounting for a further 30%. This is may be due to a comparatively high consumption rate of meat products versus that of fish products in China (Shi et al., 2009).

D4, D5 and D6 have an unusual combination of physicochemical properties exhibiting high vapor pressures and a low water solubilities resulting in high air–water partition coefficients and high K_{OW} values. They also have long media-specific half-lives resulting in high environmental persistence and bioaccumulation potential (Whelan and Breivik, 2013). Exposure via fish consumption was identified as important by both RAIDAR and ACC-HUMANsteady for D4, D5 and D6, whilst fish consumption was identified as being important for D4 and root vegetable consumption an important pathway for D5 and D6 by EUSES. Predicted dominant exposure pathways remained the same under the Chinese dietary scenario. The importance of root vegetable consumption for D5 and D6 by EUSES may have occurred as a result of the overestimation of root concentrations. Monitoring data for cyclic volatile methyl siloxanes (cVMS) in foodstuffs is scarce and concentrations are frequently below the limit of detection in many biota samples. For example, total cVMS concentrations in fish samples collected across Europe were found to be $< 0.1\ \mu g\ g^{-1}$ ww. This is possibly a result of high elimination rates through metabolism (Wang et al., 2013), which are not considered in this study. Since these models are initially designed for persistent organic chemicals, the effect of ignoring internal metabolism would be minimal. However, as stated before ignoring metabolism may overestimate the chemical concentrations in biotic media.

3.4. Potential model adaptation for Chinese scenario

A stepwise or tiered approach in which the initial step relies on conservative screening methods is commonly used to minimize costs and focus resources on the most important issues and chemicals for which there is a potential health concern. Therefore, the simplicity of current models and accepted conservative modelling results would be suitable for an initial Chinese priority setting and risk assessment scheme. Currently, there are several bottlenecks in chemical exposure assessment in China, including access to national food consumption data, difficulty with food categorization, limited data on chemical residues in food, and so on. In addition, the different exposure scenarios that are required to cover the wide variability in China need to be developed and incorporated into current models with consideration of the variation in the Chinese diet.

3.4.1. High consumption of farmed aquatic foodstuffs

According to the Chinese Total Diet Survey, the average rate of consumption of marine derived food products at the national level was approximately $29.6\ g\ d^{-1}$ (L. Zhang et al., 2013). However, in many coastal cities, located on the east coast of China, the daily fish consumption was 105 ± 182 g for a healthy adult indicating a 4–5 times higher intake rate compared to the national average (Jiang et al., 2005). Moreover, marine fish accounted for up to 98% of total fish consumption in coastal regions like Zhoushan (Jiang et al., 2005). Nevertheless, the average national picture suggests that the production of freshwater and seawater products in China is approximately equal. It is interesting to note that China produced approximately 62% of all farmed seafood in the world in 2010 (FAO Fisheries and Aquaculture Department, 2010).

In many regions of the world, wild fishery resources are declining drastically (Melinda Meador et al., 2011). As a result, farmed fish may become increasingly relevant as a source for chemical exposure to people. Compared to wild fish, farmed fish lives in a simpler food web with different feeding habits and has a higher lipid content (Hites et al., 2004). It has been reported that the concentration of organochlorine contaminants is significantly higher in farmed salmon based on the analysis results of more than two metric tons of salmon, possibly caused via their diet and higher lipid fractions (Hites et al., 2004). Most exposure models, do not consider farmed fish exposure via diet, which could potentially result in the underestimation of residues in fish and fish products (Leung et al., 2010).

The lipid content varies significantly between farmed and wild fish, as well as freshwater fish and marine fish, which can result in different levels of bioaccumulation (Cheung et al., 2007; Hamilton et al., 2005). Whereas in models like ACC-HUMANsteady, only the consumption of wild fish was considered, which may result in an important underestimation for the dietary exposure via fish for the Chinese population, especially for residents in inland cities. EUSES assumes that fish exposure occurs via freshwater fish consumption only which limits its applicability to marine fish (Rikken and Lijzen, 2004).

3.4.2. The crop model for China

One important difference between Chinese and Western dietary patterns is the consumption rate of vegetables and cereals. Cereals and vegetables play an important role in the daily diet of the Chinese population, accounting for up to 46% and 32% of the total intake (Jin, 2008). Chemical bioaccumulation in crops from soil is more likely to occur with polar, non-volatile and persistent chemicals (Trapp and Eggen, 2013). However, the previous research has demonstrated that models may not predict the behavior of polar chemicals particularly well (Dettenmaier et al., 2009). A recent study detected the highest concentrations of parabens in vegetables, followed by condiments (soy sauce, vinegar, cooking wine, ketchup, bean paste, etc.) and cereals in China, although the major sources remain unclear (Liao et al., 2013). The relevance of dietary exposure to chemicals versus direct exposure to humans via the actual use of products (e.g. home and personal care products) is also unclear.

3.4.3. Different agricultural food chains

The three models considered in this study were designed mainly for the terrestrial food chain focussing on grass-cattle-beef/dairy products, which is the typical farmland style in Western countries. However, the Chinese situation is very different. In RAIDAR and ACC-HUMANsteady, cattle are assumed to absorb chemicals through respiration, ingesting soil and consumption of water and vegetation (Arnot and Mackay, 2007; Undeman and McLachlan, 2011). In Western countries, grass provides 70% of the fodder for animals, whilst 70% animal fodder comes from grain in China (FAO, 2002). Therefore feeding regimes in the agricultural food chain are also likely to be different in China.

3.4.4. Drinking water model

RAIDAR and ACC-HUMANsteady account for exposure via drinking water by assuming that chemical concentrations in drinking water are the same as those in surface water. This probably results in an overestimation of the risk from the consumption of drinking water as no treatment is assumed. EUSES, however, considers two surface water purification systems with different storage types: system 1 includes storage in open reservoirs, while system 2 includes dune recharge. The question arises if these two systems could be extrapolated for use in a risk assessment in China, since the underlying data are based on

limited measurements for the removal of organic compounds by activated carbon adsorption and biological processes in the Netherlands (Hrubec and Toet, 1992). System 2 (dune water recharge and slow sand filtration) is atypical in China, where conventional drinking water purification processes include coagulation, sedimentation, filtration and disinfection. It is also commonplace to boil tap water before consumption, which may lead to lower concentration of volatile contaminates (Kim et al., 2004). To date, Kim et al. have developed several model algorithms to predict exposure to chemicals via consumption of drinking water, which could be considered in future model developments for more accurate predictions (Anderson et al., 2004; Kim et al., 2004).

4. Conclusions

There is no consensus on what is the best available methodology for estimating exposure via dietary intake. The different approaches used in EUSES, RAIDAR and ACC-HUMANsteady were shown to present both their own advantages and disadvantages for the estimations of dietary exposure under Western and Chinese dietary patterns. The choice for the most appropriate approach largely depends on the purpose of the corresponding risk assessment. For preliminary screening purposes, the simple empirical EUSES model appears to be useful. However, its submodels for exposure via fish and vegetable consumption were not suitable for very hydrophobic compounds. However, RAIDAR and ACC-HUMANsteady have the advantage of providing mechanistic explanations of food chain bioaccumulation. They also indicated consistent predictions for the estimation of predominant dietary exposure pathways, and were more sensitive to the Chinese dietary patterns as presented in Fig. 2. In addition, the food web chain properties of mechanistic models are easier to re-parameterized for new/novel populations.

More assessment for the performance of exposure models with several potential adaptations is required before they can be applied to China with confidence. Since China has a very large population with varying regional dietary habits, the comprehensive evaluation of sensitivity and uncertainty of dietary preference is required for future studies. The fish model, which has been developed so far based on wild marine seafood products, needs to be expanded to consider different bioaccumulation models for the freshwater food chain including farmed-fish. Furthermore, despite the importance of consumption of vegetables, especially cereals, in China there is currently no specific model for organic chemical uptake into cereals that the authors are aware of (Legind and Trapp, 2009). Therefore, the development of a more specialized crop model (like wheat) should be explored.

Acknowledgment

The authors would like to thank the Safety and Environmental Assurance Centre, Unilever for funding this research.

References

Abraham, M.H., et al., 2002. On the mechanism of human intestinal absorption. Eur. J. Med. Chem. 37, 595–605.
Anderson, P.D., et al., 2004. Screening analysis of human pharmaceutical compounds in US surface waters. Environ. Sci. Technol. 38, 838–849.
Armitage, J.M., et al., 2009. Modeling the global fate and transport of perfluorooctanoic acid (PFOA) and perfluorooctanoate (PFO) emitted from direct sources using a multispecies mass balance model. Environ. Sci. Technol. 43, 1134–1140.
Arnot, J.A., Gobas, F., 2004. A food web bioaccumulation model for organic chemicals in aquatic ecosystems. Environ. Toxicol. Chem. 23, 2343–2355.
Arnot, J.A., Mackay, D., 2007. Risk Prioritization for a Subset of Domestic Substances List Chemicals Using the RAIDAR Model.
Arnot, J.A., Mackay, D., 2008. Policies for chemical hazard and risk priority setting: Can persistence, bioaccumulation, toxicity, and quantity information be combined? Environ. Sci. Technol. 42, 4648–4654.
Arnot, J.A., et al., 2010. Multimedia modeling of human exposure to chemical substances: the roles of food web biomagnification and biotransformation. Environ. Toxicol. Chem. 29, 45–55.
Arnot, J.A., et al., 2006. Screening level risk assessment model for chemical fate and effects in the environment. Environ. Sci. Technol. 40, 2316–2323.
Bradley, E.L., et al., 2013. Exposure to phthalic acid, phthalate diesters and phthalate monoesters from foodstuffs: UK total diet study results. Food Addit. Contam. Part A—Chem. Anal. Control Expo. Risk Assess. 30, 735–742.
Cheung, K.C., et al., 2007. Residual levels of DDTs and PAHs in freshwater and marine fish from Hong Kong markets and their health risk assessment. Chemosphere 66, 460–468.
Connell, D.W., Hawker, D.W., 1988. Use of polynomial expressions to describe the bioconcentration of hydrophobic chemicals by fish. Ecotoxicol. Environ. Saf. 16, 242–257.
Czub, G., McLachlan, M.S., 2004. A food chain model to predict the levels of lipophilic organic contaminants in humans. Environ. Toxicol. Chem. 23, 2356–2366.
Dettenmaier, E.M., et al., 2009. Chemical hydrophobicity and uptake by plant roots. Environ. Sci. Technol. 43, 324–329.
Domingo, J.L., et al., 2012. Dietary intake of polychlorinated dibenzo-p-dioxins and dibenzofurans (PCDD/Fs) by a population living in the vicinity of a hazardous waste incinerator. Assessment of the temporal trend. Environ. Int. 50, 22–30.
Driffield, M., et al., 2008. Determination of brominated flame retardants in food by LC–MS/MS: diastereoisomer-specific hexabromocyclododecane and tetrabromobisphenol A. Food Addit. Contam.: Part A 25, 895–903.
European Commision, 2003. Technical Guidance Document on Risk Assessment in support of Commision Directive 93/67/EEC on Risk Assessment for New Notified Substances, Commission Regulation (EC) No. 1488/94 on Risk Assessment for Existing Substances, and Directive 98/8/EC of the European Parliament and of the Council Concerning the Placing of Biocidal Products on the Market.
FAO, 2002. Food and Agriculture Organization of the United Nations 2002 World Agriculture: Towards 2015/2030.
FAO, 2010. Fisheries and Aquaculture Department, 2010. The State of World Fisheries and Aquaculture.
Fryer, M., et al., 2006. Human exposure modelling for chemical risk assessment: a review of current approaches and research and policy implications. Environ. Sci. Policy 9, 261–274.
Guo, Y., et al., 2012. Occurrence and profiles of phthalates in foodstuffs from China and their implications for human exposure. J. Agric. Food Chem. 60, 6913–6919.
Hamilton, M.C., et al., 2005. Lipid composition and contaminants in farmed and wild salmon. Environ. Sci. Technol. 39, 8622–8629.
Harrad, S., et al., 2004. Preliminary assessment of UK human dietary and inhalation exposure to polybrominated diphenyl ethers. Environ. Sci. Technol. 38, 2345–2350.
Hattemerfrey, H.A., Travis, C.C., 1989. Pentachlorophenol – environmental partitioning and human exposure. Arch. Environ. Contam. Toxicol. 18, 482–489.
Herzke, D., et al., 2013. Perfluorinated alkylated substances in vegetables collected in four European countries; occurrence and human exposure estimations. Environ. Sci. Pollut. Res. 20, 7930–7939.
Hites, R.A., et al., 2004. Global assessment of organic contaminants in farmed salmon. Science 303, 226–229.
Hrubec, J., Toet, C., 1992. RIVM Report 714301007. Predictability of the Removal of ORGANIC Compounds by Drinking Water Treatment.
Jiang, Q.T., et al., 2005. Human health risk assessment of organochlorines associated with fish consumption in a coastal city in China. Environ. Pollut. 136, 155–165.
Jin, S., 2008. No. 10 Report of Chinese Nutrition and Health Survey in 2002. People's Medical Publishing House, China.
Kim, E., et al., 2004. Estimating exposure to chemical contaminants in drinking water. Environ. Sci. Technol. 38, 1799–1806.
Kiviranta, H., et al., 2004. Market basket study on dietary intake of PCDD/Fs, PCBs, and PBDEs in Finland. Environ. Int. 30, 923–932.
Legind, C.N., Trapp, S., 2009. Modeling the exposure of children and adults via diet to chemicals in the environment with crop-specific models. Environ. Pollut. 157, 778–785.
Leung, S.Y., et al., 2010. Risk assessment of residual DDTs in freshwater and marine fish cultivated around the Pearl River Delta, China. Arch. Environ. Contam. Toxicol. 58, 415–430.
Liao, C.Y., et al., 2013. Occurrence of parabens in foodstuffs from China and its implications for human dietary exposure. Environ. Int. 57–58, 68–74.
Mackay, D., et al., 2009. The Evolution and Future of Environmental Fugacity Models. Springer, US.
Mackay, D., et al., 1996. Evaluating the environmental fate of a variety of types of chemicals using the EQC model. Environ. Toxicol. Chem. 15, 1627–1637.
McKone, T.E., et al., 2007. Merging models and biomonitoring data to characterize sources and pathways of human exposure to organophosphorous pesticides in the salinas Valley of California. Environ. Sci. Technol. 41, 3233–3240.
Melinda Meador, M., et al., 2011. Fishery Products Annual China.
Meyer, T., et al., 2005. Illustrating sensitivity and uncertainty in environmental fate models using partitioning maps. Environ. Sci. Technol. 39, 3186–3196.
Mitchell, J., et al., 2013. Comparison of modeling approaches to prioritize chemicals based on estimates of exposure and exposure potential. Sci. Total Environ. 458, 555–567.

Remberger, M., et al., 2004. The environmental occurrence of hexabromocyclododecane in Sweden. Chemosphere 54, 9–21.
Rikken, M.G.J., Lijzen, J.P.A., 2004. RIVM report 601516011/2004. Update of Risk Assessment Models for the Indirect Human Exposure.
Rodan, B.D., et al., 1999. Screening for persistent organic pollutants: techniques to provide a scientific basis for POPs criteria in international negotiations. Environ. Sci. Technol. 33, 3482–3488.
Rosenbaum, R.K., et al., 2008. USEtox—the UNEP-SETAC toxicity model: recommended characterisation factors for human toxicity and freshwater ecotoxicity in life cycle impact assessment. Int. J. Life Cycle Assess. 13, 532–546.
Schecter, A., et al., 2013. Phthalate concentrations and dietary exposure from food purchased in New York state. Environ. Health Perspect. 121, 473–479.
Shi, Z.-X., et al., 2009. Dietary exposure assessment of Chinese adults and nursing infants to tetrabromobisphenol-A and hexabromocyclododecanes: occurrence measurements in foods and human milk. Environ. Sci. Technol. 43, 4314–4319.
Shi, Z.X., et al., 2013. Levels of tetrabromobisphenol A, hexabromocyclododecanes and polybrominated diphenyl ethers in human milk from the general population in Beijing, China. Sci. Total Environ. 452, 10–18.
Song, B., et al., 2009. Assessing the health risk of heavy metals in vegetables to the general population in Beijing, China. J. Environ. Sci.—China 21, 1702–1709.
Trapp, S., Eggen, T., 2013. Simulation of the plant uptake of organophosphates and other emerging pollutants for greenhouse experiments and field conditions. Environ. Sci. Pollut. Res. 20, 4018–4029.
Undeman, E., et al., 2010. Susceptibility of human populations to environmental exposure to organic contaminants. Environ. Sci. Technol. 44, 6249–6255.
Undeman, E., McLachlan, M.S., 2011. Assessing model uncertainty of bioaccumulation models by combining chemical space visualization with a process-based diagnostic approach. Environ. Sci. Technol. 45, 8429–8436.
US EPA, 2012. Estimation Programs Interface Suite™ for Microsoft® Windows, v 4.11. United States Environmental Protection Agency, Washington, DC, USA.
Veith, G.D., et al., 1979. Measuring and estimating the bioconcentration factor of chemicals in fish. J. Fish. Res. Board Can. 36, 1040–1048.
Vermeire, T., et al., 2005. European union system for the evaluation of substances: the second version. Chemosphere 59, 473–485.
Vermeire, T.G., et al., 1997. European Union System for the Evaluation of Substances (EUSES). Principles and structure. Chemosphere 34, 1823–1836.
Vestergren, R., et al., 2012. Dietary exposure to perfluoroalkyl acids for the Swedish population in 1999, 2005 and 2010. Environ. Int. 49, 120–127.
Wang, D.G., et al., 2013. Review of recent advances in research on the toxicity, detection, occurrence and fate of cyclic volatile methyl siloxanes in the environment. Chemosphere 93, 711–725.
Wang, H., et al., 2012. Progress of environmental management and risk assessment of industrial chemicals in China. Environ. Pollut. 165, 174–181.
Whelan, M.J., Breivik, K., 2013. Dynamic modelling of aquatic exposure and pelagic food chain transfer of cyclic volatile methyl siloxanes in the Inner Oslofjord. Chemosphere 93, 794–804.
Xia, Z.H., et al., 2010. Health risk assessment on dietary exposure to polycyclic aromatic hydrocarbons (PAHs) in Taiyuan, China. Sci. Total Environ. 408, 5331–5337.
Xiaoli, D., et al., 2010. Drinking water-related exposure factors in a typical area of northern China. Res. Environ. Sci. 23, 1216–1220.
Xu, F.L., et al., 2013. Multimedia fate modeling of polycyclic aromatic hydrocarbons (PAHs) in Lake Small Baiyangdian, Northern China. Ecol. Model. 252, 246–257.
Yu, Y.X., et al., 2013. Temporal trends in daily dietary intakes of DDTs and HCHs in urban populations from Beijing and Shenyang, China. Chemosphere 91, 1395–1400.
Zhang, L., et al., 2013. Polybrominated diphenyl Ethers (PBDEs) and indicator polychlorinated biphenyls (PCBs) in foods from China: levels, dietary intake, and risk assessment. J. Agric. Food Chem. 61, 6544–6551.
Zhang, Q.Q., et al., 2013. Multimedia modeling of the fate of triclosan and triclocarban in the Dongjiang River Basin, South China and comparison with field data. Environ. Sci.—Process. Impacts 15, 2142–2152.
Zhang, Q.Q., et al., 2014. Emission estimation and multimedia fate modeling of seven steroids at the River Basin Scale in China. Environ. Sci. Technol. 48, 7982–7992.
Zhou, P., et al., 2012. Dietary exposure to persistent organochlorine pesticides in 2007 Chinese total diet study. Environ. Int. 42, 152–159.
Zongshuang, W., et al., 2009. Human exposure factors of Chinese people in environmental health risk assessment. Res. Environ. Sci. 22, 1164–1170.

PAPER II

Modelling bioaccumulation in fish by poly-parameter linear-free energy relationships (PP-LFERs)

Shizhen Zhao[1], *Oliver Price*[2], *Kevin C. Jones*[1], *Andrew J. Sweetman**[1]

[1] Lancaster Environment Centre, Lancaster University, Lancaster, LA14YQ, UK

[2] Safety and Environmental Assurance Centre, Unilever, Sharnbrook, MK44 1LQ, UK.

*Corresponding author:

Andrew J. Sweetman

Tel: +44 (0) 1524 594715

Email: a.sweetman@lancaster.ac.uk

Abstract

A wide range of studies has characterized different types of lipids, with regards to their interactions with chemicals. This has resulted in the development poly-parameter linear free energy relationships (pp-LFER) for the estimation of partitioning of neutral organic compounds to biological phases (e.g., storage lipids, phospholipids and serum albumins). The aims of this study were to explore and evaluate the influence of implementing pp-LFERs both into a one-compartment fish model and a multi-compartment physiologically based toxicokinetic (PBTK) model and the associated implications for chemical risk assessment. For this purpose, fish were used as reference biota due to their important role in dietary exposure to humans and as a biosorbent for organic chemicals. The bioconcentration factor (BCF) was used as the evaluation metric. Overall, preliminary results indicate that models incorporating pp-LFERs (R^2=0.75) slightly outperformed the single parameter (sp) LFERs approach in the one-compartmental fish model (R^2=0.72). The pronounced enhancement was achieved for compounds with log K_{OW} between 4 and 5 with R^2 increased from 0.52 to 0.71. Meanwhile, greater improvement was observed for multi-compartmental PBTK models with consideration of metabolism, making all predictions fall within a factor of 10 compared the measurements. For screening purposes, the K_{OW}-based (sp-LFERs) approach should be sufficient to quantify the main partitioning characteristics. Further developments are required for the consideration of ionization and more accurate quantification of biotransformation in biota.

Highlights:

- Implementation of pp-LFERs resulted in greater improvement compared to sp-LFERs in the PBTK model than in the one-compartment model.
- Large uncertainties are caused by quantification of biotransformation and ionization.
- sp-LFERs approach is sufficient for screening purposes.

Keywords:

Partition coefficients, pp- LFER, bioaccumulation, membrane, biotransformation

1 Introduction

Bioaccumulation in aquatic species is a critical endpoint in the chemical assessment required by authorities such as the European Chemical Agency (ECHA) and the United States Environmental Protection Agency (Gobas et al., 2009). One widely used assessment metric is the bioconcentration factor (BCF), which assesses the bioaccumulative potential of a chemical to biota through constant aqueous exposure under well-controlled laboratory conditions (Mackay et al., 2013). One principle of the regulation is that testing of chemical on animals should be done as a last choice (Laue et al., 2014). Much effort has been devoted to developing predictive models to estimate BCFs if no *in vivo* data are available. For preliminary screening purposes, the great majority of substances are screened based on their octanol-water partitioning coefficient (K_{OW}), which are widely used as an indicator of hydrophobicity and thus the portioning of a chemical from water to lipids and other organic phases (e.g., protein) (Debruyn and Gobas, 2007).

Over several decades, equilibrium partition coefficients of organic chemicals from environmental compartments to a tissue/organism are typically estimated by the total lipid content in combination with the K_{OW} (Mackay, 2001). So chemical concentrations in an organism/tissue are often normalized to the total lipid content, assuming that all lipids have identical sorption properties and the nonlipid fraction has a negligible sorption capacity (Endo et al., 2013). However, the suitability of this simplified approach has been questioned. It has been reported that the sorption capacity varies among different types of lipids (e.g., storage and membrane lipids) (Endo et al., 2011). Furthermore, the non-lipid components (e.g., proteins and serum) could also be a significant accumulation phase for organic compounds, especially for the H-bond donor compounds (Endo et al., 2012). More importantly, correlations with K_{OW} were expected to be valid only for restricted chemical domains. As attention on contaminants in the environment with more complex structures, like hormones, pharmaceuticals and surfactants grows, the task to go beyond K_{OW} and explore more refined approaches to mechanistically modelling bioaccumulation is urgently needed.

Much effort has been made for the exploration and development of poly-parameter LFER (pp-LFER), which could account the contribution of different specific and non-specific inter-molecular interactions (Abraham et al., 1994; Abraham et al., 2015). Underman et al. (2011) estimated the total sorption capacity of human body directly using the composite tissue/organ pp-LFERs, showing limited benefit (Undeman et al., 2011). This could be attributed to inappropriately using of single pp-LFER for partitioning to composite tissue/organ (e.g., blood, liver and brain), since the specific pp-LFERs of composite tissue/organ may only work well for the calibrated chemical. If a very diverse set of studied chemicals out of the calibration domain was applied, large errors may occur. For instance, very polar compounds, which may

predominately partition into the aqueous phase, may not work well in a biological phase calibrated by compounds mainly partitioning to lipid (Geisler et al., 2011). Thus, if different chemicals have different preferred phases within a composite material (e.g., fat tissue is a composite material mainly made up by water, neutral lipid, phospholipid and protein), a pp-LFER needs to be established for individual type phase instead of the whole bulk compartment. However, the individual pp-LFERs for a separate biological phase were not available at that time.

Recently, considerable studies have characterized different types of lipids, with regards to their interaction with chemical (Endo et al., 2011). Meanwhile, pp-LFERs for estimation of partitioning of neutral organic compounds to the biological phase have also been calibrated, e.g., storage lipids (Geisler et al., 2012), phospholipids (Endo et al., 2011), serum albumins (Endo and Goss, 2011a) and muscle protein (Endo et al., 2012).In addition, preliminary evaluation has been carried out to directly compare partition coefficients to tissues calculated by pp-LFERs model and K_{OW}-based models, indicating an order-of-magnitude approximation (Endo et al., 2013). However, pp-LFERs have not been tested for the estimation of partition coefficients for non-mammalian animals such as fish (Endo et al., 2013). Consequently, a further step to explore their benefit for the prediction of bioaccumulation potential and interpretation of biomonitoring results is desirable.

The main objective of this study was to explore the influence of implementing pp-LFERs on the estimation of bioaccumulation potential in different types of fish model. Fish were used a reference biota due to their important role in daily human diet and the fact that they act as an essential biosorbent for organic chemicals. Additionally, enough data availability exists for model evaluation compared to other animals. In this study, two types of fish model: a one-compartment fish model (Arnot and Gobas, 2004) and a multi-compartment physiologically based toxicokinetic (PBTK) model (Nichols et al., 1990) were set up with incorporated sp or pp-approach. Differences between model outputs were evaluated, and predicted BCFs were used to be compared with measured BCFs. The modelling uncertainty and implications for research and regulatory practices with regard to chemical risk assessment are also discussed.

2 Methods

2.1 General approach

Two types of mechanistic fish model were selected in this study, the one-compartment fish model (Arnot and Gobas, 2004), which assumes the chemical concentration is the same throughout the organism, and the multi-compartment PBTK model (Nichols et al., 1990), which considers chemical concentration may differ between various organs and tissues. Their selection in the chemical risk assessment depends on the question being addressed and the ease of data

collection under different scenarios (Landrum et al., 1992). The one-compartment model is suitable for preliminary risk assessment with simple inputs, while the multi-compartment model is preferred in higher-tier assessment to quantify organ-specific concentration. These two representative models were implemented under both traditional sp-LFER (traditional K_{OW} - driven) and newly-developed pp-LFERs to explore their performance in term of BCF prediction.

The only difference between the two approaches is the way of calculating partition coefficients to tissues/organs. All other equations and parameterizations were identical in the two modelling approaches. Firstly, both models were run using a set of chemicals with measured descriptors. The potential error in the measurement of chemical descriptors could be eliminated by using the same chemical descriptors for both approaches. Then the compiled dataset with measured BCFs was used as the endpoint to compare with the model predictions. The ionization was not considered in this evaluation process.

2.2 General fish model

2.2.1 One-compartment model

In the one-compartment model, fish was described as a well-mixed compartment and thus the target chemical is homogeneous in the whole fish body. In this type model, K_{OW} was regarded as a surrogate of lipid to quantify partition process chemical concentration in fish (C_b, kg kg^{-1}) could be modelled using following first-order equation:

$$dC_b/dt = k_u C_w - k_e C_b \quad (1)$$

where k_u is the uptake rate constant via gill ventilation (L/kg d), C_w is the truly dissolved chemical concentration in the water column (kg L^{-1}). k_e is the total elimination rate constant (d^{-1}), including respiratory exchange back to water (k_w), fecal egestion (k_f), biotransformation (k_m) and grow dilution (k_g). In this study, the organism was assumed to be fed completely “clean” food during the entire exposure period. Thus dietary uptake was ignored. But fecal egestion was included to account for redistribution of the target compound between the organism and its gut. The detailed parameterization was illustrated in Table S1. The steady-state condition was assumed. So BCFs was used to compare the difference between predicted and observed values. Under steady state (dC_b/dt=0), chemical concentrations in the organism and BCF could be calculated by:

$C_b = k_u C_w / k_e$ (2) and $BCF = C_b / C_w = k_u / k_e$ (3)

In all calculations, the diet was assumed to be 1.5% total lipid (1.2% neutral lipid, 0.3% phospholipid for pp-LFER calculation), 15% non-lipid organic matter (NLOM) and 83.5% water (Armitage et al., 2013). Mass-based tissue fractions were converted to volume-based

tissue fractions assuming densities of 0.9, 0.9, 1.0 and 1.0 L kg^{-1} for neutral lipid, phospholipid, NLOM and water, respectively.

2.2.2 Multi-compartment PBTK model

Chemical accumulation by fish can also be simulated by the physiologically based toxicokinetic (PBTK) fish model developed by Nichols and co-workers, which treats whole fish with individual compartments, like adipose, liver, kidney separately (Nichols et al., 1990). It is particularly useful to predict chemical concentration when a specific tissue/organ is the dominant site of action. The rainbow trout was used as a reference fish, due to it is used as a standard fish in many studies and has relatively abundant data. Detailed parameterizations were presented in Table S2 but are also presented elsewhere (Nichols et al., 2007). The amount of the chemical in each compartment is calculated:

$$dA_i/dt = Q_i \times (C_{art} - C_v) \quad (4)$$

where A_i is the chemical amount in compartment i (μg), Q_i is the arterial blood low to compartment i (L h^{-1}), C_{art} is the chemical concentration in arterial blood (μg L^{-1}), C_{vi} is the chemical concentration in venous blood after compartment i (g L^{-1}).

$$C_b = \sum A_i/BW \quad (5)$$

where C_b is the average chemical concentration in the whole fish body (μg kg^{-1}), $\sum A_i$ is the chemical amount in all compartments (μg), BW is the body weight of fish (kg).

In order to facilitate the comparison, the PBTK model employed several empirical relationships given by (Arnot and Gobas, 2004), including the calculation of C_{wd} (dissolved chemical concentration in water), C_d (chemical concentration in diet), G_v (total ventilation volume) and partition coefficient between fish and water ($K_{fish/water}$). The dietary pathway was ignored in both models with assuming only ingesting completely “clean” food. The considered compartment includes the liver, fat, kidney, richly perfused compartment and poorly perfused compartment for rainbow trout (Stadnicka et al., 2012).

2.3 Biotransformation

In general, models require metabolic biotransformation information to improve estimation for chemicals that are subject to biotransformation (Arnot et al., 2008). Even slow rates of biotransformation may significantly affect bioaccumulation in fish (Mackay et al., 2013). So the treatment of biotransformation was considered and described in detail as below for the two types of fish model. However, the measured data and available models for estimating biotransformation rates (both whole body and tissue-specific) are extremely limited. The

extrapolation approach described below is just a first approximation and should be used with caution due to the existence of high uncertainty.

2.3.1 One – compartment model

For the one-compartment model, the experimental biotransformation rate constant (k_m) was selected preferentially to predicted values from BCFBAF in EPISuite (US EPA, 2012), which was normalized to a 10 g fish at 15 ℃. These were converted to mass and temperature specific $k_{m,x}$ value as:

$$k_{M,\,X} = k_M (W_X / W_N)^{-0.25} \times exp\,(0.01 \times (T_X - T_N)) \quad (6)$$

where W_x is the study-specific mass of the organism (kg), W_N is the normalized mass of the organism (0.01 kg), T_x is the study-specific temperature, T_N is the normalized water temperature (15 ℃).

2.3.2 Multi-compartmental model (in vivo-in vitro exploration)

For the PBTK model, the whole-body metabolism rate k_m was from the EPISuite database (US EPA, 2012) was used to back-calculate the metabolism rate. The experimental values were also preferred. Thus, the hepatic clearance (C_{LH}, L h^{-1} kg^{-1}) was expressed as below and was normalized to the weight of fish:

$$C_{LH} = K_m \times V_{d,blood} \quad (7)$$

where the $V_{d,blood}$ (L kg^{-1}) is the apparent volume of distribution, referenced to the chemical concentration in mixed blood. This could be regarded as the sorption capacity of the fish relative to that of blood, and can be approximated by dividing the $K_{fish\text{-}water}$ by $K_{blood\text{-}water}$ (Nichols et al., 2006). The rate of amount metabolized in the liver (RAM_l, μg h^{-1}) was calculated as the product of the chemical concentration in the artery (C_{art}, μg L^{-1}) and the hepatic clearance (C_{Lh}, L h^{-1}) (Haschek et al., 2013). If the rate of biotransformation is very high, then the C_{LH} is rate-limited by the total blood flow to the liver (Nichols et al., 1990). This is just a first approximation of extrapolation of biotransformation rates, since it will be affected by many factors, e.g., the extrahepatic metabolism and protein binding (Nichols et al., 2007).

2.4 General pp-LFERs

Poly-parameter linear free energy relationship (pp-LFERs) are multiple linear regression models that use several solute- or sorbate-specific descriptors as independent variables (Endo and Goss, 2014a). There are three widely used forms of pp-LFERs expressed as:

$$log\ K = c + sS + aA + bB + vV + eE \quad (8)$$

$$log\ K = c + eE + sS + aA + bB + lL \quad (9)$$

$$log\ K = c + sS + aA + bB + vV + lL \quad (10)$$

where K is the partition coefficient between two phases. Equation (8) is used for partitioning between a condensed phase and a gas phase, and Equation (9) is used for partitioning between two condensed phases. The capital letters stand for the chemical descriptors: S refers to dipolarity/polarizability, A and B are the hydrogen bond acidity and basicity, L is the logarithm of the partition coefficient between hexadecane and air, E is the excess molar refraction ($cm^3\ mol^{-1}/10$), and V refers to the McGowan volume ($cm^3\ mol^{-1}/100$). The lower cases letters s, a, b, v, and l are regression coefficients, which indicate the complementary properties of the partitioning system. The Equation (10) uses V and L and has the advantage of wider application to organosilicons and highly fluorinated compounds (Endo and Goss, 2014b). It is therefore preferred to use. The selected pp-LFERs in this study were summarized in Table 1. It is generally expected that the extrapolation of a model beyond its calibrated domain may cause larger prediction errors than that would be expected for interpolation. Special caution should be taken for the serum albumin, whose fitting to data was not as good as other biological systems (Endo and Goss, 2011b). The ranges of individual descriptors used in each equation are summarized in Table S5 for each biological system in this study.

Table 1. Selected pp-LFER system coefficients used for the calculation of partition coefficients (L/L), the partition coefficients between storage lipid /phospholipid and water were chosen the ones calibrated with Equation (10).

Partition coefficients	**c**	**e**	**s**	**a**	**b**	**v**	**l**	**n**	**SD**	**R^2**	**T, ℃**	**Ref**
Octanol-water	0.34	-	-1.41	-0.18	-3.45	2.41	0.43	314	0.15	0.988	25	(Goss, 2005)
Storage lipid-water	0.52	-	-1.60	-1.92	-4.16	2.04	0.58	250	0.20	0.99	37	(Endo and Goss, 2014b)
Muscle protein – water	-0.94	-	-0.59	0.21	-3.17	2.13	0.33	46	0.23	0.94	37	(Endo et al., 2012)
Phospholipid-water	0.38	-	-0.94	0.05	-4.10	2.00	0.49	134	0.31	0.97	37	(Endo and Goss, 2014b)
Bovine serum albumin-water	0.35	-	-0.46	0.20	-3.23	1.84	0.28	82	0.41	0.79	37	(Endo and Goss, 2011b)
ΔU_{AW}, kJ/mol	13.31	9.91	-2.84	32.01	41.82	-	6.35	368	3.68	0.96	-	(Mintz et al., 2007)
ΔU_{OA}, kJ/mol	6.49	1.04	-5.89	53.99	8.99	-	9.18	138	2.66	0.99	-	(Mintz et al., 2007)

2.5 Implementation of pp-LFERs

2.5.1 Incorporating pp-LFERs in the one-compartment model

In the one-compartment model, the partition coefficient between fish and water is quantified as (Arnot and Gobas, 2004):

$$K_{fish/water} = (f_{lipid} / D_{water} + f_{NLOM} \times \beta / D_{NOLM}) \, Kow + f_{water} \quad (11)$$

where f_{lipid}, f_{NLOM} and f_{water} are the volume fractions of lipid, non-lipid organic matter (NLOM) and water, as quantified in Table S2; β is the proportionally constant of *NLOM* to octanol, $\underline{D_{water}}$ and D_{NOLM} are the density of lipid and non-lipid organic matter.

Replacing the sp-LFERs by pp-LFERs, the partition coefficients are modified as:

$$K_{fish/water} = (K_{storage\ lipid/water} \times f_{storage\ lipid} / D_{lipid}) + (K_{\ phospholipid/water} \times f_{phospholipid} / D_{phospolipid}) + (K_{\ protein/water} \times f_{protein} / D_{protein} + f_{water} / D_{water}) \quad (12)$$

where $f_{storage\ lipid}$, $f_{phospholipid}$ and $f_{protein}$ are the volume fractions of storage lipid, phospholipid and protein of fish defined in Table S3, *K* values indicate the individual partition coefficients between target biological medium and water, and *D* is the corresponding density of each tissue. The densities of storage (neutral) lipid, phospholipid, protein and water are assumed to be 0.93, 1, 1.4 and 1 kg L^{-1} (Endo et al., 2013). A similar treatment was performed for the partition coefficient between gut and fish ($K_{gut\text{-}fish}$).

2.5.2 Incorporating pp-LFERs into PBTK model

In the PBTK model, the $K_{blood\text{-}water}$ was derived as (Bertelsen et al., 1998):

$$K_{blood/water} = 10^{0.72 \times \log Kow + 1.04 \log (\alpha_b)} + \gamma_b \quad (13)$$

where the α_b is the lipid content of blood tissue, γ_b is the water content of blood tissue and other partition coefficients $K_{organ/blood}$, including $K_{liver/blood}$, $K_{fat/blood}$, $K_{muscle/blood}$ and $K_{\ kidney/blood}$, are calculated from $K_{blood/water}$ as:

$$K_{organ/blood} = (10^{0.72 \times Log\ Kow + 1.04\ Log\ (\alpha_i) + 0.86} + \gamma_i) / K_{blood/water} \quad (14)$$

Where the α_i and γ_i are the lipid and water contents in the individual organ. The composition of each organ was as assumed to the defaults for rainbow trout in the original PBTK model. But in pp-LFER PBTK model, the $K_{organ/water}$ was calculated based on the biological composition of each organ, mainly containing neutral lipid, phospholipid, protein and water. The specific composition of each biological compartment (e.g., blood, kidney and liver) is presented in Table S4. It was assumed here that total lipid only contains neutral lipid and phospholipid. The fraction of bovine serum albumin (BSA) was selected from a study based on mammals (Endo et

al., 2013). The treatment of fat content in lean tissues (all compartments exclude the fat) and the temperature dependence of partitioning is detailed in the supporting information. The bovine serum albumin was only considered to be present in the blood tissue, since its existence is fairly minimal and its variation may increase the model uncertainty. The $K_{organ/blood}$ was calculated in the pp-LFERs approach as:

$$K_{organ/blood}=K_{organ/water}/K_{blood/water} \quad (15)$$

2.6 Solute descriptors

Experimentally measured solute descriptors are available for thousands of chemicals and have been compiled as a free-of-charge database (http://www.ufz.de/index.php?en=31698). The initial chemical dataset including 235 compounds (Brown and Wania, 2009), were selected from 1460 individual chemicals and considered to fall within the range environmentally relevant compounds. Several updated experimental values of descriptors were also added from the recently published literature to cover more polar and complex chemicals, including organosilicon compounds, highly polyfluorinated chemicals, flame retardants (e.g., polybrominated diphenyl ethers, hexabromocyclododecane, bromobenzenes, trialkyl phosphates), pesticides, polychlorinated biphenyls (PCBs) and heterocyclic aromatic as well as nitroaromatics compounds (Geisler et al., 2011; Stenzel et al., 2013a; Stenzel et al., 2013b). Ionization was not taken into account in this study, as the pp-LFER approaches to ionic chemicals are still a subject of ongoing research. No successful application to environmental and biological processes has been reported so far (Endo and Goss, 2014a). Selected chemicals were categorized into different polarity according to the A and B values defined here: nonpolar (both A and B $\leq$ 0.2), monopolar (including H-bond acceptor (A >0.2 but B <0.2) or H-bond donor (A <0.2 but B>0.2)), and bipolar (either A or B 0>0.2) compounds. Their individual impact on pp-LFERs is characterized.

Two subsets of compounds were added to the whole dataset. One is the chemicals with strong H-donor function (A>0.3), because substantial differences in the “aA” term have been observed for the pp-LFER equations for octanol and storage lipids for this type of chemical. Thus, partitioning to octanol and storage lipid are expected to be different, which contrasts with most typical assumptions that the octanol is a good surrogate for lipids. The other subset contained complex compounds with more than one polar functional group per molecule. The selected compounds cover hormones and hormone active compounds (e.g., estrone, bisphenol A, phthalate esters), fungicides, herbicides and mycotoxins. The representative functional groups include alcohol, amide, carbonyl, nitrite, ester, epoxide and phenyl groups. Ignorance of

ionization could potentially generate uncertainty, since the partitioning behaviour of ionic species is different from neutral species (Abraham and Acree, 2010).

2.7 Compilation of measured BCFs dataset

The main source of observed BCF data was extracted from Arnot and Gobas. (2006). It contains multiple BCF measurements of chemicals in different fish species with varying physiological conditions, which reflect realistic variations in BCFs across different fish species and system conditions. The dataset mainly contained nonpolar compounds and was firstly used to test the model performance for the one-compartment model. The majority of data points are from studies using common carp (*Cyprinus carpio*), fathead minnow (*Pimephales promelas*), zebrafish (*Danio rerio*) and rainbow trout (*Oncorhynchus mykiss*).

Secondly, chemicals with observed BCFs from studies in rainbow trout were extracted to a subset of 41 distinctive compounds and 355 data points, which was used to evaluate the PBTK model requiring specific physical fish information. In addition, other publicly available data were also compiled to cover additionally observed BCFs for complex polar chemicals. Finally, 21 additional compounds were compiled from the Pesticide Property Database (http://sitem.herts.ac.uk/aeru/ppdb/en/index.htm) and other available literature.

It is ideal to have study-specific experimental information about water temperature, fish weight, and lipid content to predict individual BCF values. However, many studies did not record such information. Consequently, a value of 5% was used as a first approximation of whole body lipid content (Arnot and Gobas, 2006). All selected experimental BCF values were lipid normalized.

2.8 Inter-comparison of models

A difficult task is to systematically compare the results from pp-LFER and sp-LFER models. One approach is to compare the predicted results directly (Gotz et al., 2007). The another is to use space maps to present the variations in models outputs as a function of partition coefficients, like K_{AW}, K_{OA} and K_{OW} (Brown and Wania, 2009). Firstly, the entire dataset was used to compare the predicted values of partition coefficients calculated by sp/pp-approach and the predicted concentration in fish. Individual contributions of different forms of intermolecular interaction to partitioning from organs/tissues to water can be compared to explore the dominant interactions. The statistical analysis was conducted using average model bias (MB) and average absolute model bias (AMB) to assess model performance as calculated below:

$$MB = \frac{\sum_{i=1}^{n} log(\frac{BCF_M}{BCF_E})}{n} \quad (16)$$

$$AMB = \frac{\sum_{i=1}^{n} ABS\left[log(\frac{BCF_M}{BCF_E})\right]}{n} \quad (17)$$

where BCF_M is the modelled bioconcentration factor, BCF_E is the measured bioconcentration factor, n is the number of observations, *ABS* means the absolute deviation. *MB* represents the average factor by which the model output deviates from the observation. It is useful to indicate the direction of any systematic bias. The root mean square error (RMSE) and the square of correlation coefficient (R^2) were also used to characterize model performance.

In this study, the only difference between model inputs is the replacement of octanol-based sp-LFER with pp-LFERs. Therefore, any observed differences will be attributable to this difference. The experimental errors in measuring the partitioning coefficients were not considered in this study. In order to reduce the uncertainty from the measurement of K_{OW}, K_{OW} used in sp-LFERs was also derived from pp-LFERs instead of using measured K_{OW} values.

3 Results & Discussion

3.1 Comparison of outputs by the sp/pp-approaches

In order to identify the types of chemicals for which the implementation of pp-LFERs would make a significant difference, the predicted concentration of fish and partition coefficients were compared for chemicals possessing a wide range of partitioning properties using the solute descriptors. The results are presented in chemical partitioning plots as a function of chemicals' octanol-air-water partitioning properties, described by K_{AW} and K_{OA} (Figure 1). In addition, the influence of the polarity is also illustrated in Figure 1 (a, b). The different categories of nonpolar, monopolar and bipolar compounds were defined based on the descriptor values of A and B defined in Section 2.6.

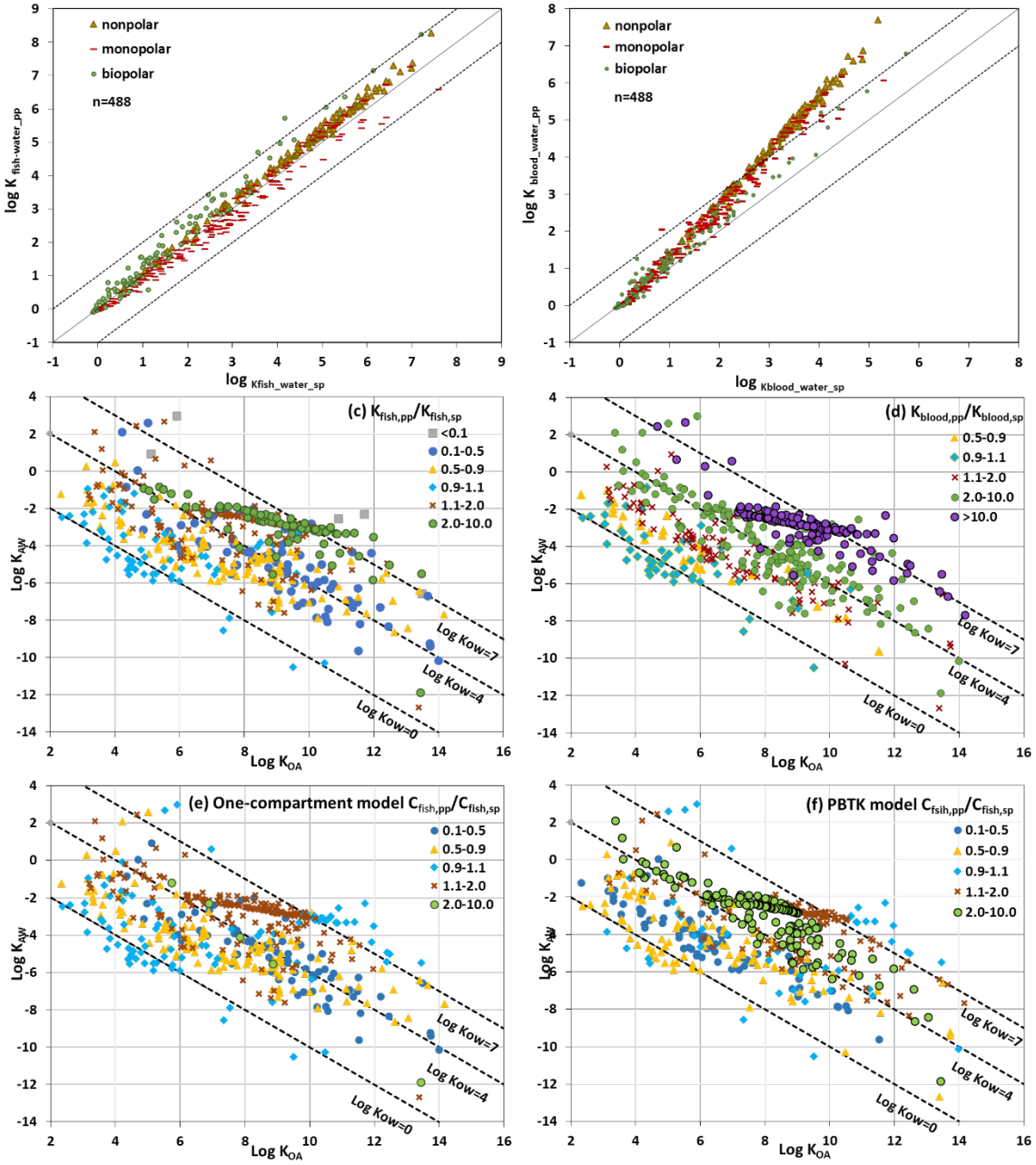

Figure 1**.** Comparison of calculated logarithmic fish-water partition coefficients (a) and blood-water partition coefficients (b) by pp-LFERs and sp-LFERs values with different defined polarities. The multiple colours and symbols represented different polarities defined by A and B. For nonpolar compounds, both A and B ≤0.2 (N=156); for monopolar compounds, either A or B is >0.2 (N=224); for bipolar compounds, both A and B >0.2 (N=108). Chemical partitioning space plots indicated the ratios of partition coefficient between water and whole fish (c) also blood (d); concentrations in fish calculated using sp and pp approach in one-compartment model (e) and in multi-compartment PBTK models (f). Different colours indicated the magnitude of the quotient. The diagonal lines indicate the log K_{OW} equal to 0, 4 and 7.

3.1.1 Comparison of $K_{fish\text{-}water}$ by the sp/pp-approaches

In general, the log $K_{fish/water}$ was estimated consistently via both sp and pp approaches. 99% of selected substances the observed differences was less than 1 log unit. Compounds with different polarities indicated slightly different deviations. For all nonpolar compounds in the dataset, the $K_{fish/water}$ calculated by pp-LFERs was larger than that calculated by sp-LFERs. However, the compounds with bipolar functional groups tended to show a larger difference between $K_{fish/water}$ calculated by these two approaches. The largest difference of log $K_{fish\text{-}water}$ was observed for bis(2-ethylhexyl) hydrogen phosphate, up to 1.5 log unit, with a strong H-bond donor/acceptor (A=0.96, B=1.12). Its log $K_{lipid/water}$ was less than log Kow by 2 log units, leading to the large deviation of calculated $K_{fish\text{-}water}$. For such compounds, there may be a chance to overestimate the bioaccumulation potential by directly using K_{OW}.

When looking at the dependency of deviation with the different range of log K_{OW} (Figure 1-c), the discrepancy also gradually raised with increased hydrophobicity. For hydrophilic compounds (log K_{OW} <0), both approaches agreed well with each other within about 10%. For chemicals with log Kow>4 and log K_{OA} >8, the pp-approach generally predicted $K_{fish\text{-}water}$ on average two times higher than that predicted by sp-approach. But the deviation did not consistently propagate to the predictions of concentration in fish. The differences between predicted concentrations by both approaches were indicated by a factor of 10 for all compounds in the partitioning map (Figure 1-e). Both approaches agreed reasonably well for hydrophilic (log Kow<0) and highly hydrophobic compounds (log Kow>7) with the quotient between 0.9-1.1, while the deviation occurred on the calculation of $K_{fish\text{-}water}$ was up to 35 times. The underlying explanation could be that $K_{fish\text{-}water}$ has different extent of impact on the determination of BCFs, which is dependent on chemical hydrophobicity. For instance, $K_{fish\text{-}water}$ was observed to have a greater contribution to the bioaccumulative potential for hydrophobic chemicals with a high tendency for bioaccumulation (Kuo and Di Toro, 2013b). While, partitioning to organic carbon (bioavailable portion) contributed more to the BCF values for highly hydrophobic compounds (Kuo and Di Toro, 2013b).

3.1.2 Comparison of $K_{blood\text{-}water}$ by sp/pp-approaches

Greater differences were observed for the log $K_{blood/water}$ calculated by the sp-LFER and pp-LFERs approaches, indicating increased divergence with higher partition coefficients between blood and water for compounds with different polarities. 72% of selected substances fell within a difference of less than 1 log unit. In the total data set, the largest difference up to 2.5 log units was found for 1, 2, 3, 4, 5, 6, 7, 8-octachloronaphthalene in the category of nonpolar compounds. This compound has a extremely high L=12.88, leading to higher partition coefficients between biological tissue and water than that between octanol and water.

A different trend was observed for the relationship between hydrophobicity and the deviations of the predictions by sp-LFERs and pp-LFERs models than that for the $K_{fish/water}$. For 86% of the selected substances, the pp-LFERs model estimated higher blood-water partition coefficients than the sp-LFERs model. Larger deviations were observed for increasing hydrophobicity for all three types of compounds. Especially for nonpolar compounds, the deviation between the sp-LFERs and pp-LFERs models indicated a positive relationship between the log K_{OW} and a high correlation coefficient of R^2=0.96 was observed between them (Figure S1-a). A higher deviation resulting from incorporating pp-LFERs were expected for polar compounds than for nonpolar compounds. The underlying reason for this could be caused by the inclusion of protein in the pp-approach, which has large deviation (1-2 log units) than $K_{storage\ lipid\text{-}water}$ for nonpolar compounds and the deviation increased with hydrophobicity (Endo et al., 2012). The absolute values of Ll+Vv terms, which describe van der Waals interactions, was plotted against hydrophobicity, since they have a fairly high cross-correlation. The sum of Ll and Vv consistently rose in all biological systems (illustrated in Figure S1). The divergences grew between the biological compositions and octanol with increased hydrophobicity. Therefore, the greater deviation probably occurs as a consequence of not properly capturing the behaviour of van der Waals' forces for chemicals with high values of L. The divergence between predicted concentrations in PBTK model is similar to that from the one-compartment model, since both models employed several identical empirical relationships, including the calculation of dissolved chemical concentration and chemical concentration in diet (Arnot and Gobas, 2004).

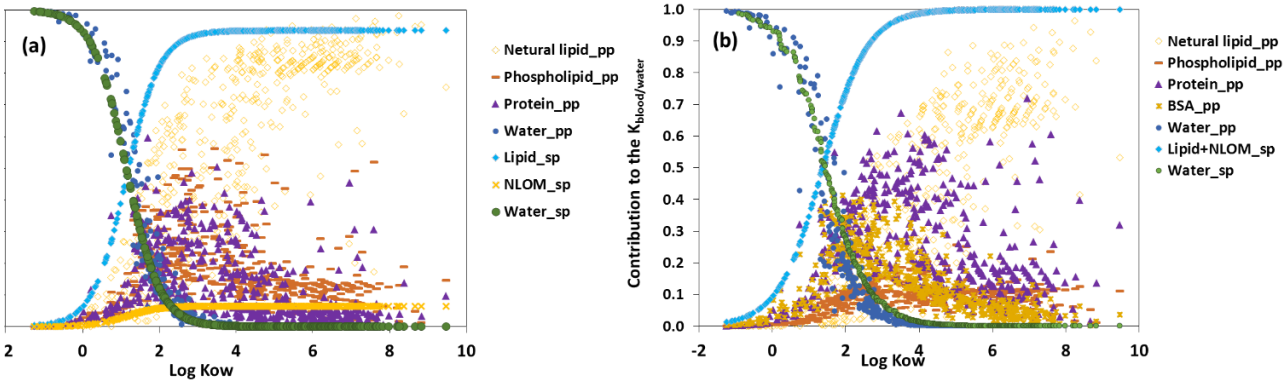

Figure 2. Contribution to total partition capacity by different biological tissues with the full range of K_{OW}: (a) individual contribution to the total $K_{fish/water}$; (b) individual contribution to the total $K_{blood/water}$.

3.2 Contribution to the total sorption capacity

In order to explore the importance of neutral lipids, phospholipids (membrane), proteins, bovine serum albumin (BSA) and water as a sorptive matrix, the contribution of each biological phase calculated via sp-LFERs and pp-LFERs were plotted as a function of log K_{OW} in Figure 2. Differences between these two approaches were due to the differences of the considered sorptive matrixes. The greatest disparity is caused by the tissue that makes the largest contribution to the total partitioning capacity. For the one-compartment fish model, the sp-LFERs model only considered neutral lipid, water and NLOM (a relative sorptive capacity proportional to lipid). Therefore, the contribution of each biological absorbent to the total partitioning capacity presented a continuous trend the change of chemical hydrophobicity (illustrated in Figure 2-a). However, the shifting trend was more complex for the pp-LFERs model, with additional consideration of protein and phospholipid without directly relating to octanol. It is obvious that the contributions of water and lipid were consistent for hydrophobic and hydrophilic chemicals for both models, since the water and lipid are the absolute predominant sorptive matrixes, respectively. For the chemical with moderate K_{OW} values ($2<\log K_{OW}<6$), the phospholipid and protein made important contributions, up to 39% for protein and 61% for phospholipid, respectively. This also helps to explain that the large deviation in calculated partitioning between fish/blood and water for a chemical with moderate hydrophobicity (Figure 1-c).

For the PBTK models employing pp-LFERs, the individual contribution was also calculated between blood and water for the whole range of K_{OW} in Figure 2-b. A similar trend was observed for predicted blood-water partitioning as the comparison for the $K_{fish/water,}$ which continuously change with the varied K_{OW} values. However, the pp-LFERs model predicted more dispersed values in the individual biological compartment. The protein and BSA also contributed to the total blood-water partitioning up to 72% and 41%, respectively Their individual contribution did not indicate a consistent shift with the increased log K_{OW}, especially for protein, whose points were scattered on a wide range of log K_{OW} between 2 and 9. This could be due to the fact that hydrophobicity is not a perfect indicator for absorption to protein. Take an example, eicosanoic acid is the most hydrophobic compound in the database with log Kow=9.47. However, protein contributes 32% to the total blood-water partition coefficients. BSAcontributed most in the moderate range of log K_{OW}=1 ~ 5, based on the currently used chemical set. Phospholipids also contributed between 10~20% for compounds with Log K_{OW} >1 peaking at about log K_{OW}=4~5. It is noteworthy that the regression relationship used for the calculation of blood-water partition coefficients, was only based on compounds with a limited log K_{OW} range from 1.46 to 4.04. Thus, any compounds outside this range may cause potential errors and should be used with caution (Bertelsen et al., 1998; Nichols, 2002). This relationship

is still commonly used in PBTK modelling (Stadnicka et al., 2012). Evaluation of the regression equation to describe tissue/water partitioning is out of the scope of this study.

From the comparison of the contribution to the total fish/blood-water partition coefficients above, it also could help to explain how the difference occurs. In the range of log K_{OW} from 2 to 6, protein models an important contribution to both partition coefficients. Using octanol as equivalent to lipid could overestimate the contribution of lipid, but the sp-LFER approach could also underestimate the contribution of protein. As a result, the total partition coefficient calculated by the sp and pp-approaches could be expected to be different within a reasonable range, since the underestimation and overestimation could proportionally cancel out with each other. The similar result was also observed in comparing the lipid-octanol model and pp-LFERs model to predicting partition coefficients of tissue-waster (Endo et al., 2013).

3.3 Comparison with experimental data

3.3.1 One-compartment model

There are 835 data points from fish species chosen from the experimental database for 110 distinct compounds (Arnot and Gobas, 2006). The chemicals covered the K_{OW} range from -0.15 to 8.67. However, most data points fell in the log K_{OW} range between 3~5 as illustrated in Figure S3. In order to examine the magnitude of the deviation correlated by the hydrophobicity between predictions and measurements, the impact of applying pp-LFER equations to the individual ranges of log K_{OW} and the whole dataset was explored and presented in Table 2. In general, the pp-LFER model performed slightly better in terms of predicting BCF, with increased coefficient of determination and absolute model bias for the whole dataset. The deviations between the sp and pp-LFERs models prediction, did not show a pronounced K_{OW} dependency. For compounds with log K_{OW} < 2, both models underestimated BCFs and the divergence increased with increased hydrophobicity. The underestimation is most severe for log K_{OW} <1 with an average 2.9 log units for both approaches. The pp-LFERs model did generally improve the coefficient of determination, for compounds with log K_{OW} <3. This is because the calculation of $K_{fish/water}$ is predominantly contributed by water (illustrated in Figure 2). Thus the effect of replacing sp with pp-LFERs is minimal. Therefore, there is no clear advantage observed for using pp-LFERs model instead of sp-LFERs for compounds with log K_{OW} < 2. For the middle range of log K_{OW} from 4 to 5, the BCFs predicted by pp-LFERs were found to getter fit observed values compared the sp-LFERs model. This is due to a better quantification of partitioning behaviour of polar compounds such as phenols in this range, by adding separate consideration of protein and phospholipid, which makes signification contribution in such case.

For very hydrophobic compounds (7<log K_{OW} <9), both models predicted the selected BCFs reasonably well(R^2=0.80-0.96). This is because the lipid is the main sorbing matrix in this K_{OW}

range. In addition, it has been demonstrated that depuration kinetics is more important for hydrophobic chemicals with higher bioaccumulation potentials while partitioning to dissolved/ particulate organic carbon (the bioavailable part) plays an important role for highly hydrophobic chemicals (Kuo and Di Toro, 2013b). Therefore, improved partition coefficients may not greatly influence the model performance using the pp-LFERs model in the high log K_{OW} range (7~9). On the other hand, chemicals with low bioaccumulative potential (log BCF≤ 2) are generally mainly determined by fish-water partitioning coefficients (K_{bw}) and thus more pronounced improvement would be expected (Kuo and Di Toro, 2013b). Consequently, the comparison should be made with caution for the very hydrophilic and super-hydrophobic compounds, due the limited data points.

Table 2. Statistical analysis of comparisons between model predictions and observations for chemicals with classified Kow ranges.

Log K_{OW}	**sp-LFER**				**pp-LFER**			
range	R^2	RMSE	MB	AMB	R^2	RMSE	MB	AMB
<1	0.65	2.91	-2.37	1.66	0.69	2.91	-2.37	1.65
1-2	0.18	1.01	-0.88	1.01	0.39	1.09	-0.87	1.06
2-3	0.09	0.13	0.00	0.44	0.28	0.28	-0.11	0.37
3-4	0.63	0.11	-0.01	0.39	0.57	0.11	0.03	0.39
4-5	0.52	0.12	-0.15	0.39	0.71	0.07	-0.01	0.30
5-6	0.45	0.07	0.25	0.73	0.48	0.09	0.43	0.74
6-7	0.44	0.17	0.28	0.44	0.45	0.16	0.27	0.43
7-8	0.96	0.08	0.33	0.33	0.96	0.09	0.35	0.35
8-9	0.80	0.09	-0.28	0.37	0.80	0.09	-0.27	0.37
Total	0.72	0.14	-0.04	0.40	0.75	0.13	0.05	0.37

3.3.2 PBTK model

In total, 41 distinct compounds with 355 data points with log K_{OW} from 2.4 to 8.7 for rainbow trout were selected. Results of statistical analysis are presented in Table 3 and Figure 3. Most compounds have low polarity, with relative small Aa and Bb values. Greater improvement was observed when pp-LFERs models were used in the PBTK model compared that in the one-compartment model. This could be attributable to more pp-LFERs equations incorporated in the model, not only for the blood-water system, but also covering kidney, liver, and fat and water partitioning composed by varied biological composition. In the one-compartment model, sp-LFERs were only replaced with the partition coefficients between whole body and water. The

501 K_{OW} -driven sp-LFERs PBTK model tended to underestimate BCFs for 96% of the selected
502 measurements. One underlying explanation could be that the partitioning behaviour could not be
503 well characterized by means of octanol-water partitioning. Particularly for highly hydrophobic
504 nonpolar compounds, the divergence increased with the increasing hydrophobicity as discussed
505 in Section 3.1.2.

506 When metabolism was included, the pp-LFER model also performed better in all the statistical
507 analysis. All deviations fell within a factor of 10. A paired t-test was conducted to indicate
508 whether there is a statistical difference ($p<0.05$). All the compounds fell within 1 log unit via
509 incorporation of pp-LFERs equations. The correlation of determination was improved from 0.67
510 to 0.80 while the absolute model bias (AMB) decreased by half from 0.68 to 0.34. The largest
511 deviation occurred for octachloronaphthalene predicted by the sp-LFERs model, which also had
512 the largest divergence when comparing the blood-water partition in the whole dataset discussed
513 previously. This further supports the fact that sp-LFERs underestimated the blood water
514 partitioning and potentially also partitioning to other biological compartments (kidney, liver and
515 fat). However, both models tended to underestimate the BCFs for the whole dataset. This could
516 be due the parameterization uncertainty, mainly from hepatic biotransformation extrapolated
517 from the whole-body metabolism rate. It has been demonstrated that biotransformation may
518 have a greater impact on the PBTK model than that in the one-compartment model, which
519 results from the different structure of both models (Nichols et al., 2007; Stadnicka et al., 2012).

520

521 Table 3. Statistical analysis of the comparison between model predictions of BCFs from the
522 PBTK model and observations.

	With metabolism		**Without metabolism**	
Approach	sp-LFER	pp-LFER	sp-LFER	pp-LFER
R^2	0.67	0.80	0.38	0.54
RMSE	0.29	0.09	0.22	0.14
MB	-0.66	-0.25	-0.39	0.02
AMB	0.69	0.34	0.58	0.38
Factor_10	86.20%	100.00%	89.30%	94.93%

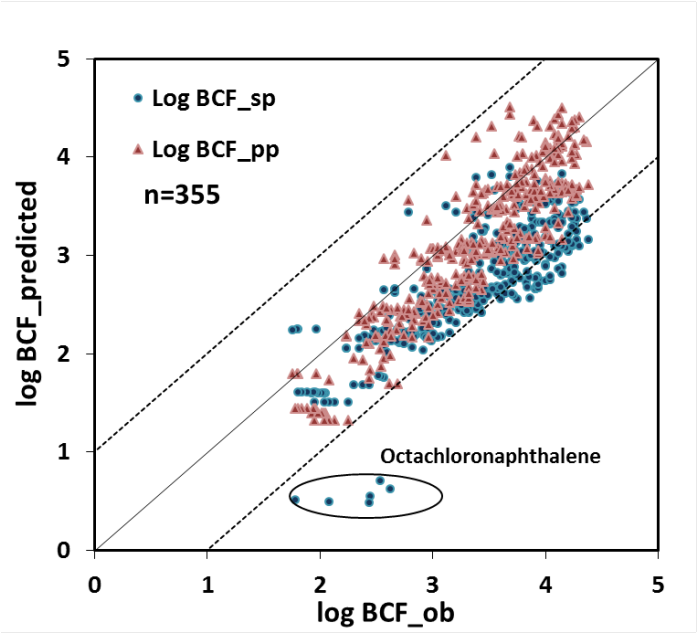

Figure 3. Comparison between measured log BCF_ob with predicted log BCF using sp/pp-approaches in the multi-compartment PBTK model. The dashed lines represent a factor of 10 between the predicted and measured BCFs.

3.4 Practical implications

pp-LFERs model can potentially give more insights about the prediction of potential bioaccumulation. The impacts of using pp-LFEs were different in the one-compartment fish model and PBTK fish model. For the one-compartment model, pp-LFERs improved model performance for chemicals with log K_{OW} from 4 to 5, via better quantifying the protein/phospholipid-water partition coefficients. However, the differences between predictions via sp-LFERs and pp-LFERs model are relatively small for the whole range of K_{OW}. This is because better quantification of individual partitioning processes does not guarantee significant improvement overall. Besides, elimination kinetics could be the most important parameters in the determination of BCFs for highly bioaccumulative substances (Kuo and Di Toro, 2013a). As a consequence, such simplified models are generally incorporated in multimedia fate models and are used for the chemical screening and risk assessment. The sp-LFERs incorporated in one-compartment fish models is, therefore, good enough for these purposes.

This situation could be different for the PBTK fish model, which offers more detailed information on organ-specific concentrations and which is potentially more insightful for understanding potential dietary exposure routes for target fish organs. The advantage of PBTK models over one-compartment models is the calculation of organ-specific concentration. It is important to understand specific pathways to target sites and bioaccumulation along food chains, if predators preferentially consume certain body parts (Stadnicka et al., 2012). Therefore, the

pp-LFERs model would clearly benefit from a better description and characterization of biological composition and water partition coefficients. Although the flawed regression equations used in this study are limited in terms of their applicable domains, the lipid was still not suggested as a good indicator to predict partition coefficients under this case as discussed above, particularly for very hydrophobic and polar compounds. In addition, the pp-LFERs model also could help with the extrapolation of partition coefficients in PBTK model to another fish species, if the biological composition in individual organ/tissues could be accurately quantified.

3.5 Limitations

In this study, all the values for solute descriptors were based on experiments, which have been reported in the literature for more than 2000 compounds and freely at http://www.ufz.de/index.php?en=31698. However, this could hamper its wide application if the solute descriptor values are not available for target compounds (Stenzel et al., 2013b). For the purpose of fast chemical screening, predictive methods only require molecular structure as desirable. Prediction models, such as ABSOLV, a commercial QSAR model that predicts the pp-LFER solute descriptors for compounds with SMILES notations (Stenzel et al., 2014), may be useful. This works well for chemicals with relatively simple molecular structures, but further development is needed for H-donor compounds and chemical with complex structures (Geisler et al., 2015).

Ionization was not taken into account in this study, as pp-LFERs approaches for ionic chemicals are still a subject of ongoing research. No successful applications to environmental and biological processes have been reported so far (Endo and Goss, 2014a). However, since many complex/ multifunction chemicals may ionize in biota, there is a strong need for the investigation of ionic chemicals (Bittermann et al., 2016; Endo and Goss, 2014a). Meanwhile, the development of one-compartment models for ionic compounds has been performed and evaluated. This indicated improved model performance via consideration of partitioning processes to phospholipids (Armitage et al., 2013). In our study, phospholipids also appeared to play an important role in distribution.

3.6 Conclusions

Overall, pp-LFERs slightly outperformed sp-LFERs for the whole dataset in a one-compartment model, especially for compounds in the log Kow range 4~5. Greater improvement was found when pp-LFERs were incorporated into a multi-compartment PBTK model. The impact of pp-LFERs incorporation could be further evaluated by the organic-specific concentrations/bioaccumulative potential. Therefore, for screening purposes, the sp-LFERs

approach is probably good enough to quantify the main partition characteristics in most cases. For more detailed study aimed to understand toxicity pathways to target sites, or dietary exposure for predators preferentially consuming certain organs/tissues, the pp-LFERs would be suggested to incorporate in the PBTK model to improve the accuracy of the description of partition processes.

4 Acknowledgements

We thank Unilever and the China Scholarships Council (CSC) for funding this research. Thanks to John Nichols for offering guidance on the implementation of PBTK fish model. Thanks to Satoshi Endo for offering comments on the preliminary draft. Thanks to Emma Undeman for offering suggestions on applying pp-LFERs.

5 References

Abraham MH, Acree WE, Jr. Equations for the transfer of neutral molecules and ionic species from water to organic phases. J Org Chem 2010; 75: 1006-15.

Abraham MH, Chadha HS, Whiting GS, Mitchell RC. Hydrogen-Bonding .32. An Analysis of Water-Octanol and Water-Alkane Partitioning and the Delta-Log-P Parameter of Seiler. Journal of Pharmaceutical Sciences 1994; 83: 1085-1100.

Abraham MH, Gola JMR, Ibrahim A, Acree Jr WE, Liu X. A simple method for estimating in vitro air-tissue and in vivo blood-tissue partition coefficients. Chemosphere 2015; 120: 188-191.

Armitage JM, Arnot JA, Wania F, Mackay D. Development and evaluation of a mechanistic bioconcentration model for ionogenic organic chemicals in fish. Environmental Toxicology and Chemistry 2013; 32: 115-128.

Arnot JA, Gobas F. A food web bioaccumulation model for organic chemicals in aquatic ecosystems. Environmental Toxicology and Chemistry 2004; 23: 2343-2355.

Arnot JA, Gobas FAPC. A review of bioconcentration factor (BCF) and bioaccumulation factor (BAF) assessments for organic chemicals in aquatic organisms. Environmental Reviews 2006; 14: 257-297.

Arnot JA, Mackay D, Bonnell M. Estimating metabolic biotransformation rates in fish from laboratory data. Environmental Toxicology and Chemistry 2008; 27: 341-351.

Bertelsen SL, Hoffman AD, Gallinat CA, Elonen CM, Nichols JW. Evaluation of log K_{OW} and tissue lipid content as predictors of chemical partitioning to fish tissues. Environmental Toxicology and Chemistry 1998; 17: 1447-1455.

Bittermann K, Spycher S, Goss K-U. Comparison of different models predicting the phospholipid-membrane water partition coefficients of charged compounds. Chemosphere 2016; 144: 382-391.

Brown TN, Wania F. Development and exploration of an organic contaminant fate model using poly-parameter linear free energy relationships. Environmental Science & Technology 2009; 43: 6676-6683.

Debruyn AMH, Gobas FAP. The sorptive capacity of animal protein. Environmental Toxicology and Chemistry 2007; 26: 1803-1808.

Endo S, Bauerfeind J, Goss KU. Partitioning of neutral organic compounds to structural proteins. Environ Sci Technol 2012; 46: 12697-703.

623 Endo S, Brown TN, Goss KU. General model for estimating partition coefficients to organisms
624 and their tissues using the biological compositions and polyparameter linear free energy
625 relationships. Environ Sci Technol 2013; 47: 6630-9.
626 Endo S, Escher BI, Goss KU. Capacities of membrane lipids to accumulate neutral organic
627 chemicals. Environ Sci Technol 2011; 45: 5912-21.
628 Endo S, Goss K-U. Serum Albumin Binding of Structurally Diverse Neutral Organic
629 Compounds: Data and Models. Chemical Research in Toxicology 2011a; 24: 2293-
630 2301.
631 Endo S, Goss KU. Serum albumin binding of structurally diverse neutral organic compounds:
632 data and models. Chemical Research in Toxicology 2011b; 24: 2293-301.
633 Endo S, Goss KU. Applications of polyparameter linear free energy relationships in
634 environmental chemistry. Environ Sci Technol 2014a; 48: 12477-91.
635 Endo S, Goss KU. Predicting partition coefficients of Polyfluorinated and organosilicon
636 compounds using polyparameter linear free energy relationships (PP-LFERs). Environ
637 Sci Technol 2014b; 48: 2776-84.
638 Geisler A, Endo S, Goss K-U. Partitioning of polar and non-polar neutral organic chemicals into
639 human and cow milk. Environment International 2011; 37: 1253-1258.
640 Geisler A, Endo S, Goss KU. Partitioning of organic chemicals to storage lipids: elucidating the
641 dependence on fatty acid composition and temperature. Environ Sci Technol 2012; 46:
642 9519-24.
643 Geisler A, Oemisch L, Endo S, Goss K-U. Predicting storage-lipid water partitioning of organic
644 solutes from molecular structure. Environmental Science & Technology 2015.
645 Gobas FA, de Wolf W, Burkhard LP, Verbruggen E, Plotzke K. Revisiting bioaccumulation
646 criteria for POPs and PBT assessments. Integrated environmental assessment and
647 management 2009; 5: 624-637.
648 Goss KU. Predicting the equilibrium partitioning of organic compounds using just one linear
649 solvation energy relationship (LSER). Fluid Phase Equilibria 2005; 233: 19-22.
650 Gotz CW, Scheringer M, Macleod M, Roth CM, Hungerbuhler K. Alternative approaches for
651 modeling gas-particle partitioning of semivolatile organic chemicals: Model
652 development and comparison. Environmental Science & Technology 2007; 41: 1272-
653 1278.
654 Haschek WM, Rousseaux CG, Wallig MA. Haschek and Rousseaux's handbook of toxicologic
655 pathology: Academic Press, 2013.
656 Kuo DTF, Di Toro DM. Biotransformation model of neutral and weakly polar organic
657 compounds in fish incorporating internal partitioning. Environmental Toxicology and
658 Chemistry 2013a; 32: 1873-1881.
659 Kuo DTF, Di Toro DM. A reductionist mechanistic model for bioconcentration of neutral and
660 weakly polar organic compounds in fish. Environmental Toxicology and Chemistry
661 2013b; 32: 2089-2099.
662 Landrum PF, Lee H, Lydy MJ. Toxicokinetics in Aquatic Systems - Model Comparisons and
663 Use in Hazard Assessment. Environmental Toxicology and Chemistry 1992; 11: 1709-
664 1725.
665 Laue H, Gfeller H, Jenner KJ, Nichols JW, Kern S, Natsch A. Predicting the bioconcentration of
666 fragrance ingredients by rainbow trout using measured rates of in vitro intrinsic
667 clearance. Environ Sci Technol 2014; 48: 9486-95.
668 Mackay D. Multimedia Environmental Models: The Fugacity Approach, Second Edition:
669 Taylor & Francis, 2001.
670 Mackay D, Arnot JA, Gobas F, Powell DE. Mathematical relationships between metrics of
671 chemical bioaccumulation in fish. Environmental Toxicology and Chemistry 2013; 32:
672 1459-1466.
673 Mintz C, Clark M, Acree WE, Abraham MH. Enthalpy of solvation correlations for gaseous
674 solutes dissolved in water and in 1-octanol based on the abraham model. Journal of
675 Chemical Information and Modeling 2007; 47: 115-121.
676 Nichols J. Modeling the Uptake and Disposition of Hydrophobic Organic Chemicals in Fish
677 Using a Physiologically Based Approach. In: Krüse J, Verhaar HM, de Raat WK,

678 editors. The Practical Applicability of Toxicokinetic Models in the Risk Assessment of
679 Chemicals. Springer Netherlands, 2002, pp. 109-133.
680 Nichols JW, Fitzsimmons PN, Burkhard LP. In vitro-in vivo extrapolation of quantitative
681 hepatic biotransformation data for fish. II. Modeled effects on chemical
682 bioaccumulation. Environmental Toxicology and Chemistry 2007; 26: 1304-1319.
683 Nichols JW, McKim JM, Andersen ME, Gargas ML, Clewell HJ, 3rd, Erickson RJ. A
684 physiologically based toxicokinetic model for the uptake and disposition of waterborne
685 organic chemicals in fish. Toxicol Appl Pharmacol 1990; 106: 433-47.
686 Nichols JW, Schultz IR, Fitzsimmons PN. In vitro–in vivo extrapolation of quantitative hepatic
687 biotransformation data for fish: I. A review of methods, and strategies for incorporating
688 intrinsic clearance estimates into chemical kinetic models. Aquatic Toxicology 2006; 78:
689 74-90.
690 Stadnicka J, Schirmer K, Ashauer R. Predicting concentrations of organic chemicals in fish by
691 using toxicokinetic models. Environ Sci Technol 2012; 46: 3273-80.
692 Stenzel A, Goss KU, Endo S. Determination of polyparameter linear free energy relationship
693 (pp-LFER) substance descriptors for established and alternative flame retardants.
694 Environ Sci Technol 2013a; 47: 1399-406.
695 Stenzel A, Goss KU, Endo S. Experimental determination of polyparameter linear free energy
696 relationship (pp-LFER) substance descriptors for pesticides and other contaminants:
697 new measurements and recommendations. Environ Sci Technol 2013b; 47: 14204-14.
698 Stenzel A, Goss KU, Endo S. Prediction of partition coefficients for complex environmental
699 contaminants: Validation of COSMOtherm, ABSOLV, and SPARC. Environmental
700 toxicology and chemistry 2014; 33: 1537-1543.
701 Undeman E, Czub G, McLachlan MS. Modeling bioaccumulation in humans using poly-
702 parameter linear free energy relationships (PPLFERS). Science of The Total
703 Environment 2011; 409: 1726-1731.
704 US EPA. Estimation Programs Interface Suite™ for Microsoft® Windows, v 4.11, United
705 States Environmental Protection Agency, Washington, DC, USA., 2012.

706

Supporting information for "Modelling bioaccumulation in fish by poly-parameter linear-free energy relationships (PP-LFERs)"

Shizhen Zhao[1], Oliver Price[2], Kevin C. Jones[1], Andrew J. Sweetman[*1]*

[1] Lancaster Environment Centre, Lancaster University, Lancaster, LA14YQ, UK

[2] Safety and Environmental Assurance Centre, Unilever, Sharnbrook, MK44 1LQ, UK.

Contents

Treatment of fat content in lean tissues

The lipid content of lean tissue (all compartments exclude the fat) was assumed not to depend on the lipid content of whole body (Nichols et al., 1990). So, the lipid content of lean tissue (lipid_lean) was calculated based on lipid fraction on each lean tissue (liver, kidney, richly perfused and poorly perfused). The richly perfused compartments mainly contain the gut, gastrointestinal tract, spleen and gonads. The lipid content in the gut was used to be representative of the lipid content in the richly perfused tissues, which was calculated following the same method and assumed the same diet input as the one-compartment model. Based on measured total lipid content (lipid_total) in each study, the volume of fat compartment (V_f) was expressed as (Stadnicka et al., 2012):

V_f=BW× (lipid_total-lipid_lean)/(lipid_fat-lipid_lean)

Bovine serum albumin was only considered to be present in the blood tissue, since its existence is fairly minimal and its variation may increase the model uncertainty.

Temperature dependence

The partition coefficients are typically measured at 37℃ for mammals or around 25 ℃ for the experimental condition. For predicting bioaccumulation in fish, partition coefficients need to be adjusted to the corresponding environmental water temperature. As a result, log K_{AW} and log K_{OA} were adjusted to the environmental concentration based on the enthalpies of partitioning (ΔH_i) based on the van't Hoff equation as:

$\Delta Hi=-(\log K_i(t_1)-\log K_i(t_2))\times R\times 2.303/(1/t_1-1/t_2)$

But the relationship was less rarely developed for other biological phases. Only one study found was about the fat (Geisler et al., 2012). The equation for enthalpies of partitioning was fitted based on the descriptor combination L, S, A, B and V, but it's is less diverse than that for log $K_{\text{storage lipid-water}}$. According to the extrapolation, the log $K_{\text{lipid-water}}$ was calculated at 281K, which is very close to that at 310K. In practice, the temperature dependence for many compounds is small (Geisler et al., 2012). So the temperature dependence of other partitioning coefficients between biological phases and water are assumed to be independent of temperature in the range of fish body temperature.

Table S 1. Table 1 Parameters/equations used in the one-compartment bioaccumulation model for fish.

Parameters	**Units**	**Value/Equation**	**References**
Dissolved organic carbon	kg L^{-1}	2.9×10^{-6}	(Nichols et al., 2007)
Particulate	kg L^{-1}	0.5×10^{-6}	(Nichols et al., 2007)
Bioavailable solute fraction	-	Φ=1/(1+Cpoc*Dpoc*αpoc*Kow+Cdoc*Ddoc* αdoc*Kow)	(Arnot and Gobas, 2004)
Lipid	-	0.92	(Arnot and Gobas, 2004)
NLOM	-	0.60	(Arnot and Gobas, 2004)
Water	-	0.70	(Arnot and Gobas, 2004)
Dissolved oxygen	mg L^{-1}	7.1	(Arnot and Gobas, 2006)

Table S 2 The biological composition in fish, following (Armitage et al., 2013; Arnot and Gobas, 2004; Hendriks et al., 2005), and assumed the none-lipid organic matter was replaced by protein and phospholipid.

Fish	**Neutral lipid,%**	**Phospholipid, %**	**Protein,%**	**Water,%**
volume fraction, m^3 m^-	4	1	15	80

Table S 3. Parameters used in the PBTK fish model, the scaled parameters were the same Nichols and his co-workers (Nichols et al., 1990).

Parameters	**Values/Equations**	**References**
Cardiac output (Q_c, L h^{-1})	$Q_c=(0.23\times T_{water}-0.78)\times (BW/500)^{0.1}\times BW^{0.75}$	(Erickson and Mckim, 1990)
Effective respiratory volume (Q_w, L h^{-1})	$Q_w=0.65*G_v$	(Nichols et al., 2007)

Table S 4 Composition of blood and other organs for the rainbow trout used in the PBTK model.

Organ/tissue	Total lipid, %	Neutral lipid,%	Phospho lipid,%	Serum albumin, %	Protein, %	Water, %	References
Blood	1.4	0.7	0.7	1.6	13.1	83.9	(Bertelsen et al., 1998; Endo et al., 2013)
Fat	94.2	93.4	0.8	-	0.8	5.0	(Bertelsen et al., 1998)
Liver	4.5	1.8	2.7	-	20.9	74.6	(Bertelsen et al., 1998)
Kidney	5.2	3.7	1.5	-	15.9	78.9	(Bertelsen et al., 1998)

Poorly perfused compartment	3.0	2.2	0.8	-	20.1	76.9	(Bertelsen et al., 1998)
Richly perfused compartment	0.38	0.31	0.08	-	19.2	80.4	Calculated from one-compartment model

Table S 5. The range of each chemical descriptor in the calibration procedures for used biological systems.

Biological system	**Range of each descriptor in the calibration chemical set**					
	S	A	B	L	V	Ref
Neutral lipid-water	0.3~1.72	0~0.76	0~0.97	-0.82~8.83	0.25~2.36	(Geisler et al., 2015)
Phospholipid-water	0~3.29	0~1.14	0~1.63	0.97~13.26	0.31~2.62	(Endo et al., 2011)
Muscle protein-waster	0~1.59	-0.03~0.69	0~1.28	3~10.48	0.793~2.274	(Endo et al., 2012)
Serum albumin-water	0 ~2.05	0~0.99	0~1.38	1.75~13.26	0.715~2.281	(Endo and Goss, 2011)

Additional results

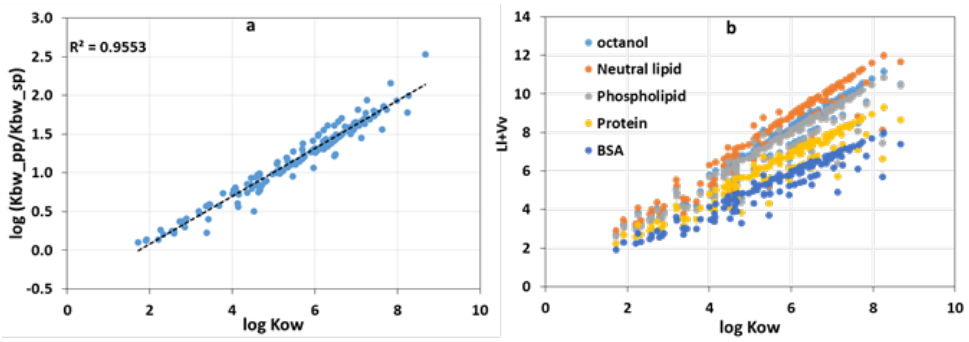

Figure S 1. The dependency of predicted deviations on $K_{blood\text{-}water}$ (K_{bw}) between pp-LFERs and sp-LFERs and the varied log Kow values for nonpolar compounds in the dataset (both A and B ≤0.2, N=156) (a) and the absolute value of Ll+Vv terms in considered biological tissue and octanol-water (b).

Contributions of molecular interactions

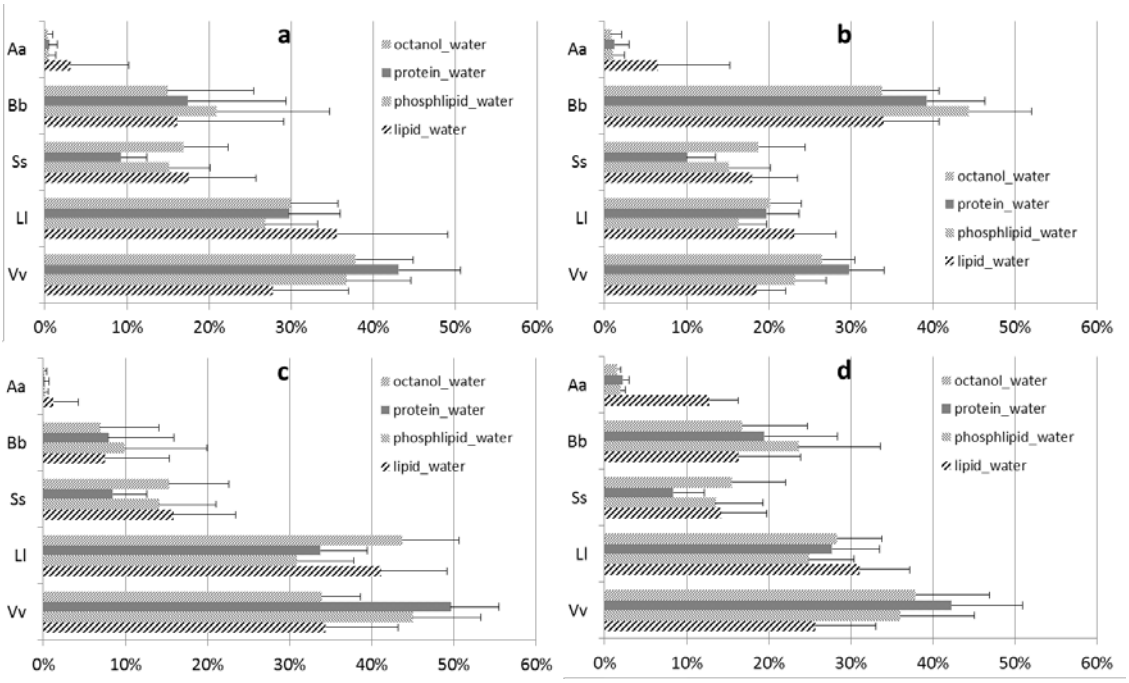

Figure S 2. Mean contribution of the absolute value of each descriptor in pp-LFERs to the sum of the absolute values of all terms for octanol-water, protein-water, phospholipid-water and neutral lipid-water for chemical with a) whole dataset (n=498) b) log Kow≤1 (n=44) c) log Kow≥4 (n=249) d) A≥0.5 (n=61). The error bars indicate the standard deviation.

A quantitative assessment of the relative contribution of the different solute descriptors in the pp-LFERs for the partition coefficients between octanol/water, protein/water, phospholipid/ water and neutral lipid/water was carried out for the whole dataset and multiple sub-datasets. The inter-molecule interaction was captured mostly by Ll representing Van der Waals' force (see Figure S 2), except for the subset of hydrophilic compounds with log K_{OW} <1 (Figure S 2-b). Meanwhile, the H-bond acceptor (B) is significant for compounds with log K_{OW} <1, which also explains the large deviation caused by chemicals with the strong H-bond acceptor.

The descriptor Aa, which describes the H-bond donor, was not a dominant descriptor in the dataset and each subset. It accounted up to 3% in the total dataset, which is relatively minimal. Even in the subset of compounds with A≥0.5, its highest contribution was 13% for lipid-water partitioning as indicated in Figure S 2-d. Since a<0, Aa makes a negative contribution to total $K_{lipid/water}$. Thus, the $K_{fish/water}$ would be overestimated by using Kow for H-donor compounds with high A values (e.g., eicosanoic acid). According to the analysis of the contribution of each descriptor in terms of relative contribution, K_{OW} could characterize the general contribution as the individual biological phases. However, it should be taken caution for compounds with H-bond donor and acceptor.

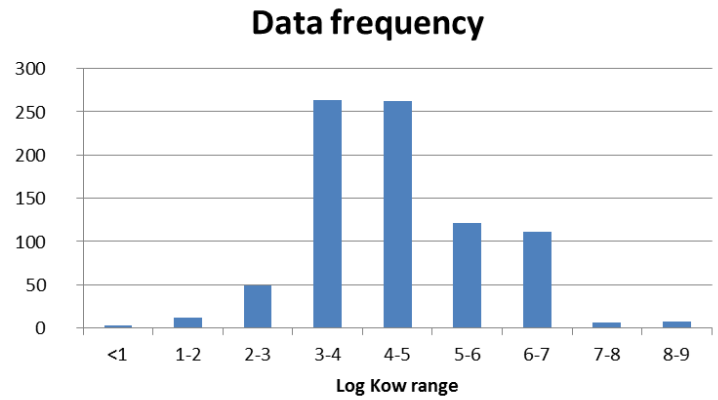

Figure S 3. The distribution of the measured data points in different categories of log Kow values.

References

Armitage JM, Arnot JA, Wania F, Mackay D. Development and evaluation of a mechanistic bioconcentration model for ionogenic organic chemicals in fish. Environmental Toxicology and Chemistry 2013; 32: 115-128.

Arnot JA, Gobas F. A food web bioaccumulation model for organic chemicals in aquatic ecosystems. Environmental Toxicology and Chemistry 2004; 23: 2343-2355.

Arnot JA, Gobas FAPC. A review of bioconcentration factor (BCF) and bioaccumulation factor (BAF) assessments for organic chemicals in aquatic organisms. Environmental Reviews 2006; 14: 257-297.

Bertelsen SL, Hoffman AD, Gallinat CA, Elonen CM, Nichols JW. Evaluation of log K_{OW} and tissue lipid content as predictors of chemical partitioning to fish tissues. Environmental Toxicology and Chemistry 1998; 17: 1447-1455.

Endo S, Bauerfeind J, Goss KU. Partitioning of neutral organic compounds to structural proteins. Environ Sci Technol 2012; 46: 12697-703.

Endo S, Brown TN, Goss KU. General model for estimating partition coefficients to organisms and their tissues using the biological compositions and polyparameter linear free energy relationships. Environ Sci Technol 2013; 47: 6630-9.

Endo S, Escher BI, Goss KU. Capacities of membrane lipids to accumulate neutral organic chemicals. Environ Sci Technol 2011; 45: 5912-21.

Endo S, Goss KU. Serum albumin binding of structurally diverse neutral organic compounds: data and models. Chemical Research in Toxicology 2011; 24: 2293-301.

Erickson RJ, Mckim JM. A model for exchange of organic-chemicals at fish gills - flow and diffusion limitations. Aquatic Toxicology 1990; 18: 175-197.

Geisler A, Endo S, Goss KU. Partitioning of organic chemicals to storage lipids: elucidating the dependence on fatty acid composition and temperature. Environ Sci Technol 2012; 46: 9519-24.

Geisler A, Oemisch L, Endo S, Goss K-U. Predicting storage-lipid water partitioning of organic solutes from molecular structure. Environmental Science & Technology 2015.

Hendriks AJ, Traas TP, Huijbregts MAJ. Critical body residues linked to octanol-water partitioning, organism composition, and LC50 QSARs: Meta-analysis and model. Environmental Science & Technology 2005; 39: 3226-3236.

Nichols JW, Fitzsimmons PN, Burkhard LP. In vitro-in vivo extrapolation of quantitative hepatic biotransformation data for fish. II. Modeled effects on chemical bioaccumulation. Environmental Toxicology and Chemistry 2007; 26: 1304-1319.

Nichols JW, McKim JM, Andersen ME, Gargas ML, Clewell HJ, 3rd, Erickson RJ. A physiologically based toxicokinetic model for the uptake and disposition of waterborne organic chemicals in fish. Toxicol Appl Pharmacol 1990; 106: 433-47.

Stadnicka J, Schirmer K, Ashauer R. Predicting concentrations of organic chemicals in fish by using toxicokinetic models. Environ Sci Technol 2012; 46: 3273-80.

PAPER III

Long-term temporal trends of PCBs and their controlling sources in China

Shizhen Zhao[1], *Oliver Price*[2], *Guorui Liu*[3], *Minghui Zheng*[3], *Kevin C. Jones*[1], *Andrew J. Sweetman*[*1]

[1] Lancaster Environment Centre, Lancaster University, Lancaster, LA14YQ, UK

[2] Safety and Environmental Assurance Centre, Unilever, Sharnbrook, MK44 1LQ, UK.

[3] State Key Laboratory of Environmental Chemistry and Ecotoxicology, Research Centre for Eco-Environmental Sciences, Chinese Academy of Sciences, P.O. Box 2871, Beijing 100085, China.

*Corresponding author:

Andrew J. Sweetman

Tel: +44 (0) 1524 594715

Email: a.sweetman@lancaster.ac.uk.

Abstract

Polychlorinated biphenyls (PCBs) are industrial organic contaminants which have been identified as persistent, bioaccumulative, toxic (PBT) and subject to long-range transport (LRT) with global scale significance. They are regulated by the Stockholm Convention to protect environmental and human health with a global production of 1.3 million tons. Although total production and usage in China was relatively minor (<1%) compared to global rates, the potential risks from on-going sources cannot be ignored owing to their PBT properties. This study focuses on a reconstruction and prediction of the long-term emission trends of intentionally produced $\sum_7$ PCBs with additional consideration of the potential importance of unintentionally produced PCBs (UP-PCBs from the manufacture of steel, cement and sinter iron) and re-emission from secondary sources (e.g., soils and vegetation), using a dynamic fate model (BETR-Global). Contemporary emission estimates combined with predictions from a multimedia fate model suggested that primary sources still dominate environmental burdens, PCB-28 produced by unintentional sources is predicted to become a main contributor by 2035. China could become a potential source to neighbouring regions with a net output of 444 kg year^{-1} in the case of PCB-28 by 2050 without effective controlling measures. The influence of e-waste could be potentially shifted from regional to a national level in future. Calculation of the future significance of the sources of UP-PCBs involves large uncertainties but could be improved significantly with further domestic measurements of emission factors, which would enable more accurate determination of emission trends.

Highlights:

- Long-term environmental emission trends were simulated for PCBs in China.
- Unintentionally sources and secondary sources were explored for emissions of PCBs in China.
- Primary sources still predominate for PCB-28 currently, and unintentional sources are predicted to dominate from 2040.
- China could possibly change from being a net PCB receiver to a potential net source to neighbouring regions in future.

Keywords:

Polychlorinated biphenyls; primary emissions; secondary emissions; multimedia dynamic fate model; controlling sources

1 Introduction

Polychlorinated biphenyls (PCBs) are industrial organic contaminants identified as persistent, bioaccumulative, toxic and subject to long-range transport (LRT) with global scale significance. They are among the twelve persistent organic pollutants (POPs) initially regulated by the Stockholm Convention (UNEP, 2001) in order to protect environmental and human health from these hazardous compounds. The cumulative global production of PCB was approximately 1.3 million tonnes with 10 thousand tonnes produced in China (Breivik et al., 2002a). These chemicals were mainly emitted as a direct result of intentional historical production, consecutive use and disposal or accidental release of products containing PCBs (Breivik et al., 2002c). Though they have been banned for several decades, they are still of great concern because of its persistence in the environment, bioaccumulation in biota and potential toxicity (Jones and de Voogt, 1999; Nizzetto et al., 2010).

PCBs can be emitted from both primary and secondary sources. Primary sources are considered to account for the main direct releases of PCBs to the environment from their major use categories while the secondary sources represent the re-emission from environmental reservoirs including soils, sediments and other environmental compartments contaminated in the past. Secondary sources can be viewed as “capacitors” that were charged with pollutants deposited from the atmosphere when emissions were higher and may now be net sources to the atmosphere (Nizzetto et al., 2010). Primary emissions of PCBs to the environment in industrialized countries were at their height during the main production phase, which peaked in the early 1970s and largely occurred through the leakage and losses from the PCB-containing products and systems. More recently secondary sources have been demonstrated to represent a significant fraction of the total source inventory, especially in some remote areas (Nizzetto et al., 2010). Under such conditions, the reduction in primary emissions of PCBs may not be directly manifested in declines of atmospheric concentrations due to on-going releases from secondary sources. An understanding of both primary and secondary emissions is, therefore, important to provide guidance on the potential success of control measures.

In China, although production volume of PCBs only accounts up to 1% of the global production, China could also additionally receive PCB from long-range atmospheric transport (LRAT) or trans-boundary movement of e-waste products containing PCBs (Breivik et al., 2014). Therefore, the manner of PCBs released into the environment could be a combination of primary emission and re-volatilization from contaminated environmental compartments. There are several studies suggesting that contaminated soil could be a secondary source particularly contributing to low molecular weight PCBs by determining the equilibrium status between air and soil (Li et al., 2010; Wang et al., 2012a). These studies have demonstrated a diffusion

gradient from soil to air along with a wide temperature-driven seasonal variation (Wang et al., 2012b). So the relative significance of primary emission and secondary emission is still under debate. On other hand, studies carried out in remote regions of China, such as the Tibetan Plateau, have reported high proportions of tetra-PCBs in ambient air samples which could be being supplied from LRAT (Wang et al., 2010). The relative importance of on-going primary emissions from largely historical sources, from by-products of unintentional production and secondary sources in China, are still not fully understood.

There are two types of primary PCB emissions into the atmosphere, intentionally-produced (IP-PCB) and unintentionally produced PCBs (UP-PCBs) (Cui et al., 2015; Cui et al., 2013). Emissions of IP-PCBs, which have been predicted by on a global scale by Breivik and his co-workers (Breivik et al., 2002a; Breivik et al., 2002b; Breivik et al., 2007), show a constantly decreasing trend since the middle of the 1970s when production was phased out. This emission inventory has been recently updated to include the contribution of e-waste. Since the ban on manufacture and use of commercial products containing PCBs, the UP-PCBs are likely to become relatively more important compared to going forward primary emissions from products containing intentionally produced PCBs (Liu et al., 2013). Hogarh et al. (2012) reported that ambient air concentrations in China have increased by one order of magnitude over the period 2004 to 2008, which could be mainly related to widespread industrial combustion process (Hogarh et al., 2012). As the economy in China grows, there is an increasing demand for construction materials such as steel and concrete. China has contributed around 45% of global steel production and has become the world's largest consumer of iron ore since 1993 (Feng, 1994). Consequently, the temporal trends and historical/future contribution of UP-PCBs needs to be further explored. To understand which factors are controlling PCB burdens in environmental compartments in China, it is important to quantify the relative significance of primary emissions (controllable) versus secondary emission (uncontrollable). An overestimate of the relative importance of primary emission could lead to costly and unnecessary measures to reduce future environmental exposure, whereas an underestimation of the importance of secondary emissions could lead to an over-optimistic assessment of reducing environmental and human exposure to PCBs (Breivik et al., 2004). A further important question would be what are the most important primary sources, 'intentional' or 'unintentional'? These questions are of key interest for policy makers since it will affect their perception of the potential need to reduce or eliminate primary emissions and the potential effectiveness of emission reduction strategies.

The main aims of this study were 1) to explore the potential contribution of primary sources (imported e-waste and unintentionally produced emission) and secondary sources both from domestic sources and the importance of LRAT; 2) to evaluate modelling results using observations and discuss remaining uncertainties; 3) provide a assessment of study output for

policy makers on the potential for success of control measures. These objectives were achieved mainly by using BETR Global, a dynamic level IV fate and transport model, which has been evaluated and applied successfully for a range of organic contaminants, including PCBs (Lamon et al., 2009).

2 Methods

2.1 Emission data and selected PCBs

In this study, the emission, fate and transport, covering both intentionally and unintentionally produced PCBs, were explored under several scenarios for $\sum_7$ PCBs (PCB-28, 52, 101, 118, 138,153, and 180). These were selected in this study due to their representative physicochemical properties and extensive use in China. The assembled usage and emission data were distributed into a 1°× 1° latitude/longitude grid system based on a global population density database (Li et al., 1996). The physical-chemical properties of selected congeners are presented in Table S1 (Breivik et al., 2010; Schenker et al., 2005).

2.1.1 IP-PCBs emission in China

The recently revised global emission inventory by Breivik and his co-workers was utilized in this study (Breivik et al., 2015) as they have pioneered work on global emission inventories for 22intentionally produced PCB congeners over the period 1930 to 2100 (Breivik et al., 2002a; Breivik et al., 2002c; Breivik et al., 2007). The revised global emission scenarios accounting for transport of e-waste were assumed to represent an improvement compared to the previous one produced in 2002 (Breivik et al., 2015; Breivik et al., 2002b). The global emissions of 22 selected PCB congeners were estimated over the period 1930 to 2100.

In China, about 10,000 tonnes of PCBs were produced from 1965 to 1974, mainly composed of tri-PCB and penta-PCB (Fu et al., 2003). Around 90% was utilized in the electrical supply and distribution industry (e.g. as dielectric fluid in capacitors and transformers), mostly made up of tri-PCB. The remaining function was used as additives for paint with penta-PCB being the dominant component. Therefore, tri-PCBs are the main homologue group used in China accounting for 56% among all Chinese products (Frame et al., 1996). The highly chlorinated homologue groups, including the hexa-PCB and hepta-PCB, accounted for 2.5%, which was much lower compared to commercial products produced in Europe and North America (Jiang et al., 1997).

2.1.2 UP-PCBs emission in China

Three major UP-PCB emission contributors have been identified as representing significant contributions to UP sources (Cui et al., 2015; Cui et al., 2013). These are cement kilns, electric

arc furnaces (EAF) used in steel making and the iron ore sintering process. This information was based on an investigation of the main industrial thermal processes in China by Liu et al. (2013). However, it is possible that there are other UP-PCB sources, such as coking, secondary aluminium production, and thermal power stations, and so this could represent an underestimation of the total (Cui et al., 2013). In addition, large uncertainties may also exist within each source category as a range of individual plants may produce a range of emissions depending on operating conditions (Cui et al., 2013). As emission inventories are generally uncertain by at least an order of magnitude, with many parameters affecting the estimates, the resulting predictions from models using such data also need to be considered as highly uncertain (Breivik et al., 2002c). Two scenarios were used to explore this potential uncertainty: (1) the default scenario using measured emission factors taken from Liu et al. (2013); and (2) a 'high' scenario using the measured emission factors multiplied by a factor of 10 as the conservative assumption. An inventory from the Netherlands has indicated that emission factors are uncertain by an order of magnitude (Annema et al., 1995).

The relative importance of the three source types (IP-PCB, UP-PCB and secondary sources) was considered for past and future emission scenarios. The recorded and estimated production volume of cement, EAF produced steel and sinter iron are illustrated in Figure 1. The population density was regarded as a surrogate for spatial distribution. The estimated annual emission data were assigned onto a 1°×1° grid map based on the method by Li et al. (1996). These estimates represent a first approximation, which may not be appropriate for some large plants located near sources of raw materials and thus, would not correlate with population density.

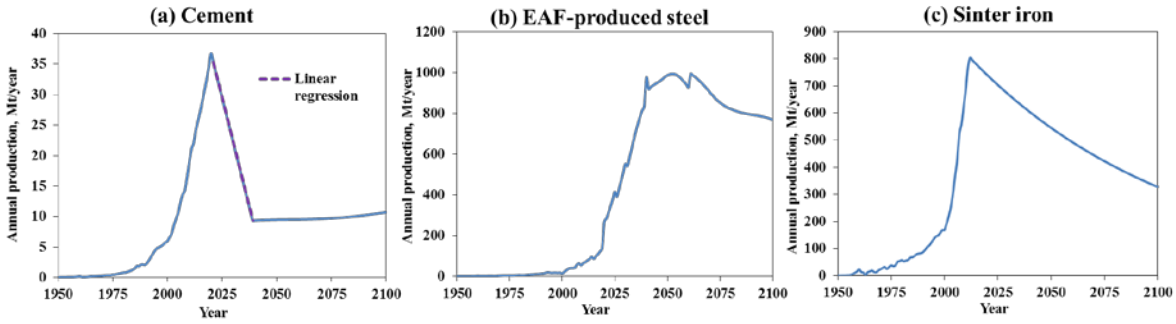

Figure 1. The recorded and estimated production and for cement (a), EAF-produced steel (b) and sinter iron (c) during 1949-2100.

2.2 Selected fate model and study region

The BETR Global model was used to predict the fate and distribution of PCBs with a spatial resolution of 15° latitude ×15° longitude and 288 grid cells (MacLeod et al., 2011). It has been

applied successfully and evaluated for a range of organic contaminants, including PCBs (Macleod et al., 2005). Each grid cell consists of up to 7 bulk compartments, which are oceanic water, fresh water, planetary boundary layer (PBL), free atmosphere, soil, freshwater sediments and vegetation (Macleod et al., 2005). The model accounts for advective transport between the regions by air/ water and inter-compartment transport processes such as dry and wet deposition and reversible partitioning (Lamon et al., 2009).

The study region focussed on China and is illustrated in Figure 2. The model was used to simulate the period from 1930 to 2100 using a dynamic level IV structure that assumes non-steady state conditions. The total emission was allocated to the individual 288 grid cells according to the methodology by Breivik et al. (2007). The only emission to the lower air compartment was considered. The initial model concentration in all compartments was assumed to be zero.

2.3 Estimation of source-receptor relationships

Multiple emission inventory scenarios were investigated to explore the different source-receptor relationships. The employed emission profiles were defined as: i) baseline and worst-case IP only scenario with or without consideration of imported e-waste as detailed inBreivik et al. (2015), which were used to compare the contribution of imported e-waste to the grid cells covering the most of China. The UP sources were added based on the worst-case IP scenario, since it has been demonstrated to work well in Breivik et al. (2015); ii) default scenario (IP+UP): UP-PCBs and IP-PCBs sources combined, with UP-PCBs calculated using measured emission factors from Liu et al. (2013).; iii) high scenario combined worst-case IP-PCBs and “high” UP-PCBs using the a factor of 10 as defined in section 2.1.2, to explore the uncertainty range for 7 UP-PCBs.

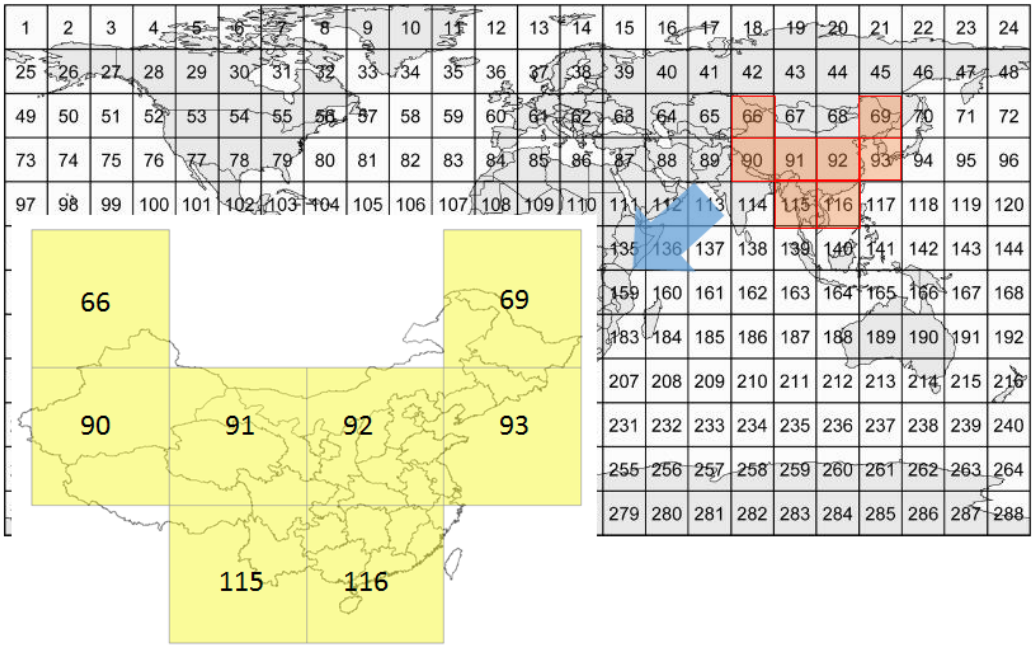

Figure 2. The grid structure of BETR-Global and the defined study region of China.

The emission scenarios of baseline IP, worst-case IP and default IP+UP were first investigated allowing contaminants from both primary and secondary emissions in environmental reservoirs to increase over time to look at the individual contribution from imported e-waste and UP-PCBs over a temporal trend for seven indicator UP/IP-PCBs. Secondly, in order to distinguish primary from secondary sources, the default IP+UP scenario was repeated with re-emission from the surface compartments blocked. The blocked processes from surface-to-air included the diffusion from soil, water and vegetation to air, as well as re-suspension from soils via dust and from oceans via marine aerosol production (Wohrnschimmel et al., 2012). Thirdly, in order to explore the role of China in its global context (sink or source), the model was also run using only the emission estimated within China while the emission to other parts of the world disabled.

3 Results and Discussion

3.1 Evaluation with measurements

First, the modelling results were evaluated with available measurements to build confidence for further exploration. A model such as the one presented here can only be validated to a limited extent, especially for a region where measurement data is scarce. However, it is also useful to assess the accuracy of model predictions where possible. The output from the model with the default scenario (IP+UP), over a limited period, was compared with available measured PCBs data in air and soil. As the BETR Global model does not provide information on urban-rural gradients, model predictions were compared against observed background concentrations.

Atmospheric PCBs concentration have been measured in China by several researchers over the last decade (Jaward et al., 2005; Xing et al., 2005). Surveys providing PCB concentration data for background soils have been conducted in 2005 and 2013 (Ren et al., 2007; Zheng et al., 2014) and normalized using total organic carbon (TOC). For comparisons to be made with studies that do not distinguish between PCB congeners 28 and 31, it has been assumed that PCB-28 represents 0.55 of the combined total (Breivik et al., 2010). This is a reflection of the composition of the technical mixtures.

Figures S8 and S9 compare predicted and observed time trends in air and soil for PCB congeners. According to the comparison with observations over the period 2001 to 2008, the model generally captures the main trends during this period. The agreement between predicted and observed air concentrations is better for heavier PCBs than that for the lighter congeners (PCB-28/52). Most modelled concentrations are within a factor of 3 compared to the limited observations in background air. The model tended to underestimate the atmospheric concentrations for PCB-28 and PCB-52 with the largest difference occurring in 2001 by a factor of 7 for PCB-52. This could be potentially caused by the underestimation of the emission at that time based on a limited dataset. The peak concentration, which happened around 1970 as predicted by modelling, is difficult to confirm with measurements. However, several preliminary findings from dated sediment cores could potentially support the model estimation. The historical trend was shown to increase until the mid-1970s in a dated sediment core from Yangtze River Estuary adjacent to the East Sea region and Pearl River Delta (Mai et al., 2005; Yang et al., 2012). Predicted concentrations increase again from the 1980s, mainly associated with the imported electrical equipment containing PCBs and e-waste recycling activities in nearby regions (Mai et al., 2005; Yang et al., 2012).

Soil responds much slower to changes in emissions compared to air, especially for the heavier and more persistent PCB congeners. Measured surface soil concentrations from 2005 (Ren et al., 2007) and 2013 for forest soil (Zheng et al., 2014) were compared with model predictions and agreed well, within a factor of 4 except for tri-PCB, although the measured concentrations varied over a wide range. The largest deviation was observed for PCB-28 for both studies, which indicated the model greatly underestimated soil concentrations by a factor of 165. The underestimation could be a consequence of the underestimation of secondary sources for more volatile congeners, since the soil is the main reservoir for atmospheric PCBs. The measurement data were limited to two years 2005 and 2013, but showed evidence of a decrease for PCB-28 and PCB-101. However, for PCB-138 and PCB-153 an increase was observed from 0.28 to 0.42 ng/g OC (dw) for PCB-153 and from 0.09 to 0.31 ng/g OC (dw) for PCB-153. These differences are small but could be attributed to the more recalcitrant nature of heavier PCB congeners (Zhang et al., 2008).

Many contaminant studies have been conducted around heavily polluted areas (i.e. ‘hotspots’), and much fewer data are available for national background areas. Therefore, the high spatial variability of PCB concentrations in soil with relatively low numbers of measurements at the background sites, makes it difficult to draw a reliable conclusion. A much larger dataset would be required to establish reliable ranges for background concentrations to determine the whole picture of POPs pollution in China.

The homologue profiles of PCBs during the simulation period of 1930 to 2100 were also compared (see Figure S7). At the beginning of the simulation, the tri-PCB and penta-PCB dominated the atmospheric profile, and both are predicted to continue to increase until they achieved a steady state condition around 2045. The hepta-PCB contributed the least during the entire simulation period, up to about 11% initially, and it was assumed to be mainly from extra-regional emission. Its contribution is predicted to decrease rapidly, becoming negligible accounting for less than 0.5% of the total at the end of the simulation. The change in the homologue trend is generally consistent with the profile of the emission measurements (Zhang et al., 2008).

3.2 Temporal trend of UP-PCBs in China

The predicted time trends for the past and future emissions of PCB-28 /153 and their individual contribution from imported e-waste and unintentionally sources are illustrated in Figure 3 Other congeners profiles presented in Fig S1. Since the optimum scenarios of unintentional-sources are difficult to confirm with measurements, the default scenario (IP + UP) based on measured emission factors was assumed to be most representative of reality and used for further discussion. In addition, the impact of an uncertainty factor of 10 on UP emissions from $\sum_7$ PCBs was also explored (see Figure S2).

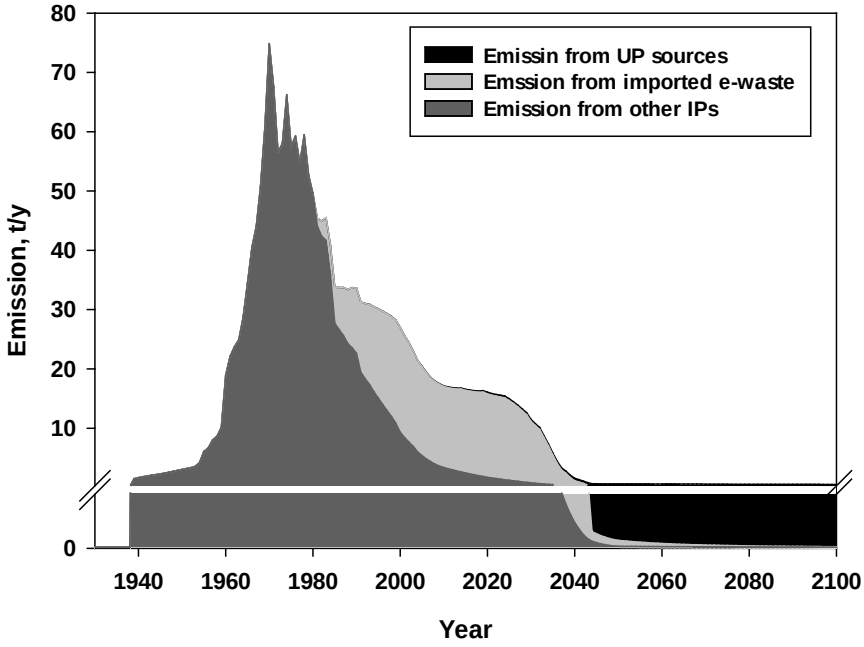

Figure 3. Predicted trends of total PCBs emission in China from 1930 to 2100 under the default scenario (IP+UP).

The cumulative intentionally produced emission of $\sum_7$ PCBs from 1930 to 2040 was estimated at 2300 tonnes in China (illustrated in Figure 3) with future emission estimated to be about 2 tonnes from 2040 to 2100. Emissions of $\sum_7$ UP-PCBs were predicted to be 9.5 tons between 1949 and 2040. However, their future estimation (2040-2100) were estimated around 23 tons under the default scenario with measured emission factors. As a result, emissions from $\sum_7$ UP-PCB sources only account for a minor portion (of the total PCBs emission, approximately 0.4% during the period of 1930-2040 while they would play an increasingly important role in the distant future (2040-2100) accounting for up to 91% among the $\sum_7$ PCB (UP+IP).

The predicted atmospheric concentrations were almost identical for the three emission scenarios, over the period 1930 to 2010 for $\sum_7$ PCBs (see Figure S2). This further supports the assumption that UP-PCBs did not contribute significantly over that period. After 2010, however, predicted air concentrations started to diverge differently for each congener, attributed to different congener abundances UP-PCB sources. In addition, the identification of markers could be informative for future monitoring activities. Previously, PCB-118 was demonstrated to be a good marker congener to describe and evaluate the emission trends from the industrial thermal process, since it falls in both classes of dl-PCBs and indicator PCBs (Liu et al., 2013). On the other hand, PCB-28 was also demonstrated to have a significant correlation with seven congeners (Cui et al., 2015). In this study, both correlation relationships were explored for PCB-

28 and PCB-118, a correlation coefficient (R^2) of 0.98 and 0.90 was observed ($p<0.001$), respectively. Therefore, PCB-28 was suggested to be a useful indicator congener.

For UP sources, PCB-28 was the dominant congener of the $\sum_7$ PCBs emission, accounting for approximately 78% during 1930-2100. It also contributes about 28% of the $\sum_7$ PCBs (IP+UP) emissions over the period dominated by IP-PCBs (1940-2010). The historical predominance of IP-PCB-28 was anticipated, as tri-PCBs were dominant in commercial mixtures used in China. In addition, atmospheric concentrations of PCB-28 indicate the largest difference under three scenarios, which is up to 6 orders of magnitude (Figure 4-a). This difference is minimal for PCB-153 in Figure 4 -b. UP sources are more important for lighter PCBs (PCB28/52) than heavier ones (PCB138/153), contributing less than 50% concentrations in air. In addition, atmospheric concentrations of different congeners will be dominated by unintentional sources at different times. For example, PCB-28 is predicted to be dominated by the UP-PCBs from 2035, due to high abundance among UP-PCBs sources while PCB-52 will be dominated by UP sources after 2040 with a relatively gradual shift.

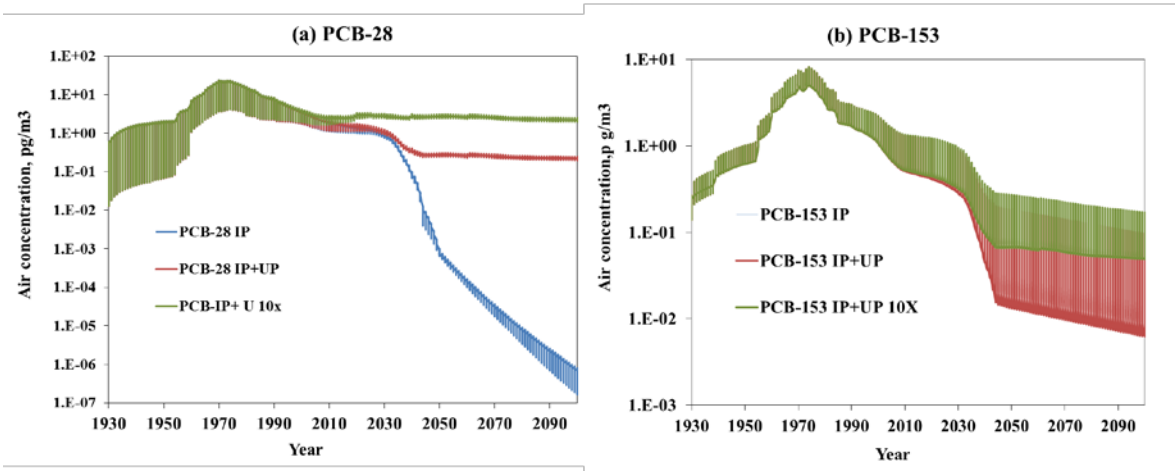

Figure 4. Predicted atmospheric concentrations under three scenarios for PCB-28 and PCB-153 in central China (Grid 92).

3.3 Contribution from imported (national or regional) e-waste

The trans-boundary movements of e-waste from developed countries to developing countries has made it a potentially substantial inventory and emission source of PCBs (Breivik et al., 2014; Breivik et al., 2015). Therefore, the contribution of imported e-waste was explored to identify its potential influence (national or regional in China). The cumulative emissions from imported e-waste are predicted to contribute around 30% to the total emissions for seven congeners during 1930-2100. PCB-180 received the highest percentage (45%) from imported e-waste. In terms of the cumulative atmospheric concentration in different study grids (see Fig S3), the

337 contribution of e-waste was largest for Grid 116 (which included most e-waste recycling sites in
338 South China), making up more than 30% of all congeners.

339 The influence of e-waste varied in different sampling years as illustrated in Figure 5. The e-
340 waste started to be imported into China from about 1980. So it is obvious that the grid 116
341 received the highest burden in atmosphere contributed by the imported e-waste, since the main
342 e-waste recycling sites (e.g., Guiyu and Qingyuan) with potential informal recycling activities
343 are located here (Breivik et al., 2014). Evident regional differences are predicted in terms of
344 influence from imported-waste, e.g., Grid cell 61 (mainly covering Xinjiang) received the least
345 e-waste associated PCBs, possibly due to its far distance from the e-waste recycling sites. In
346 addition, its influential scale may be potentially shifted from local/regional source to a national
347 level. Imported e-waste is predicted to play an increasing role until 2020-2030 on a national
348 scale, when Grid cell 116 receive more than 90% of input contributed by imported e-waste. The
349 impact scale of e-waste expanded and the remote regions received increasing portion from e-
350 waste recycling sites. However, after 2030, the relative contribution from imported e-waste is
351 diminishing (Figure 5-c, d) to present less than 5% to the total modelled air concentration on
352 2100.

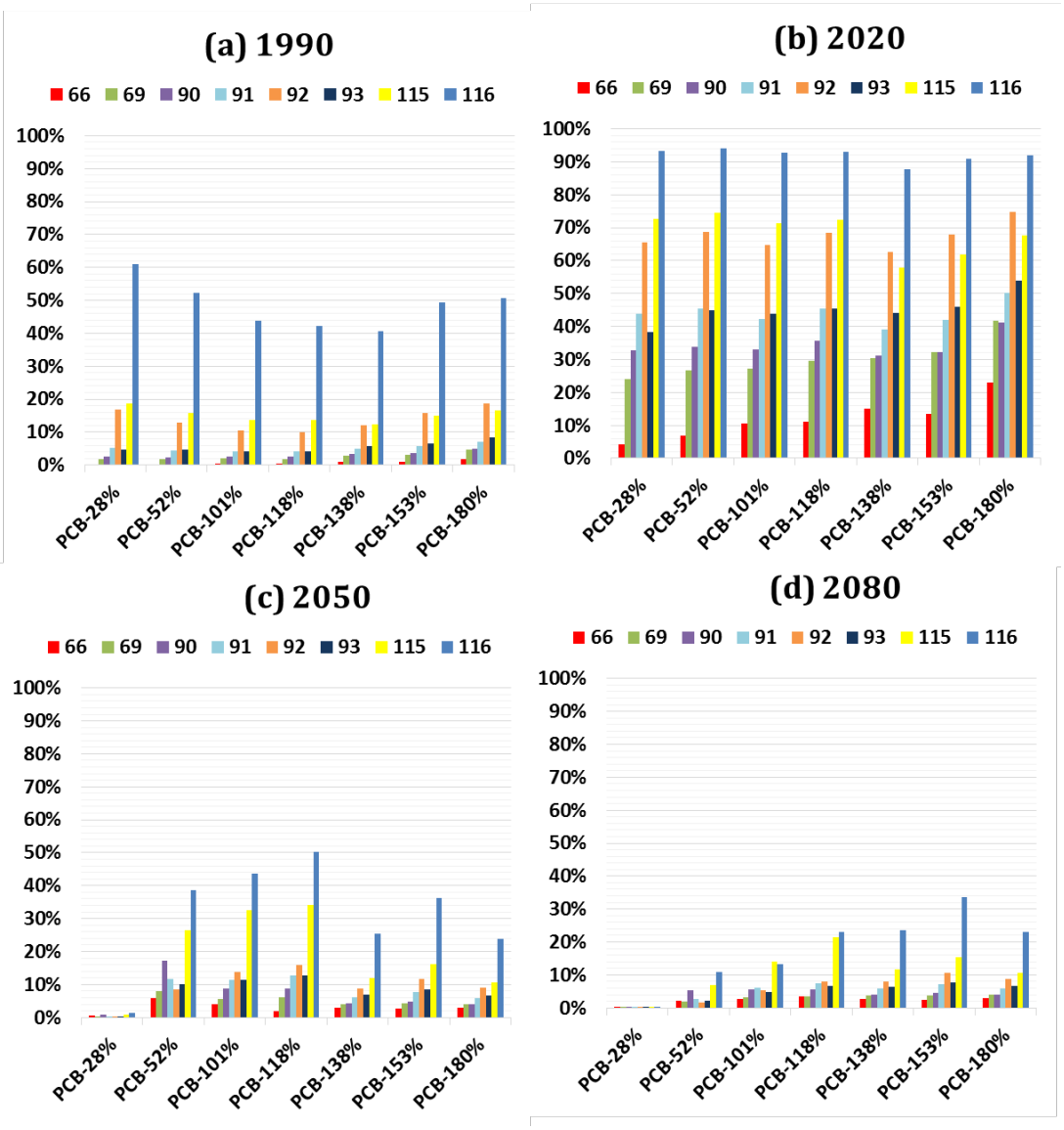

Figure 5. Imported e-waste contribution (sum of domestic generation and foreign import) to the total environmental concentration in 1990 (a), 2020 (b), 2050 (c) and 2080 (d) in specified grid cell numbers (66, 69, 91, 92, 115, 116).

3.4 Contribution from secondary sources

Being able to distinguish between primary and secondary sources is important for understanding our ability to control sources and to aid policy makers to develop the most effective control measures. The advection into (and out of) China from the wider Asian region also needs to be quantified to place China's activities into a regional context. Therefore, the primary and secondary sources from China (region) and out of China (extra-region) were estimated for PCB-28 and PCB-153 (see Figure S4-a, b). In addition, the individual contribution of secondary sources from soil, water and vegetation to air, was explored (Figure S4 c, d), where regional primary/secondary emission represent emissions from the domestic sources (China) while extra-regional/primary emission represents the emissions from outside China, as result of LRAT.

When separating secondary sources into regional and extra-regional, the profiles for PCB-28 and PCB-153 were similar until 2030 (see Figure S4). The extra-regional primary and secondary sources dominate the emission during the initial period from 1930 to 1960 for both PCB-28 and PCB-153. During that period, China did not have any domestic production or usage of PCBs. Therefore, LRAT would have been responsible for supplying PCB to the Chinese environment. However, when China started to produce PCBs in 1964, primary sources became increasingly important and had provided a constant contribution of approximately 70% which is predicted to continue until around 2030. Afterwards, both congeners are predicted to behave differently behaviour. Future pattern of PCB-28 was mainly dominated by regional primary emission while PCB-153 was mostly controlled by extra-regional secondary sources. This could be because that PCB-28, mainly being supplied by ongoing and increasingly important UP sources as discussed in Section 3.2. Instead, the primary sources of PCB-153 may be gradually ceased within China with secondary extra-regional emission gradually replacing this role.

Several studies suggest that the main contribution to PCB emission should move from the primary to secondary sources as production and use of PCBs declines (Cousins et al., 1999; Harner et al., 1995). In China, the same trend is seen for PCB-28 when simulations were performed only considering IP-PCBs (see Figure S5). However, when taking UP-PCB into account, it appeared that the primary sources remained dominant over the whole simulation period. As for the individual sources of UP-PCBs, the main contribution to emissions is converted cement kilns to EAF production over the period 2010 to 2020 (see Figure S6). EAF allows steel to be made from 100% scrap, and as a result, it could greatly reduce energy consumption (Pauliuk et al., 2013). So this technology is being strongly promoted. However, without effective control measures, EAF may have potential to cause increased emission of UP-PCBs

3.4.1 Re-emission from soil-air

The exchange of POPs across the air-soil interface is one of the most important process determining their long-term environmental fate, as the soil is thought to be the major sink in the terrestrial environmental (Cousins et al., 1999). When individual contributions from soil and vegetation to the secondary sources for PCB-153 were explored (see Figure S4-c, d), vegetation is predicted to dominate until 2030 with soil gradually becoming the main secondary source. This is a reflection of the relative size of vegetation and soils as storage compartments. Delayed re-emissions normally occur from compartments that are slow to respond to changes in atmospheric concentrations such as soils and the oceans (Wohrnschimmel et al., 2012). Therefore, soil represents an initial sink for PCBs until it reaches equilibrium with air, after which it becomes a net source as primary emissions reduce (Li et al., 2010). It is important to

take into account that these calculations assume a soil depth of 20 cm and increasing the depth would increase soil capacity (Sweetman et al., 2005) and vice versa.

Secondary emissions also occur from vegetation, although over a much shorter time-scale as vegetation responds rapidly to the changes in atmospheric concentrations (Wohrnschimmel et al., 2012), The model suggests that vegetation is the dominant secondary source for the whole simulation period for PCB-28 (see Figure S4-c). This may be because primary sources are controlling the emission to the atmosphere, with soils acting as a reservoir during the simulated period. It has also been demonstrated that atmospheric deposition is the main contamination pathway for vegetation, rather than uptake from the soil, based on a study of paddy rice in China (Bi et al., 2001).

3.4.2 Analysis of compartment response times (VZ/D)

The importance of soil and vegetation compartments as secondary sources can also be explained in terms of model calculations. Taking air (A), soil (S) and vegetation (V) as examples. The fugacity capacities of each medium can be calculated using compartment volume (V, m^3) and fugacity capacity (Z, mol m^{-3} Pa^{-1}). For PCB-28, the V_SZ_S is 2.6×10^{15} mol Pa^{-1}, VvZv is 2.5×10^{12} V_AZ_A is 7.4×10^{11} mol Pa^{-1}. Thus, the soil has approximately 3500 times the storage capacity of the air and has approximately 1000 times capacity of the vegetation The transport parameter D value for soil-to-air transfer D_{SA} is 2.3×10^{9} mol $Pa^{-1}h^{-1}$ and vegetation-to-air transfer $D_{V,A}$ is 9.6×10^{9} mol Pa^{-1} h^{-1}. The characteristic time (VZ/D), is the average time that a chemical spend in a single compartment and is the first indication of persistence (Mackay, 2001). This was calculated to be about 92 years and ten days in soil and vegetation, respectively (Sweetman et al., 2002). Therefore, the PCB-28 in the atmosphere will rapidly exchange with the vegetation as it attempts to approach equilibrium. In addition, the pathways of air-to-soil and vegetation-to-soil were also calculated to compare the relative importance of these two pathways. The calculations suggest that the characteristic time from air to soil are 3 and 18 days while vegetation to soil is about one year. However, the leaf area can be much bigger than the soil surface area covered by vegetation (Moeckel et al., 2009). So vegetation may take a lot more PCBs to the soil then directly deposit from air to soil can account for.

3.5 Atmospheric advection

The importance of atmospheric advection between study regions (covered main China) and extra-region was investigated and the results presented in Figure 6 for two contrasting years 1980 and 2050, representing the ‘in-use’ and ‘phase-out’, respectively. PCB production and use were restricted around 1974 (Breivik et al., 2002a), and peak emissions were expected around 1980. At that time, the central part of China (represented by grids 66, 69, 90, 91, 92,115 and 116) acted as a PCB storage reservoir while the west and east of the country as industrialized areas

acted as sources of PCBs to the regions. It is interesting to note that the western parts of the country, which are not highly industrialized, have been acting as a net source of PCB-28, which may be attributed to its volatility and advection from the rest of the world. When looking at future predictions until 2050, the central part of China is still predicted to receive PCBs from the industrialized regions although with the decreasing quantity. The direction of the net flux changes from the west and northeast. Therefore, the Chinese region has a high potential to change from a source to a sink. When examining China a whole, the model predicts that the country has moved from a net sink with a net input of 800 kg year^{-1} to acting as a potential source to neighbouring regions with a net output of 444 kg year^{-1}.

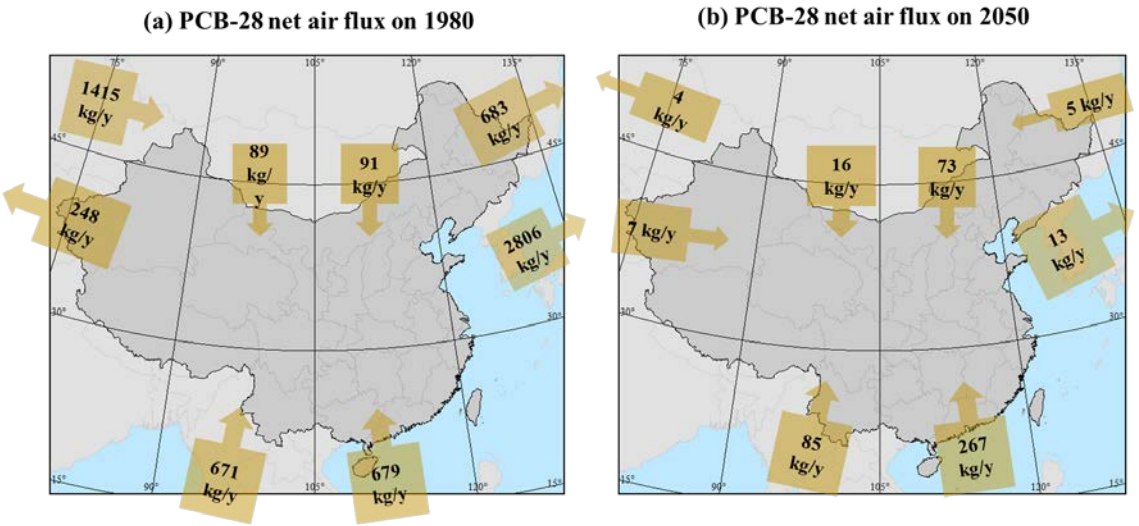

Figure 6. The net flux of air between region and extra-region on 1980 (a) and 2050 (b), reflecting the default emission scenario (IP+UP).

3.6 Uncertainty

The emission inventory and environmental concentrations estimated in this study contain high levels uncertainty caused by a wide range of factors. The first issue is on the identification of comprehensive of e-waste sources. Although the domestically generation of e-waste and its import have generally been captured in the current inventory, several types of electronic equipment were not considered (e.g., large household appliances and telecommunication equipment), which are still on the rise combined with shortened lifespan. These may be considered in future work, though PCB production has been banned (Breivik et al., 2014). Another concern has been the difficulty in tracking illicit import of e-waste without effective regulation in China. A complementary approach to tracking the sources, flows and destination

of e-waste could provide further insights into the emission of e-waste pollutants (Breivik et al., 2014).

For the emission of UP-PCBs, only three major industrial processes were considered and explored in this study. Other industrial sources could also contribute to the emission of UP-PCBs, such as secondary zinc smelting and thermal wire reclamation (Liu et al., 2013). However, the individual congener profile of many industrial processes is lacking, and using emission factors from other countries has been shown to be misleading. Fox example, when comparing the emission factors used in this study (Liu et al., 2013) with those reported from other countries, large differences were observed. For example, emission factors for cement production were up to 1000 times lower here than those used in the Japanese Toolkit (Cui et al., 2013). This could be that the industrial thermal process used as the waste incinerators fed on alternative waste material in China is not very common, leading to less emission of toxic chemicals via thermal processes. In addition, the composition of the raw materials fed to the sinter plant, would potentially enhance the chlorination formation of PCBs. Even within this study, there were wide variations observed in the same type of plants in China with up to 100 times difference in the most extreme case (Liu et al., 2013). Therefore, using the emission factors from other countries would only be recommended when domestic measurements are not available. Even then, caution should be taken. These differences also highlight the need for a more systematic survey of emission sources on a national scale to provide an unbiased and comprehensive reference for the emission inventory. A better characterization of emission factors is essential to help to produce a more accurate estimation of the time trends in future.

The actual sources of PCBs via the industrial process also need to be further scrutinized. Since PCBs are not only formed by *de novo* synthesis or precursors, they may also be present in the raw materials (Roudier et al., 2013). For example, PCB concentrations in iron ores were reported to be around 1-1.6 mg t^{-1} in a European sinter plant (Fisher et al., 2005). They are likely to be destroyed mostly in the combustion zone but may be driven off due to their volatility. Therefore, it is very important but also, a great challenge to differentiate the portion existing in the raw material and from the new formation, in order to avoid double accounting for emission estimation and customized the most effective control strategies.

In the cement industry, China uses the coal almost exclusively as the fuel (Hasanbeigi et al., 2010). In addition, there is very little use of alternative fuels (defined as waste materials with heat value more than 4000 kcal kg^{-1} for cement clinker burning) or compressing with waste materials (defined as the incineration of wastes for disposal purposes) in cement production. However, Chinese laws and policies now tend to encourage industry to use alternative fuels and waste materials (Hasanbeigi et al., 2010). This may have an increased trend if the more recycled waste material is used to feed the cement production.

In the steel and iron industries, the raw materials are mainly from self-produced steel scrap, collected from society and imported from aboard. The process of scrap preheating used in EAF may result in higher emissions of PCBs from contaminated scrap with paints and lubricants containing PCBs, which could be minimized post-combustion using additional oxygen burners (Fisher et al., 2005). However, the related information is very limited in China. For recycled scrap, it is forbidden to have hazardous material with more than 50 mg kg^{-1} PCBs regulated by the Chinese government (GB13015-91). So the impact caused by the presence of PCBs in raw materials for steel industry is assumed negligible.

In this study, population density was used distribute PCB emission to each grid cell. For the UP-PCBs, high uncertainty may exist due to the recent movement of industrial sources from urban to rural or semi-rural areas. For example, most PCB-containing equipment is stored at special sites after they are out of use. Due to poor management and storage conditions, PCBs from some of these special storage locations have leaked into the environment of surrounding areas, especially to the soil (Xing et al., 2005; Zhang et al., 2008).

3.7 Implications for control measures

The environmental response to regulatory measures for the control of persistent chemicals can be very slow and substance-specific (Lammel and Stemmler, 2012). Meanwhile, a regional difference is also anticipated, particularly for a large country with varied geographical information and levels of economic development like China. For this reason, an effective strategy should be developed and implemented as early as possible. Results from this study suggest that the effectiveness of emission control measures may vary significantly for individual substances and specific regions. For example, primary sources are still predominant for PCB-28, which means the controllable sources could be effectively mitigated via implementing policy and regulations, especially for controlling the UP-PCBs from industrial processes. Although the techniques have been developed for reducing the emissions of individual POPs, further work is needed to control POPs from industrial activities, and on-site monitoring is lacking (Liu et al., 2015). Nevertheless, this may not work well for PCB153 and PCB-180, since imported e-waste is a more important contributor at this stage, particularly in the southern part of China (Grid 116). The situation is also different in western of China, where both imported e-waste and UP-PCBs do not play a significant role.

4 Conclusions

The contribution of unintentional sources and imported e-waste to the total emission and atmospheric burden of $\sum_7$ PCBs were explored in this study. A dynamic Level IV multimedia fate model (BETR-Global) was shown to be a useful tool to reconstruct and assess the historical

emission trend as well as to predict the environmental behaviour of this classical POP category. China could become a potential source to neighbouring regions with a predicted net output of 444 kg $year^{-1}$ for PCB-28 by 2050 without effective control measures. The influence of e-waste could be potentially shifted from a regional to a national level by 2020. The predictions suggest that UP-PCBs have had little impact on the past emission profile, but may potentially provide a greater contribution from around 2050, if current industrial thermal processes, continue without further control strategies. Contemporary emission estimates combined with predictions from a multimedia fate model suggests that primary sources still predominate environmental burdens, with PCB-28 produced by unintentional sources becoming a main contributor around 2035. Calculation of the future significance of UP-PCBs sources involves large uncertainties but could be improved significantly with systematic measurements of emission factors, which would enable more accurate determination of emission trends.

5 Acknowledgment

We would like to thank Unilever for funding this research. Thanks to Matthew MacLeod and Henry Wohrnschimmel from Stockholm University for their guidance on using BETR-Global model. Thanks to Dr. Stefan Pauliuk and Pro Zeyi Jiang for offering data estimated production of EAF and iron sinter. Thanks to Prof. Knut Breivik for providing the data on the updated emission inventory and offering comments on a preliminary draft.

6 References

Annema J, Beurskens J, Bodar C. Evaluation of PCB fluxes in the environment. Report no.601014011. National Institute for Public Health and the Environment (RIVM) 1995.

Bi X, Chu S, Xu X. Transport of PCB in contaminated paddy fields. Acta Scientiae Cirumstantiae 2001; 21: 454-458.

Breivik K, Alcock R, Li YF, Bailey RE, Fiedler H, Pacyna JM. Primary sources of selected POPs: regional and global scale emission inventories. Environmental Pollution 2004; 128: 3-16.

Breivik K, Armitage JM, Wania F, Jones KC. Tracking the global generation and exports of e-waste. Do existing estimates add up? Environ Sci Technol 2014; 48: 8735-43.

Breivik K, Armitage JM, Wania F, Sweetman AJ, Jones KC. Tracking the global distribution of persistent organic pollutants accounting for e-waste exports to developing regions. Environ Sci Technol 2015.

Breivik K, Czub G, McLachlan MS, Wania F. Towards an understanding of the link between environmental emissions and human body burdens of PCBs using CoZMoMAN. Environ Int 2010; 36: 85-91.

Breivik K, Sweetman A, Pacyna JM, Jones KC. Towards a global historical emission inventory for selected PCB congeners - a mass balance approach 1. Global production and consumption. Science of the Total Environment 2002a; 290: 181-198.

Breivik K, Sweetman A, Pacyna JM, Jones KC. Towards a global historical emission inventory for selected PCB congeners - a mass balance approach 2. Emissions. Science of the Total Environment 2002b; 290: 199-224.

572 Breivik K, Sweetman A, Pacyna JM, Jones KC. Towards a global historical emission inventory
573 for selected PCB congeners — a mass balance approach: 2. Emissions. Science of The
574 Total Environment 2002c; 290: 199-224.
575 Breivik K, Sweetman A, Pacyna JM, Jones KC. Towards a global historical emission inventory
576 for selected PCB congeners — A mass balance approach: 3. An update. Science of The
577 Total Environment 2007; 377: 296-307.
578 Cousins IT, Beck AJ, Jones KC. A review of the processes involved in the exchange of semi-
579 volatile organic compounds (SVOC) across the air-soil interface. Science of the Total
580 Environment 1999; 228: 5-24.
581 Cui S, Fu Q, Ma W-L, Song W-W, Liu L-Y, Li Y-F. A preliminary compilation and evaluation
582 of a comprehensive emission inventory for polychlorinated biphenyls in China. Science
583 of The Total Environment 2015; 533: 247-255.
584 Cui S, Qi H, Liu LY, Song WW, Ma WL, Jia HL, et al. Emission of unintentionally produced
585 polychlorinated biphenyls (UP-PCBs) in China: Has this become the major source of
586 PCBs in Chinese air? Atmospheric Environment 2013; 67: 73-79.
587 Feng L. China's steel industry: Its rapid expansion and influence on the international steel
588 industry. Resources Policy 1994; 20: 219-234.
589 Fisher R, GARCIA CARCEDO E, ALAIZ ALVAREZ E, Pietruck R. Influence of sinter mix
590 materials on the environmental impact of high productivity iron ore sintering. EUR
591 2005: 1-101.
592 Frame GM, Cochran JW, Bøwadt SS. Complete PCB congener distributions for 17 Aroclor
593 mixtures determined by 3 HRGC systems optimized for comprehensive, quantitative,
594 congener‐specific analysis. Journal of High Resolution Chromatography 1996; 19:
595 657-668.
596 Fu J, Mai B, Sheng G, Zhang G, Wang X, Peng Pa, et al. Persistent organic pollutants in
597 environment of the Pearl River Delta, China: an overview. Chemosphere 2003; 52:
598 1411-1422.
599 Harner T, Mackay D, Jones KC. Model of the long-term Exchange of PCBs between soil and
600 the atmosphere in the southern U.K. Environ Sci Technol 1995; 29: 1200-9.
601 Hasanbeigi A, Price L, Lu H, Lan W. Analysis of energy-efficiency opportunities for the
602 cement industry in Shandong Province, China: A case study of 16 cement plants.
603 Energy 2010; 35: 3461-3473.
604 Hogarh JN, Seike N, Kobara Y, Habib A, Nam J-J, Lee J-S, et al. Passive air monitoring of
605 PCBs and PCNs across East Asia: A comprehensive congener evaluation for source
606 characterization. Chemosphere 2012; 86: 718-726.
607 Jaward TM, Zhang G, Nam JJ, Sweetman AJ, Obbard JP, Kobara Y, et al. Passive air sampling
608 of polychlorinated biphenyls, organochlorine compounds, and polybrominated diphenyl
609 ethers across Asia. Environmental Science & Technology 2005; 39: 8638-8645.
610 Jiang K, Li L, Chen Y, Jin J. Determination of PCDD/Fs and dioxin-like PCBs in Chinese
611 commercial PCBs and emissions from a testing PCB incinerator. Chemosphere 1997;
612 34: 941-950.
613 Jones KC, de Voogt P. Persistent organic pollutants (POPs): state of the science. Environmental
614 Pollution 1999; 100: 209-221.
615 Lammel G, Stemmler I. Fractionation and current time trends of PCB congeners: evolvement of
616 distributions 1950–2010 studied using a global atmosphere-ocean general circulation
617 model. Atmos. Chem. Phys. 2012; 12: 7199-7213.
618 Lamon L, Von Waldow H, Macleod M, Scheringer M, Marcomini A, Hungerbuhler K.
619 Modeling the global levels and distribution of polychlorinated biphenyls in air under a
620 climate change scenario. Environ Sci Technol 2009; 43: 5818-24.
621 Li YF, Harner T, Liu L, Zhang Z, Ren NQ, Jia H, et al. Polychlorinated biphenyls in global air
622 and surface soil: distributions, air-soil exchange, and fractionation effect. Environ Sci
623 Technol 2010; 44: 2784-90.
624 Li YF, McMillan A, Scholtz MT. Global HCH usage with 1 degrees x1 degrees
625 longitude/latitude resolution. Environmental Science & Technology 1996; 30: 3525-
626 3533.

627 Liu G, Zheng M, Jiang X, Jin R, Zhao Y, Zhan J. Insights into the emission reductions of
628 multiple unintentional persistent organic pollutants from industrial activities.
629 Chemosphere 2015; 144: 420-424.
630 Liu GR, Zheng MH, Cai MW, Nie ZQ, Zhang B, Liu WB, et al. Atmospheric emission of
631 polychlorinated biphenyls from multiple industrial thermal processes. Chemosphere
632 2013; 90: 2453-2460.
633 Mackay D. Multimedia Environmental Models: The Fugacity Approach, Second Edition:
634 Taylor & Francis, 2001.
635 Macleod M, Riley WJ, Mckone TE. Assessing the influence of climate variability on
636 atmospheric concentrations of polychlorinated biphenyls using a global-scale mass
637 balance model (BETR-global). Environmental Science & Technology 2005; 39: 6749-
638 6756.
639 MacLeod M, von Waldow H, Tay P, Armitage JM, Wöhrnschimmel H, Riley WJ, et al. BETR
640 Global–A geographically-explicit global-scale multimedia contaminant fate model.
641 Environmental Pollution 2011; 159: 1442-1445.
642 Mai BX, Zeng EY, Luo XJ, Yang QS, Zhang G, Li XD, et al. Abundances, depositional fluxes,
643 and homologue patterns of polychlorinated biphenyls in dated sediment cores from the
644 Pearl River Delta, China. Environmental Science & Technology 2005; 39: 49-56.
645 Moeckel C, Nizzetto L, Strandberg B, Lindroth A, Jones KC. Air-boreal forest transfer and
646 processing of polychlorinated biphenyls. Environ Sci Technol 2009; 43: 5282-9.
647 Nizzetto L, Macleod M, Borgå K, Cabrerizo A, Dachs J, Guardo AD, et al. Past, Present, and
648 Future Controls on Levels of Persistent Organic Pollutants in the Global Environment.
649 Environmental Science & Technology 2010; 44: 6526-6531.
650 Pauliuk S, Milford RL, Muller DB, Allwood JM. The steel scrap age. Environ Sci Technol 2013;
651 47: 3448-54.
652 Ren N, Que M, Li YF, Liu Y, Wan X, Xu D, et al. Polychlorinated biphenyls in Chinese surface
653 soils. Environ Sci Technol 2007; 41: 3871-6.
654 Roudier S, Sancho LD, Remus R, Aguado-Monsonet M. Best Available Techniques (BAT)
655 Reference Document for Iron and Steel Production: Industrial Emissions Directive
656 2010/75/EU: Integrated Pollution Prevention and Control. Institute for Prospective and
657 Technological Studies, Joint Research Centre, 2013.
658 Schenker U, MacLeod M, Scheringer M, Hungerbuhler K. Improving data quality for
659 environmental fate models: a least-squares adjustment procedure for harmonizing
660 physicochemical properties of organic compounds. Environ Sci Technol 2005; 39:
661 8434-41.
662 Sweetman AJ, Cousins IT, Seth R, Jones KC, Mackay D. A dynamic level IV multimedia
663 environmental model: Application to the fate of polychlorinated biphenyls in the United
664 Kingdom over a 60-year period. Environmental Toxicology and Chemistry 2002; 21:
665 930-940.
666 Sweetman AJ, Valle MD, Prevedouros K, Jones KC. The role of soil organic carbon in the
667 global cycling of persistent organic pollutants (POPs): interpreting and modelling field
668 data. Chemosphere 2005; 60: 959-972.
669 Wang X-p, Sheng J-j, Gong P, Xue Y-g, Yao T-d, Jones KC. Persistent organic pollutants in the
670 Tibetan surface soil: Spatial distribution, air–soil exchange and implications for global
671 cycling. Environmental Pollution 2012a; 170: 145-151.
672 Wang XP, Gong P, Yao TD, Jones KC. Passive air sampling of organochlorine pesticides,
673 polychlorinated biphenyls, and polybrominated diphenyl ethers across the tibetan
674 plateau. Environ Sci Technol 2010; 44: 2988-93.
675 Wang Y, Cheng Z, Li J, Luo C, Xu Y, Li Q, et al. Polychlorinated naphthalenes (PCNs) in the
676 surface soils of the Pearl River Delta, South China: Distribution, sources, and air-soil
677 exchange. Environmental Pollution 2012b; 170: 1-7.
678 Wohrnschimmel H, MacLeod M, Hungerbuhler K. Global multimedia source-receptor
679 relationships for persistent organic pollutants during use and after phase-out.
680 Atmospheric Pollution Research 2012; 3: 392-398.

Xing X, Lu YL, Dawson RW, Shi YJ, Zhang H, Wang TY, et al. A spatial temporal assessment of pollution from PCBs in China. Chemosphere 2005; 60: 731-739.
Yang H, Zhuo S, Xue B, Zhang C, Liu W. Distribution, historical trends and inventories of polychlorinated biphenyls in sediments from Yangtze River Estuary and adjacent East China Sea. Environmental Pollution 2012; 169: 20-26.
Zhang Z, Liu L, Li Y-F, Wang D, Jia H, Harner T, et al. Analysis of Polychlorinated Biphenyls in Concurrently Sampled Chinese Air and Surface Soil. Environmental Science & Technology 2008; 42: 6514-6518.
Zheng Q, Nizzetto L, Mulder MD, Sanka O, Lammel G, Li J, et al. Does an analysis of polychlorinated biphenyl (PCB) distribution in mountain soils across China reveal a latitudinal fractionation paradox? Environmental Pollution 2014; 195: 115-122.

Supporting information for

"Long-term temporal trend of PCBs and their controlling sources in China"

*Shizhen Zhao[1], Oliver Price[2], Guorui Liu[3], Minghui Zheng[3], Kevin C. Jones[1], Andrew J. Sweetman[*1]*

[1] Lancaster Environment Centre, Lancaster University, Lancaster, LA14YQ, UK

[2] Safety and Environmental Assurance Centre, Unilever, Sharnbrook, MK44 1LQ, UK.

[3] State Key Laboratory of Environmental Chemistry and Ecotoxicology, Research Centre for Eco-Environmental Sciences, Chinese Academy of Sciences, P.O. Box 2871, Beijing 100085, China.

Contents

Physical-chemical properties of selected congeners

Table S1. The molecular weight (MW, g mol^{-1}), partition coefficients at 25 ℃ (K, dimensionless), internal energies of phase transfer (ΔU, kJ mol^{-1}), air reaction half-life (HL_{air}, h), and the activation energy for reaction in air (E_{air}, kJ mol^{-1}). Partition coefficient and internal energy of phase changes from (Schenker et al., 2005), degradation half-life was from (Sinkkonen and Paasivirta, 2000).

Chemical	**MW**	**log K_{OW}**	**log K_{OA}**	**Log K_{AW}**	**ΔU_{OW}**	**ΔU_{OA}**	**E_{air}**	**HL_{air}**
PCB-28	257.54	5.66	7.85	-1.93	-26.6	-78.4	10	161
PCB-52	291.99	5.95	8.22	-1.96	-27.5	-81.3	10	268
PCB-101	326.43	6.38	8.83	-2.08	-19.3	-84.4	10	444
PCB-118	326.43	6.65	9.44	-2.36	-24.5	-89.8	10	444
PCB-138	360.88	7.19	9.67	-1.97	-22.2	-86.9	10	739
PCB-153	360.88	6.86	9.45	-2.13	-26.6	-94.8	10	737
PCB-180	395.32	7.15	10.17	-2.51	-26.1	-95.2	10	1224

Prediction of UP-PCBs

Cement production volume prediction

The production volume of cement in China was taken from the Statistical Yearbooks (1949-2014) (http://www.stats.gov.cn/tjsj/ndsj/, accessed on 27/09/2015). Production volumes beyond 2014 were estimated and assumed that China will follow the growth trend of cement production of developed countries based on historical analysis of past consumption patterns. The key point is to decide the timing when per capita will reach the maximum level, so the gap could be filled by extrapolation between now and then. As economic growth is not evenly distributed in China the year in which capita stock saturation occurs will also be different. The more developed regions, mostly in eastern China, would be expected to enter a period of capital stock saturation earlier than the relatively undeveloped regions in eastern China, due to the higher speed of construction. To simplify the prediction of the point in time when the cement production started to decrease, the year 2020 was predicted by historical analysis for the western countries was selected to stand for the whole countries (Shi, 2011). Cement production was estimated to remain stable from 2040 with an average consumption rate of 0.6 tonne $capita^{-1}year^{-1}$ as a worst case. The Chinese population growth data were estimated by the United Nations with the high fertility scenario being used (http://esa.un.org/wpp/Excel-Data/population.htm, accessed on 26/06/2015). The gap between the peak year 2020 and 2040 was filled assuming a linear relationship.

As a result, the production volume was estimated to peak around the year 2020 then reduce slightly becoming stable at 0.5-0.6 tonne for per person in China (Shi, 2011). For the growth

period (2014~2020) the elastic coefficient method was used to predict the cement production volume (Shi, 2011):

$P_{t+n}=P_n\times(1+E\times y)^t$

Where the P_n is the known production volume (t y^{-1}) of the previous year (starting from 2013), E is the elastic coefficient of cement production, y is the economic growth rate, n is the number of years. In this study, E was calculated from the average after the year of 1985. Thus E=0.572 and y=10.8%.

Predicting electric arc furnace (EAF) made steel production

The main techniques used to manufacture steel include basic oxygen furnace (BOF) and electronic arc furnace (EAF). EAF allows steel to be made from a 100% scrap metal feedstock, and so EAF will gradually replace BOF driven by the high demand for sustainable metal use in China (Pauliuk et al., 2012). In the past decade, the share of EAF-produced steel only accounted for around 10% of total steel production in China compared 30% and 57% globally and in the USA (Wang and Yang, 2010). In order to improve resource utilization and facilitate sustainable development, a rapid increase was foreseen for EAF-produced steel using recycled scrap (Pauliuk et al., 2012). A model comprising all stages of the life cycle of steel was used to provide a complete cycle in China based on future utilization of steel, which performed a stock-driven quantification of steel demand and supply of old scrap until 2100 (Pauliuk et al., 2012). The approach was developed by Pauliuk and Equation (S1) below was used to model the approach to saturation (Pauliuk et al., 2013):

$$S(t)=\frac{\hat{s}}{1+\left(\frac{\hat{s}}{s_0}-1\right)\cdot exp\left(c\cdot\left(1-exp(d\cdot(t-t_0))\right)\right)} \quad (S1)$$

where the parameters are: t: time, $\hat{s}$: saturation level, S_0: stock at a given t_o, c and d are numerical value for further boundary conditions. The long-term regression coefficients of Chinese per capita steel stock demand by a range of industries were simulated based on the data between 1975-2010 (Wang et al., 2014) as shown in Table 1. The total in-use stocks were determined by multiplying population forecasts with the perspective per capita stock patterns. Steel stock in China was estimated to saturate around 2050 (Wang et al., 2014). The scenario assumed that the Chinese government would take effective measures on the recycling of scrap steel, and as a result the recycle rate was estimated to reach 80% by 2020 and increase to 95% by 2060, which is equivalent to the level for developed countries (Wang et al., 2014).

Table 1. The long-term regression coefficients of Chinese per capita steel stock by industries (Wang et al., 2014).

Sectors	$\hat{s}$	**a**	**b**	R^2	**Lifetime, year**
Construction	5	1.224	0.035	0.998	29
Transportation	1.9	1.132	0.035	0.993	11
Machinery	2.3	1.113	0.031	0.986	15
Products	0.3	0.191	0.075	0.974	11
Other	0.5	0.927	0.041	0.952	13

Production of sinter iron

The production of sinter iron was recorded in the Statistical Yearbook of Iron and Steel for the period 1949 to 2011 (National Bureau of Statistics of the People's Republic of China, 2014). After the year of 2011, the volume of iron oxide in sinter/pellets was estimated using the mass balance flow of the stock driven model, which considered stocks of steel in construction and all other metal-bearing as a driving force behind the steel cycle. The detailed description could be found elsewhere (Pauliuk et al., 2012). It was assumed that 1.6 tonnes of sinter contain about 1 tonne of iron (Pauliuk, personal communication). However, based on the historical analysis of modelling results and recorded statistics, the realistic production volume of the sinter iron was four times higher than the prediction. To make the prediction consistent, a factor of four was multiplied to ensure that the trend was consistent. It is important to recognise that this represents a first approximation based on a mass balance approach. It is clear that uncertainty may exist using the different strategies/methods used for iron recycling (Pauliuk et al., 2012).

Additional model results

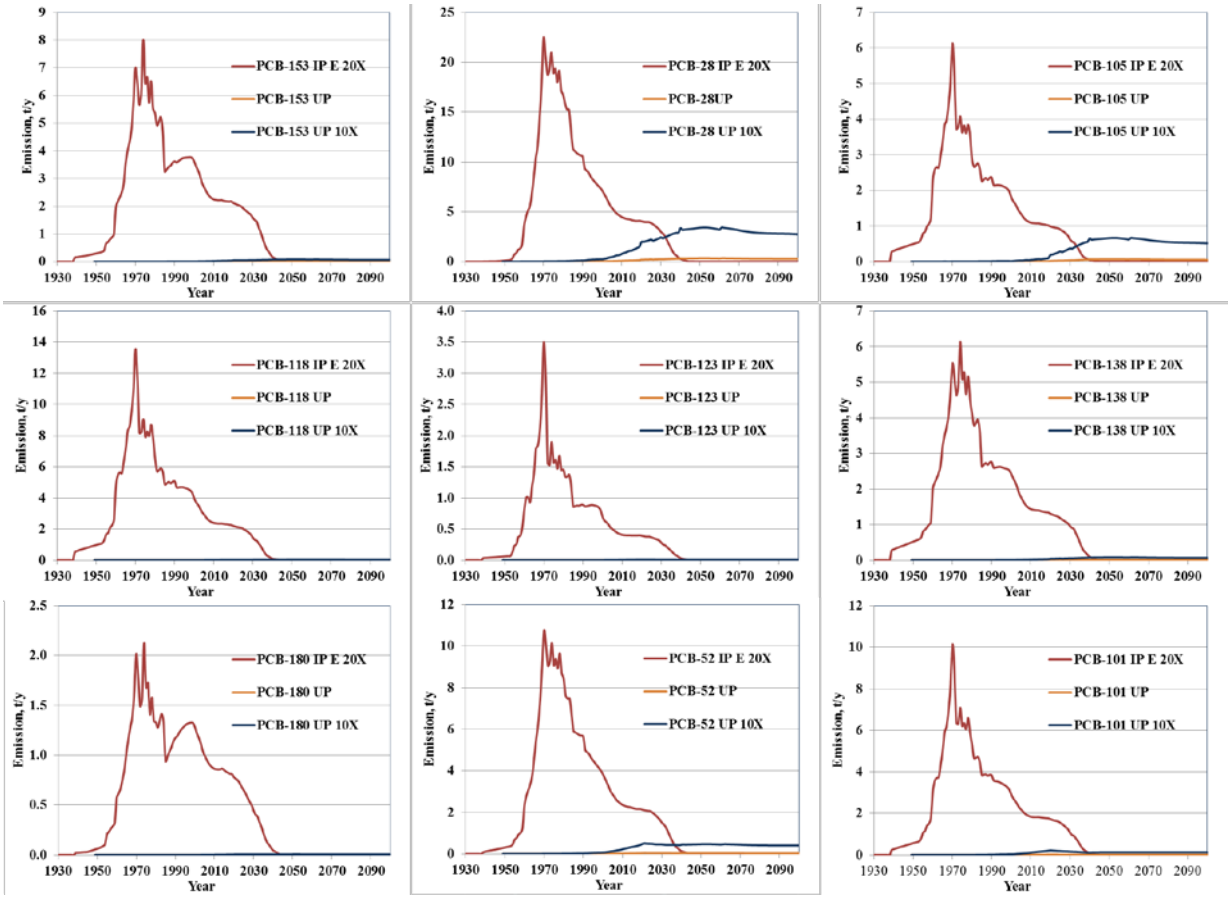

Figure S 1. Predicted emission inventories under three scenarios for all PCB congeners.

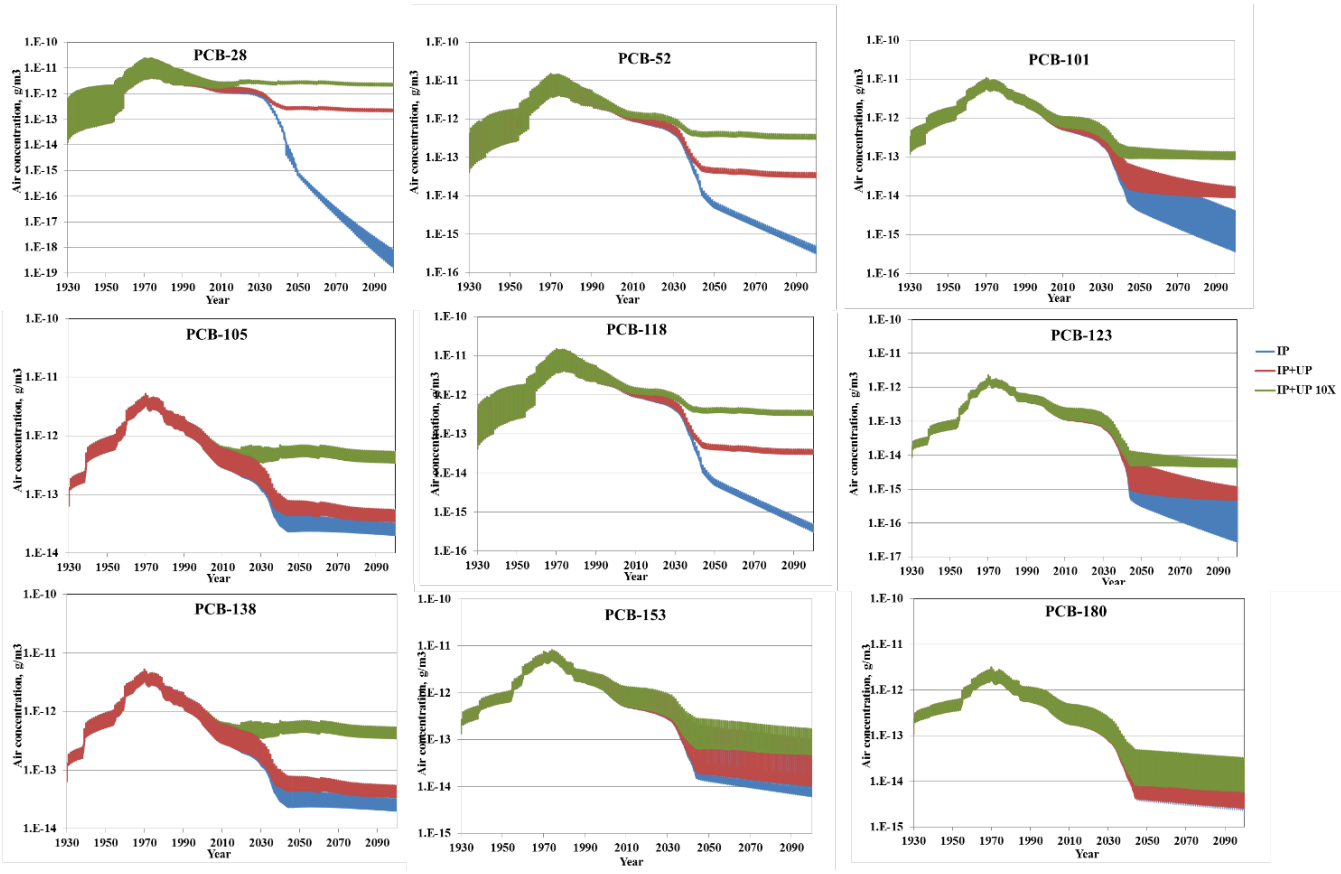

Figure S 2. Predicted atmospheric concentrations under three scenarios for PCB congeners in central China (Grid 92)

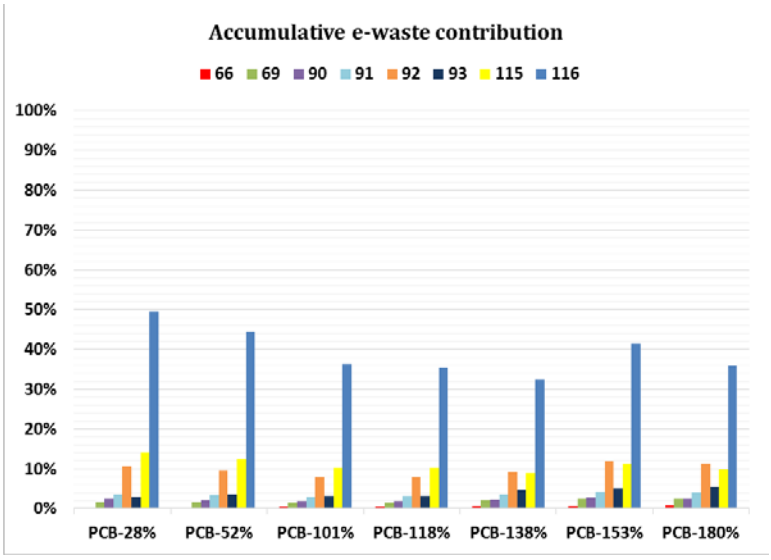

Figure S 3.The cumulative contribution of e-waste to the atmospheric concentrations of PCBs from 1930 to 2020 for different grid cells.

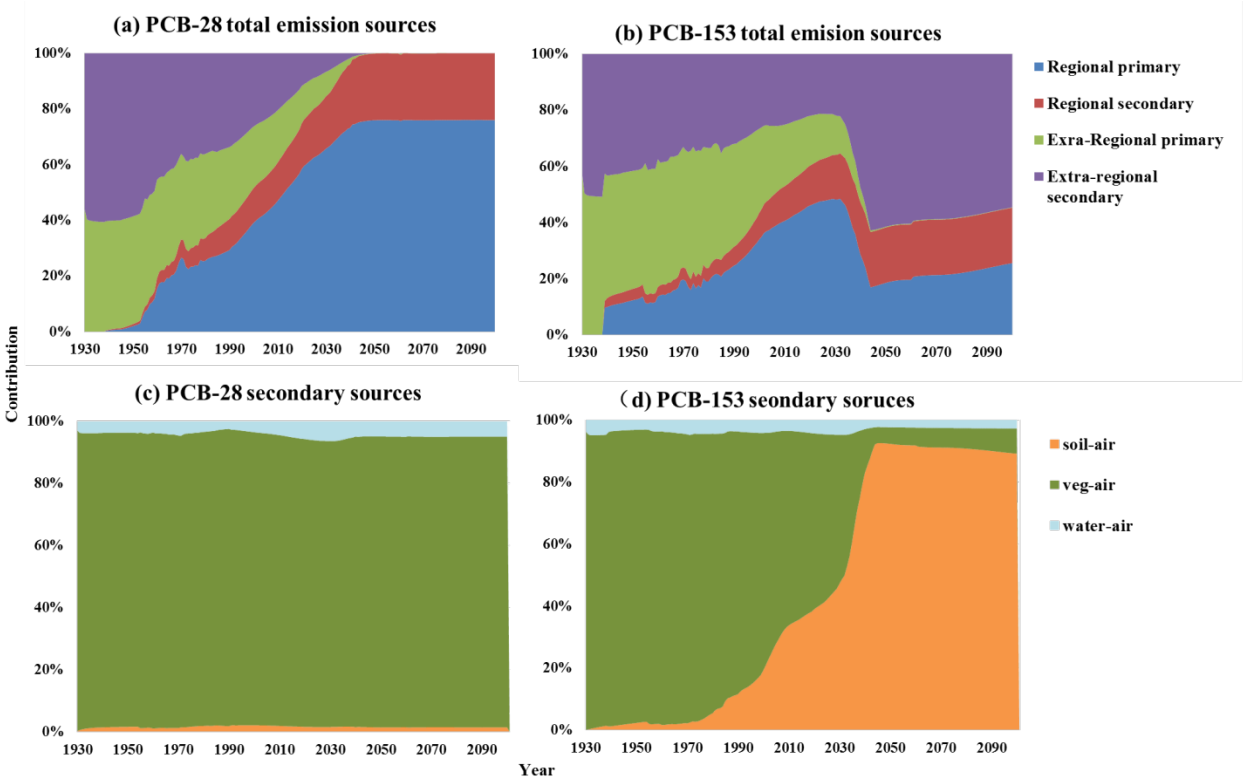

Figure S 4.The relative contribution of primary and secondary emission to total emission, and the individual contributions of soil, vegetation and water to secondary emission under default (IP+UP) scenario.

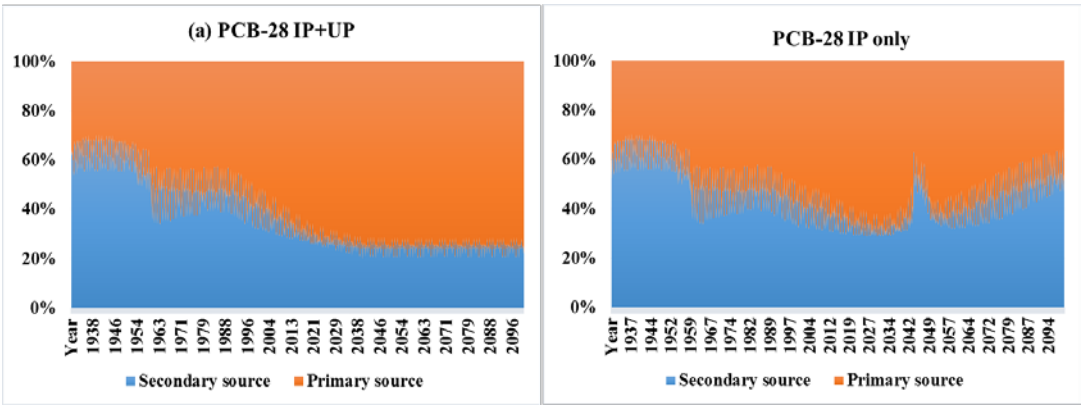

Figure S 5. Contribution of secondary sources with the default scenario (IP+UP) and only IP-PCB (b) for PCB-28.

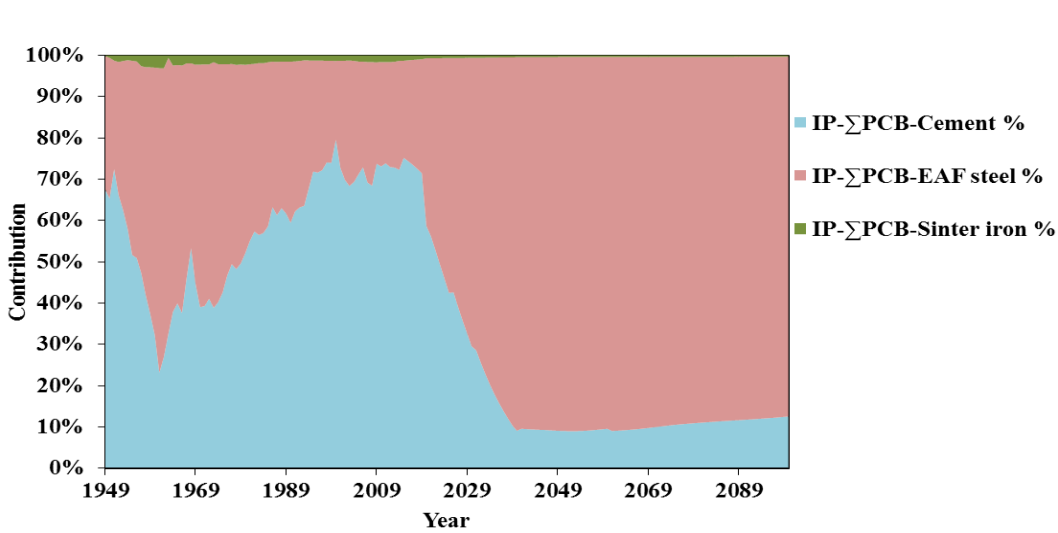

Figure S 6. Individual contribution of cement, EAF produced steel and sinter iron to the total unintentionally emission sources versus time trend.

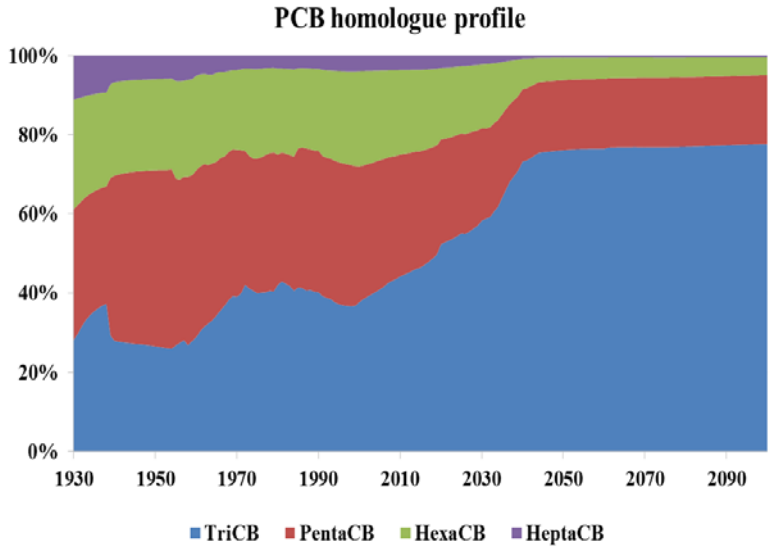

Figure S 7. Modelled temporal trend of homologue profile.

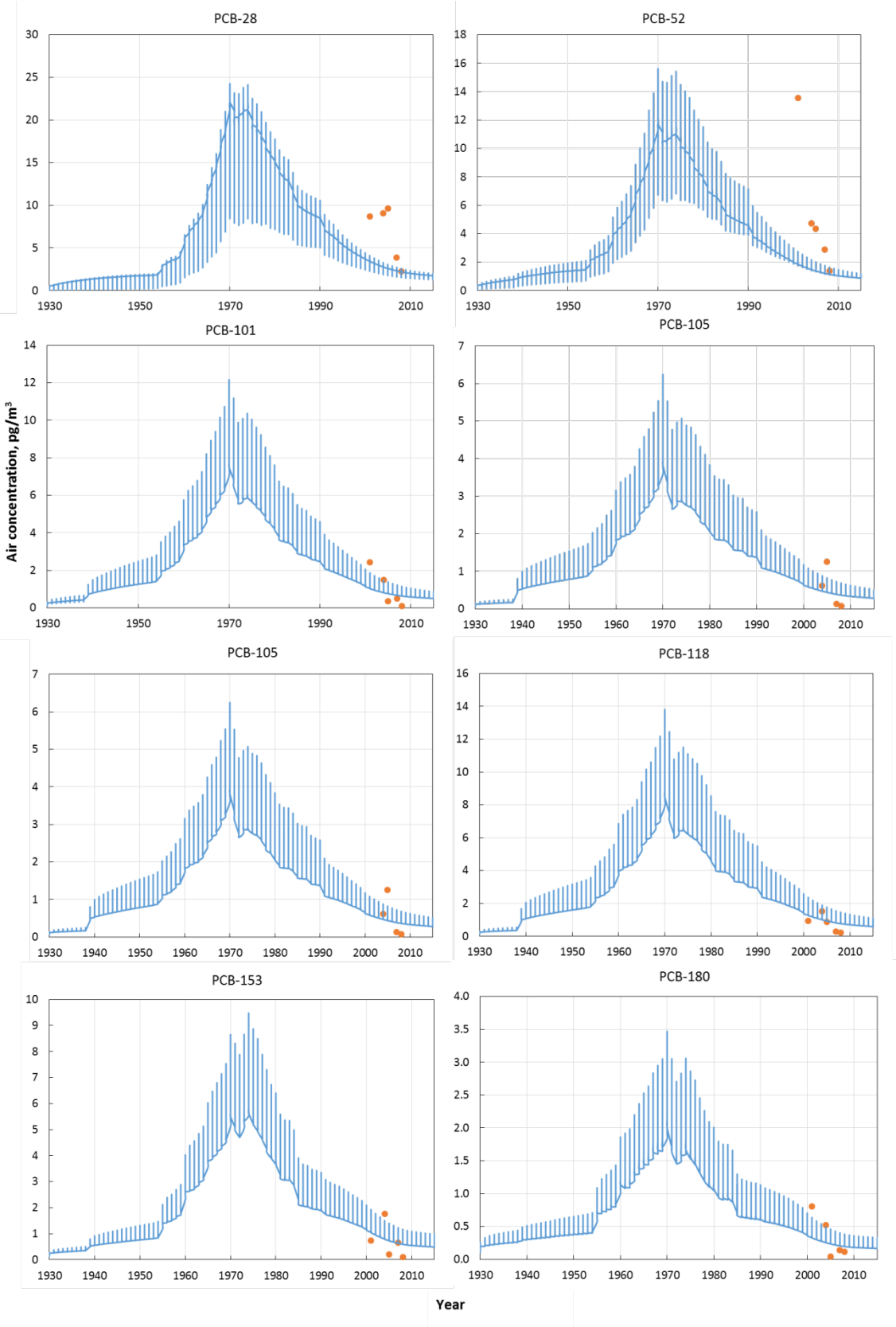

Figure S 8.The compared modelled concentration of different PCBs in air (blue line) along with measurements (orange dots).

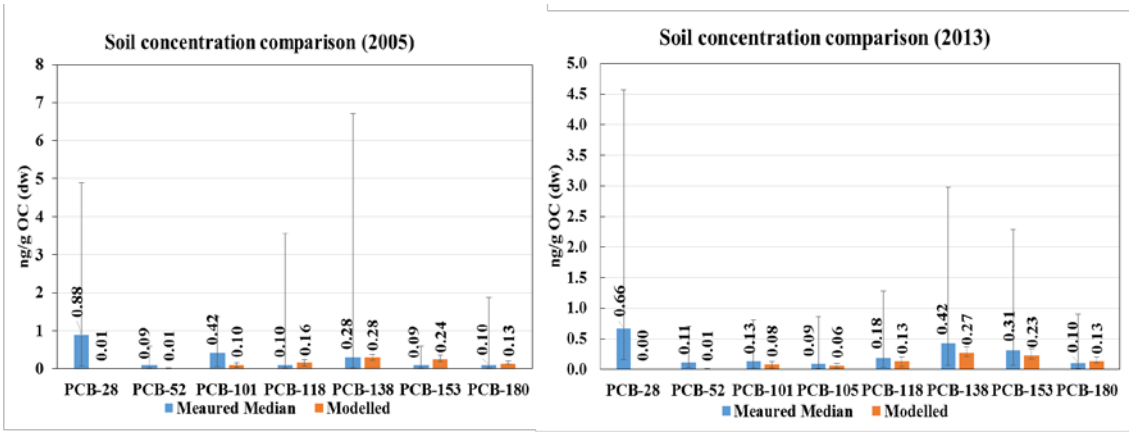

Figure S 9. The comparison of modelled and measured soil concentration on 2003 for surface soil (Ren et al., 2007) and 2013 for forest soil (Zheng et al., 2014).

References

National Bureau of Statistics of the People's Republic of China. China Statistical Yearbook (1949-2014), 2014.

Pauliuk S, Milford RL, Muller DB, Allwood JM. The steel scrap age. Environ Sci Technol 2013; 47: 3448-54.

Pauliuk S, Wang T, Muller DB. Moving toward the circular economy: the role of stocks in the Chinese steel cycle. Environ Sci Technol 2012; 46: 148-54.

Ren N, Que M, Li YF, Liu Y, Wan X, Xu D, et al. Polychlorinated biphenyls in Chinese surface soils. Environ Sci Technol 2007; 41: 3871-6.

Schenker U, MacLeod M, Scheringer M, Hungerbuhler K. Improving data quality for environmental fate models: a least-squares adjustment procedure for harmonizing physicochemical properties of organic compounds. Environ Sci Technol 2005; 39: 8434-41.

Shi W. The cement deman prediction from 2011 to 2050 in China. (in Chinese), 2011, pp. 16-25.

Sinkkonen S, Paasivirta J. Degradation half-life times of PCDDs, PCDFs and PCBs for environmental fate modeling. Chemosphere 2000; 40: 943-949.

Wang M-x, Yang J-x. The sustainabiliy assessment of steel-making technologies and sustainable developmen of steel industry. China population, resources and environment. 2010; 20: 125-128.

Wang P, Jiang Z-y, Zhang X-x, Geng X-y, Hao S. Long-term scenario forecast of production routes, energy consumption and emissions for Chinese steel industry. Journal of University of Science and Technology Beijing 2014; 36: 1684-1693.

Zheng Q, Nizzetto L, Mulder MD, Sanka O, Lammel G, Li J, et al. Does an analysis of polychlorinated biphenyl (PCB) distribution in mountain soils across China reveal a latitudinal fractionation paradox? Environmental Pollution 2014; 195: 115-122.

PAPER IV

Time-variant dietary exposure of POPs in China – a PCB case study

Shizhen Zhao[1], *Oliver Price*[2], *Kevin C. Jones*[1], *Andrew J. Sweetman**[1]

[1] Lancaster Environment Centre, Lancaster University, Lancaster, LA14YQ, UK

[2] Safety and Environmental Assurance Centre, Unilever, Sharnbrook, MK44 1LQ, UK.

*Corresponding author:

Andrew J. Sweetman

Tel: +44 (0) 1524 594715

Email: a.sweetman@lancaster.ac.uk

Abstract

Although total production and usage of polychlorinated biphenyls (PCBs) in China was relatively minor (<1%) compared to many other parts of the world, potential human exposure cannot be ignored because of their persistence in the environment with bioaccumulation and potential toxicity. The main objective of this study was to reconstruct historical exposure profiles under the combined effect of changing temporal emissions and dietary transition using seven indicator PCBs as a case study. A long-term (1930-2100) dynamic simulation using realistic emission estimates combined with dietary transition trends was conducted using a multimedia fate model (BETR-Global) linked to a bioaccumulation model (ACC-HUMAN). The female lipid-normalized body burden (ng g^{-1} lipid) was used as the evaluation metric over time. An approximately 30-year delay in the period of peak concentration for PCB-153 in humans was suggested for a 30-year-old Chinese female compared to their European counterpart following a Swedish diet. This was mainly attributed to the rapid diet transition and intensive e-waste imported into China. A fish-based diet predicted to eight times higher body burden in the future (2010-2100) compared to a vegetable-based diet. Furthermore, replacing all local food with imported food items from a heavily polluted region (central Europe) may result in four times higher PCB-153 body burdens. A comprehensive tracking system to record geographical information for food sources and a biobank network to facilitate data collection of human samples, would help to improve the accuracy of dietary exposure profiles and hence risk assessment for human health.

Highlights:

- The historical PCBs exposure profile was estimated and future trends were explored for Chinese female cohorts 1930-2100.
- A peak delayed by 30 years was observed for Chinese compared to Western women due to combined effects of rapid diet transition and the emission trend.
- The Chinese human body burden of PCB-153 may exceed the Western peers from 2030.
- A comprehensive tracking system to record the geographical information of food sources and a biobank network to facilitate human data collection are recommended.

Keywords:

Human exposure; polychlorinated biphenyls; diet pattern; human body burden; Chinese population; e-waste

1 Introduction

Polychlorinated biphenyls (PCBs) are one of twelve legacy persistent organic pollutants (POPs) targeted by the Stockholm Convention on POPs (UNEP, 2001), because they are stable in the environment, undergo long-range atmospheric transport (LRAT), and possess bioaccumulative ability through the food chain with potential threat to humans and biota (Jones and de Voogt, 1999). China started to produce PCBs in 1965 and ceased production at the end of 1974 (Xing et al., 2005). Over the years, the accumulated amount of production has reached approximately 10,000 tonnes, accounting for about 0.8% of total global PCB production. Although China has not been a main producer of PCBs and has banned them for several decades, these chemicals are still of great concern and are frequently detected in the environment and in organisms (Chen et al., 2014; Cimenci et al., 2013; Wang et al., 2010; Zhang et al., 2011a).

Continuous biomonitoring could help to assess human exposure to the ambient environment. In China, several biomonitoring studies have been conducted in heavily polluted regions, e.g., the e-waste recycling regions in the southern and eastern parts of the country (Bi et al., 2007b; Shen et al., 2012; Wang et al., 2010; Zhang et al., 2011b). However, due to limited funds, long-term cross-sectional and longitudinal bio-monitoring studies in control areas are very rare. Uncertainties also arise from potentially ongoing primary emissions, e.g. the extent of contributions from e-waste to the total human body burden. This is likely to play a significant role, given that China may receive more than 70% of the total exported e-waste from the rest of the world since 2006 (Breivik et al., 2014; Liu et al., 2006). The combination of a multimedia fate model and a bioaccumulation model could be an efficient methodology to close some of the information and knowledge gaps by tracking back the exposure history for a target population, predicting potential future exposure and exploring the age-versus-burden effects (Quinn et al., 2014).

Many factors will affect human exposure to organic contaminants. Dietary exposure is an important source of PCBs, accounting up to 90% of the total intake, especially for foods of animal-origin rich in lipids (Shen et al., 2012). It may, therefore, overwhelm any other potential effects of global climate change on human exposure to organic contaminants in remote regions (e.g., the Arctic) (Quinn et al., 2012). Quinn et al. (2012) reported a 6 to 13 fold decrease in PCB-153 body burden from 1980-2020 due to dietary transition for Arctic population (e.g., less reliant on seal meat, (Quinn et al., 2012). Meanwhile, the Chinese population has also changed dietary habits hugely with 17, 3 and eight times higher consumption of meat, milk and fish from 1950 to 2013, respectively (FAOSTA: http://faostat3.fao.org/home/E). Here, the combined influence of PCB emission trends and dietary transition on the human body burden were explored for the Chinese population.

The relationship between age and human body burden for POPs has been broadly discussed, but no agreement reached so far (Quinn and Wania, 2012). The influential factors mainly include exposure history, metabolic/depuration half-lives, sources and exposure pathways. Concentrations of POPs in the human body have frequently been reported to be positively associated with age in human cross-sectional studies due to long-term exposure and poor ability to metabolize these substances (Covaci et al., 2008; Hardell et al., 2010; Jursa et al., 2006), where age, and birth cohort effects are confounded. However, a decreasing trend in serum concentrations with age was also observed, which may be due to steady-state exposure levels being reached (Covaci et al., 2008). In addition, growth dilution would reduce the human body burdens for people aged younger than 16 years (Bu et al., 2015). Several studies reported no significant correlation between concentrations in humans and age of participants in an industrialized area (Kunisue et al., 2004; Shen et al., 2009; Sun et al., 2006) while Sun et al., observed a positive relationship between age and dioxins like PCB concentrations (Sun et al., 2010). However, all studies were conducted after the ban on PCBs and were based on limited sample sizes. Therefore, there is an urgent need to rebuild the exposure history for the Chinese population and systematically explore the age burden relationship under historic dynamical emission and dietary patterns.

The purposes of the study were: 1) to reconstruct the historical exposure profile and predict future exposure trends under multiple scenarios for Chinese female cohorts, using PCBs as a case study; 2) to assess the combined effect of dietary transition and emission trends on human exposure over the longitudinal and cross-sectional trends for organic contaminants; 3) to explore the role of imported e-waste and unintentional sources of total human body burden. Modelled lipid-normalized body burdens have been used primarily to characterize the potential variability in human exposure caused by different dietary consumption pattern and multiple emission sources.

2 Methods

2.1 Conceptual approach

Assessing implications of emission trends and dietary transition on human exposure to organic contaminant requires an integrated approach combining chemical fate and bioaccumulation modelling. In this study, the overall approach was modified after Quinn et al. (2012) and the following elements were developed and synthesized (Quinn et al., 2012): 1) emission rates over time (1930-2100) worldwide and in China were developed; 2) environmental concentrations responding to the emission scenarios were predicted; 3) food web bioaccumulation covering the main pathways of chemical accumulation in the Chinese population (e.g. water-fish-human); 4)

scenarios of different dietary patterns were explored; 5) scenarios defining trends of the dietary transition in future and human exposure to PCBs were explored. Simulations were performed to calculate human body burdens (ng g^{-1} lipid) as a function of time (year), i.e., longitudinal body burden versus age trends.

2.2 Emission scenarios

Breivik and co-workers have pioneered work on global emission inventories for intentionally produced PCBs, which estimated global emissions of 22 selected PCB congeners from 1930 to 2010 (Breivik et al., 2015; Breivik et al., 2002; Breivik et al., 2007). The worst-case scenario in the revised PCBs emission inventory, which accounts for imported e-waste was used (Breivik et al., 2015). This scenario has been used in a number of modelling studies and has been demonstrated to make reasonable comparisons between predictions and observations (Breivik et al., 2015). Also, the baseline emission scenario, without consideration of the transport of e-waste, was also used to estimate the impact of emissions on the human body burden in China. Unintentionally produced emissions from cement production, electronic arc furnace steel production and iron sintering have also been added to explore their contributions to human body burdens. These three industrial thermal processes were selected due to their large production volumes in China, which could potentially lead to high emissions. They have been identified as important emission sources for PCBs (Liu et al., 2013). A detailed description is given elsewhere (Zhao et al., 2015b). The default emission scenario was defined as the sum of the worst-case scenario, imported e-waste and unintentionally produced emissions. Except for the section to explore the role of imported e-waste and unintentional emissions, the default emission scenario was used as the input into the BETR-Global model for the remaining simulations (Macleod et al., 2005; MacLeod et al., 2011). PCB-153 was selected to explore the contemporary exposure profile, as it is a good indicator congener for human exposure. The other six indicator PCB congeners (PCB-28, 52,101, 105, 138 and 180) were also selected to discuss the behaviour of congener mixtures. The assembled emissions of PCB 153 and other six indicator PCBs (28, 52, 101, 105, 138 and 180) were allocated to a 1° latitude × 1° longitude grid system based on a global population density database (Li et al., 1996).

2.3 Selected models

2.3.1 Fate model

To generate the ambient environmental levels of selected PCB congeners in the global environment over time, the emission inventory (Breivik et al., 2015) was used as input to the multimedia fate model BETR-Global (Macleod et al., 2005; MacLeod et al., 2011). This model has been evaluated and successfully applied previously for PCBs (Lamon et al., 2009; Macleod et al., 2005; MacLeod et al., 2011). The study region and covered grid cells (assigned numbers

of Grid 66, 69, 90, 91, 92, 93, 115, 116) are illustrated in Figure S1. The model has a spatial resolution of 15° latitude ×15° longitude, consisting of 288 grid cells. Each of these regions consists of up to 7 bulk compartments, which are coastal water, fresh water, planetary boundary layer (PBL), lower air, soil, freshwater sediments and vegetation. The model describes advective transport between the regions in air, water and inter-compartment transport processes, e,g., dry/wet deposition and reversible partitioning. The total emissions were allocated to the 288 grid cells. The only emission to lower air was considered, and the initial model concentration was assumed to be zero. The model was run for the period 1930 to 2100 using a dynamic level IV evaluation. The physicochemical properties of the seven indicator congeners were the same as that reported by (Breivik et al., 2010).

2.3.2 Bioaccumulation model

Chemical bioaccumulation in food chains was modelled by a mechanistically based, non-steady state bioaccumulation model (ACC-HUMAN), which has been demonstrated to predict reasonable results for concentrations of PCBs in target biota along the food chain (Breivik et al., 2010; Czub and McLachlan, 2004; Norström et al., 2010). It is subdivided into an agricultural and a marine system. The human is assumed to be made up of two compartments, which are the digestive tract and the remaining body parts (Czub and McLachlan, 2004). ACC-HUMAN assumes equilibrium distribution of test chemicals in different tissues without consideration of kinetic distribution within the human body. The considered uptake pathways of contaminants are diet and inhalation, while the elimination pathways are metabolism, percutaneous excretion, digestive tract excretion and exhalation. Childbirth and breastfeeding were additionally considered for females.

Environmental concentrations (output from BETR-Global) were used as inputs along with physical-chemical properties of a given PCB congener. Using these inputs, the model calculated the time course of lipid-normalized PCBs concentrations in human tissues. All the parameters suggested in Czub and McLachlan (2004) were adopted, except for dietary pattern transition and human characteristic (e.g., growth curve, lipid content and body weight), which was modified for the Chinese population as illustrated in Figure 1 (c) and (d). The different scenarios for dietary habits are defined in Section 2.4.

Cross-sectional data generated through biomonitoring studies are based on groups of different individuals sampled at the same time, whereas the longitudinal estimates derived from ACC-HUMAN are for a single individual over a person’s entire lifetime. Cross-sectional trends were determined from the model-derived longitudinal estimates of lipid-normalized concentrations for individual females born at 10-year intervals. This reduces the confounding effect of the birth cohort on the human body burden.

2.4 Composition and transition of diet

The food supply data for domestic utilization from 1959 to 2013 (http://faostat3.fao.org/browse/FB/CL/) was used as the default dietary pattern to represent the dietary transition trends on a national average level. This was calculated based on the food production plus imports minus exports. The domestic food supply of meat, milk and fish increased by about a factor of 17, 3 and 8 (illustrated in Figure 1-c), on a national scale during the period from1959 to 2013. For the period from 1930 to 1959, the dietary pattern was assumed to be same as 1959. This is a first approximation to gain a general overview of dietary transition in China. Potential uncertainties include regional supply variances between different sub-populations.

The default lipid content in ACC-HUMAN used for fish was 3.5% and for milk. It was 4.4%. These were reset to 5.2 % and 3.2% for Chinese food products (Yang, 2007). For meat intake, pork is the main meat type consumed in China (Du et al., 2001). Pigs were treated identically to cattle. The pork was assumed to be obtained from the same processes as beef from cattle in ACC-HUMAN. However, pork has the highest lipid content among all food categories (Yang, 2007). As a result, its lipid content was modified to 30 % (Yang, 2007). The only pork meat was considered for the Chinese population as a worst-case scenario. The dietary transition excluded data for vegetables, based on national diet surveys, with average vegetable consumption remaining relatively stable at around 276 to 310 g day^{-1} per person (He et al., 2005). Considering the relatively low PCB concentrations in vegetables, the resulting variation is minimal. Therefore, a default of 300 g day^{-1} of vegetable intake was used.

2.4.1 Scenarios for future trends

Multiple dietary scenarios were defined to explore human body burdens of Chinese populations, and specific values of each diet pattern are presented in Table S1: 1) The Chinese population maintain current dietary patterns until the end of the simulation (2100); 2) The Chinese population follows the dietary trends of populations from developed countries after 2013; 3) The Chinese populations d follows the Chinese Dietary Guidelines suggested by the Chinese Nutrition Society (Chinese Nutrition Society, 2008) until 2100; (4) Only vegetables are consumed; (5) The Chinese population adheres to a meat-rich diet; (6) The Chinese population maintains a fish-based diet.

2.4.2 Food origin assumptions

All food was assumed to be produced locally unless defined otherwise. Therefore, the food web bioaccumulation modelling was driven by ambient environmental levels calculated for the modelled regions. However, China is one of the largest food consumers in the world, and the domestic demand is still increasing (Huang et al., 1997), due to increasing population and limited ability to self-supply. Also, due to domestic food security issues (Chen, 2007), Chinese

residents tend to purchase food imported from foreign countries. Consequently, the influence of imported food on human body burden was also explored. However, it is difficult to track the origin of all imported food. Therefore, the environmental concentrations of a heavily polluted region (Grid 61, mainly covering central Europe) was selected to represent a reasonable worst-case scenario. Meanwhile, the human body burdens in individual grid cells covering most of the China (66, 69, 90, 91, 92, 93, 115 and 116) were compared to the reference year 2002 based on different diet patterns.

2.5 Human characteristics

Dietary transitions were evaluated by comparing the lipid-normalized body burden of a 30-year old female over time under various dietary transition scenarios. By focusing on a single age group, the influence of longitudinal changes in the body burden of an individual will be eliminated (Quinn et al., 2011). Chinese women were chosen as the target receptors for simulations, as most studies did not observe significant sexual differences in human body burdens (Zhao et al., 2010). All women were assumed to be the first-born child to a 29-year-old mother and deliver one child at the age of 29. Each child was breastfed for six months as suggested by WHO (WHO, 2002). Their whole-body lipid contents were re-parametrized based on Chinese population data following (Jiang, 2006). All children were assumed to be born on their mother's birthday. Both newborns and breast milk were assumed to have equal fugacity with the mother.

3 Results and Discussion

3.1 Evaluation with observations

3.1.1 General trend

Using the integrated modelling approach, the outputs from the fate model (BETR-Global) and the bioaccumulation model (ACC-HUMAN) were combined to calculate the body burdens of women living in China, which are schematically presented in Fig 1. All the results are presented based on predictions from the central China grid cell (92) unless mentioned otherwise. In order to build confidence in the model, the predicted human body burdens from the default scenario of emission and diet pattern were compared with measurements in the literature (summarized in Table S2).

To our knowledge so far, there are no studies reporting both the dietary profiles and PCB levels in a single population at more than one-time point in China. Therefore, it is difficult to evaluate rigorously these predictions against historical measurements. The data available for the Chinese population was summarized in Table S2 and varies over one order of magnitude. For example,

Wang et al. (2010) measured PCB-153 body burden concentrations between 3.28~31.29 ng g^{-1} lipid in adipose samples for 15-91 years old females living in Anhui provenience and 2.49~29.5 ng g^{-1}lipid for 18~88 years old people living in Jiangsu province in 2009 (Wang et al., 2010). Although there are many assumptions and uncertainties (e.g. the dietary consumption pattern, food origins and lipid content in food) in this modelling exercise, the modelled human body burden broadly corresponds to the varied biomonitoring data within a factor of two as illustrated in Figure 1 (f) for PCB-153.

In developed countries, a falling trend of summed serum POP concentrations has been observed in human body samples between 1979 and 2007 (Nost et al., 2013). However, Sun et al. (2011) reported that the dioxin like-PCBs level increased from 2002 to 2007 in human milk from northern China, which is consistent with the trend of human body burdens predicted in our study as illustrated in Fig 1(f). In addition, several studies confirmed that the PCB-138 and PCB-153 were predominant congeners in human body burdens as illustrated in Figure S4 (Wang et al., 2010; Zhang et al., 2011b). As a result, the default scenario was assumed to capture the main bioaccumulation behaviour of PCBs and is used in the following discussions.

3.1.2 Body burden versus age trends

In order to understand the relationship between age and human body burden based on data modelled at different times, the cross-sectional and longitudinal body burden versus age trends (CBATs/LBATs) of PCB-153 were calculated and sampled every 10 years from 1960 to 2050 for Chinese women between 0-80 years old as presented in Figure 1-(h) and (g). The short dashed lines present the period of increasing emission while the long-short dashed lines show modelling results after all intentional emissions have ceased.

The relationships between age and human body burden in cross-sectional and longitudinal studies were strongly dependent on the year of sampling, which means that a straightforward positive or negative relationship is not observed between age and human body burdens. During the time of increasing intentional emission (1930-1970), the cross-sectional human body burden peaked at the age of 10 years, which reflects the increasing prenatal exposure and relatively low body lipid content at a younger age. For a single person born during this period, the human body burden generally increased with age as illustrated in Figure 1-(h). This is attributed to accumulative exposure in a contaminated environment with increasing emission. At the time of decreasing intentional emission (1980-2010), the age at which the maximum body burden occurred in CBAT depends on the length of time after the emission peak. The predictions suggest that the peak age of human body burden happen at increasingly higher ages as time elapses after emissions ceased. For an person, the predicted human body burden was highest for

a child at age one and reduced substantially due to growth dilution. This trend is consistent with the observations of Quinn and Wannia (2012).

It is challenging to confirm the predictions of cross-sectional and longitudinal body burden versus age trends with measurements, particularly for findings before the PCB ban (1930-1970). The earliest national survey of human milk was conducted in 2008 (Li et al., 2011) and no evidence could identify the historical exposure profile during the pre-ban period. In addition, no biomonitoring studies have been conducted on a single sub-population at different time points in China. This makes it difficult to confirm the main findings from this study, which indicates that the peak of human body burden occurred around 2010. Several cross-sectional studies conducted after the banning of PCBs have confirmed the significance of age, dietary habits and geographical factors in determining human exposure in China (Zhang et al., 2011b). However, most studies surveyed have limited sample sizes and narrow age ranges, and did not reach a consistent agreement on the relationship between age and human body burden. This leads to difficulties in confirming the model predictions. For example, Sun et al. (2011) and Wang et al. (2010) reported that human tissues positively correlated with age (Sun et al., 2011; Wang et al., 2010) while Kunisue et al. (2004) did not find any relationship between age and human body burden (Kunisue et al., 2004).

3.2 Impact of dietary pattern on future body burden

Each cohort was assumed to consume a constant dietary pattern, although they will have a wide range of preferences in reality. In order to test the influence of different types of dietary pattern on future exposure trends and offer recommendations on how to maximise the reduction of human body burdens, future dietary exposure profiles were explored under multiple scenarios defined in Section 2.4. There are illustrated in Figure S3. Only the vegetable-based diet was expected to rapidly decrease/dilute the human body burden while the fish-based diet represented the highest exposure. The 2020 born cohort mainly eating fish would have around eight times higher human body burden than those eating mainly vegetables. The elevated human body burden from eating fish reflects bioaccumulation along the aquatic food chain, which is approximately two orders of magnitude higher than in the meat food chain in the same region. The differences between other scenarios were relatively small by less than a factor of two.

3.3 Implications for long-term human exposure

In a dynamic simulation, the environmental compartments and the biota living within these compartments will directly reflect the variability in the emission profile when primary emissions dominate. Since dietary intake is the main exposure pathway for humans to PCBs, variable chemical concentrations in food and multiple diet patterns will lead to variable human body burdens (Zhang et al., 2011b). In particular, under non-steady state emissions human body

328 burdens will depend on the age when the exposure began to reflect changes in the emission
329 profile (Quinn and Wania, 2012).

330

331

332

333

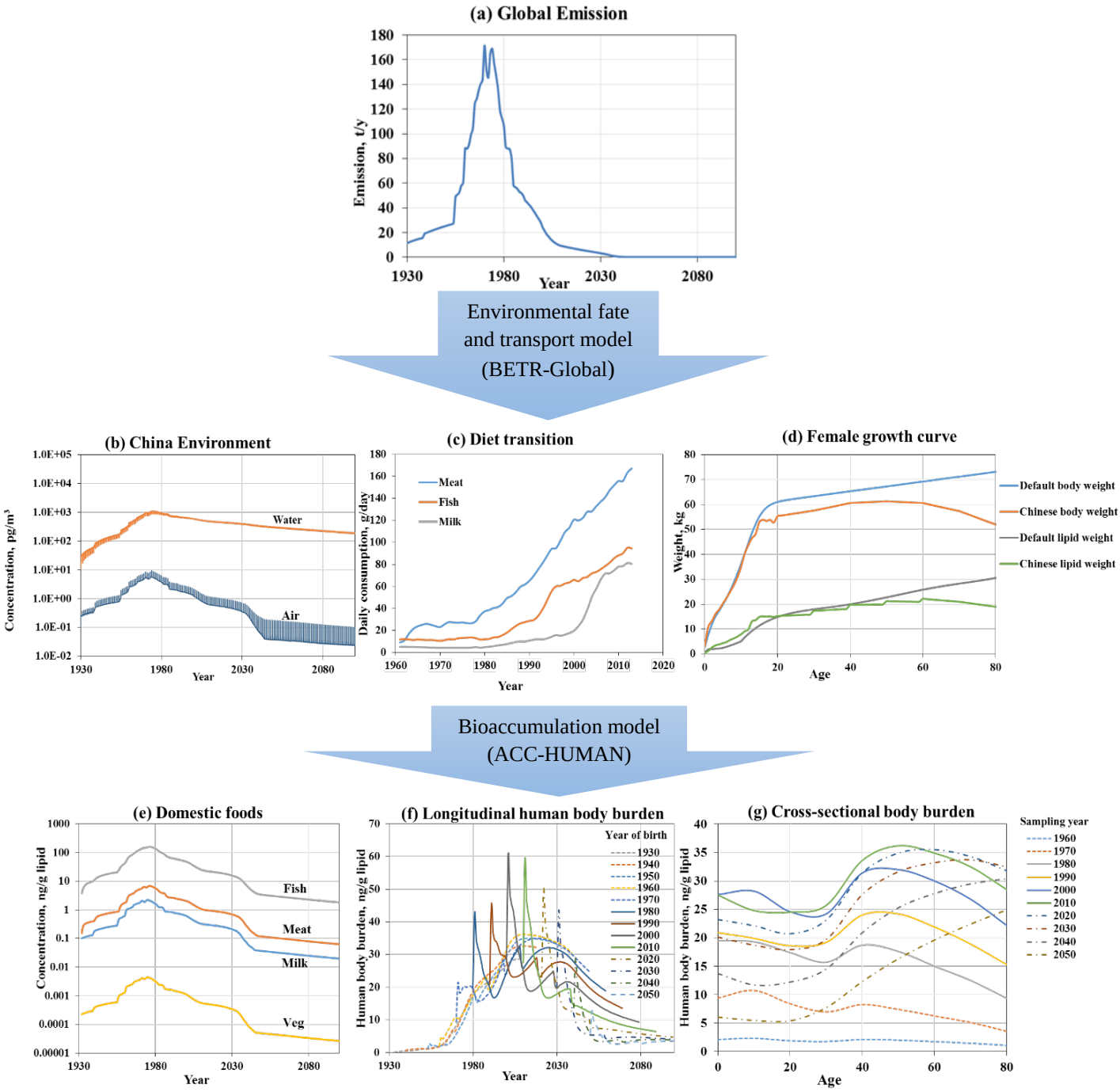

Figure 1. Schematic overview of the modelling approach employed to assess the combined effect of emission trends and dietary transition on human exposure to PCB-153 for the Chinese population. The approach was modified after Quinn et al. (2012).(Quinn et al., 2012)The global emission estimate for PCB-153 over the period 1930-2100 (a) was used as input to a global fate and transport model (BETR-Global) to produce the ambient environmental concentrations target regions (b). The estimated environmental concentrations (b) combined specified transition of diet (c) and female growth curve (d) are used as input to bioaccumulation model (ACC-HUMAN) to predict the concentration in respective food items (e) and the human body burden for a 30-year-old Chinese female (f). The cross-sectional versus age dependence was modelled every ten years from 1930 to 2050 (g).

3.3.1 Historical exposure profile

Under the combined effect of changing emissions and cohort dietary transition, the body burden of the 30-year-old female cohort increased 75 times over the last 70 years (1940-2010), despite a 4-fold reduction in Chinese environmental concentrations driven by declining emission. The dietary transition may cause an additional increase in human body burden of more than two orders of magnitude during the simulated time range. In addition, the peak time of human body burden is predicted to have occurred in 2010 for the 30-year-old female cohort of the Chinese population while this occurred in 1980 for Western females (Figure 2). The Western temporal trend of human body burden was assumed to be represented by a typical European female following Swedish dietary pattern parameterized as in Breivik et al. (2010). The combined effect of changing emission trends and dietary transition resulted in an approximately 30-year difference between the peak of human body burdens in the Chinese and European populations. This time lag could be attributed to two main reasons. One is the relatively fast dietary transition from 1959-2010 with rapidly increasing consumption of food of animal origin (milk, meat and fish) in China. A change in PCB exposure was also observed for Arctic populations when replacing locally-sourced traditional food (with high concentrations of PCBs) with imported food. In this case, Quinn et al. (2012) reported that the rapid diet transition could cause up to a 50-fold reduction in PCB's body burden over a 40-year period (Quinn et al., 2012). Another reason could be more intensive on-going emission sources in China compared to Western countries, although the manufacture of PCBs has been ceased around the world. For instance, China was estimated to receive more than 70% of global e-waste production since 2006 (Liu et al., 2006). In addition, it is now the largest industrial country in the world and unintentionally emitted PCBs from varied industrial thermal processes (e.g., production of steel and cement) may also contribute to the human body burden (Liu et al., 2015). Therefore, the roles of these two emission sources affecting the human body burden have been further explored for the Chinese population in Section 3.4.1.

The exposure profile of the European population followed the emission trends relatively closely, peaking about ten years after the emissions peak in 1970. This could be due to their relatively stable diet compared with Chinese population, with only about a two-fold increase in animal-derived food from the 1960s to 1990s (Moreno et al., 2002). In addition, the cumulative human body burden of 175 ng g^{-1} lipid in the Chinese population was an order of magnitude lower than the Western body burden during the period from 1930 to 2100. However, the difference is mainly associated with historical exposure (1930-2010). During this period, the cumulative body burden accounts for more than 90% of the total body burden (during 1930-2100) for the Western population while it only accounts for up to 54% for the Chinese population for PCB-153. From 2030, the Chinese human body burden is predicted to exceed that of the Europeans

for the first time. This may be caused by higher continued emissions as discussed below. For instance, UP-PCB sources were estimated to start contributing significantly to the total emissions from around 2030 and become the dominant emission source from 2040 (Zhao et al., 2015b).

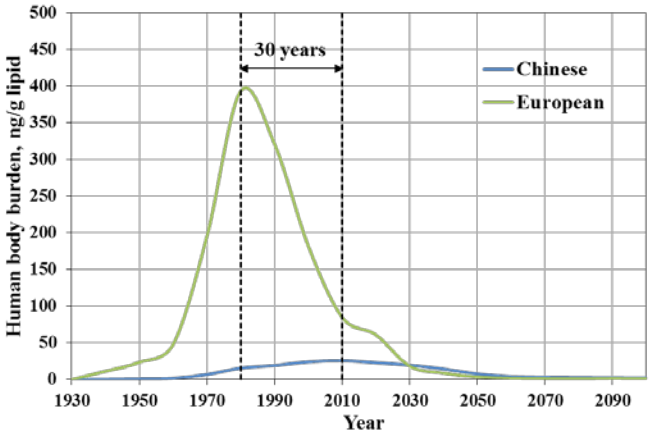

Figure 2. The human body burden (ng g^{-1} lipid) of PCB-153 for a 30-year-old female cohort in central China (Grid 92) and for a European (Grid 61). Both populations were assumed to eat locally produced food only.

3.3.2 Roles of imported e-waste and UP-PCBs

The contribution of imported e-waste and unintentionally produced PCBs (UP-PCBs from a cement kiln, electronic arc furnace-produced steel and iron sinter) to the total human body burden has been estimated for PCB 153 and $\sum_7$ PCBs (Figure 3). Since the imported e-waste contribution would be expected to vary spatially based on the physical distance from the main e-waste recycling sites (mostly located in the southeast-Grid116), the Northeast (Grid 66) was selected as a background region receiving less than 5% of the total emission of $\sum_7$ PCBs from imported e-waste during 1930-2100. The southeast region (Grid 116) was chosen to represent a typical e-waste polluted region, receiving more than 40% of the emissions of $\sum_7$ PCBs caused by imported e-waste (1930-2100). These two regions were compared in terms of the individual contribution from the imported e-waste and unintentionally produced emissions.

During the period 1930 to 1990, contributions from imported-e-waste and unintentional emissions were negligible. This is because China did not start to import e-waste until 1980 and sources of UP-PCBs were minimal. In terms of the cumulative human body burden for $\sum_7$ PCBs from 1930 to 2100, imported e-waste contributed more than 62% in Grid cell 116 while it was only approximately 4% in Grid cell 66. The UP sources contributed less than 1% of $\sum_7$ PCBs in both two grids. Since 2000, the contribution of imported e-waste to total human body burdens

started to become dominant (46% in 2000 with an increasing trend over time) in Grid 116 peaking in 2040 when it is predicted to account for more than 90% of $\sum_7$ PCBs. If the exposure from imported e-waste was excluded, the peak of human body burden in Grid cell 116 would occur in the year 2000, but it is peak in 2020 with the inclusion of import of e-waste. Consequently, the on-going imported e-waste may result in a 20-year time lag of the peak human body burden.

To explore further the potential sources contributing to total human body burden, congener profiles were compared with observations of people living around e-waste sites and in background sites. These two studied sources have different congener-specific contributions to the total exposure profiles (see Figure 3-b, c). Elevated body burdens were mainly caused by the heavier PCBs from imported e-waste, partial why PCB-153 which contributed the greatest proportion. The main contributors to the $\sum_7$ PCBs in humans were PCB-153 and PCB-138 in both e-waste zone (Grid cell 116) and he background zone (Grid cell 66). This agrees with measurements where PCB-138 was found to be the most abundant congener in the samples from participants living in the e-waste disassembly sites of Zhejiang Province and Guangdong Province (Bi et al., 2007a; Zhao et al., 2009). In a national survey of mother's milk, PCB-153 and PCB-138 were also the most abundant congeners with levels found to be similar to those in other developed countries (Zhang et al., 2011b). Moreover, Zhang et al. (2010) observed different PCB congener profiles in residents from e-waste and background zones, where PCB-28 and PCB-153 contributed most to the total human body burden in the e-waste zone and PCB-28 was the dominating congener in the background zone (Zhang et al., 2010). The lower contribution of PCB-28 predicted in this study may be caused by the underestimation of emission for lighter PCBs (PCB-28 and PCB-52) in China. Consequently, this could lead to underestimation of environmental concentrations compared to observations in environmental compartments (Zhao et al., 2015b). Given that dietary intake accounts for up to 90% to the total exposure (Zhao et al., 2015a), the large uncertainty about food origins may be another source of significant uncertainty in the model results.

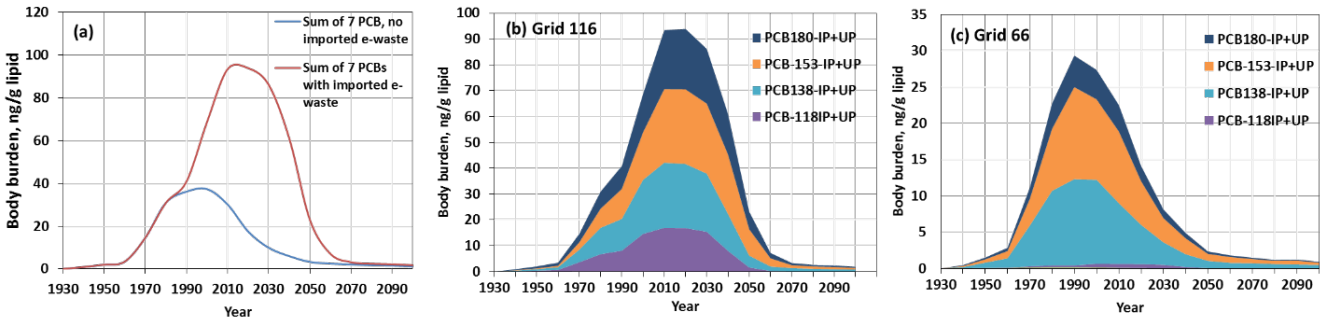

Figure 3. The individual contribution of imported e-waste to the total human burden for 1930-2100 for $\sum_7$ PCBs in Grid cell 66 (a) and the congener pattern in Grid 116 (b) and Grid cell 66 (c).

3.3.3 Regional differences in dietary exposure in 2002

A large variation in dietary patterns can be observed in the Chinese population. The year 2002 was used as a reference year to explore differences in human body burdens with different dietary patterns (recorded in Total Diet Study) and corresponding environmental concentrations within Chinese regions. All the surveyed locations of the TDS were allocated to the grid and the average concentrations at each site were compared. Although the sampling site of Xinjiang is outside the domain of Grid cell 66, it was still assumed to represent the diet pattern in Xinjiang province and was hence used as diet pattern input for Grid cell 66.

The percentage of fish and dairy products contributing to the total diet pattern varied widely between 1% and 20% and 1% and 33%, respectively. In the western part of China (Grid cell 61 and 90), dairy takes up a much higher portion (33%) than in the other regions. In south-eastern parts (Grid cells 93 and 116), large amounts of fish are consumed (up to 20% of the total diet) (see Figure S2). As a combined result of environmental concentrations and dietary pattern, the highest human body burden of 29 ng g^{-1} lipid was predicted in 30-year-old females living in Grid cell 116, mainly covering Guangdong, Fujian and Hunan provinces. The population living in Grid cell 92 had the lowest body burden, equivalent to that of only a third of that in Grid cell 116. However, this regional difference in human body burdens is relatively small compared to long-term trends. It should be noted that the spatial resolution of BETR-Global is relatively coarse (15°×15°) and “hot spots” could not be recognized in this study. This uncertainty may result in missing potentially high-risk regions.

3.3.4 Impact of food origins

The previous model simulations assumed that residents only eat locally produced food. However, in reality, many Chinese residents prefer imported food from developed countries instead of purchasing local food due to issues around food safety, especially with regards to

meat and milk (Huang et al., 1997). For example, the import of liquid milk cumulatively rose by 800% in China from 2005 to 2013 (He, 2014). The influence of eating imported food was explored for the entire simulation period (1930 – 2100) by comparing the human body burden of people only eating local food to an extreme scenario of a person exclusively eating imported food from regions with high PCB levels (Figure 4). In terms of the cumulative human body burden for PCB-153 (1930-2100), people only eating imported food were predicted to reach levels four times higher than people only consuming local food. The largest difference occurred in 1980, when the European population had an approximately 7-fold higher human body burden than the Chinese population. This can be attributed to China not starting to manufacture PCBs until 1965, resulting in a relatively low exposure of Chinese people eating locally-sourced food. The peak burden occurred in 1990 for people completely relying on imported food while it is predicted to occur in 2010 for people eating local food. In reality, people typically choose about 23% of dairy products (Chen and Yang, 2012), 23% fish and 3 % meat products from abroad (Yi et al., 2015). This food source pattern is predicted to result in 15% higher human body burdens compared to people eating local food only. Consequently, populations with a high preference for imported food may receive higher PCB doses than people eating locally.

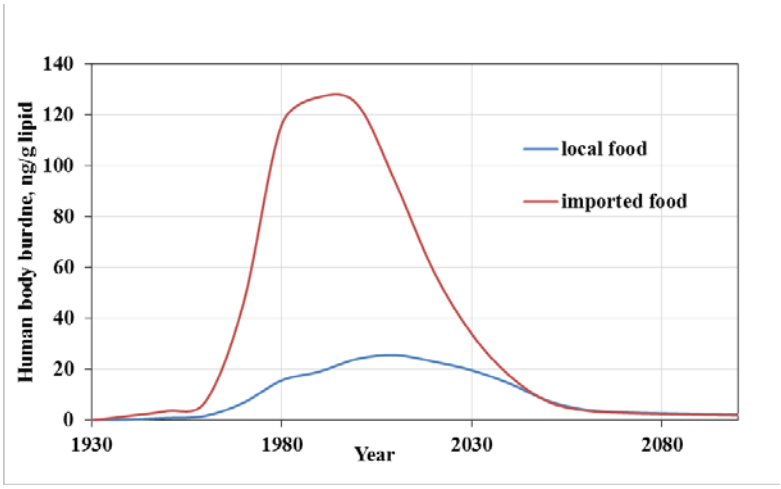

Figure 4. Comparison of human body burden for a 30-year-old female only eating local diet and only eating imported food from a heavily polluted area in the case of PCB-153.

3.4 Uncertainty and Limitations

While insight can be gained through the combined application of fate and bioaccumulation models, substantial uncertainties and data gaps remain and limit further exploration of existing data. Reproductive behaviour was simplified to an initial approximation in this study for the Chinese female cohort assuming a single child at age 30. This should be modified the recently-

493 released two-child policy. The age when giving birth, the number of children and the type of
494 milk (formula or breast milk) are factors that may affect the prenatal and postnatal exposure of a
495 child as well as the cumulative lifetime exposure of the adult (Quinn et al., 2011). Large
496 uncertainty also exists in the intrinsic elimination parameters (i.e., changes in body weight and
497 ongoing exposure) (Ritter et al., 2011). The confounding processes of on-going exposure,
498 changes in body size/composition and other factors that would influence concentration over
499 time, will make the intrinsic human elimination half-life of the Chinese population different
500 from that in Western populations. Consequently, this study can only offer a general view of the
501 exposure profile for the Chinese population. A more detailed investigation of the exposure of
502 target populations could be achieved by improved parameterization.

503 The origin of food consumed in China is difficult to assess. In this study, it was demonstrated
504 that food from background sites has a minimal influence on the elevation or decrease of human
505 body burdens. The gradient between urban and rural regions as well as 'hot spots' was outside
506 the scope of this modelling study. However, many studies have reported that PCB levels in food
507 from 'hot spots' can be elevated by several orders of magnitude, resulting in high body burdens
508 in local residents, particularly in regions near e-waste cycling sites (Chan et al., 2013; Wang et
509 al., 2011a; Wang et al., 2011b; Wu et al., 2008; Zhao et al., 2009).

510 # 4 Conclusions

511 This study has combined a complex array of factors, which determine human exposure to PCBs
512 for the Chinese population. It highlighted the role of dietary pattern and two specific emission
513 sources in the long-term simulation of human body burdens. With respect to the interpretation
514 of biomonitoring data, the long-term simulation of PCBs illustrated the key roles of emission
515 profile and dietary composition in determining the absolute human body burden and potential
516 variability between different cohorts. A 30-year delay was predicted between people body
517 burdens in European and Chinese populations due the combined effect of dietary transition and
518 temporal emission trends, particularly influenced by imported e-waste, compared with European
519 cohort. Furthermore, replacing all local food with imported food items may result in an
520 increased accumulation (up to four times) of PCB-153 compared to people eating locally-
521 sourced food. These results highlight possible sources of variability observed in human
522 biomonitoring data in China. For instance, the geographical source of the diet (from domestic or
523 foreign counties), dietary transition trends and distributions, are paramount for estimating the
524 human body burden in a population of interest.

525 Potential improvements to enhance future predictions of human body burdens could include: 1)
526 more detailed information on diet (e.g. the geographic origin of consumed food) and its
527 transition (continued diet survey) in target populations; 2) the reproductive behaviour (age when

giving birth, number of childbirths) in the target population; 3) applying higher spatially-resolved fate/transport data to better distinguish local/remote food as well gradients between urban and rural areas, particularly for 'hot spots'. Food preparation processes may also affect pollutant concentrations in final ready-to-eat food items. Cooking processes have shown to cause losses of more than 30% of total PCBs via the loss of fat (Tsutsumi et al., 2002). Therefore, identifying scenarios based on different cooking process may be useful. In addition, a large-scale national biobank network program would be a valuable asset to facilitate data collection on human contaminant profiles (Elliott and Peakman, 2008). For instance, cryogenic repositories for biological samples can be used in retrospective and prospective biomonitoring studies (Zhu et al., 2011).

PCBs were used as a case study here representing very persistent chemicals. Therefore, biotransformation did not play a key role in their fate and bioaccumulation along food chains. Similar simulations could be easily repeated for other well-documented persistent organic contaminants. However, even for such persistent organic contaminants, large variations were still observed for individual congeners with the age-cohort-effect. Quinn et al., (2012) suggested the half-life may have a significant influence here (Quinn and Wania, 2012). As a result, for chemicals which are more susceptible to biotransformation, uncertainty from the metabolic potential in humans and other biota needs to be accurately parameterized, in order to improve predictions.

Acknowledgement

We would like to thank Unilever and the China Scholarship Council (CSC) for funding this research. Thanks to Dr Emma Underman from Stockholm University for guidance on using ACC-HUMAN model. Thanks to Prof. Knut Breivik from NILU for providing the updated emission inventory.

5 References

Bi X, Thomas GO, Jones KC, Qu W, Sheng G, Martin FL, et al. Exposure of electronics dismantling workers to polybrominated diphenyl ethers, polychlorinated biphenyls, and organochlorine pesticides in South China. Environmental Science & Technology 2007a; 41: 5647-5653.

Bi XH, Thomas GO, Jones KC, Qu WY, Sheng GY, Martin FL, et al. Exposure of electronics dismantling workers to polybrominated diphenyl ethers, polychlorinated biphenyls, and organochlorine pesticides in South China. Environmental Science & Technology 2007b; 41: 5647-5653.

Breivik K, Armitage JM, Wania F, Jones KC. Tracking the global generation and exports of e-waste. Do existing estimates add up? Environ Sci Technol 2014; 48: 8735-43.

Breivik K, Armitage JM, Wania F, Sweetman AJ, Jones KC. Tracking the global distribution of persistent organic pollutants accounting for e-waste exports to developing regions. Environ Sci Technol 2015.

566 Breivik K, Czub G, McLachlan MS, Wania F. Towards an understanding of the link between
567 environmental emissions and human body burdens of PCBs using CoZMoMAN.
568 Environ Int 2010; 36: 85-91.
569 Breivik K, Sweetman A, Pacyna JM, Jones KC. Towards a global historical emission inventory
570 for selected PCB congeners - a mass balance approach 2. Emissions. Science of the
571 Total Environment 2002; 290: 199-224.
572 Breivik K, Sweetman A, Pacyna JM, Jones KC. Towards a global historical emission inventory
573 for selected PCB congeners — A mass balance approach: 3. An update. Science of The
574 Total Environment 2007; 377: 296-307.
575 Bu Q, MacLeod M, Wong F, Toms L-ML, Mueller JF, Yu G. Historical intake and elimination
576 of polychlorinated biphenyls and organochlorine pesticides by the Australian population
577 reconstructed from biomonitoring data. Environment International 2015; 74: 82-88.
578 Chan JKY, Man YB, Wu SC, Wong MH. Dietary intake of PBDEs of residents at two major
579 electronic waste recycling sites in China. Science of the Total Environment 2013; 463:
580 1138-1146.
581 Chen B, Yang XW. Analysis report of dairy industry in China 4th dairy conference of China.
582 Dairy Association of China, Nanchang, China, 2012.
583 Chen J. Rapid urbanization in China: A real challenge to soil protection and food security.
584 Catena 2007; 69: 1-15.
585 Chen SJ, Tian M, Zheng J, Zhu ZC, Luo Y, Luo XJ, et al. Elevated levels of polychlorinated
586 biphenyls in plants, air, and soils at an E-waste site in Southern China and
587 enantioselective biotransformation of chiral PCBs in plants. Environ Sci Technol 2014;
588 48: 3847-55.
589 Chinese Nutrition Society. Chinese Diet Guidelines: Tibet People's Publishing House, 2008.
590 Cimenci O, Vandevijvere S, Goscinny S, Van Den Bergh M-A, Hanot V, Vinkx C, et al.
591 Dietary exposure of the Belgian adult population to non-dioxin-like PCBs. Food and
592 Chemical Toxicology 2013; 59: 670-679.
593 Covaci A, Voorspoels S, Roosens L, Jacobs W, Blust R, Neels H. Polybrominated diphenyl
594 ethers (PBDEs) and polychlorinated biphenyls (PCBs) in human liver and adipose
595 tissue samples from Belgium. Chemosphere 2008; 73: 170-175.
596 Czub G, McLachlan MS. A food chain model to predict the levels of lipophilic organic
597 contaminants in humans. Environmental Toxicology and Chemistry 2004; 23: 2356-
598 2366.
599 Du S, Lu B, Wang Z, Zhai F. Transition of dietary pattern in China. Journal of Hygiene
600 Research 2001; 30: 221-225.
601 Elliott P, Peakman TC. The UK Biobank sample handling and storage protocol for the
602 collection, processing and archiving of human blood and urine. International Journal of
603 Epidemiology 2008; 37: 234-244.
604 Hardell E, Carlberg M, Nordström M, van Bavel B. Time trends of persistent organic pollutants
605 in Sweden during 1993–2007 and relation to age, gender, body mass index, breast-
606 feeding and parity. Science of The Total Environment 2010; 408: 4412-4419.
607 He S. China's dairy industry statistics: Dairy Association of China, 2014.
608 He Y-n, Guan-sheng M, Li Y-p, Wang Z-h, Hu Y-s, Zhao L-y, et al. Study on the current status
609 and trend of food consumption among Chinese population. Chinese Journal of
610 Epidemiology 2005; 26.
611 Huang J, Rozelle S, Rosegrant MW. China's food economy to the twenty-first century: Supply,
612 demand, and trade. Vol 19: Intl Food Policy Res Inst, 1997.
613 Jiang C. Study on lipid distribution and estimation method of body fat rate in China. Physical
614 education and training. Doctoral. Beijing Sport University, 2006.
615 Jones KC, de Voogt P. Persistent organic pollutants (POPs): state of the science. Environmental
616 Pollution 1999; 100: 209-221.
617 Jursa S, Chovancová J, Petrík J, Lokša J. Dioxin-like and non-dioxin-like PCBs in human serum
618 of Slovak population. Chemosphere 2006; 64: 686-691.

Kunisue T, Someya M, Kayama F, Jin Y, Tanabe S. Persistent organochlorines in human breast milk collected from primiparae in Dalian and Shenyang, China. Environmental Pollution 2004; 131: 381-392.

Lamon L, Von Waldow H, Macleod M, Scheringer M, Marcomini A, Hungerbuhler K. Modeling the global levels and distribution of polychlorinated biphenyls in air under a climate change scenario. Environ Sci Technol 2009; 43: 5818-24.

Li J, Zhao Y, Wu Y. A review for the body burden of persistent organic pollutants in China. Environmental Chemistry 2011; 30: 5-19.

Li YF, McMillan A, Scholtz MT. Global HCH usage with 1 degrees x1 degrees longitude/latitude resolution. Environmental Science & Technology 1996; 30: 3525-3533.

Liu G, Zheng M, Jiang X, Jin R, Zhao Y, Zhan J. Insights into the emission reductions of multiple unintentional persistent organic pollutants from industrial activities. Chemosphere 2015; 144: 420-424.

Liu GR, Zheng MH, Cai MW, Nie ZQ, Zhang B, Liu WB, et al. Atmospheric emission of polychlorinated biphenyls from multiple industrial thermal processes. Chemosphere 2013; 90: 2453-2460.

Liu X, Tanaka M, Matsui Y. Generation amount prediction and material flow analysis of electronic waste: a case study in Beijing, China. Waste management & research 2006; 24: 434-445.

Macleod M, Riley WJ, Mckone TE. Assessing the influence of climate variability on atmospheric concentrations of polychlorinated biphenyls using a global-scale mass balance model (BETR-global). Environmental Science & Technology 2005; 39: 6749-6756.

MacLeod M, von Waldow H, Tay P, Armitage JM, Wöhrnschimmel H, Riley WJ, et al. BETR Global–A geographically-explicit global-scale multimedia contaminant fate model. Environmental Pollution 2011; 159: 1442-1445.

Moreno L, Sarrıa A, Popkin B. ORIGINAL COMMUNICATION The nutrition transition in Spain: a European Mediterranean country. European journal of clinical nutrition 2002; 56: 992-1003.

Norström K, Czub G, McLachlan MS, Hu D, Thorne PS, Hornbuckle KC. External exposure and bioaccumulation of PCBs in humans living in a contaminated urban environment. Environment international 2010; 36: 855-861.

Nost TH, Breivik K, Fuskevag OM, Nieboer E, Odland JO, Sandanger TM. Persistent organic pollutants in Norwegian men from 1979 to 2007: intraindividual changes, age-period-cohort effects, and model predictions. Environmental Health Perspectives 2013; 121: 1292-1298.

Quinn CL, Armitage JM, Breivik K, Wania F. A methodology for evaluating the influence of diets and intergenerational dietary transitions on historic and future human exposure to persistent organic pollutants in the Arctic. Environment International 2012; 49: 83-91.

Quinn CL, van der Heijden SA, Wania F, Jonker MT. Partitioning of polychlorinated biphenyls into human cells and adipose tissues: evaluation of octanol, triolein, and liposomes as surrogates. Environ Sci Technol 2014; 48: 5920-8.

Quinn CL, Wania F. Understanding differences in the body burden-age relationships of bioaccumulating contaminants based on population cross sections versus individuals. Environ Health Perspect 2012; 120: 554-9.

Quinn CL, Wania F, Czub G, Breivik K. Investigating intergenerational differences in human PCB exposure due to variable emissions and reproductive behaviors. Environ Health Perspect 2011; 119: 641-6.

Ritter R, Scheringer M, MacLeod M, Moeckel C, Jones KC, Hungerbühler K. Intrinsic Human Elimination Half-Lives of Polychlorinated Biphenyls Derived from the Temporal Evolution of Cross-Sectional Biomonitoring Data from the United Kingdom. Environmental Health Perspectives 2011; 119: 225-231.

672 Shen H, Han J, Tie X, Xu W, Ren Y, Ye C. Polychlorinated dibenzo-p-dioxins/furans and
673 polychlorinated biphenyls in human adipose tissue from Zhejiang Province, China.
674 Chemosphere 2009; 74: 384-388.
675 Shen HT, Ding GQ, Wu YN, Pan GS, Zhou XP, Han JL, et al. Polychlorinated dibenzo-p-
676 dioxins/furans (PCDD/Fs), polychlorinated biphenyls (PCBs), and polybrominated
677 diphenyl ethers (PBDEs) in breast milk from Zhejiang, China. Environment
678 International 2012; 42: 84-90.
679 Sun S-J, Kayama F, Zhao J-H, Ge J, Yang Y-X, Fukatsu H, et al. Longitudinal increases in
680 PCDD/F and dl-PCB concentrations in human milk in northern China. Chemosphere
681 2011; 85: 448-453.
682 Sun S-J, Zhao J-H, Liu H-J, Liu D-W, Ma Y-X, Li L, et al. Dioxin concentration in human milk
683 in Hebei province in China and Tokyo, Japan: Potential dietary risk factors and
684 determination of possible sources. Chemosphere 2006; 62: 1879-1888.
685 Sun S, Zhao J, Leng J, Wang P, Wang Y, Fukatsu H, et al. Levels of dioxins and
686 polybrominated diphenyl ethers in human milk from three regions of northern China
687 and potential dietary risk factors. Chemosphere 2010; 80: 1151-1159.
688 Tsutsumi T, Iida T, Hori T, Nakagawa P, Tobiishi K, Yanagi T, et al. Recent survey and effects
689 of cooking processes on levels of PCDDs, PCDFs and co-PCBs in leafy vegetables in
690 Japan. Chemosphere 2002; 46: 1443-1449.
691 UNEP. The Stockholm Convention on Persistent Organic Pollutants. United Nations
692 Environmental Programme, 2001.
693 Wang N, Kong D, Cai D, Shi L, Cao Y, Pang G, et al. Levels of polychlorinated biphenyls in
694 human adipose tissue samples from southeast China. Environ Sci Technol 2010; 44:
695 4334-40.
696 Wang Y, Luo CL, Li J, Yin H, Li XD, Zhang G. Characterization and risk assessment of
697 polychlorinated biphenyls in soils and vegetations near an electronic waste recycling
698 site, South China. Chemosphere 2011a; 85: 344-350.
699 Wang Y, Luo CL, Li J, Yin H, Li XD, Zhang G. Characterization of PBDEs in soils and
700 vegetations near an e-waste recycling site in South China. Environmental Pollution
701 2011b; 159: 2443-2448.
702 WHO. Report of the expert consultation on the optimal duration of exclusive breastfeeding.,
703 Geneva, Switzerland, 2002.
704 Wu J-P, Luo X-J, Zhang Y, Luo Y, Chen S-J, Mai B-X, et al. Bioaccumulation of
705 polybrominated diphenyl ethers (PBDEs) and polychlorinated biphenyls (PCBs) in wild
706 aquatic species from an electronic waste (e-waste) recycling site in South China.
707 Environment International 2008; 34: 1109-1113.
708 Xing X, Lu YL, Dawson RW, Shi YJ, Zhang H, Wang TY, et al. A spatial temporal assessment
709 of pollution from PCBs in China. Chemosphere 2005; 60: 731-739.
710 Yang Y. Manuual for pratical food nutrition analysis: China Light Industry Press, 2007.
711 Yi A, Xu M, An J. China's pork and is by-prodcuts import: scale, structure and prospect. World
712 Agriculture 2015; 7: 103-107.
713 Zhang HB, Li XH, Luo YM, Li QB. Depth distribution of polychlorinated biphenyls in soils of
714 the Yangtze River Delta region, China. Geoderma 2011a; 160: 408-413.
715 Zhang J, Jiang Y, Zhou J, Wu B, Liang Y, Peng Z, et al. Elevated Body Burdens of PBDEs,
716 Dioxins, and PCBs on Thyroid Hormone Homeostasis at an Electronic Waste Recycling
717 Site in China. Environmental Science & Technology 2010; 44: 3956-3962.
718 Zhang L, Li J, Zhao Y, Li X, Yang X, Wen S, et al. A national survey of polybrominated
719 diphenyl ethers (PBDEs) and indicator polychlorinated biphenyls (PCBs) in Chinese
720 mothers' milk. Chemosphere 2011b; 84: 625-633.
721 Zhao GF, Wang ZJ, Zhou HD, Zhao Q. Burdens of PBBs, PBDEs, and PCBs in tissues of the
722 cancer patients in the e-waste disassembly sites in Zhejiang, China. Science of the Total
723 Environment 2009; 407: 4831-4837.
724 Zhao SZ, Price O, Liu ZT, Jones KC, Sweetman AJ. Applicability of western chemical dietary
725 exposure models to the Chinese population. Environmental Research 2015a; 140: 165-
726 176.

727 Zhao SZ, Price OR, Liu GR, Zheng MH, Jones KC, Sweetman A. Long-term temporal trend of
728 PCBs and its controlling sources in China, 2015b.
729 Zhao X-R, Qin Z-F, Yang Z-Z, Zhao Q, Zhao Y-X, Qin X-F, et al. Dual body burdens of
730 polychlorinated biphenyls and polybrominated diphenyl ethers among local residents in
731 an e-waste recycling region in Southeast China. Chemosphere 2010; 78: 659-666.
732 Zhu YG, Ioannidis JP, Li H, Jones KC, Martin FL. Understanding and harnessing the health
733 effects of rapid urbanization in China. Environ Sci Technol 2011; 45: 5099-104.

734

735

736

737

Supporting information for "Time-variant dietary exposure of POPs in China –a PCB case study"

Shizhen Zhao[1], Oliver Price[2], Kevin C. Jones[1], Andrew J. Sweetman[1]*

[1] Lancaster Environment Centre, Lancaster University, Lancaster, LA14YQ, UK

[2] Safety and Environmental Assurance Centre, Unilever, Sharnbrook, MK44 1LQ, UK.

Contents

Table S 1. Defined scenarios on different diet patterns to predict future trends for the Chinese population.

Scenarios	Dietary weight, g/capital/day			
	Fish	Milk	Meat	Veg
Keep the current diet pattern	94	81	167	300
Followed diet from developed countries diets, following a Swedish diet as an example	75	1394	43	310
Followed the official guidance	100	300	75	400
Veg-based	-	-	-	500
Meat based	100	-	220	110
Fish based	100	-	220	110

Table S 2. Summary of PCB measured concentrations in humans for populations living in background sites of China.

PCBs analysed	Sampling time	Sampling sites	Exposure group	Human tissues	∑PCBs	References
PCB-153	N/A	Guangzhou	27 mothers	Serum and breast milk	0.27-73 ng/g lipid	(Bi et al., 2006)
PCBs	08.2005	Guiyu vs Haojiang	47 residents	Serum	52 vs 63 ng/g lipid	(Bi et al., 2007)
PCBs	11-12.2002	Dalian and Shenyang	40 mothers	Human milk	8.8-100 ng/g lipid	(Kunisue et al., 2004)
PCBs	2001	Shanghai	5 women	Mammary glands	32-135 ng/g lipid	(Nakata et al., 2002)
dl-PCBs	2006	Zhejiang	24 patients	Adipose tissue	4.1-125 ng/g lipid	(Shen et al., 2009)
dl-PCBs	2002	Shijiazhuang and Hebei	41 mothers	Human milk	3564 pg/g lipid	(Sun et al., 2006)
12 PCBs	11.2006-04.2007	Northern China	158 mothers	Human milk	1.17-3.38 TEQ pg/g lipid	(Sun et al., 2010)
62 PCBs	04.2008-06.2009	Jiangsu and Anhui province	14-90 years old residents	Adipose tissue	27.2 μg/kg lipid 14.2 μg/kg lipid	(Wang et al., 2010)
PCBs	06.1999-07.2000	Hong Kong and Guangzhou	169 mothers	Human milk	0.033-0.042 μg/g lipid	(Wong et al., 2002)
PCBs	04,2009-2010.10	Tianjin	56 workers and residents (35:21)	Serum	44.1 vs 12.4 ng/g lipid	(Yang et al., 2013)
PCBs	04.2007-12.2007	Southeast China e-waste vs. control area	50 pregnant women	Cord blood	43.22~1167.01 pg/g lipid	(Zhang et al., 2010)
6 PCBs	08-11.2007	National	1237 mothers	Human milk	10.05ng/g lipid	(Zhang et al., 2011)
23 PCBs	10.2003-06.2005	Pingqiao, Zhejiang	16 mothers	Human milk	69.22–677.29 ng/g lipid	(Zhao et al., 2007)
27 PCBs	04.2007~01.2008	Wenling	32-94 years old cancer patients	Kidney, liver and lung	257.9 -455.1 ng/g lipid	(Zhao et al., 2009)
dl-PCBs	11.2007	National	1237 mothers	Human milk	1.69 TEQ pg/g lipid	(Li et al., 2009)
PCBs	2002	Guizhou	34 humans	Adipose tissues	1.1-110 ng/g lipid	(Nakata et al., 2005)
12 PCBs	2002-2007	Shijiazhuang	50 mothers	Human milk	2.29 TEQ pg/g lipid	(Sun et al., 2011)

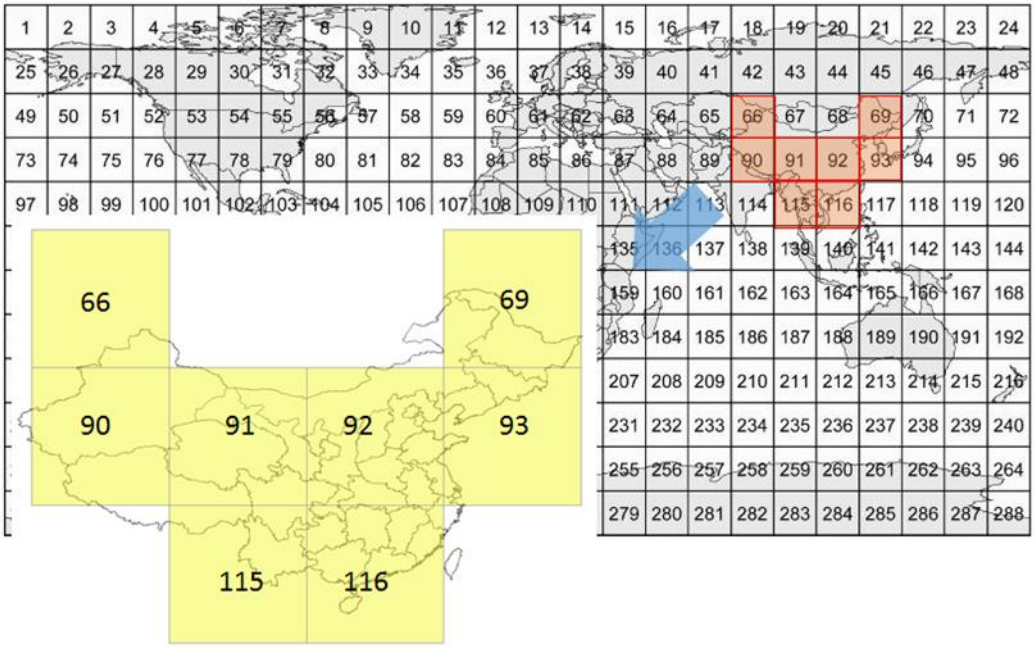

Figure S 1. The defined study region of China together with the BETR-Global grid.

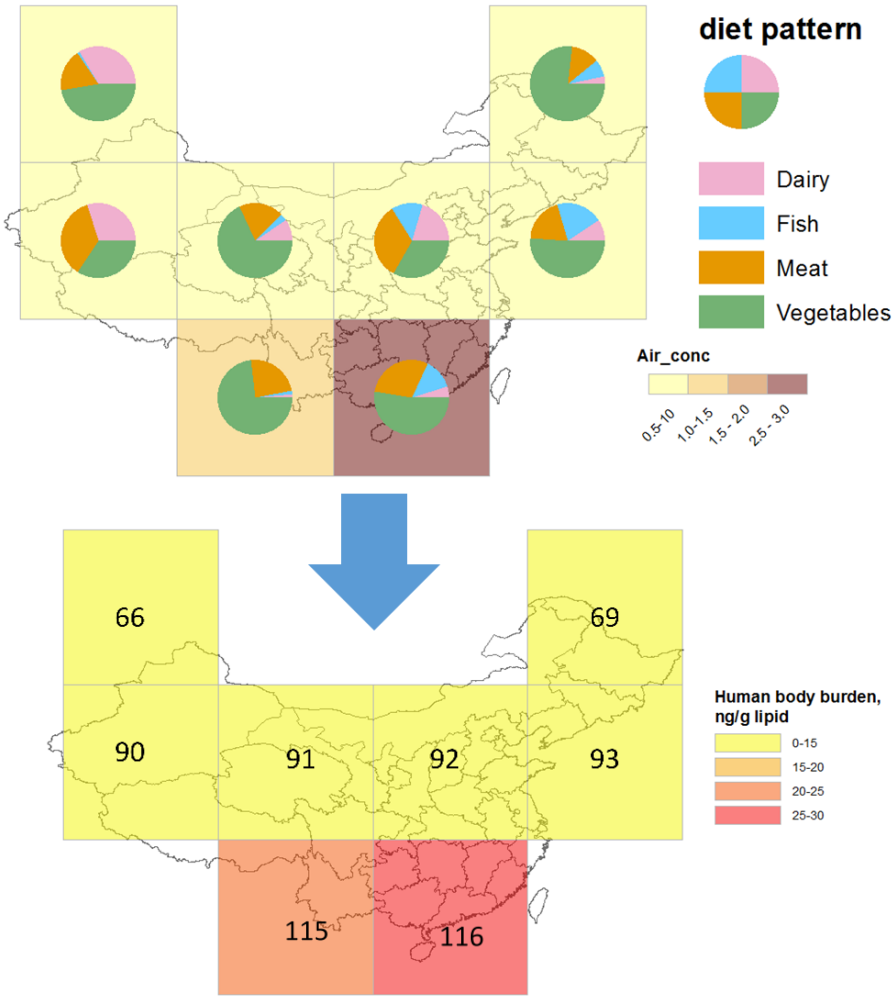

Figure S 2. Regional human body burden for a 30-year-old female in 2002 as a reference year under the combined effect of local emission and diet preference in target grids cells.

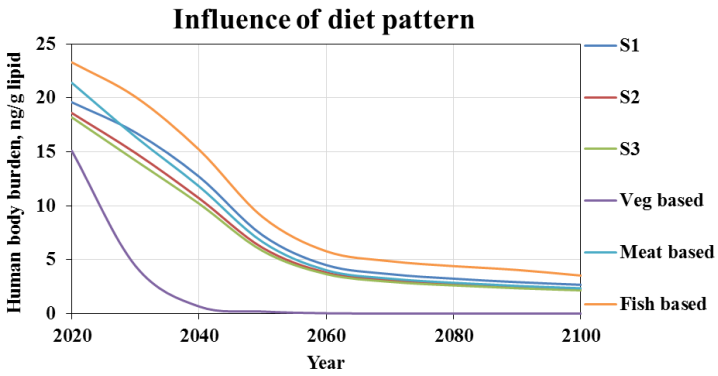

Figure S 3. Predicted future trends of human body burden in a 30-year-old female living in Grid cell 92 from 2010 to 2100 under three scenarios assuming local or imported food from Grid cell 61 (representing a very contaminated foreign site): (a) S1: keeping current diet pattern; (b) S2: following the diet pattern of Western (Swedish) population; (c) S3: following the diet pattern suggested by official diet guidance (d) Veg based: keeping the vegetable-based diet; (e) Meat based: keeping meat-based diet pattern; (f) Fish based: keeping fish-based diet pattern.

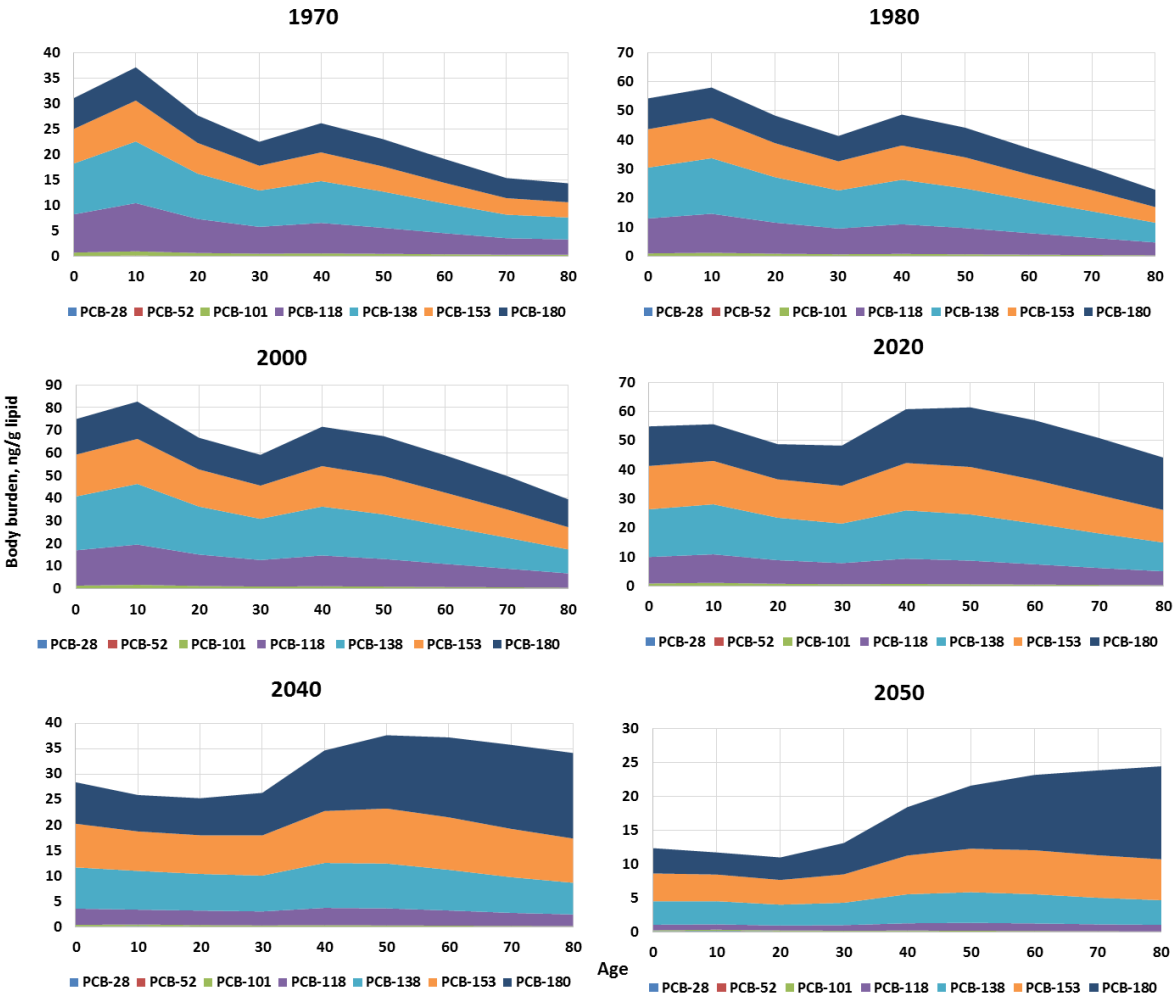

Figure S 4. Cross-sectional body burden trends for the selected seven indicator PCBs congeners in different time points.

References

Bi X, Thomas GO, Jones KC, Qu W, Sheng G, Martin FL, et al. Exposure of electronics dismantling workers to polybrominated diphenyl ethers, polychlorinated biphenyls, and organochlorine pesticides in South China. Environmental Science & Technology 2007; 41: 5647-5653.

Bi XH, Qu WY, Sheng GY, Zhang WB, Mai BX, Chen DJ, et al. Polybrominated diphenyl ethers in South China maternal and fetal blood and breast milk. Environmental Pollution 2006; 144: 1024-1030.

Kunisue T, Someya M, Kayama F, Jin Y, Tanabe S. Persistent organochlorines in human breast milk collected from primiparae in Dalian and Shenyang, China. Environmental Pollution 2004; 131: 381-392.

Li J, Zhang L, Wu Y, Liu Y, Zhou P, Wen S, et al. A national survey of polychlorinated dioxins, furans (PCDD/Fs) and dioxin-like polychlorinated biphenyls (dl-PCBs) in human milk in China. Chemosphere 2009; 75: 1236-1242.

Nakata H, Kawazoe M, Arizono K, Abe S, Kitano T, Shimada H, et al. Organochlorine pesticides and polychlorinated biphenyl residues in foodstuffs and human tissues from china: status of contamination, historical trend, and human dietary exposure. Arch Environ Contam Toxicol 2002; 43: 473-80.

Nakata H, Nasu T, Abe S, Kitano T, Fan QY, Li WH, et al. Organochlorine contaminants in human adipose tissues from China: Mass balance approach for estimating historical Chinese exposure to DDTs. Environmental Science & Technology 2005; 39: 4714-4720.

Shen H, Han J, Tie X, Xu W, Ren Y, Ye C. Polychlorinated dibenzo-p-dioxins/furans and polychlorinated biphenyls in human adipose tissue from Zhejiang Province, China. Chemosphere 2009; 74: 384-388.

Sun S-J, Kayama F, Zhao J-H, Ge J, Yang Y-X, Fukatsu H, et al. Longitudinal increases in PCDD/F and dl-PCB concentrations in human milk in northern China. Chemosphere 2011; 85: 448-453.

Sun S-J, Zhao J-H, Liu H-J, Liu D-W, Ma Y-X, Li L, et al. Dioxin concentration in human milk in Hebei province in China and Tokyo, Japan: Potential dietary risk factors and determination of possible sources. Chemosphere 2006; 62: 1879-1888.

Sun S, Zhao J, Leng J, Wang P, Wang Y, Fukatsu H, et al. Levels of dioxins and polybrominated diphenyl ethers in human milk from three regions of northern China and potential dietary risk factors. Chemosphere 2010; 80: 1151-1159.

Wang N, Kong D, Cai D, Shi L, Cao Y, Pang G, et al. Levels of polychlorinated biphenyls in human adipose tissue samples from southeast China. Environ Sci Technol 2010; 44: 4334-40.

Wong CKC, Leung KM, Poon BHT, Lan CY, Wong MH. Organochlorine hydrocarbons in human breast milk collected in Hong Kong and Guangzhou. Archives of Environmental Contamination and Toxicology 2002; 43: 364-372.

Yang QY, Qiu XH, Li R, Liu SS, Li KQ, Wang FF, et al. Exposure to typical persistent organic pollutants from an electronic waste recycling site in Northern China. Chemosphere 2013; 91: 205-211.

Zhang J, Jiang Y, Zhou J, Wu B, Liang Y, Peng Z, et al. Elevated Body Burdens of PBDEs, Dioxins, and PCBs on Thyroid Hormone Homeostasis at an Electronic Waste Recycling Site in China. Environmental Science & Technology 2010; 44: 3956-3962.

Zhang L, Li J, Zhao Y, Li X, Yang X, Wen S, et al. A national survey of polybrominated diphenyl ethers (PBDEs) and indicator polychlorinated biphenyls (PCBs) in Chinese mothers' milk. Chemosphere 2011; 84: 625-633.

Zhao GF, Wang ZJ, Zhou HD, Zhao Q. Burdens of PBBs, PBDEs, and PCBs in tissues of the cancer patients in the e-waste disassembly sites in Zhejiang, China. Science of the Total Environment 2009; 407: 4831-4837.

Zhao GF, Xu Y, Li W, Han GG, Ling B. PCBs and OCPs in human milk and selected foods from Luqiao and Pingqiao in Zhejiang, China. Science of the Total Environment 2007; 378: 281-292.